Addendum to thesis

Some image panels in chapters 3 and 5 were duplicated accidentally and should be disregarded.

Chapter 3
Loading controls in panels 3.7a and 3.12a are duplicated.
Loading controls in panels 3.9a, 3.10a, 3.11a are duplicated.
Loading controls in panels 3.10a, 3.12a are duplicated.

Chapter 5
Figure 5.3 (2nd image) and 5.6 are duplicated.

Some images in chapter 4 are duplicated or erroneously altered and should be disregarded.

Chapter 4
Images in panels 4.9a, 4.10c, 4.11b and 4.12a are erroneously altered.
Loading controls in panels 4.7a, 4.7c and 4.7c are duplicated and erroneously altered.

Partnerships and Phosphorylation of Cyclic AMP Phosphodiesterase-4A5

Kirsty Faye MacKenzie

2011

A thesis for the degree of Doctor of Philosophy

at

University of Glasgow

Department of Neuroscience and Molecular Pharmacology

Wolfson Link Building

University of Glasgow

University Avenue

Glasgow

G12 8QQ

Abstract

Phosphodiesterase 4 enzymes hydrolyse the second messenger cyclic AMP and therefore are set to play an important role in cell signaling. In this thesis I investigate the phosphorylation and protein-protein interactions of the cAMP hydrolyzing phosphodiesterase isoform, PDE4A4/5.

In the first of my studies I show that PDE4A4/5 can be phosphorylated by MAPKAPK2 (MK2) the downstream kinase of the p38 MAPK signalling pathway. This phosphorylation reaction attenuates the degree of activation of PDE4A5 elicited through phosphorylation by Protein Kinase A. I also show that MAPKAPK2 can bind directly to PDE4A4/5 and map the two binding sites required by peptide array technology.

In the second of my studies I show that PDE4A4/5 interacts with the low affinity neurotrophin receptor, p75NTR. This interaction inhibits normal fibrin breakdown in an *in vitro* model. I also show that phosphorylation of PDE4A5 by MAPKAPK2 enhances the inhibition of fibrin breakdown and increases PDE4A5:p75NTR complex formation.

In the final study described in this thesis I show that long form PDE4 isoforms contain a potential multi-functional docking site where several partner proteins are able to bind.

In conclusion, the work described in this thesis provides a valuable insight into PDE4A4/5, its interacting proteins, phosphorylation status and the potential for exploitation of this novel information therapeutically.

Acknowledgements

I first and foremost want to thank my supervisor Prof. Miles Houslay for his constant, support, encouragement, insight, optimism and bad jokes. It would have been impossible without him. Who would have thought that one set of third year undergraduate tutorials would help shape my future.

Secondly I want to thank everyone in the Gardiner Lab. In particular I want to thank George Baillie for his support, help and additional bad jokes. Allan Dunlop for being the most unbelievably helpful and friendly, I don't know how the lab will function without him. Irene Gall for all of her help with mutagenesis and our mutual love of cats. Elaine Huston and Angela MacCahill for keeping me sane and helpful advice. Martin Lynch for helping me get started. Kim Brown, Dave Henderson, Ruth McLeod, York Cheung, Dong Meng and Shelley Li for lab fun. And of course Helen Edwards for listening to my rants and panics, letting me vent and keeping me calm.

I'd like to also thank my boyfriend Tom for putting up me for the entirety of my PhD. Hopefully I can do the same for you now! Thank you for making me food, bringing me Diet Coke, taking me to the zoo and generally being awesome.

And thank you to my brother Alasdair for always being there to support me, take me out for Nandos and listening to me get excited about science!

And most importantly I want to thank my parents. I want to thank my dad for always knowing and believing I could do it and constantly trying to help and decipher what I do. And to my mum for putting up with my 'drama queen' moments, keeping me grounded, being constantly supportive and always pushing me to finish this thesis! I owe this to both of you.

Table of Contents

Figures

Tables

Abbreviations

AKAP	A Kinase Anchoring Proteins
AMP	Adenosine monophosphate
ATP	Adenosine triphosphate
BDNF	Brain Derived Neurotrophic Factor
cAMP	Cyclic Adenosine Monophosphate
CaMK	Calcium/Calmodulin dependent protein kinase
cGMP	Cyclic Guanosine Monophosphate
COPD	Chronic Obstructive Pulmonary Disease
DD	Death Domain
DISC	Disrupted in Schizophrenia
EPAC	Exchange Protein directly Activated by cAMP
ERK	Extracellular signal Regulated Kinase
FSK	Forskolin
GAF	cGMP-binding PDEs, adenylyl cyclases and Escherichia coli (FhlA)
GDP	Guanosine Diphosphate
GEF	Guanine nucleotide Exchange Factor
GPCR	G-Protein Coupled Receptor
GRK	G-protein coupled Receptor Kinase
GTP	Guanosine Triphosphate
IBMX	3-isobutyl-1-methylxanthine
ICD	IntraCellular Domain
JNK	c-Jun N terminal Kinase
KIM	Kinase Interaction Motif
LPS	Lipopolysaccharide
LR	Linker Region
MAPK	Mitogen Activated Protein Kinase
MAPKAPK	Mitogen Activated Protein Kinase Activated Protein Kinase
MAPKK	Mitogen Activated Protein Kinase Kinase
MAPKKK	Mitogen Activated Protein Kinase Kinase Kinase

MNK	MAPK interacting protein kinase
MSK	Mitogen and Stress-activated protein Kinase
NADPH	Nicotinamide adenine dinucleotide phosphate
NGF	Nerve Growth Factor
NT	Neurotrophin
p75NTR	p75 Neurotrophin Receptor
PAS	Per Arnt Sim
PKA	Protein Kinase A
PKB	Protein Kinase B
PKC	Protein Kinase C
PLC	Phospholipase C
RACK	Receptor for Activated C-Kinase
RIP	Ribosome Inhibiting Protein
TLR	Toll Like Receptor
TNF	Tumour Necrosis Factor
TRAF	TNF Receptor Associated Factor
UCR	Upstream Conserved Region

Publications and Conferences

MACKENZIE, K.F., TOPPING, E.C., BUGAJ-GAWEDA, B., DENG, C., CHEUNG, Y.F., OLSEN, A.E., STOCKARD, C.R., HIGH MITCHELL, L., BAILLIE, G.S., GRIZZLE, W.E., DE VIVO, M., HOUSLAY, M.D., WANG, D. & BOLGER, G.B. (2008). Human PDE4A8, a novel brain-expressed PDE4 cAMP-specific phosphodiesterase that has undergone rapid evolutionary change. *Biochem J*, **411,** 361-9.

SACHS, B.D., BAILLIE, G.S., MCCALL, J.R., PASSINO, M.A., SCHACHTRUP, C., WALLACE, D.A., DUNLOP, A.J., MACKENZIE, K.F., KLUSSMANN, E., LYNCH, M.J., SIKORSKI, S.L., NURIEL, T., TSIGELNY, I., ZHANG, J., HOUSLAY, M.D., CHAO, M.V. & AKASSOGLOU, K. (2007). p75 neurotrophin receptor regulates tissue fibrosis through inhibition of plasminogen activation via a PDE4/cAMP/PKA pathway. *J Cell Biol*, **177,** 1119-32.

Conferences

2009 Biochemical Basis of Respiratory Disease (Loughborough, UK)

2009 EU Thera-cAMP focus group meeting (Glasgow, UK)

2008 EU Thera-cAMP focus group meeting (Kassel, Germany)

2008 British Pharmacology Society: Focus meeting on Cell Signalling (Leicester, UK)

2007 EU Thera-cAMP focus group meeting (Cambridge, UK)

2007 Life Sciences (Glasgow, UK)

2006 FEBS Spatiotemporal Signalling Focus Group (Oslo, Norway)

Chapter 1 Introduction

Understanding how cells communicate with each other in health and disease is a major topical issue that will impact considerably on human health. The mechanisms that underpin signal transduction in cells are complex and unravelling them provides a major challenge.

With the exception of steroid hormones, most hormones and neurotransmitters cannot penetrate the cell membrane and must therefore elicit their response within the cell via signal transduction pathways that traverse the cell plasma membrane, radiate through the cell interior and, where appropriate, into intracellular organelles such as the nucleus. This process involves the conversion of an extracellular biological signal to an intracellular response. Initiation of this pathway begins through activation of a cell-surface receptor by an agonist.

The second messenger concept was developed through studies on the 3', 5' cyclic adenosine monophosphate (cyclic AMP or cAMP) signalling system [Beavo and Brunton, 2002]. The receptor-mediated stimulation of cAMP generation (Figure 1.1) [Beavo and Brunton, 2002] envisages that when an agonist binds to a G Protein Coupled Receptor (GPCR) it is able to associate with a specific G-Protein, called Gs. This causes activation of Gs through GDP/GTP exchange, with the release of GTP-bound γ-subunit of Gs and a αβ complex. The GTP-bound, Gs γ-subunit, in turn, activates the membrane bound enzyme adenylyl cyclase, which leads to the production of cAMP from ATP and therefore an increase in intracellular levels of cAMP. Cyclic AMP can then activate important proteins like Protein Kinase A (PKA), Exchange Protein Activated by cAMP (EPAC) and cyclic nucleotide gated ion channels. This confers regulation on a myriad of fundamental cellular processes such as transcription, proliferation, cardiac function, learning and memory and apoptosis [Tasken and Aandahl, 2004].

Cyclic nucleotide phosphodiesterases, which degrade cAMP to 5'-AMP, are pivotal to signal transduction, not only as regards signal termination and therefore negative regulation of cAMP within the cell, but also in shaping gradients of cAMP for compartmentalised cAMP signalling [Houslay. 2010].

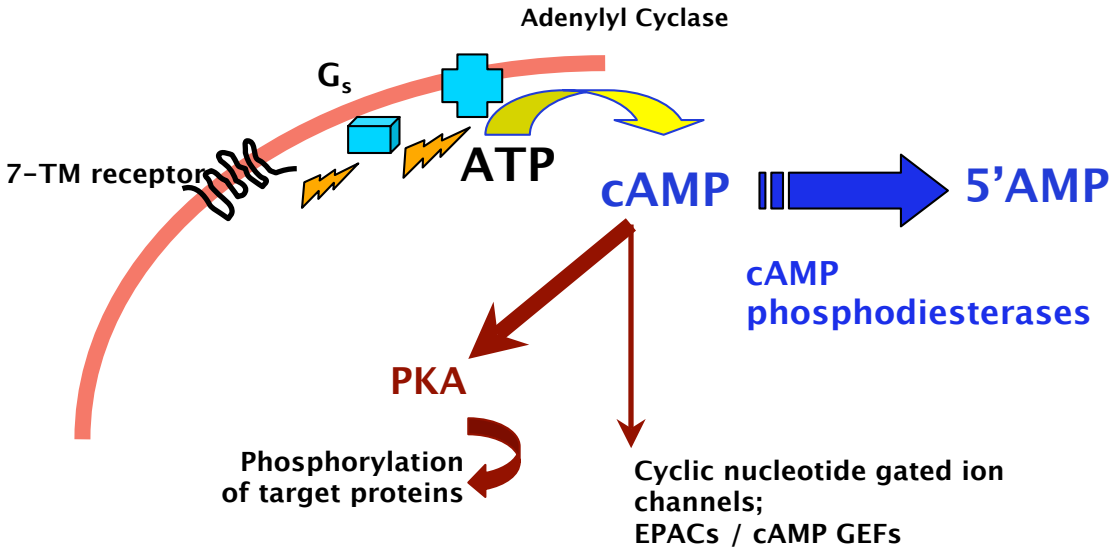

Figure 1.1 - cAMP cascade (adapted from Prof Miles Houslay).

1.1 G-Protein Coupled Receptors

For the cAMP signalling pathway to be fully understood each of its components must be looked at in depth. Signalling is initiated by an agonist binding to G-Protein Coupled Receptors. GPCRs are the widest and most diverse family of cell surface receptors [Fredholm et al., 2007]. Structurally they consist of seven transmembrane α-helices that span the plasma membrane. These seven α-helices are linked by alternate intracellular and extracellular loops. They can vary in length and can be subjected to N-linked glycosylation at their extracellular surface [Hollmann et al., 2005]. The third transmembrane domain contains an amino acid essential for ligand specificity, which is situated C-terminally to a conserved cysteine residue [Yin et al., 2004]. If the 'ligand specificity' amino acid is basic the agonist binding the GPCR will most likely be a peptide but if the 'ligand specificity' amino acid is acidic then the agonist will most likely be an amine [Simon, Strathmann and Gautam, 2001]. The C terminal region of a GPCR consists of approximately 50 amino acids that are reasonably conserved through most GPCRs. The second and third cytoplasmic loop work in conjunction with the C-terminal to confer ligand binding specificity [Simon, Strathmann, Gautam, 2001].

G-Protein Coupled Receptors are now widely thought to form dimers which confer important functional attributes such as signal transduction and plasma membrane localisation [Milligan, 2004].

1.1.1 Desensitisation of GPCRs

Continuous exposure of GPCRs to their ligand causes a profound and rapid desensitization of signalling [Kohout and Lefkowitz, 2003]. Desensitization occurs as a result of phosphorylation of the C-terminal by G-protein coupled receptor kinases (GRK). Indeed, GRK activity can itself be regulated by PKA and Extracellular-signal Regulated Kinase (ERK) phosphorylation. The functional consequence of

phosphorylation by GRK is to trigger the binding of cytosolic β-arrestin to the membrane-localised GPCR, which sterically blocks its G-protein coupling, causing a rapid desensitization [Li et al., 2006]. In cells where the cAMP degrading PDE4D5 isoform is present then a complex of this isoform together with β-arrestin can be delivered to an agonist-activated GPCR, thus delivering an active cAMP degrading system to the site of cAMP synthesis at the plasma membrane [Houslay, 2010]. This can form an additional part of the desensitization mechanism for cAMP signalling in cells.

Receptor internalisation can lead to long-term desensitisation. This works through a similar mechanism involving β-arrestin but in this case the binding of β-arrestin causes localisation of the GPCR to clatherin coated vesicles. Through interaction with clatherin and AP-2 this then leads to endocytosis of the complex. The β-arrestin-bound GPCR can then either become de-phosphorylated via Protein Phosphatase 2 (PP2) in the early endosomes, after which it is recycled and returned to the cell surface or sent for degradation in lysosomes, with concomitant down-regulation of cell surface receptor levels and signalling [Hollmann et al., 2005]. Certain processes within the cell can prevent receptor recycling, such as palmitoylation, which involves the covalent attachment of palmitic acid to appropriate cysteine residues in the GPCR. Other means of regulation involve ubiquitination, which is the attachment of ubiquitin peptides to the GPCR, affecting its recycling and facilitating its degradation.

1.2 G-Proteins

The second step in the cAMP signalling pathway comes in the form of G-Proteins. G-proteins are guanine nucleotide binding proteins [Cabrera-Vera et al, 2003]. These interact with the second and third intracellular loops and the C-terminal of GPCRs. There are four major classes; Gs, Gi/o, Gq/11 and G12/13. G-proteins are heterotrimeric and are composed of three subunits; Gα, Gβ and Gγ. In the inactive state the Gα unit is bound to GDP, which facilitates binding to a Gβ-Gγ complex that keeps the G-protein bound to the plasma membrane [Hollmann et al., 2005]. Activation of the

GPCR leads to a conformational change in its intracellular loops causing activation of the guanine exchange factor, which results in GTP being substituted for GDP at the Gα subunit. This causes dissociation of Gα from the Gβ-Gγ complex, which leads to reduction of agonist binding [Hollmann et al., 2005].

Each of these classes demonstrates an affinity for particular partner GPCRs. The classes of G-proteins can bind GPCRs out with their partners but with a much lower affinity. However this low affinity can be increased through phosphorylation and palmitoylation. For example, when the β_2-adrenoceptor is phosphorylated by protein kinase A (PKA) this reduces its affinity for its partner G-protein G_s but increases its affinity for the G-protein Gi/o [Hollmann et al., 2005].

1.3 Adenylyl Cyclases

Following on from G-Proteins in the signalling cascade are the membrane-bound adenylyl cyclases. Adenylyl cyclases are a group of membrane-associated glycoprotein enzymes that convert ATP to cyclic AMP [Taskén and Aandahl, 2004]. There are 10 adenylyl cyclase isoforms that all exhibit individual tissue specific patterns of localisation and specific means of regulation.

They have two trans-membrane helical domains which cause membrane targeting and two cytosolic domains which become the catalytic site when they are in the correct conformation. Regulation of these active sites is controlled by the G-proteins upstream of them.

1.4 cAMP signalling

When cyclic AMP was first proposed to be a second messenger eliciting signals from within the cell the theory of its role was controversial. It was not understood how one small molecule could play a role in so many different, independent, physiological roles [Beavo and Brunton, 2002]. However it is now understood that when cAMP is produced, by different adenylyl cyclase isoforms, it is diffused throughout the cell into distinct compartmentalised pools restricted by effector proteins such as AKAPs, PKA and PDEs [Baillie, 2009; Zaccolo et al., 2002; Houslay, 2010]. cAMP has a basal concentration of 1 μM in resting cells but this can rise to 10-20 μM in milliseconds to elicit a response. If it was left uncontrolled within the cell this would lead to disruption of compartmentalisation and uniform distribution which would result in an inappropriate response from the cell.

1.4.1 Protein Kinase A

The first cAMP effector identified, PKA is a Ser/Thr protein kinase that phosphorylates a wide range of target proteins at the consensus site Arg-Arg-Xaa-[Ser/Thr]-$X_{hydrophobic}$. It is a heterotetramer with two regulatory and two catalytic domains. These are differentially expressed in different PKA holoenzymes on a cell type specific basis. Four genes encode the regulatory domains; RIα, RIβ, RIIα, RIIβ. RI encodes PKA for subcellular cytosolic localisation whereas RII encodes it for targeting to AKAPs. The differences in these two forms are in the N-terminal portion of the regulatory subunits. The catalytic domain of PKA is encoded by three genes; Cα, Cβ, Cγ. PKA activation occurs when cAMP binds to the two regulatory subunits (2 cAMP molecules per subunit), causing dissociation and activation of the catalytic subunits allowing for phosphorylation of target proteins [Taskén and Aandahl, 2004]. However

the catalytic domains are subject to interactions with the PKA inhibitor PKI that replaces PKA at the active site and abolishes PKA activity.

1.4.2 EPAC

When cAMP signalling was first being investigated it was initially thought that its only effectors were PKA and cAMP-gated ion channels. However now it is widely appreciated the cAMP also targets an exchange protein known as Epac (exchange protein directly activated by cAMP). This protein was initially identified through database screening of an RT-PCR product to explain the PKA-independent activation of Rap, a small G protein, through cAMP activation [de Rooij et al., 1998]. Subsequently two isoforms of Epac were discovered, Epac 1 and Epac 2 [Kawasaki et al., 1998]. Structurally they are multi-domain proteins containing and N-terminal regulatory domain, a C-terminal exchange factor domain and linking these a Ras-assocation domain [de Rooij et al., 2000]. Both isoforms are present in most tissues with different expression levels. Epac 1 is most abundant in adipose tissue, blood vessels, and the ovaries to name but a few, whereas Epac 2 is most abundant in the central nervous system and pancreas [Kawasaki et al., 1998].

Functionally Epac proteins act as guanine exchange factors (GEFs) for the Rap family of small G-proteins. Their role is to catalyse the exchange of GDP to GTP on these G-proteins and therefore activate them [de Rooij et al., 2000]. Various effectors proteins downstream of Rap have been identified and it has been shown that Epac plays roles in cardiac function, insulin secretion, cerebral function and even immune response [Gloerich and Bos, 2010].

1.4.3 AKAPs

AKAPs are A-Kinase (PKA) Anchoring Proteins [Langeberg and Scott, 2005] which, despite not being direct cAMP effectors play a very important role in cAMP signalling. To date more than 50 members of the AKAP family have been identified

[Wong and Scott. 2004] and these are thought to play a key role in compartmentalisation and precision of cAMP signal transduction through binding of PKA into spatial specific areas throughout the cell [Carnegie et al., 2009]. Despite a lack of primary sequence homology between the AKAP isoforms they have been identified through the presence of three common features: an anchoring PKA domain, their ability to bind other signalling enzymes (such as phosphodiesterases) and their ability to target these enzymes and kinases to specific sites within the cell [Wong and Scott, 2004]. The first of these features, the anchoring site for PKA, has been widely studied. The majority of AKAPs bind PKA through its RII regulatory subunit [Carnegie et al., 2009] however dual specificity AKAPs which bind both RII and the other regulatory component of PKA the RI subunit have also been identified [Huang et al., 1997]. This R subunit binding configures PKA to a specific site within the cell, near other cAMP regulating components such as PDEs and allows for compartmentalisation of signalling [Baillie. 2009]. A small 24mer peptide, Ht31, has been developed that binds the PKA binding site on AKAPs with nanomolar affinity and this is now being used in disruption studies to help identify the cellular and physiological function of AKAPs [Carr et al., 1992]. Indeed at a cellular level this has already been used to highlight the role of AKAPs in regulation of L-type calcium channels [Johnson et al., 1994] where when Ht31 is used cAMP regulation of the receptor is lost, most likely due to a lack of cAMP compartmentalisation.

Despite these advances in the identification of a large number of AKAPs and the elucidation of their ability to anchor PKA, their physiological role is not greatly understood. Studies on *Drosophila melanogaster* have now shown that AKAPs play a role in learning and memory [Terman and Kolodkin, 2004]. However the development of knockout mice models for AKAPs has been less successful due to high levels of embryonic lethality or conversely lack of an obvious phenotype [Carnegie et al., 2009].

1.5 Cyclic Nucleotide Phosphodiesterases

Cyclic Nucleotide Phosphodiesterases (PDEs) play a major role in cell signalling by hydrolysing the cyclic nucleotides cAMP and cGMP into their 5' mononucleotides. Due to their diversity they are found in many locations throughout the cell such as the cytosol, the plasma membrane, the cytoskeleton and the nucleus [Houslay and Adams, 2003]. The PDE super-family is represented by 11 gene families (PDE1-11). However the occurrence of mRNA splicing and multiple genes within various families leads to the potential for a large number of PDE isoforms being expressed. Some PDE families specifically hydrolyse cAMP (PDE4, 7, 8) some both cAMP and cGMP (PDE1, 2, 3, 10, 11) and others which can hydrolyse only cGMP (PDE5, 6, 9) [Conti and Beavo, 2007; Lugnier, 2006]. The structure of the catalytic units of various PDEs has been solved recently and this has identified the cyclic nucleotide binding pocket and given insight into the catalytic mechanism [Zhang et al., 2004]. Structural studies have also given insight into the basis of selectivity of active site targeted competitive PDE inhibitors and aided in the development of more potent and selective inhibitors [Ke and Wang, 2007; Zhang et al., 2004; Card et al., 2005]. Use of these inhibitors has then given an insight into the functional role of specific PDEs within the body and led to the development of several therapeutics. Examples of these are the selective PDE4 inhibitors in development for treating inflammatory diseases [Houslay et al., 2005], PDE3 inhibitors that are used to treat intermittent claudication [Thompson et al., 2007] and, of course, the most famous PDE inhibitor to date, namely Sildenafil (Viagra), which is a PDE5 specific inhibitor used to treat erectile dysfunction and infant and, more recently, adult pulmonary hypertension [Francis and Corbin, 2005; Huddleston et al., 2009; Singh, 2010]. Along with the therapeutic advances developed through research into PDE isoforms, research into PDE4 enzymes in particular has helped to develop the understanding of compartmentalisation of cAMP signalling and the role of PDEs in cross-talk between signalling pathways [Houslay and Adams, 2003; Houslay, 2010].

Table 1.1: Classification of PDE enzyme super-family.

PDE	Genes	Substrates		Regulation	Regulatory Domains
		cAMP	cGMP		
1	A, B and C	√	√	Ca^{2+}/CaM PKA and CaMK	Ca^{2+}/CaM Binding
2	A	√	√	Activated by cGMP Phosphorylated by PKC	GAF-A, GAF-B
3	A and B	√	x	Inhibited by cGMP Phosphorylated by PKA, PKB/Akt & PI3-K	
4	A, B, C and D	√	x	Phosphorylated by PKA and ERK1/2	UCR1, UCR2
5	A	x	√	Binds cGMP Phosphorylated by PKA and PKG	GAF-A, GAF-B
6	A, B and C	x	√	Activated by Rhodopsin and Transducin (G_t)	GAF-A, GAF-B
7	A and B	√	x		
8	A	√	x		PAS
9	A	√	√		REC

10	A	√	√	Inhibited by cAMP	GAF-A, GAF-B
11	A	√	√		GAF-A, GAF-B

1.5.1 Phosphodiesterase 1

Phosphodiesterase 1 (PDE1) enzymes are encoded by 3 genes (A-C), expressed as multiple splice variants [Wang et al., 1990]. They can hydrolyse both cAMP and cGMP but have a lower Km value for cGMP and therefore shows higher affinity for it than for cAMP (Km values = 1-100 μM for cAMP and 1-5 μM for cGMP) [Francis et al., 2001]. Structurally PDE1 enzymes consist of two paired Ca^{2+} calmodulin domains (CaM) which, with the binding of four calcium ions, cause activation of enzymatic activity [Huang et al., 1981]. This means that increased intracellular calcium levels generate a fall in cAMP/cGMP levels by activating PDE1, thus providing a point of cross talk. Regulation of PDE1 enzymes is thought to occur through phosphorylation by PKA and CaM kinase II which down-regulate its action by attenuating CaM binding [Sharma, 1991; Sharma & Wang, 1986].

PDE1 isoforms are differentially expressed in cells; with particularly high levels found in the central nervous and cardiac systems [Yan et al., 1994; Miller et al., 2009]. In the central nervous system the enzymes exists in an auto-inhibited state but can also be inhibited by vinpocetine and nicardipine [Yan et al., 1996; Lefievre et al., 2002]. In recent years specific PDE1 inhibitors have been developed with the hope of development of a potential therapeutic for Parkinsons disease however the results of this work are as yet inconclusive [Laddha and Bhatnagar, 2009]. In the cardiac system a role for the PDE1A isoform has been implied to regulate pathological cardiomyocyte hypertrophy through a cGMP/PKG dependent mechanism. This demonstrates cross-talk between cGMP and Ca^{2+} signalling pathways during cardiac hypertrophy [Miller et al., 2009].

1.5.2 Phosphodiesterase 2

Phosphodiesterase 2 (PDE2) enzymes are encoded by one gene and have 3 splice variants [Francis et al., 2001]. They can hydrolyse both cAMP and cGMP and are unique in that they are activated by a decrease in Km rather than an increase in Vmax as is usually observed in the other members of the PDE family [Erneux et al., 1981]. The Km value is 15-30 μM for both cAMP and cGMP [Erneux et al., 1981].

Structurally PDE2 enzymes have paired cGMP-binding GAF domains [Ho et al., 2000]. The GAF acronym is derived from the names of the first 3 classes of proteins recognized to contain this domain, namely cGMP-binding PDEs, Anabaena adenylyl cyclases and Escherichia coli (FhlA) [Aravind and Ponting, 1997]. There are now more than 1400 proteins in the non-redundant database that are predicted to contain a GAF domain [Zoraghi et al., 2004]. These GAF domains promote hydrolysis of cAMP in a positively homotrophic/ cooperative fashion with a hill coefficient of >1 [Erneux et al., 1981]. This means, therefore, that small increases in intracellular cGMP concentration can lead to a decrease in intracellular cAMP concentration in cells or compartments where PDE2 is located [Martinez et al., 2002; Mongillo et al., 2006]. However, higher levels of cGMP will then compete out cAMP for binding to the PDE2 active site and thus inhibit cAMP hydrolysis by this enzyme.

PDE2 is expressed in many different parts of the body with the main sites of expression being the adrenal medulla, heart, liver and brain [Yanaka et al., 2003; Coudray et al., 1999]. It is essentially a soluble, cytosolic enzyme. However, alternative mRNA splicing yields isoforms with N-terminal regions that confer membrane association.

PDE2 is thought to play a major feedback role for cyclic nucleotides under hormonal regulation and plays an important role in feedback between cAMP and cGMP. Two PDE2 selective inhibitors are EHNA (erythro-9-(hyroxy-3-nonyl) adenite) and Bay

60-7550. EHNA binds to both the catalytic and the regulatory sites of PDE2 [Michie et al., 1996]. However, EHNA also acts as an adenosine deaminase inhibitor. Recently it has been discovered that PDE2 may play an important role in cardiac inotrophy [Mongillo et al., 2006] and mediating angiogenesis through Rac1 and NADPH oxidase, providing a potential new therapeutic target for endothelial dysfunction, oxidative stress, vascular proliferation and angiogenesis [Diebold et al., 2009].

1.5.3 Phosphodiesterase 3

Phosphodiesterase 3 (PDE3) enzymes are encoded by 2 different genes [He et al., 1998]. They specifically hydrolyse cAMP but this hydrolysis can be competitively inhibited by cGMP [Lugnier, 2006]. The Km value of hydrolysis of both cAMP and cGMP is 0.1-0.8 μM however cAMP has a higher Vmax value for hydrolysis [Francis, 2001]. This therefore means that PDE3 enzymes provide a means by which increased intracellular cGMP can lead to increased intracellular cAMP by selective inhibition of PDE3.

PDE3 enzymes play a key role in metabolic signalling, specifically in adipocytes and hepatocytes [Meacci et al., 1992; Wechsler et al., 2002]. Here it mediates the functional consequences of insulin on cAMP concentration [Zhao et al., 2002]. Insulin triggers Protein Kinase B (PKB/Akt) to phosphorylate and activate PDE3, thereby decreasing cAMP concentration and inhibiting lipolysis, gluconeogenesis, and glycogenolysis [Geoffroy et al., 2001] where it is critical in underpinning insulin action adipocytes, counteracting action of adrenaline.

Another important role for PDE3 has been found in the cardiac system. Here PDE3 has been shown to play several roles including control of myocyte contraction and relaxation through regulation of cAMP at L-type Ca^{2+} channels and through modulating calcium current by facilitating the constitutive association of SERCA2 with PI3 Kinase [Kakkar et al., 1999].

Selective inhibitors of PDE3 have been generated and these have been shown to exert a marked effect on cardiac function [Moos et al., 1987]. These inhibitors were originally developed as positive ionotropic agents for treating congestive heart failure [Bristol et al., 1984]. The compound milrinone in particular is a moderately selective, first generation PDE3 inhibitor with a Ki value of 0.5 μM [Mongillo et al., 2004]. Milrinone, however, was withdrawn from clinical use due to side effects, namely arrhythmias, probably because it also could exert effects on other PDEs, including PDE4. However, the pure PDE3 selective inhibitor cilostazol is now considered safe and used clinically to treat intermittent claudication by inhibiting platelet aggregation [Liu et al., 2001].

1.5.4 Phosphodiesterase 4

This family of cAMP specific enzymes is discussed in detail below (see Section 1.6).

1.5.5 Phosphodiesterase 5

Phosphodiesterase 5 (PDE5) enzymes are encoded by one gene which has 5 splice variants [Lin et al., 2002]. They specifically hydrolyses cGMP and are most commonly known as the target for Viagra (Sildenafil) used to treat Erectile Dysfunction [Coquil et al., 1980; Boolell et al., 1996]. Structurally they have two paired GAF domains that are a site for cGMP binding with a Km of 5-20 μM [Francis et al., 2001]. This binding initially alters activation and conformation of PDE5 and is also thought to influence phosphorylation by PKA and Protein Kinase G [Francis et al., 2002].

PDE5 is expressed throughout the body with highest expression levels seen in the lungs, heart, blood vessels and brain [Giordano et al., 2001]. The most famous inhibitor of PDE5, Viagra, promotes smooth muscle relaxation and increases the blood

flow to the corpus cavernosum by preventing the PDE5 hydrolysis of cGMP [Lin et al., 2003]. More recently it has also been used to treat infantile and severe adult pulmonary hypertension [Huddleston et al., 2009; Singh, 2010].

1.5.6 Phosphodiesterase 6

Phosphodiesterase 6 (PDE6) enzymes are encoded by three genes with multiple splice variants [Gillespie & Beavo, 1989]. PDE6 specifically hydrolyses cGMP with a Km value of 5-20 μM [Miki et al., 1975]. Structurally they contain two paired GAF domains and appear to be a tetramer with one alpha catalytic subunit, one beta catalytic subunit and two gamma regulatory (inhibitory) subunits [Gillespie & Beavo, 1989].

PDE6 is membrane bound and found exclusively in the rods and cones of the eyes [Francis et al., 2001 and Houslay, 2001]. PDE6 is light activated via rhodopsin, which couples to the G-protein, transducin [Chabre et al., 1988]. Rod PDE6 enzymes consist of one α, one β, two γ subunits whereas cone PDE6 enzymes consist of two α and two γ subunits [Artemyev et al., 1996]. Rhodopsin absorbs a photon of light, which then physically interacts with transducin causing an exchange of GDP for GTP. The GTP-bound transducin undergoes a conformational change such that it interacts with and activates, membrane bound PDE6 by triggering the release of the inhibitory gamma subunits from this enzyme [Morin et al., 2001; Pugh & Lamb, 1990]. The consequential increase hydrolyses cGMP to GMP allowing the closure of cGMP-gated channels located in the plasma membrane of photoreceptors [Beavo, 1995].

Recently a potential role for PDE6 in retinal malignant melanoma has been identified. In these melanoma cells activation of PDE6 through the Wnt5a–Frizzled-2-transducin cascade leads to a decrease in cGMP allowing for a build-up of calcium which in turn can regulate the metabolism of the melanoma cells [Bazhin et al., 2010]. If this pathway occurs in cells out with the eyes inhibition of PDE6 may provide a potential non-invasive therapeutic for malignant melanoma.

1.5.7 Phosphodiesterase 7

Phosphodiesterase 7 (PDE7) enzymes are encoded by two genes, one of which has splice variants [Beavo, 1995]. They are specific for cAMP for which they have been shown to have an extremely low Km value of 0.01-0.05 μM [Michaeli et al., 1993]. PDE7A is ubiquitously expressed throughout the body but is particularly well expressed in the pro-inflammatory and immune system [Smith et al., 2003] whereas PDE7B is expressed throughout the heart, skeletal and brain tissues but its expression is lower than PDE7A in the immune system [Hetman et al., 2000].

The majority of PDE7 research has focussed on the role of PDE7A. In T-cells in particular a functional role for PDE7A has been proposed where it is envisaged that PDE7 may regulate T-cell proliferation and activation. In T-cells the main PDE isoforms present in resting cells are PDE3 and PDE4, however it was shown that upon T-cell activation PDE7A is up-regulated and if this is up-regulation of PDE7 is inhibited there is a loss of T cell proliferation [Li et al., 1999; Smith et al., 2003]. As a result of this discovery several PDE7 inhibitors have been developed. These include several unnamed pyrimidine inhibitors shown that selectively inhibit PDE7A and have been shown to have some effect in vitro on T cell proliferation [Guo et al., 2009] and ASB16165, a novel inhibitor for PDE7A, that suppresses IL-12-induced IFN-γ production by mouse activated T lymphocytes in vitro [Kadoshima-Yamaoka et al., 2009]. However it should be noted that studies using knock-out animals have not supported the notion of any particular role of PDE7 inhibitors as regulators of T-cell functional and potential as anti-inflammatory agents and PDE7 selective inhibitors have no shown any particular promise as anti-inflammatory agents [Guo et al., 2009; Yang et al., 2003].

Despite PDE7B only having low level expression in the immune system in normal circumstances its expression has been found to be up-regulated in B cells and peripheral blood mononuclear cells in chronic lymphocytic leukaemia, the most common form of adult leukaemia. It has also been shown that inhibition of PDE7 in

these leukaemia cells leads to apoptosis in vitro, providing a potential therapeutic target for treatment of this form of leukaemia [Zhang et al., 2008].

1.5.8 Phosphodiesterase 8

Phosphodiesterase 8 enzymes are encoded by two genes and many splice variants [Fisher et al., 1998; Hayashi et al., 1998]. They are specific for cAMP with a very low Km value of 0.06 μM [Francis et al., 2001]. They are one of the only known PDE subfamily members that are insensitive to inhibition by IBMX (isobutylmethylxanthine) [Hayashi et al., 1998; Lavan et al., 1989]. Structurally they contain a single Per-ARNT-Sim (PAS) domain that has been shown in other proteins to mediate protein-protein interaction so may regulate PDE8's intracellular distribution [Wang et al., 2001]. Expression of PDE8 is highest in the testis [Soderling et al., 1998] but it has also been shown to be involved in regulation of T-cell activation and chemotaxis of activated lymphocytes [Glavas et al., 2001; Dong et al., 2006].

Unfortunately until recently purification of PDE8 was not possible therefore its crystal structure could not be solved and in turn selective PDE8 inhibitors have not been developed. However recent structural studies may help solve this problem and lead to the development of inhibitors [Wang et al., 2008]. This may be of major potential therapeutic benefit as a recent clinical study has shown that PDE8 is up-regulated in the hippocampus of end stage patients with Alzheimers Disease [Perez-Torres et al., 2003].

1.5.9 Phosphodiesterase 9

Phosphodiesterase 9 (PDE9) enzymes are encoded by one gene but it is thought to be a rather complicated isoform as up to 20 splice variants have been identified [Rentero and Puigdomenech, 2006]. They are cGMP specific and have the lowest Km value for cGMP known to date at 0.07 μM [Fisher et al., 1998]. Structurally they are not

thought to contain GAF domains but may contain REC domains instead [Lugnier, 2006]. CheY-like phosphoacceptor (or receiver (REC)) domain is a common module in a variety of response regulators of the bacterial signal transduction systems. REC domains have a propensity to regulate dimerisation and protein-protein interactions [Galperin, 2006]. Thus they may be involved in either targeting of PDE9 or regulation by dimerisation.

PDE9A isoforms are expressed in several regions of the brain where it has been implied to play a role in cognition [Reyes-Irisarri et al., 2007] and has also been proposed to play a role in diabetes as PDE9 knockout mice developed an diabetes like phenotype when placed on a high fat diet [DeNinno et al., 2009]. PDE9 isoforms are insensitive to IBMX but their actions are attenuated by zaprinast and SCH 51866 [Soderling et al., 1998]. Few selective PDE9 inhibitors have been developed. However of those that have the novel selective PDE9 inhibitor BAY 73-6691 has been shown to improve learning and memory in rodents [van der Staay et al., 2008].

1.5.10 Phosphodiesterase 10

PDE10 enzymes are encoded by one gene and have been indicated to have many splice variants [Kotera et al., 1999; O'Connor et al., 2004]. They can hydrolyse both cAMP and cGMP with Km values of 0.05-0.26 μM and 3-7.2 μM respectively and a Vmax value 5 times higher for cAMP than cGMP [Lugnier, 2006]. Structurally they have two paired GAF domains but so far there is no evidence that these can bind cGMP [Lugnier, 2006]. IBMX, dipyridamole and zaprinast all inhibit PDE10.

It is ubiquitously expressed throughout all human tissues [Soderling et al., 1999] but its unique distribution of expression in the brain has lead to a great amount of research. In the brain PDE10 expression is very high in the caudate putamen, nucleus accumbens, and the olfactory tubercle, however expression is minimal in cortex, hippocampus, and cerebellum [Kelly and Brandon, 2009]. This distribution has lead to a

great deal of interest in the potential role of PDE10 in schizophrenia. In PDE10A knockout mice a decrease in basal locomotor activity and impaired learning of a conditioned avoidance task was observed which is consistent with a model of schizophrenia [Siuciak et al., 2008]. These mice also show increased sensitivity to indirect dopaminergic agonists [Siuciak et al., 2008]. Indeed it has also been shown that selective PDE10 inhibitors developed by Wyeth modulate the dopamine striatal pathways and can improve both the positive and negative symptoms of schizophrenia [Grauer et al., 2009].

1.5.11 Phosphodiesterase 11

PDE11 enzymes are encoded by just one gene and have 4 splice variants [Hetman et al., 2000]. It exhibits dual specificity in a similar way to PDE10 but has a Km value of about 0.75 μM for both cAMP and cGMP [Francis et al., 2001]. Only some of its isoforms express two paired GAF domains in a way that is similar to the expression of UCR domains in PDE4. The presence of these GAF domains may allow for regulation by PKA and PKG phosphorylation [Yuasa et al., 2000].

The range of tissues that express this enzyme is controversial and little is understood about its function. Studies into its expression in the brain have shown that expression is limited but through knockout mice models it has been shown to play a vital role in brain function with lack of this enzyme leading to hyperactivity and loss of social function [Kelly et al., 2010]. Other research using PDE11 knockout mice has shown that these mice exhibit reduced sperm concentration and live spermatozoa after ejaculation implying that this isoform plays an important role in reproduction [Wayman et al., 2005].

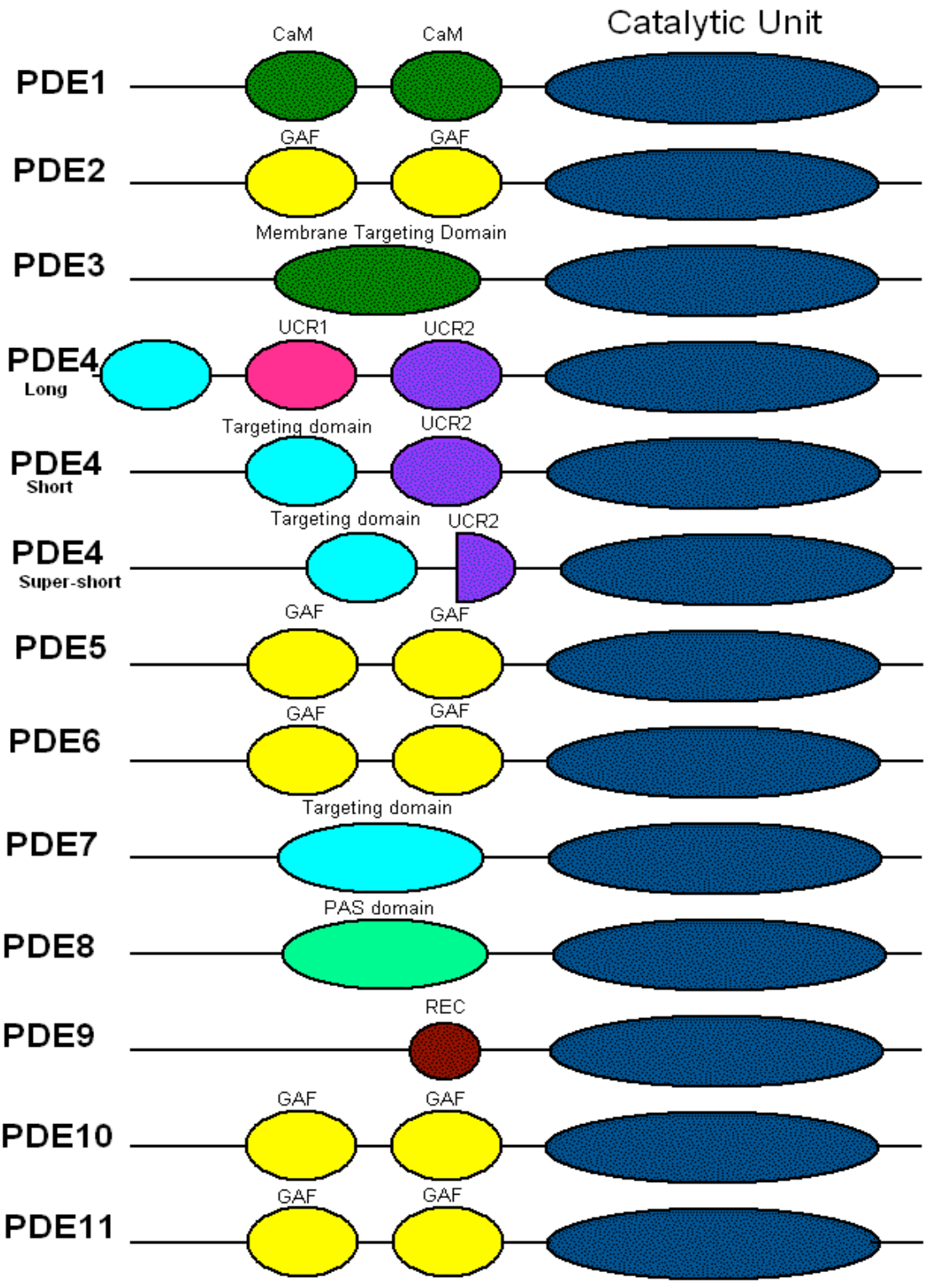

Figure 1.2 - Modular structure of PDE enzyme super-family.

1.6 Phosphodiesterase 4

PDE4 enzymes specifically hydrolyse cAMP. They are encoded by four genes (PDE4A, PDE4B, PDE4C and PDE4D), which are located on three chromosomes in humans [Houslay et al., 1998; Houslay and Adams, 2003; Houslay, 2010]. The genes for both PDE4A and PDE4C, are located at 19p13.2 and 19p13.1, respectively, on chromosome 19 [Milatovich et al., 1994 and Sullivan et al., 1999]. The PDE4B and PDE4D genes are located on chromosomes 1p31 and 5q12 respectively [Milatovich et al., 1994 and Szpirer et al., 1995]. These four PDE4 genes in turn encode upwards of 20 different isoforms each of which is characterised by a unique N-terminal region [Houslay and Adams, 2003]. The N-terminal region of each isoform is encoded by unique 5' exons. As well as this unique N-terminal region, PDE4 isoforms exhibit two Upstream Conserved Regions (UCR1 and UCR2), a conserved catalytic unit and a C-terminal region that is unique to each of the four PDE4 subtypes. The two UCR regions are joined together by regions known as Linker Region 1 (LR1) and Linker Region 2 (LR2). Figure 1.3 details the encoding of these exons.

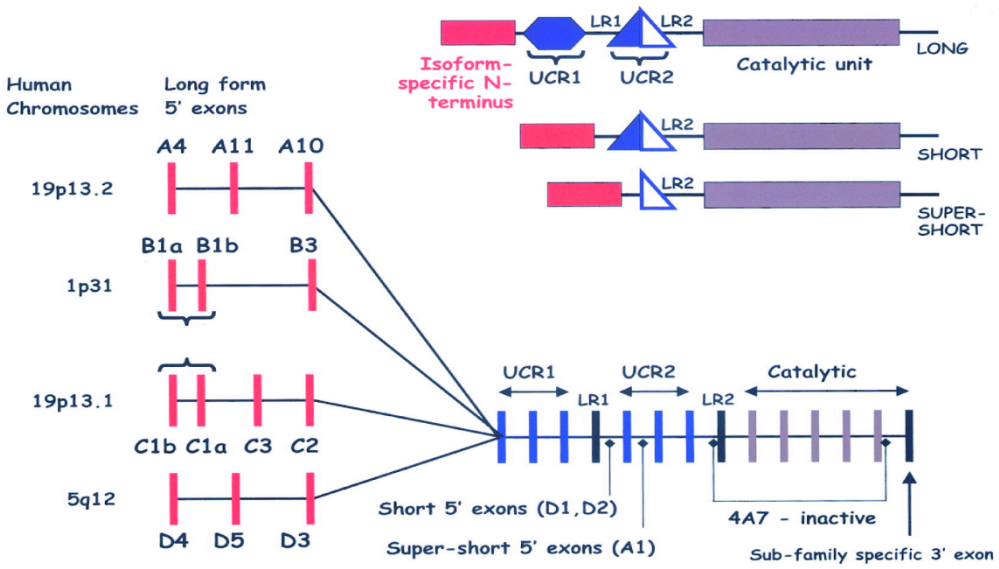

Figure 1.3: Structure and encoding of PDE4 Isoforms (Houslay and Adams, 2003).

1.6.1 N-Terminal

One of the most important roles of the unique N-terminal region in PDE4 is to confer intracellular targeting of the isoforms leading to compartmentalisation within the cell. It invariably confers the ability of the PDE4 isoform to interact specifically with other signalling complexes [Houslay, 2010]. One example of this is the interaction of PDE4A4/5 with the Src tyrosyl kinase Lyn [McPhee et al., 1999], which will be discussed in detail later and another is the binding of PDE4D5 to the signalling scaffolds, RACK1 and β-arrestin [Bolger et al., 2006].

1.6.2 UCR1 and UCR2

As seen in Figure 1.3, PDE4 isoforms can be sub-grouped into long, short, super-short and dead-short forms depending on the presence of the regulatory UCR1 and UCR2 regions and, in the case of dead-short variants, a severe C-terminal truncation [Houslay, 2001; Houslay and Adams, 2003; Houslay et al., 2007]. Long forms have both UCR1 and UCR2 present as well as linker regions LR1 and LR2 that, respectively, connect UCR1 to UCR2 and UCR2 to the catalytic unit whereas short forms possesses an intact UCR2 but lack UCR1 and LR1. Super-short forms also lack UCR1 and LR1 but possess a truncated version of UCR2. The dead short forms lack both regulatory and linker regions and are both N and C-terminally truncated into the catalytic units such that they are uniquely enzymatically inactive and, as such may have a scaffolding function [Johnston et al., 2004].

UCR1 and UCR2 can interact with each other to form a regulatory module that interacts with and regulates the catalytic domain [Beard et al, 2000]. As recent structural data shows, this is achieved by the binding of UCR2 alongside and across the active site of the catalytic unit [Houslay and Adams, 2010; Burgin et al., 2010].

1.6.3 Catalytic Domain

The catalytic unit of all PDE4 isoforms consists of 17 α-helices, which form 3 distinct sub-domains. These sub-domains comprise of eight, four and six helices respectively and a short β-hairpin [Houslay and Adams, 2003 and Xu et al., 2000]. UCR2 is known to exhibit an auto-inhibitory effect on the core catalytic domain although the structural reason for this remained unclear until recently. Thus the recent elucidation of the UCR2-bound catalytic region greater insight into the function of this region has been discovered [Burgin et al., 2010]. In this structure an α-helical sequence within UCR2 was shown to bind across the catalytic pocket, thereby forming a gate controlling substrate and inhibitor access to it [Burgin et al., 2010]. Uncapping of this UCR2 'gate' allows cAMP to bind to the PDE.

Hydrophobic residues and residues with negatively charged side chains form a cAMP-binding pocket between the three sub-domains [Houslay, 2001]. This pocket contains two divalent cation binding sites. The first binding site tightly binds a Zn^{2+}, which is co-ordinated by four amino acids (His-238, His-274, Asp-275 and Asp-392) The second site usually binds Mg^{2+} but may also bind either Zn^{2+} or Mn^{2+} [Houslay and Adams, 2003]. This binding is co-ordinated by five amino acids (His-274, Glu-304, His-307, Thr-345 and Asp-392). The nine amino acids involved in the binding of these metal ions are highly conserved across all 11 members of the PDE family. The metal ions are essential for cAMP hydrolysis [Laliberté et al., 2002]. Interestingly, it is changes in the side-chain orientation of a single amino acid within the active site of different PDE families that confers selectivity between cAMP and cGMP [Wang et al., 2007].

Recent structure studies have helped give greater insight into how inhibitors of PDE4 bind and help to explain their somewhat complicated inhibitor kinetics. Certain inhibitors such as RS25344 interact favourably with the gating sequence of UCR2, stabilizing the UCR2 into the capped state whereas inhibitors like Roflumilast, which has recently gained approval in Europe for treating COPD, interact less favourably with the capped UCR2 and instead preferentially occupies the uncapped catalytic pocket.

Interestingly the more complicated PDE4 inhibitors, in terms of the range of affinities shown for enzyme preparations from different tissues, such as Rolipram are now understood to have affinity for the catalytic pocket in both the UCR2 capped and uncapped states. This may explain why the action of inhibitors like rolipram can be altered by PKA phosphorylation of long forms and by protein-protein interactions involving PDE4 [Burgin et al., 2010; Houslay and Adams, 2010].

1.6.4 C-terminal

The C-Terminal domain of PDE4 isoforms is differs somewhat between each of the four sub-families. The functional significance of this is unknown, although recent structural studies suggest that the C-terminal portion of the catalytic unit can, like, UCR2, cap the active site. This may point to a potential regulatory role for the C-terminal [Burgin, 2010]. Interestingly the C-Terminal domain of PDE4B, C and D, but not PDE4A, shows conservation between mammalian species and the significance of this divergence for PDE4A remains to be elucidated [Hoffmann et al., 1998].

1.7 Phosphodiesterase 4 Isoforms

1.7.1 Phosphodiesterase 4A

PDE4A has several different isoforms some of the most notable being PDE4A4 [Huston et al., 1996], 4A5 [McPhee et al., 1995], 4A8 [Huston et al., 2000; MacKenzie et al., 2008], 4A10 [Rena et al., 2001] and 4A11 [Wallace et al., 2005]. The function of this group of enzymes is only recently being uncovered as they are present at notoriously low levels endogenously, there are no selective inhibitors and genetically modified (KO) animals have not been generated. The PDE4A isoforms are unusual

amongst the PDE4 gene families because their C-terminal regions are not conserved across humans and rats [Houslay and Adams, 2003]. A good example of this is that PDE4A4 is expressed in humans and is the homologue of the rat enzyme PDE4A5 [Terry et al., 2003]. Both of these isoforms are long form phosphodiesterases with similar molecular weights (99kDa and 94kDa respectively [Huston et al., 1996 and McPhee et al., 1995]), however the rat homologue has a significantly lower cytosolic Vmax value than the human homologue [Houslay and Adams, 2003].

PDE4A8 is expressed in rats and humans and is a long isoform of 88kDa [MacKenzie et al., 2008; Bolger et al., 1996]. PDE4A10 and 4A11 are also long isoforms, with a molecular weight of 93kDa but these are expressed in both humans and rats [Wallace et al., 2005].

1.7.1.1 PDE4A Brain Distribution Patterns

PDE4A isoform brain expression has been studied [McPhee et al., 2001] in relation to the two long form isoforms, PDE4A5 and PDE4A10 and the short for PDE4A1. PDE4A5 and PDE4A10 expression was shown to be highest in the olfactory bulb and both displayed a very similar distribution pattern throughout the brain except for in the major island of Calleja where only PDE4A10 is present. This suggests that the two long forms may have similar promoter regions but are likely to have distinct functional roles within the cells. The short PDE4A1 isoform was shown to be distributed highest in the olfactory bulb, the cerebellum and the paraflocculus [McPhee et al., 2001]. More recent work has also shown that the long PDE4A8 isoform is also distributed throughout the brain, in particular in the cortex, spinal cord and cerebellum [MacKenzie et al., 2008].

Several partner proteins have been identified for the different PDE4A isoforms. These are described in detail below.

1.7.1.2 PDE4A aggregation and p62 (sequestosome1, SQSTM1)

Chronic challenge of PDE4A4 with rolipram causes it to form reversible intracellular aggregates. These aggregates are not stress processing bodies or stress granules as they do not contain the regulating proteins necessary to make these complexes. PDE4A4 aggregates have also been shown to not be autophagosomes or aggresomes. However microtubule disruptors do prevent the aggregates from forming. Instead it has been shown that PDE4A4 interacts with p62 protein (sequestosome1, SQSTM1) in these aggregates, and loss of p62 from this complex, via the mTor inhibitor rapamycin, prevents aggregation from occurring. The purpose for this is proposed to be a novel regulatory mechanism where a sub-population of p62-interacting PDE4A4 aggregates form in a rapid, reversible manner which is thought to be used to sequester the PDE4A4 away from its important functional site within the cell [Christian et al., 2010].

1.7.1.3 PDE4A and Src Homology 3 binding domains

The Src Homology 3 (SH3) binding domain is a distinct small protein domain of roughly 60 amino acids which are self-folding. It allows protein-protein interaction by binding to proline rich motifs on acceptor proteins. It is found in a variety of families of proteins such as the Src tyrosyl family kinases [Pawson, 1995]. Certain PDE4A isoforms (PDE4A4B and PDE4A5) contain proline- and arginine-rich sites for interaction with SH3 domains. The Src family tyrosyl kinases interact with PDE4A5 through SH3 domain binding in PDE4A5s N-terminal region [O'Connell et al., 1996]. The SH3 domain of the Src tyrosyl kinase Lyn has also been shown to interact with the human homologue of PDE4A5 which is PDE4A4B. This interaction occurs at a proline and arginine rich motif (RPRPSQP) within the LR2 region of the enzyme [McPhee et al., 1999]. PDE4A4B can exhibit two different sensitivities for the PDE4 specific inhibitor rolipram dependent on where it is located in the cell. When it is located in the

cytoplasm it exists in a low affinity rolipram binding state (LARBS) whereas if it is membrane bound it exists in a high affinity rolipram binding state (HARBS) which is approximately 60 times more sensitive to rolipram [Huston et al., 1996]. Interestingly interaction of the SH3 domain of Lyn with PDE4A4B mimics HARBS throughout the cell [McPhee et al., 1999]. This is now thought that this may be because Lyn can still interact with, and elicit its effect on PDE4A4B even when the inhibitor rolipram is bound to the catalytic site of the enzyme [Burgin et al., 2010; Houslay and Adams, 2010].

1.7.1.4 PDE4A and the immunophilin XAP2

XAP2/Ara9 is an immunophilin that was first identified as a protein that interacts with the X protein of the hepatitis B virus [Kuzhandaivelu et al., 1996]. It is 38kDa long and contains an N-terminal immunophilin homology domain and a C-terminal tetratricopeptide repeat (TPR) domain. It has been shown to interact with heat shock protein 90 (Hsp90), the aryl hydrocarbon receptor and certain phosphodiesterases, specifically PDE4A5 [Bolger et al., 2003].

PDE4A5 has a highly conserved TPR domain in its UCR2 region which allows for binding to XAP2 along with another binding region in its unique N-terminal domain [Bolger et al., 2003]. This is the only PDE isoform that XAP2 can interact with in this way except for its human orthologue, PDE4A4, which has the same binding residues conserved within its sequence. Although XAP2 doesn't bind directly to the catalytic site of PDE4A5 it inhibits its enzymatic activity. It therefore must be working as a non-competitive inhibitor. XAP2 association also results in a marked increase in sensitivity to inhibition which indicates that its presence, although not directly on the catalytic domain, is causing altered conformation of the catalytic unit [Bolger et al., 2003].

Interestingly although XAP2 has only been found to associate with these two closely related isoforms of PDE4 it has very recently been found to associate with

PDE2A [de Oliveira et al., 2007]. In this enzyme it binds to a site located within the GAF-B regulatory domain although this site appears to show no similarity to the site of binding in UCR2, which suggests a different mode of binding. The association of XAP2 with PDE2A also differed from its association with PDE4A5 in that it does not altered the enzymatic activity of PDE2A but does appear to guide it towards the aryl hydrocarbon receptor complex [de Oliveira et al., 2007].

1.7.2 Phosphodiesterase 4B

There are four known phosphodiesterase 4B isoforms, PDE4B1, 4B2, 4B3 and 4B4. Unlike the PDE4A enzymes their endogenous expression in cells is higher so they can be detected more easily. Phosphodiesterase 4B1 and 4B3 are both long isoforms with a molecular weight of 83kDa [Huston et al., 1997] whereas PDE4B2 is a short isoform with a molecular weight of only 64 kDa [Bolger et al., 1994]. PDE4B4 is the most recently cloned and characterised member of this family, it is found in the rat and has a molecular weight of 73kDa [Shepherd et al., 2003].

1.7.2.1 PDE4B knockout mice

The development of PDE4B knockout mice has given a huge insight into the functional purpose of this PDE4 sub-family. It has in particular highlighted the importance role of PDE4B isoforms in the immune response. In mouse peritoneal macrophages from PDE4B knockout mice it has been shown that loss of this PDE4 isoform impacted LPS TLR signalling and TNFα production [Jin et al., 2005]. In neutrophil studies it has also been shown that knockout of PDE4B leads to an inhibition of neutrophil migration [Ariga et al., 2004]. In addition to the role in the immune system, knockout mice studies have also highlighted behavioural and neurochemical phenotypes that appear to be PDE4B dependent. In PDE4B knockout mice it was observed that spontaneous locomotive activity was decreased when compared to wild

type [Siuciak et al., 2008], and that these knockout mice also exhibited depression and anxiety like behaviour [Zhang et al., 2008].

1.7.2.2 PDE4B and DISC1

Perhaps one of the most important discoveries made in relation to PDE4B is its potential role in schizophrenia. The disrupted in schizophrenia 1 (*DISC1*) gene locus was first identified as a disrupted gene in a large Scottish family presenting with schizophrenia and bipolar disorder [Blackwood et al., 2001]. It has subsequently been shown that DISC1, the scaffold protein encoded by the *DISC1* gene, can interact with the UCR2 domain of the PDE4B isoform PDE4B2 [Millar et al., 2005]. It was then proposed that this interaction lead to DISC1 sequestering PDE4B2 in resting cells and releases it in an activated state to deal with elevated cAMP levels [Millar et al., 2005]. It is proposed that disruption of this DISC1-PDE4B complex may be involved in the molecular mechanism of schizophrenia and therefore could provide a therapeutic target for treatment of schizophrenia [Millar et al., 2007]. In addition to this work it has subsequently been shown that other PDE4 isoforms can bind to DISC1 [Murdoch et al., 2007].

1.7.3 Phosphodiesterase 4C

Like the PDE4A gene family PDE4C isoforms exist at very low endogenous expression levels in the cell. Due to this there has not been much work done on members of this gene family. However, three long isoforms of this enzyme, PDE4C1, 4C2 and 4C3 have been identified [Bolger et al., 1993; Swinnen et al., 1989].

Distribution in the human brain of PDE4C is restricted to the cortex, thalamic nuclei and cerebellum whereas in monkeys distribution is seen in the olfactory bulb [Perez-Torres et al., 2000].

1.7.4 Phosphodiesterase 4D

The PDE4D gene family is probably the best studied out of all of the PDE4 enzymes. There are thought to be 11 isoforms PDE4D1 to 4D11. The most notable of these are PDE4D3, 4D4 and 4D5 which are all long isoforms with molecular weights between 77kDa and 91kDa [Bolger et al., 1997]. PDE4D3 and PDE4D5 are both expressed at relatively high levels endogenously. The short form PDE4Ds, PDE4D1 and PDE4D2 have a more limited expression pattern [Vicini and Conti, 1997]. Little, however, is known about the more recently discovered PDE4D6-11 species, although the *PDE4D7* gene locus has been linked to stroke [Houslay, 2005].

1.7.4.1 PDE4D knockout mice

In a similar way to PDE4B, a great deal of the functional role of PDE4D has been elucidated through the generation of PDE4D knockout mice. Neurological studies have shown that PDE4D knockout mice presented an anti-depressant like phenotype (measured through mobility in response to stress tests) and this is thought to imply that PDE4D is the essential mediator of the antidepressant-like effects of rolipram [Zhang et al., 2002]. In further neurological studies it has also been shown that there may be a role for PDE4D in long term memory formation [Rutten et al., 2008]. However PDE4D knockout models have shown far wider ranging effects than just within the neurological system, for example within the airway smooth muscle it has been shown that PDE4D plays a key role in balancing relaxation of contraction of smooth muscle, playing a role in controlling airway tone [Mehats et al., 2003]. In addition to this PDE4D knockout has been shown to have a small but still significant effect on neutrophil migration within the immune system while also reducing chemotaxis in response to the cytokines KC and MIP2 [Ariga et al., 2004].

1.7.4.2 PDE4D and β-arrestin

G-protein coupled receptors (GPCRs) couple to Gs, upon activation, and activate adenylyl cyclase to produce cAMP. Desensitisation of these GPCRs involves phosphorylation by G-protein coupled receptor kinases (GRKs) and subsequent recruitment of cytosolic signalling scaffold proteins, β-arrestins [Lefkowitz and Shenoy, 2005]. The presence of β-arrestin then blocks further GPCR coupling to Gs. β-arrestin has been shown to interact with all isoforms of PDE4 regardless of whether they are long, short or super-short through a region in their catalytic domain [Perry et al., 2002]. Binding occurs through the N-terminal and C-terminal regions of β-arrestin [Baillie et al., 2007]. Interaction of β-arrestin with PDE4 seems to recruit the enzymes to the site of agonist occupied, GRK phosphorylated GPCRs where they regulate PKA phosphorylation of the receptor by lowering the local level of cAMP.

However the PDE4 isoform PDE4D5 shows greater affinity for β-arrestin than all other PDE4 isoforms [Bolger et al., 2006; Bolger et al., 2003; Lynch et al., 2005; Li et al., 2006]. This is due to two separate factors: the presence of an extra β-arrestin binding domain located at amino acids 70-88 within its unique N-terminal region [Perry et al., 2002; Baillie et al., 2007] and ubiquitination of PDE4D5 by Mdm2 guiding it to bind more β-arrestin [Li et al., 2009]. These interactions do not affect the enzymatic activity of PDE4D5.

Recently it has also been discovered that the binding site on the N-terminal overlaps with the binding site of RACK1 for PDE4D5 [Bolger et al., 2006].

1.7.4.3 PDE4D and RACK1

Receptor for activated C-Kinase 1 (RACK1) is a 36 kDa protein which has a high affinity for partner protein binding. It has a seven bladed propeller like structure

composed of β-sheets which allow it to scaffold Protein Kinase C (PKC) [McCahill et al., 2002]. RACK1 can interact with proteins in two different ways: constitutively or stimulus dependent. The individual blades of its propeller structure have multiple sites for protein interactions which would indicate that it has the ability to associate with many different proteins classes.

RACK1 specifically interacts with the PDE4 isoform PDE4D5 through two sites. This first site is a RACK1 interaction domain (RAID1) in the unique N-terminal of 4D5 [Yarwood et al., 1999, Bolger et al., 2006]. The functional reason for this association is yet unknown but it is thought that it may be to alter the sensitivity of RACK1 surrounding proteins to PKA phosphorylation [McCahill et al., 2002]. The second interaction site is found in the third sub-domain of the catalytic region of PDE4D. While this site is essential for PDE4D5 binding it is not a strong enough binding site itself to elicit binding of RACK1 without the N-terminal. This is why, despite the presence of this catalytic site across the other PDE4 isoforms no RACK1 binding is observed [Bolger et al., 2006]. It has also been proposed that RACK1 and β-arrestin partner PDE4D5 in a mutually exclusive fashion therefore if one of these scaffolding proteins is knocked out of the cell it allows for the other to bind [Bolger et al., 2006]. The functional reason for the interaction of PDE4D5 and RACK1 has been proposed in the past few months where it has been shown that RACK1 may serve as the molecular bridge linking FAK to the recruitment of PDE4D5. The FAK/RACK1/PDE4D5 complex then acts as a novel 'direction-sensing' complex that acts to recruit specific components of the cAMP second-messenger system to the leading edge of polarizing cells [Serrels et al., 2010].

1.7.4.4 PDE4D and its genetic link to disease states

Two major gene studies have been carried out in relation to the PDE4D gene and disease states. The first of these studies looked at the role of the PDE4D gene in bone mineral density [Reneland et al., 2005]. In this study it was show that variants in the gene that encodes PDE4D accounts for some of the genetic contribution to bone mineral density variations observed in humans. This work corresponds well with the fact that PDE4 inhibitors have been shown to increase bone mass in mouse studies [Reneland et al., 2005]. The second of these studies was carried out across a wide-ranging population and uncovered the role of the PDE4D gene in asthma-susceptibility through a series of different mutations and SNPs [Himes et al., 2009].

1.8 PDE4 Phosphorylation

One of the main modes of control of PDE4 activity is through its phosphorylation. The main kinases that can phosphorylate PDE4 are PKA and ERK and both of these kinases have different resultant effects.

1.8.1 Protein Kinase A

Long isoforms of PDE4 can all be phosphorylated by PKA, which leads to activation [Sette and Conti, 1996; Hoffmann et al., 1998; MacKenzie et al., 2002]. This phosphorylation occurs at a single conserved serine residue in UCR1 which is contained in the PKA consensus RRES*F [MacKenzie et al., 2002]. This phosphorylation increases PDE4 activity in cells by around 60% but it appears that PDE4A4 and 4D3 show the greatest increase in activation [Laliberte et al., 2002; Sette and Conti, 1996; MacKenzie et al., 2002], although the reason for this is unknown.

In PDE4D3 two sites for PKA phosphorylation, the conserved one at Ser54 in UCR1 together with another one at Ser13, that is located within its unique N-terminal region [Hoffmann et al., 1998; Sette and Conti, 1996]. The N-terminal site has no effect on activity, but is involved in targeting, increasing the association of PDE4D3 with mAKAP [Carlisle Michel et al., 2004] and reducing its interaction with the scaffold protein, Ndel1 [Collins et al., 2008].

Interestingly PKA-phosphorylated forms of both PDE4A4 and 4D3 show enhanced sensitivity to stimulation by Mg^{2+}, a cation found in the catalytic site which is necessary for PDE activity [Oki et al., 2000; Perry et al., 2002]. It has recently been shown [Burgin et al., 2010] that in the absence of UCR1 phosphorylation of PDE4 by PKA the UCR2 domain adopts a 'closed' conformation over catalytic pocket. However when PKA phosphorylation occurs the interactions between UCR1 and UCR2 are altered causing the UCR2 helix to move into an 'open' active conformation, activating the enzyme and increasing its Vmax without affecting Km.

1.8.2 Extra-cellular Signal Regulated Kinase (ERK)

The Mitogen-Activated Protein (MAP) Kinase signalling cascade is a pivotal signalling pathway where growth factors, cytokines and hormones [Pearson et al., 2001] exert crucial effects on cell survival and growth. ERK1 and ERK 2 are members of the MAPK family. All PDE4 enzymes, except for PDE4A species, contain a consensus motif for ERK binding (Pro-Xaa-Ser-Pro) in their catalytic unit within which a serine can be phosphorylated [MacKenzie et al., 2000]. However for ERK binding to occur there must be the presence of ERK docking sites at either side of the consensus motif. These consist of a kinase interaction motif (KIM) which is found approximately 135 amino acids N-terminal of the consensus site and a Phe-Xaa-Phe (FQF) motif found approximately 16 amino acids C-terminal of the consensus site. The presence of these two docking sites allows for specificity of ERK1/2 phosphorylation over other kinase phosphorylations that can occur here, such as c-Jun N-terminal kinase (JNK)

phosphorylation [Sharrocks et al., 2000]. These recognition/binding sites have been identified in PDE4 and shown to be functional as regards being essential for PDE4 to be phosphorylated by ERK in cells [MacKenzie et al., 2000].

ERK phosphorylation exerts different effects on PDE4 enzymes which are dependent on whether the enzyme is long or short form. In short form PDE4s it leads to activation of the PDE4 enzymes with an increase in intracellular activity of 40% [MacKenzie et al., 2000 and Baillie et al., 2000]. In contrast to this, in long form PDE4s then phosphorylation by ERK causes inhibition of enzymatic activity by around 40%. However, this is a transitory effect that can be overcome if ERK inhibition of PDE4 long forms cause cAMP levels to rise enough to activate PKA, which can then phosphorylate the long form and overcome the ERK inhibitory effect, leading to a net activation [Houslay and Kolch, 2000 and Baillie at al., 2000]. This inhibition is now understood to be caused by the ERK phosphorylated serine on the C-terminus of the enzyme interacting directly with the UCR2 region stabilising it in a 'closed' conformation over the catalytic pocket [Burgin et al., 2010].

1.9 New partner proteins for PDE4A

The work detailed in this thesis will introduce two new partner proteins for the long form PDE4A isoform PDE4A5 and will highlight the presence of a potential multi-functional docking domain on this, and other long form PDE4 isoforms.

1.9.1 MAPKAPK2

The p38 MAPK pathway is a key signal transduction pathway involved in the control of cellular immune, inflammatory and stress responses [Hommes et al., 2003].

One of its downstream effectors is the kinase mitogen-activated protein kinase-activated protein kinase 2 (MAPKAPK2). In chapter 3 is it described how MAPKAPK2 interacts with PDE4A5.

1.9.2 p75NTR

Another important protein shown to interact with PDE4A5 in chapter 4 of this thesis is the low affinity neurotrophin receptor p75NTR. This 75 kDa neurotrophin receptor is pivotal in neuronal signalling and inflammatory responses. It gets its name from its ability to bind several different neurotrophins at a low affinity [Barker, 2009]. This protein will be discussed in more detail in Chapter 4.

Chapter 2 Materials and Methods

2.1 Materials

All materials, chemicals and equipment were supplied by Sigma-Aldrich® unless otherwise stated.

2.2 Plasmid Preparation

All plasmid work was carried out in a sterile environment and all buffers used were molecular biology grade. Buffers were sterilised by sterile filtration or autoclaving.

2.2.1 Transformation of Competent Cells

Competent cells are bacterial cells that can incorporate foreign DNA plasmids. Not all cells have this ability but can often be manipulated to be electrically or chemically competent. Most competent cells have an optimal transformation protocol, often provided by the manufacturers, but these protocols all follow same general principle. Competent cells were stored at -80^{o}C and thawed on ice. 1-10ng of DNA was added to 50μL of competent cells and incubated on ice for 15 mins, although longer incubation periods generally have no effect on transfection efficiency. The cells were then heat shocked at 42^{o}C for 45-90s before being returned to ice for 2 mins. 450μL of pre-warmed L-Broth media (1% (w/v) bacto-tryptone, 0.5% (w/v) bacto-yeast extract and 170mM NaCl) was then added to the cells and incubated shaking at 37^{o}C for one hour. Agar plates were produced using L-Broth media and 1.5% (w/v) agar. This solution was autoclaved and cooled to less then 50^{o}C then the appropriate antibiotic for the plasmid was added (commonly used antibiotics and their concentrations are shown in Table 2.1) before being poured out and set in 90mm plates. 50-250μL of transformation mix was then spread on the agar plates and incubated at 37^{o}C for 14-18

hours. Colony growth indicated successful cell transformation. Plates were stored at 4°C for up to one month before being discarded.

Antibiotic	Stock Concentration	Storage	Working Concentration
Ampicillin	100mg/ml in H_2O	-20°C	100 μg/ml
Kanamycin	10mg/ml in H_20	-20°C	50 μg/ml
Zeocin (Invitrogen)	100mg/ml in HEPES	-20°C	25 μg/ml

Table 2.1 – Concentrations of commonly used antibiotics.

2.2.2 Isolation of Plasmid DNAs

From agar plates single colonies were picked and grown overnight in 5mL L Broth media containing the appropriate antibiotic in an orbital shaker at 37°C. 1ml of the bacterial culture was saved for production of a glycerol stock (see section 2.2.3). The remaining bacterial stock was used for plasmid isolation using the QIAGEN® QIAprep® Miniprep Kit. Alternatively, the 5 ml overnight bacterial culture was used to inoculate a larger L Broth media culture of 500 ml, supplemented with the appropriate antibiotic, for overnight growth and isolation of significantly greater plasmid DNA concentrations and volumes using the QIAGEN® QIAprep® Maxiprep Kit. For in-depth details of the plasmid DNA isolation protocols please refer to the manufacturers instructions. Purified plasmid DNA was stored at 4°C, if eluted in 10mM Tris-Cl; pH 8.5, and –20°C, if eluted in sterile water.

2.2.3 Storage of Plasmid DNAs

To produce a glycerol stock 1ml of overnight culture (see section 2.2.2 above) was removed and mixed with 500μl sterile filtered glycerol in a sterile cryo-vial. This was then snap-frozen on dry ice and stored at -80°C until required. Generally the E.Coli bacterial strain JM109 was used for storage as long-term glycerol stocks.

Glycerol stocks were used to inoculate culture media (L Broth) by scrapping the frozen stock with a sterile pipette tip, which is then transferred into 5ml of sterile L Broth media containing the appropriate antibiotic for the plasmid in which they were cultured or the bacterial host strain. This culture was then incubated in an orbital shaker overnight at 37^{o}C. The plasmid isolation can then be carried out as described in Section 2.2.2 and 2.3.

2.2.4 Analysis of Plasmid DNA

2.2.4.1 Agarose Gel Electrophoresis

Agarose gel electrophoresis is a method used to analyse DNA molecules by size. This is achieved by moving negatively charged nucleotides through an agarose matrix with an electric field. Shorter molecules migrate faster than larger molecules and DNA is resolved into fragments between 0.5-10 kilobases with 20-500ng of DNA per band. 1% agarose was dissolved in 40mM Tris-Cl; pH 8.5, 0.114% (v/v) glacial acetic acid and 2mM EDTA (TAE) by heating in a microwave oven until the agarose dissolved. The 1% agarose solution was cooled to 55^{o}C and 0.5µg/ml ethidium bromide was added. The solution was then poured into the Bio-Rad® Sub-Cell GT gel apparatus, with the well comb in place, and allowed to set. For more details about the Bio-Rad® Sub-Cell GT gel apparatus please consult the manufacturers instructions. Once set for 30-40 min the comb was removed and the gel was placed in a gel tank with 1x TAE buffer (40mM Tris, 20mM Acetic Acid, 1mM EDTA) to a level of 1mm above the gel. 1kb DNA ladder was also loaded to an appropriate well of the gel to allow the size of the DNA plasmid or fragment within the sample to be determined. For DNA samples 6x loading buffer (0.25% (w/v) bromophenol blue, 0.25% (w/v) xylene cyanol FF and 40% (w/v) sucrose) was diluted 1:6 into the DNA solution and mixed gently. The gels were then run at 100V for approximately one hour and were then removed from the tank and analysed under ultra violet light where ethidium bromide stained DNA can be visualised. Images of the gels were then captured using an ultra violet light box.

2.2.4.2 Quantification of DNA Concentration

The concentration of purified DNA was determined using the Nanodrop 2000 spectrophotometer from Thermo Scientific which measures DNA concentration at absorbance of 260 nm.

2.2.4.3 DNA Sequencing

DNA samples for sequencing were sent to the University of Dundee Sequencing Service (www.dnaseq.co.uk) where sequencing of 500bp lengths of DNA was carried out using standard or custom primers. Analysis of DNA sequencing was carried out using Gene Jockey Version 2.2 or Geneious computer software programs.

2.2.5 Site-Directed Mutagenesis of Plasmid DNA

Site-directed mutagenesis of plasmid DNA was carried out using the QuikChange® Site-Directed Mutagenesis Kit. In short, Polymerase Chain Reaction (PCRs) samples were set up in 10x reaction buffer containing various concentrations of purified, template DNA (5-50ng). Primer pairs used for site directed mutagenesis were designed using Gene Jockey or Genious computer software and manufactured by Thermo Bioscience. 125ng of each primer and 1µl of deoxynucleotide tri-phosphate (dNTP) mix were added to the PCR reaction and it was made up to a total volume of 50µl with RNAase, DNAase free water. 1µl of Pfu Turbo polymerase was added to each reaction. PCR was then carried out using the MJ Research Peltier Thermal Cycler 200 with conditions set as 95^{o}C for 30s, and 18 cycles of 95^{o}C for 30s, 55^{o}C for 1min, and 68^{o}C for 1min per kb of the plasmid length. Once this reaction is complete 1-4µl of the Dpn I restriction enzyme was added to each reaction and incubated at 37^{o}C for 1h. 1µl of the Dpn I-treated DNA was used to transform 50µl of XL-Blue super-competent cells as described above and plasmid DNA was then isolated from single colonies on agar plates, cultured, purified and sequenced as described above to assess whether site

directed mutagenesis was successful. I wish here to thank Mrs Irene Gall, who carried out all the site-directed mutagenesis for this project.

2.3 Expression and Purification of Recombinant Fusion Proteins

2.3.1 Maltose Binding Protein (MBP) Fusion Proteins

Competent E.coli BL21 cells were transformed, as described in Section 2.2.1, with the appropriate pMAL plasmid, as described in Table 2.2, and grown in 30ml or sterile L-Broth media, supplemented with 100μg/ml ampicillan, overnight in an orbital shaker at 37^{o}C. 450ml of L-Broth media, containing 100μg/ml ampicillan was then inoculated with the 30ml overnight culture and grown in the orbital shaker at 37^{o}C for a further 1-2 hours. A 1ml sample of the culture was taken at regular intervals, placed in a plastic cuvette and its optical density was measured at 600nm (OD600) against an uncultured L-Broth media control. Once this density reached a value of between 0.6 and 1 expression of the fusion protein was induced with 0.2mM isopropyl-β-D-thiogalactopyranoside (IPTG). An OD600 at this level ensured that the culture was in the logarithmic phase, where bacteria will grow exponentially. The culture was then grown for a further 4 hours in an orbital shaker set at 30^{o}C. Hourly 1ml samples were removed to monitor protein expression. These samples (including the samples used for OD600 measurement) were centrifuged at 13000rpm, the supernatant was discarded and the pellet was re-suspended in 100μl SDS sample buffer for analysis by SDS-PAGE and Coomassie staining as described in Section 2.7. The cells from the 450ml culture were then harvested by centrifugation at 4000rpm for 10 min. The cells were re-suspended in 12ml of 50mM Tris-HCl; pH 8.0, 10mM NaCl and 10mM β-mercaptoethanol containing a 1x solution of Roche Diagnostics protease inhibitor cocktail tablets. The re-suspended cells were then frozen at -80^{o}C overnight. Cells were thawed on ice and lysozyme was added at a final concentration of 1mg/ml and the cell suspension subjected to sonication to ensure sufficient cell lysis occurred. A final concentration of 0.05% NP-40 was added to aid cell lysis and the cells were centrifuged at 13000rpm for 15 min to remove cell

debris. 1ml of amylose resin (New England BioLabs) was pre-equilibrated with re-suspension buffer containing 0.05% NP-40. The cell supernatant was applied to the pre-equilibrated resin and incubated end-over-end at 4^{o}C for 1h to bind the expressed fusion protein. The resin was the collected by centrifugation at 2000rpm for 2min and washed three times with 1ml of re-suspension containing 0.05% NP-40. The fusion protein was eluted from the amylose resin with 500µl of 10mM maltose, 50mM Tris-HCL; pH8.0 by incubation end over end for 20 min at 4^{o}C. This was repeated up to three times, if necessary. The eluted fractions were pooled and dialysed using Pierce® Slide-A-Lyser® dialysis cassettes against three 750ml volumes of 100mM NaCl, 50mM Tris-HCL; pH 8.0 and 5% glycerol for 1h each at 4^{o}C. The purified fusion protein was frozen on dry ice, and stored as aliquots of 25µl at -80^{o}C. The expression time-course and final purification products were analysed by SDS-PAGE and Coomassie® staining, described in Section 2.7.

2.3.2 Glutathione-S-Transferase (GST) Fusion Proteins

The E.coli expression and purification of recombinant GST fusion proteins is extremely similar to the purification of MBP protein described above in Section 2.3.1. Competent E.coli BL21 cells were transformed, as described in Section 2.2.1, with the appropriate pGEX plasmid, as described in Table 2.2. Cultures were grown, induced, harvested and lysed as described above however for the purification of GST fusion proteins glutathione sepharose resin (Amersham Biosciences) was used and elution required an elution buffer composed of 10mmM glutathione, 50mM Tris-HCl; pH 8.0. The expression time-course and final purification products were analysed by SDS-PAGE and Coomassie® staining, described in Section 2.7.

2.3.3 Histidine (His) Fusion Proteins

The E.coli expression and purification of recombinant His fusion proteins is extremely similar to the purification of MBP and GST protein described above in Section 2.3.1 and Section 2.3.2. Competent E.coli BL21 cells were transformed, as

described in Section 2.2.1, with the appropriate (pEX-His) plasmid, as described in Table 2.2. Cultures were grown, induced, harvested and lysed as described above however for the purification of His fusion proteins nickel resin (Qiagen) was used and elution required an elution buffer composed of (6M Urea, 20mM Tris pH 7.5, 100mM NaCl); pH 8.0. The expression time-course and final purification products were analysed by SDS-PAGE and Coomassie® staining, described in Section 2.7.

2.4 Mammalian Cell Culture

All cell culture techniques were carried out in a class two hood using aseptic techniques and reagents had been filter sterilised or autoclaved to ensure sterilisation.

2.4.1 Maintenance of Cell Lines

Cells of a low passage number were stored at -200^{o}C, in cryovials containing freezing cell media (70% serum, 10% DMSO), to ensure their long-term integrity. To revive cells from the temperature individual vials were quickly thawed and added directly to 10ml of growth media pre-warmed to 37^{o}C, under sterile conditions. Once the cell line is established and confluent, further aliquots of cells were re-suspended in freezing cell media and initially frozen at -80^{o}C before being transferred to -200^{o}C for long-term storage.

2.4.1.1 COS1 Cells

COS1 cell lines are derived from African green monkey kidney cells and have been transformed with the SV40 virus. The cells were propagated in growth media containing Dulbecco's modified Eagle's medium (DMEM) supplemented with 0.1% penicillin/streptomycin (10000U/ml), 2mM glutamine and 10% foetal bovine serum (FBS). The cell line was maintained at 37^{o}C in an atmosphere of 95% air and 5% CO_2. The cells were passaged when approximately 70-90% confluence was reached. To passage the cells the growth media was removed and 5ml of sterile pre-warmed

phosphate buffer saline (PBS) was added to gently wash the cells. The PBS was removed and 5ml of trypsin-EDTA solution was added and cells were incubated for 5 min at 37^{o}C. The cells were vigorously agitated and then analysed under the microscope to ensure complete cell detachment. 5ml of growth media was then added to inactivate the trypsin-EDTA solution. The cells were collected by centrifugation at 10,000rpm for 3 min at room temperature. The growth media and trypsin-EDTA solution was removed and the cell pellet was re-suspended in 5ml of fresh growth media. Once fully re-suspended 1ml of cells were added to fresh growth media in sterile flasks, 100mm or six well plates. The cells were incubated at 37^{o}C in an atmosphere of 95% air and 5% CO_2 until required or confluent.

2.4.1.2 HEK293 Cells

The human embryonic kidney 293, (HEK293) cell line has epithelial morphology. These cells were maintained as described in Section 2.4.1.1 for COS1 cells.

2.4.1.3 NIH3T3 Cells

NIH3T3 cells are fibroblasts from Swiss mouse embryo tissue with the '3T3' designation referring to the abbreviation of "3-day transfer, inoculum 3 x 10^5 cells". These cells were grown in Dulbecco's modified Eagle's medium (DMEM) supplemented with 0.1% penicillin/streptomycin (10000U/ml), 2mM glutamine and 10% newborn calf serum (NCS) and maintained as described in Section 2.4.1.1. A stable NIH3T3 cell line expressing p75NTR-GFP was provided by the laboratory of Dr Katerina Akassoglou (Gladstone Research Institute, San Francisco, USA). These cells were maintained in the same manner as above with the growth media supplemented with 100μg/ml Hygromycin B. These cells were maintained as described in Section 2.4.1.1 for COS1 cells.

2.4.1.4 Mouse Embryonic Fibroblasts (MEFs)

Mouse Embryonic Fibroblasts (MEFs) are fibroblast cells isolated from the bodies of c57 black mouse embryos. The cells were propagated in growth media containing Dulbecco's modified Eagle's medium (DMEM) supplemented with 0.1% penicillin/streptomycin (10000U/ml), 2mM glutamine and 10% foetal bovine serum (FBS). The cell line was maintained at 37^{o}C in an atmosphere of 95% air and 5% CO_2. These cells were maintained as described in Section 2.4.1.1 for COS1 cells. PDE4A (-/-) and PDE4B (-/-) MEFs were a generous gift from Dr Marco Conti (UC San Francisco, USA).

2.5 Mammalian Cell Transfection of Plasmid DNA

A list of DNA plasmids used for the transfection of the mammalian cell lines are described in Table 2.2.

2.5.1 PolyFect® Transient Transfection

The PolyFect® the method of mammalian cell transfection, from QIAGEN®, was used for transfection of COS1, HEK293 and NIH3T3 cell lines. Flasks of confluent cells were passaged the day prior to transfection and plated to ensure 40-80% confluency on the day of transfection. These plates were incubated overnight at 37^{o}C in an atmosphere of 95% air and 5% CO2. The amount of DNA required for each plate was dependent on the cell line and number of cells to be transfected and should be scaled accordingly. The protocol described is accurate for 100mm plates of 40-80% confluent cells in 6ml growth media. See manufacturers instructions for the amount of DNA required for different plate sizes. 4μg of the desired DNA plasmid for the transfection of COS1 or NIH3T3 cells was diluted in antibiotic and serum free DMEM to a final volume of 300μl. 8μg of the desired DNA plasmid for the transfection of HEK293 cells was diluted in antibiotic and serum free DMEM to a final volume of 300μl. 25μl of PolyFect® Transfection Reagent was added to the DNA solution for

COS1 and NIH3T3 cell transfections whereas 80µl was required for efficient transfection of HEK293 cells. The transfection reagents were incubated at room temperature for 5-10min to allow complex formation. Where co-transfection of two DNA plasmids was required the amount indicated above of each plasmid was diluted in 300µl of antibiotic and serum free DMEM before the addition of the specific volume of PolyFect® Transfection Reagent indicated above for the cell type. During the incubation period the growth media was removed and replaced with 6ml of fresh DMEM supplemented with 0.1% penicillin/streptomycin (10000U/ml), 2mM glutamine and the relevant serum for the cell line. Following incubation, 1ml of supplemented DMEM containing the antibiotics and serum was added to the DNA-DMEM- PolyFect® complex. This was mixed gently and added directly to the appropriate transfection plate. The plates were then incubated for 24-72 hrs at 37^{o}C in an atmosphere of 95% air and 5% CO2 prior to any cell treatments and harvesting. Details of ligands and inhibitors used for cell treatments post-transfection are described in Table 2.3.

2.5.2 Nucleofector Transfection

Transfection of MEF cells cannot be successfully carried out using Polyfect transient transfection therefore Amaxa Nucleofector nucleoporation transfection was instead carried out using their MEF transfection kit according to manufacturers instructions.

Vector	Construct
pcDNA	PDE4A5 – Wild Type
pcDNA	PDE4A5 – Ser147Ala
pcDNA	PDE4A5 – Ser147Asp
pcDNA	PDE4A5 – Ser161Ala
pcDNA	p75NTR – Wild Type
pcDNA	PDE4D3 – Wild Type
pcDNA	PDE4D3 – Ser61Ala
pcDNA	PDE4D3 – Ser61Asp
pcDNA	PDE4A4 – Wild Type
pcDNA	PDE4A1 – Wild Type
pcDNA	PDE4A10 – Wild Type
pcDNA	PDE4A11 – Wild Type
pMAL	PDE4A5 MBP
pMAL	PDE4A4 MBP
pMAL	PDE4A1 MBP
pMAL	PDE4A10 MBP
pMAL	PDE4A11 MBP
pGEX	p75NTR GST
pGEX	MAPKAPK2 GST
pGEX	Lyn GST
pGEX	UBC9 GST
pGEX	GST alone
pGEX	β-Arrestin GST
pGEX	ERK GST
pEX-His	p75NTR

Table 2.2 List of Plasmids

Agonists/ Inhibitors	Role	Concentration	Reference
Anisomycin	p38 MAPK activator	10 µg/ml	Cuenda et al., 1995
TNFα	TNFα signalling cascade activator p38 MAPK activator	10 µM	Winston et al., 1997
SB203580	p38 MAPK cascade inhibitor	25 µM	Cuenda et al., 1995
Forskolin	Adenylate cyclase activator	100 µM	Seamon et al., 1981
IBMX	Broad spectrum PDE inhibitor	100 µM	Essayan, 2001
Rolipram	PDE4 inhibitor	10 µM	Watchel, 1982

Table 2.3 – Agonists and Inhibitors.

2.6 Preparation of Cell Lysates

2.6.1 Whole Cell Lysate

Confluent cells were harvested at 4^{o}C using buffers that had been previously chilled to minimise protein degradation. The culture media was aspirated and the cells were washed three times with ice cold sterile PBS. The cell plates were drained thoroughly and an appropriate volume of cell lysis buffer was added. For a 100mm plate 500µl of lysis buffer was used whereas for a 6 well plate 300µl was added to each well. For the production of whole cell lysate 3T3 lysis buffer was used. This composed of 25mM HEPES-OH: pH 7.5, 50mM NaCl, 10% glycerol, 1% Triton, 50mM NaF, 30mM Na pyrophosphate, 5mM EDTA and 1x solution of Roche Diagnostics (Mannheim,

Germany) protease inhibitor cocktail tablets. The cells were incubated for 5 min on ice then scraped using a disposal scraper. The lysate was then collected into a 1.5ml Eppendorf tube. The cell lysates were centrifuged in a refrigerated, bench-top at 13.000rpm at 4^{o}C and the supernatant was retained. The cell lysates were then snap frozen in dry ice and stored at -80^{o}C until required.

2.6.2 Sub-cellular Fractionation

Confluent cells were harvested at 4^{o}C using buffers that had been previously chilled to minimise protein degradation. The culture media was aspirated and the cells were washed three times in ice cold PBS. The cell plates were drained thoroughly and an appropriate volume of cell lysis buffer was added. For a 100mm plate 500µl of lysis buffer was used whereas for a 6 well plate 300µl was added to each well. For the production of sub-cellular fractions, 500µl sterile 50mM KCl, 50mM HEPES; pH 7.2, 10mM EGTA, 1.92mM $MgCl_2$, 1mM dithiolthreitol (DTT) and 1x solution of Roche® Diagnostics (Mannheim, Germany) protease inhibitor cocktail tablets (KHEM) was added to the cells and incubated at 4^{o}C for 5 min. The lysate was then collected into a 1.5ml Eppendorf tube. The cells were homogenised on ice by drawing through a 26G needle and 1 ml syringe, approximately 20 times, and centrifuged at 2,000rpm in a refrigerated, bench-top centrifuge at 4^{o}C for 10 min. The pellet formed was the P1 fraction (unbroken cells and nuclei). The supernatant was transferred to a plastic ultra-centrifuge tube and centrifuged at 75,000rpm in a Beckman TLA-100 ultra-centrifuge for 30 min at 4^{o}C. The pellet formed at this stage was the P2 fraction (plasma membrane, Golgi vesicles, endoplasmic reticulum, endosomes and lysosomes). The supernatant from this fraction was retained as the S fraction (enriched cytosolic proteins) and the volume noted. P1 and P2 fractions were both washed twice in 500µl if KHEM. The P1 fraction was washed at 2,000rpm for 10 min and the P2 fraction at 75,000rpm for 30 min. The pellets were then re-suspended in an appropriate volume of KHEM buffer. To asses sub-cellular distribution of a given protein in each fraction they were subjected to SDS-PAGE and Western-immuno-blotting as described in section 2.7.

2.6.3 Determination of Protein Concentration

The protein concentration of cell lysates and purified recombinant proteins was determined using bovine serum albumin (BSA) in a standard spectrophotometric, Bradford assay [Bradford, 1976]. The assays were undertaken in 96-welll micro-titre plates. As standard curve of know BSA concentrations between zero and 5μg was generated diluted in sterile water to a final volume of 50μl in triplicate. The protein sample of interest was assayed at various dilutions (1:100, 1:50, 1:25) in a final volume of 50μl to ensure it was within the range of the standard curve. Bradford reagent from Bio-Rad (Hemel Hempstead, U.K.) was diluted 1:5 with sterile water and 200μl was added to each well of the micro-titre plate. The 96-well plate was analysed with a 590nm test filter using a Dynex MRX micro-titre plate reader controlled through Dynex Revelation, Version 3.04 computer software. The intensity of the colour change (brown to blue) is directly proportional to protein concentration and this was determined by plotting the standard curve and using least squared regression analysis to obtain the line of best fit. The equation of the line was used to determine the concentration of the protein samples. This concentration was then adjusted to account for any dilution factor.

2.7 Protein Analysis

2.7.1 SDS-PAGE

Sodium dodecyl sulphate-polyacrylamide gel electrophoresis (SDS-PAGE) is a method used to separate proteins by virtue of their molecular weight. Protein samples of 1-100μg were denatured and reduced by dilution in 10% SDS, 300mM Tris-Cl; pH6.8, 0.05% bromophenol blue, 50% glycerol and 10% B-mercaptoethanol (5x SDS Hannah sample buffer). The samples were boiled for 3 min and then loaded directly to an Invitrogen (Paisley, U.K.) NuPAGE 4-12% Bis-Tris polyacrylamide gel immersed in Invitrogen NuPAGE MES or MOPS SDS running buffer. 5μl of Bio-Rad pre-stained

molecular weight protein marker was loaded to the first well of the gel, to assess the molecular weight of proteins being analysed, and protein sample were loaded to the subsequent wells. The gel was then run at 200V for 1.5 hours. For more details of the Invitrogen Nu-PAGE pre-cast gels and associated X-Cell II apparatus please consult the manufacturer's instructions (http://www.invitrogen.com/site/us/en/home/Products-and-Services/Applications/Protein-Expression-and-Analysis/Protein-Gel-Electrophoresis.html).

2.7.2 Coomassie Staining

Proteins separated by SDS-PAGE can be visualised by a variety of methods. For Coomassie staining gels were removed from the pre-cast gel cassette and washed in sterile water to remove residual running buffer. Coomassie stain consists of 1.25g Coomassie Brilliant Blue R250, 444ml methanol, 56ml acetic acid in a final volume of 1,000ml sterile water. 50ml of stain was added to the gel and placed gently shaking at room temperature for 2h. The Coomassie stain was then removed and replaced with Coomassie de-stain, 444ml methanol and 56ml acetic acid in a final volume of 1,000ml sterile water. The gel was then incubated with de-stain for 6h after which was replaced with fresh de-stain for another 6h. This removed all residual Coomassie background staining, leaving the remaining stain bound to the proteins showing detection of all proteins present in the sample. Proteins were then be measured against the molecular weight marker to determine their identity. The gel was then washed in sterile water with 10% glycerol to aid the prevention of gel cracking following drying.

2.7.3 Western Immuno-Blotting

Proteins separated by SDS-PAGE can be visualised by a variety of methods. Western-blotting allows the detection of individual proteins using specific anti-sera. The proteins separated by SDS-PAGE were transferred to a nitrocellulose membrane using Invitrogens X-Cell II blotting modular and Nu-PAGE transfer buffer containing 20% methanol. The proteins were transferred with an applied voltage of either 25V for 2h or

10V for 15h. Full transfer of the pre-stained molecular weight marker onto the nitrocellulose membrane indicated successful transfer of the proteins. Following transfer the nitrocellulose membrane was incubated or "blocked" in 5% milk powder (Marvel) re-constituted in 20 m< Tris-Cl; pH 7.6, 150mM NaCl and 0.1% Tween20 (TBST), for 1h at room temperature with gentle agitation. Primary antibody, for the protein wishing to be detected, was then added at the appropriate dilution (general dilution range 1:100 to 1:10,000) to a 1% milk powder TBST solution. Details of the primary antibodies used as show in Table 2.4. The nitrocellulose membrane was then sealed in and airtight plastic carrier containing 10ml of the primary antibody TBST solution. This was then incubated at either room temperature for 2h or overnight at $4^{o}C$ both with vigorous agitation. The membrane was then removed from the plastic carrier and washed 3 times in TBST for 5 min at room temperature. The appropriate horseradish peroxidase (HRP) conjugated anti-immunoglobulin G (IgG) secondary antibody diluted 1:5,000 in 1% milk powder TBST solution in a sealed, airtight plastic carrier. This was then incubated for 1h at room temperature with vigorous agitation. The membrane was washed again 3 times with TBST before employing the Amersham Biosciences (Little Chalfont, U.K.) enhanced chemiluminescence (ECL) Western Immuno-blotting kit as the visualisation protocol for detecting bound antibodies. In brief, the bound antibodies were detected by exposure of the membrane, following washing in ECL solution, to blue-light sensitive autoradiography film and developed using the Kodak X-Omat Model 2000 processor.

Protein	Specificity	Type	Dilution*	Source	Supplier
Human PDE4A	Conserved C-terminal region of human PDE4A isoforms	Serum	1:5000	Goat	In-house
Rat PDE4A	Conserved C-terminal region of rat PDE4A isoforms	Serum	1:2500	Rabbit	In-house
PDE4B	Conserved C-terminal region of PDE4B isoforms in all species	Serum	1:2500	Goat	In-house
PDE4D	Conserved C-terminal region of PDE4D isoforms in all species	Serum	1:5000	Goat	In-house
PKA phosphorylated PDE4	Phosphorylated Ser residue in RRES*F motif in UCR1 of all PDE4 long isoforms	Serum	1:1000	Rabbit	In-house
MAPKAPK2 phosphorylated PDE4	Phosphorylated Ser residue in LYRSDS* motif in UCR1 of all PDE4 long isoforms	Polyclonal	1:1000	Rabbit	Custom – Cambridge Research Biochemicals

Protein	Specificity	Type	Dilution*	Source	Supplier
p38 MAPK	Endogenous levels of p38 MAPK	Polyclonal	1:1000	Rabbit	Cell Signaling Technology®
Activated p38 MAPK	Endogenous levels of phosphorylated p38 MAPK at Thr180 & Tyr182	Polyclonal	1:1000	Rabbit	Cell Signaling Technology®
MAPKAPK2	Endogenous levels of MAPKAPK2	Polyclonal	1:1000	Rabbit	Cell Signaling Technology®
Activated MAPKAPK2	Endogenous levels of phosphorylated MAPKAPK2 at Thr334 only & not Thr25, Thr222 & Ser272	Polyclonal	1:1000	Rabbit	Cell Signaling Technology®
p75NTR	Endogenous levels of p75NTR. Targetted to the c-Terminal end.	Polyclonal	1:1000	Mouse	Santa-Cruz
GST	Recognises GST-tag fusion proteins	Polyclonal	1:1000	Rabbit	In-house
VSV	Recognises an epitope containing the five C-terminal amino acids of VSV glycoprotein	Monoclonal	1:5000	Mouse	Sigma-Aldrich®
FLAG	Recognises an epitope containing DYKDDDDK	Monoclonal	1:5000	Mouse	Sigma-Aldrich®

Table 2.4 – Anti-sera used for Western immuno-blotting.

*Dilution factor is correct for Western immuno-blotting. Antibody titrations should be undertaken for immuno-precipitation and immuno-histochemistry.

2.8 Fusion Protein Interactions

2.8.1 Pull-down Assays

The expression and purification of GST fusion proteins in E.coli was undertaken as described in Section 2.3. COS1 cells were transfected to transiently express specific PDE4A isoforms as described in Section 2.5 and subjected to sub-cellular fractionation as described in Section 2.6. Assessment of the interaction of PDE4A isoforms with GST fusion proteins has been described previously [McPhee et al., 1999, Huston et al., 2000 and Rena et al., 2001]. Briefly, 400µg of the GST fusion protein, or GST alone as a control, was immobilised on a 40µl bed volume of Amersham Biosciences (Little Chalfont, U.K.) glutathione sepharose resin. The resin was pelleted by centrifugation at 2500rpm for 5min at 4^{o}C using a refrigerated bench-top centrifuge. The supernatant was discarded. The pellets were then re-suspended in 500µl (approximately 200µg of protein) of cytosolic, or S fraction, produced from COS1 cells expressing equal immuno-reactive amounts of PDE4A isoforms, as determined by Western immuno-blotting with a PDE4A C-terminal specific anti-serum. The protein samples were diluted in KHEM, the buffer used for sub-cellular fractionation of mammalian cells. The immobilised fusion protein and cytosol were incubated together for 1h end-over-end at 4^{o}C. The glutathione sepharose resin was then collected by centrifugation at 2500rpm for 5min at 4^{o}C. The supernatant was retained for Western immuno-blotting to measure the extent of PDE4A remaining unbound to the GST fusion protein. The beads were washed three times with 500µl of KHEM by centrifugation at 2500rpm for 5min at 4^{o}C. The supernatant was discarded and the beads re-suspended in 40µl of SDS sample buffer to elute the bound proteins. Protein samples of PDE4A expressed in cytosolic cell lysate, PDE4A bound to GST, PDE4A unbound to the GST fusion protein and PDE4A bound to the GST fusion protein were analysed by SDS-PAGE, as described in

Section 2.7, and immuno-probed for PDE4A using a C-terminal, species and sub-family specific anti-serum, as described in Section 2.7.

2.8.2 Peptide Arrays

Peptide arrays are Whatman® 50 cellulose membranes on which peptide sequences are directly synthesised [Reineke et al., 2001 and Frank, 2002]. These peptide arrays are able to bind purified recombinant proteins and provide evidence for direct protein interaction and the elucidation of the critical domains and residues involved [Espanel and Hooft van Huijsduijnen, 2005 and Bolger et al., 2006]. The peptide arrays used in the experiments detailed in this thesis were kindly produced by Dr. E. Klussmann (Forschungsinstitut für Molekulare Pharmakologie, Berlin, Germany) using the Intavis Bioanalyical Instruments (Köhn, Germany) AutoSpot-Robot ASS 222 and utilising Fmoc-chemistry. Recombinant GST fusion proteins were produced to homogeneity, as described in Section 2.3. The peptide arrays were activated by immersion in 100% ethanol and then washed in TBST for 10min at room temperature on an orbital shaker. The peptide arrays were then incubated or blocked with 5% milk powder (Marvel®), re-constituted in 20mM Tris-Cl; pH 7.6, 150mM NaCl and 0.1% Tween20 (TBST) for 1h at room temperature with vigorous agitation. 3-10µg/ml of recombinant GST fusion protein, or GST alone as a control, was then diluted in 1% milk powder TBST solution and incubated with the peptide array in an airtight plastic carrier overnight at 4^{o}C with vigorous agitation. The peptide array was then subjected to three 10min washes in TBST. The recombinant GST fusion protein was then detected for direct binding to the peptide array by probing with a specific primary anti-serum or an anti-serum specific for GST. As a general rule the primary anti-sera were used at two-fold less than the recommended dilution for Western immuno-blotting. Details of the primary antibodies used in the experiments described in this thesis are shown in Table 2.4. The membrane was then washed several times with TBST before application of the appropriate horseradish peroxidase (HRP) conjugated anti-immunoglobulin G (IgG) secondary antibody diluted 1:5000 in 1% milk powder TBST solution in a sealed, airtight plastic carrier. Similarly, this was incubated for 1h at room temperature, or

overnight at 4oC, with vigorous agitation. The membrane was again washed several times with TBST before employing the Amersham Biosciences (Little Chalfont, U.K.) enhanced chemiluminescence (ECL) Western immuno-blotting kit as the visualisation protocol for detecting bound antibodies. Briefly, the bound antibodies were detected by exposure of the peptide array, following washing in ECL solution, to blue-light sensitive autoradiography film and developed using the Kodak® X-Omat Model 2000 processor. For a more detailed description of this kit or the autoradiography film processor please consult the manufacturers instructions. The resolution of spots, distinct from the GST control peptide array, on the autoradiography film were indicative of a positive interaction of the recombinant fusion protein with the peptide array and the critical sequences were analysed for putative consensus sites or binding motifs.

2.8.3 Co-immunoprecipitation

Mammalian cell lines were co-transfected, as described above in Section 2.5 and cell lysates were produced by sub-cellular fractionation as described above in Section 2.6. The protein concentrations of the cytosolic, or S fractions were determined, as described above, and the concentrations equalised for all samples to contain approximately 250µg of protein in a 500µl volume of ice-cold KHEM. A 30µl sample of the diluted lysate was removed for Western immuno-blotting to determine the relative immuno-reactive inputs of the co-expressed proteins for the co-immuno-precipitation experiment. Anti-FLAG or anti-VSV agarose beads were pre-equilibrated in ice-cold KHEM to produce a 50% slurry. 60µl of the slurry was added to each 500µl protein sample and these were incubated end-over-end for 2h at 4^{o}C. The samples were centrifuged at 13000rpm for 5min at 4^{o}C using a bench-top refrigerated centrifuge. 30µl of supernatant was removed to screen for unbound proteins. The agarose resin was washed three times in 500µl of ice-cold KHEM and once in 500µl of ice-cold PBS by centrifugation at 13000rpm for 1min at 4^{o}C. Bound proteins were then eluted in SDS sample buffer and subjected to SDS-PAGE and Western immuno-blotting, as described previously. The quantification, by densitometry, of the immuno-reactive amounts of the co-expressed proteins, in both the initial cell lysate and following co-immuno-

precipitation, was determined using The Discovery Series™ Quantity One® 1-D Analysis Software, Version 4.4.0. These data were used to compare the interaction efficiency of the two proteins and assess conditions that may facilitate modulation of the specific interaction. Control immuno-precipitations were undertaken in a similar manner with cell lysates produced from cells singly transfected with the protein that was to be co-immuno-precipitated to screen for non-specific binding to the chosen agarose bead conjugate.

2.9 Cell Based Assays

2.9.1 Phosphodiesterase Activity Assay

To measure PDE activity a radioactive cAMP hydrolysis assay was employed. This procedure has been described previously [Marchmont and Houslay, 1980] and is a modification of a historical two-step procedure [Thomson and Appleman, 1971]. PDE enzymes hydrolyse cAMP, which results in the formation of 5' AMP. In this assay, both [8-3H] adenosine 3', 5'- cyclic mono-phosphate from Amersham Biosciences (Little Chalfont, U.K.) and adenosine 3', 5'- cyclic monophosphate are hydrolysed. Addition of Snake Venom from Ophiophagus Hannah prevents re-circularisation of uncharged 5' AMP by further hydrolysis to adenosine and the Dowex slurry binds charged, un-hydrolysed cAMP.

2. 9.1.1 Activation of Dowex 1x8-400 Anion Exchange Resin

Dowex 1x8-400 was prepared and activated by dissolving 400g of Dowex resin in 4l of 1M NaOH. The solution was stirred for 15min at room temperature and the resin allowed to settle. The supernatant was removed and the Dowex resin extensively washed thirty times with 4l of distilled water and allowed to settle after each wash. After thirty washes the resin was washed with 4l of 1M HCl for 15min at room temperature and allowed to settle. The resin was then washed a further 5 times with distilled water and stored at 4^{o}C as 1:1 slurry with distilled water. Following this

procedure generally produced approximately 1l of Dowex slurry. This Dowex slurry was utilised in the PDE assay as a 2:1 solution of slurry to 100% ethanol.

2.9.1.2 Assay Procedure

The entire assay procedure was undertaken using 1.5ml Eppendorf® tubes per reaction. The cAMP substrate solution for the assay was composed of 2µl of 1mM 3', 5' cyclic adenosine mono-phosphate and 3µl of [8-^{3}H] 3', 5' cyclic adenosine mono-phosphate per millilitre of 20mM Tris-Cl; pH 7.4 and 10mM $MgCl_2$. The appropriate volume of purified protein or cell extract was diluted to a final volume of 50µl in 20mM Tris-Cl; pH 7.4. 50µl in 20mM Tris-Cl; pH 7.4 was used as the blank control. The exact volume of purified protein or cell extract required in the assay was pre-determined in a pilot assay using increasing concentrations of protein samples. 50µl of cAMP substrate was added to 50µl of the PDE containing sample, mixed, and these were then incubated in a water bath at 30^{o}C for 10min. The samples were then placed in a boiling bath for 2min to inactivate the PDE and stop the reaction. The tubes were then cooled on ice for a minimum of 15min. 25µl of 1mg/ml snake venom from Ophiophagus Hannah was then added to the reaction tubes, mixed, and incubated for a further 10min at 30^{o}C. 400µl of Dowex/ethanol solution was added to each reaction tube, mixed, and incubated on ice for a further 15min. Following incubation the tubes were then mixed again and centrifuged at 13,000rpm for 3min at 4^{o}C in a refrigerated bench-top centrifuge. 1ml of Opti-Flow SAFE 1 scintillant was added to fresh 1.5ml Eppendorf® tubes. 150µl of supernatant from the reaction tubes was added to an individual tube containing scintillant with 50µl of cAMP substrate solution added to a scintillant vial to determine total counts per minute for the assay. All tubes containing scintillant were mixed and hydrolysed 3', 5' cyclic adenosine mono-phosphate and [^{8}-3H] 3', 5' cyclic adenosine mono-phosphate was measured using a Wallac® 1409 Liquid Scintillation Counter.

2.9.1.3 Determination of Phosphodiesterase Activity

To determine specific PDE activity contained within any reaction tube the following formula was applied, 2.61 x (value – blank / average total) x 10-11 x 1012 x (1000 / μg protein) resulting in PDE activity in ρmoles/min/mg protein. To assess the effect of PDE inhibition, the activity of samples containing inhibitor were directly compared to an uninhibited control reaction and was expressed as the percentage of the aforementioned uninhibited control.

2.9.2 Thermal Stability Assays

Twenty assay tubes were set-up for a PDE activity assay, as described in Section 2.10.1. Each tube contained a pre-determined volume of cell extract, expressing the desired PDE4A, in a final volume of 50μl in 20mM Tris-Cl; pH 7.4. The assay tubes were placed in a 55^{o}C water bath and one assay tube was removed to ice every 30s until none were remaining. 50μl of cAMP substrate was then added to 50μl of the de-natured PDE sample and the activity assay continued as described above. The $\log_{10}$ residual PDE activity was determined against a control cell extract and the thermal stability profile plotted as a function of time, with the half-life ($t_{1/2}$) determined as the time in which 50% of the activity remained.

2.9.3 cAMP assay

Intracellular cAMP was determined by using the 'Cyclic AMP Competitive ELISA' kit (Product: EMSCAMPL; ThermoFisher/Pierce).

2.9.4 Fibrin Breakdown Assay

Fibrin matrices were prepared by addition of 0.1 U/mL thrombin to a mixture of 2.5 U factor XIII, 2 mg fibrinogen, 2 mg Na-citrate, 0.8 mg NaCl, and 3 µg plasminogen per mL DMEM medium. 300 µL of this mixture was added to each well of a 12 well plate. After clotting at room temperature, the fibrin matrices were soaked with 0.5 mL DMEM supplemented with 10% NCS, and penicillin/streptomycin. NIH3T3 and MEF cells were seeded at high density to obtain confluent monolayers cultured in DMEM without indicator supplemented with 10% NCS, 2 mmol/L L-glutamine and penicillin/streptomycin. Incubations were for 8 to 12 days, and test compounds were added together with fresh medium where appropriate. The medium was collected and replaced every 2 to 3 days along with new test compounds. Invading cells in the three-dimensional fibrin matrix were analyzed by phase contrast microscopy. To quantify the amount of fibrin degradation, the supernatant was aspirated and the remaining gel weighed using an analytical balance. The decrease in gel weight corresponds to the increase in fibrin degradation.

Chapter 3 Phosphorylation of PDE4A5 by MAPKAPK2

3.1 Introduction

3.1.1 Mitogen-Activated Protein Kinases

Mitogen activated protein kinases (MAP Kinases or MAPKs) were discovered approximately 20 years ago and provide among the most extensive means of cell regulation [Avruch, 2007; Kyriakus and Avruch, 2001]. MAPKs form phosphorylation cascades that control various cellular functions such as cell differentiation, cell proliferation, cell death, embryogenesis and immune and inflammatory responses [Pearson et al., 2001]. Their role in such a diverse range of functions has led to their being implicated in a wide range of diseases, such as asthma, COPD, cancer, cardiac hypertrophy and rheumatoid arthritis [Pearson et al., 2001; Dong et al., 2002].

The basic components of all MAP Kinase cascades are three core members, the mitogen activated protein kinase kinase kinases (MAPKKK), the mitogen activated protein kinase kinases (MAPKK) and the mitogen activated protein kinases (MAPK). The first stage in the phosphorylation cascade is activation of the MAPKKK proteins through exposure to a mitogen. This results in threonine and tyrosine phosphorylation in the kinase domain of MAPKKK. The MAPKKK is then able to phosphorylate specific serine and threonine residues in the MAPKK kinase domain, leading to activation of this downstream protein kinase. Activated MAPKK then, in turn, is able to phosphorylate the MAPK kinase domain at serine and tyrosine residues in a conserved Ser-Xaa-Tyr region (where Xaa is any amino acid), leading to its activation and the furtherance of downstream signalling [Kyriakus and Avruch, 2001]. Within the super-family of MAPK proteins there are three members, p38 MAPK, c-Jun N-terminal kinase (JNK) and extra-cellular signal-regulated protein kinase (ERK). The difference in specificity between these three MAPKs is conferred by the Xaa in the phosphorylation site motif, as

described above. In the case of p38 MAPK this amino acid is a glycine, in the case of JNK it is a proline and in the case of ERK it is a glutamate. The signal specificity arising from this comes into play when p38 MAPK is activated by MAPKK3 and MAPKK6, JNK is activated by MAPKK4 and MAPKK7 and ERK is activated by MAPKK1 and MAPKK2. However, despite this linear specificity, crosstalk between the p38 MAPK and JNK pathways can occur upon activation of MAPKK4, which can activate both pathways [Pearson et al., 2001].

Once the MAPK components of the phosphorylation cascades have been activated they can go on to have a diverse range of downstream effects through a diverse range of final substrates. These substrates can be anything from other protein kinases, transcription factors and scaffold proteins to enzymes such as PDE4 [Dong et al., 2002]. Critically, these potent signalling effects are, however, reversible and this is achieved by dephosphorylation that is mediated by the actions of a family of protein phosphatases [Lang, 2006].

3.1.2 p38 Mitogen Activated Protein Kinase.

The p38 mitogen activated protein kinase signalling cascade plays a key role in inflammation and is sometimes known as a stress-activated protein kinase cascade. In this, its main activating stimuli are stress factors such as cytokines, heat shock, osmotic shock, oxidative stress and ultra-violet radiation [Avruch, 2007].

There are four different isoforms of p38, namely p38α, p38β, p38δ and p38γ. p38α was the first of these isoforms to be discovered, is thought to be primarily responsible for regulation inflammation and is ubiquitously expressed. p38β is also ubiquitously expressed and shares more than 70% sequence homology with p38α [Zhang et al., 2006]. The biological roles of p38δ and p38γ are less well understood although these isoforms are thought to be tissue specific with p38δ predominantly found

in skeletal muscle and p38γ found in the small intestines, testes and pancreas [Schindler et al., 2007].

3.1.2.1 Activation and Inhibition of p38 MAP Kinase

The p38 MAP kinase can be activated by many different extracellular factors, as stated above and listed in Table 3.1. Stimulation by these factors works through various MAPKKKs to elicit activation of MAPKK3, MAPKK4 or MAPKK6, which go on to activated p38. MAPKK3 and MAPKK6 show the highest levels of activity towards p38, with MAPKK3 favouring the α and β isoforms, whereas MAPKK6 can activate all four isoforms [Enslen et al., 2000]. MAPKK4 has also, somewhat curiously, been shown to activate p38 under certain cellular conditions. This is unusual and is still being questioned as MAPKK4 is a component of the JNK pathway and was, originally, thought to only operate on this pathway [Brancho et al., 2003]. Pharmacologically the p38 MAP Kinase pathway can be activated by Anisomycin. Anisomycin is an antibiotic that inhibits protein synthesis and activates the stress activated protein kinase pathways, including p38 MAPK, which may be through actions on Rac and Cdc42 [Grollman, 1967; You et al., 2005]. Its structure is shown in Figure 3.3. Similarly TNFα can activate the p38 MAPK cascade through the TNFα receptor and recruitment of its signal scaffold proteins RIP and TRAF [Wajant and Scheurich, 2001]. Both of these activation pathways are shown in Figure 3.1. Inhibitors of the p38 MAPK pathway have been widely studied with limited clinical success [Cohen, 2009]. Pyridinyl imidazole inhibitors contributed to the discovery and characterisation of p38 MAPK through their ability to inhibit the p38 MAPK cascade and now provide the most common experimentally used p38 inhibitors, of which one example is SB203580, whose structure is shown in Figure 3.3 [Zhang et al., 2007].

3.1.2.2 Downstream Effects of p38 MAP Kinase

Once p38 MAPK has been activated it can then go on to activate downstream effectors which, when activated, transduce signals to target proteins in the cell that are not directly targeted by the MAP kinase. Downstream effectors of p38 MAPK tend to be protein kinases, with the most prominent group of these being the mitogen activated protein kinase activated protein kinases or MAPKAPKs. Three such isoforms can be activated by p38 MAPK, namely MAPKAPK2, MAPKAPK3 and MAPKAPK5 [Clifton et al., 1996; Ni et al., 1998]. Other protein kinases targeted downstream of the p38 MAPK pathway include the MAPK signal-integrating kinases (MNKs), and mitogen- and stress-activated protein kinases (MSKs) [Roux, 2004; Arthur, 2008].

The MAPKAPK family is a curious one as, despite its members having overlapping structural properties and substrate spectrums, they do not appear to have a common function. Of the three isoforms activated by p38 MAPK, MAPKAPK2 and MAPKAPK3 are activated directly by the p38α and β isoforms of the MAPK. However MAPKAPK5, also known as the p38-regulated and activated kinase (PRAK), is activated by both ERK and p38 MAPK

MAPKAPK2 is the most investigated substrate of p38 MAPK. Structurally it consists of an N-terminal proline-rich domain, a catalytic domain and contains both a putative nuclear localisation signal (NLS) and a nuclear export signal (NES) within its C-terminal domain [Meng et al., 2002]. Upon stimulation of the p38 MAPK cascade, p38 MAPK becomes activated and phosphorylates MAPKAPK2 at Thr222 and Ser272 in the catalytic domain and at Thr334 in the C-terminal domain [Gaestel, 2006; Lukas et al., 2004]. In resting cells an inactive, auto-inhibitory complex of p38α-MAPKAPK2 is found in the nucleus where the nuclear localisation signal on MAPKAPK2 is functional. Under stress stimulation MAPKK6 activates p38α that, in turn, phosphorylates MAPKAPK2. This phosphorylation, in particular the phosphorylation of Thr334, leads to “unmasking” of the nuclear export signal of the protein and allows for translocation

of the p38α-MAPKAPK2 complex out of the nucleus, allowing a population of active p38α-MAPKAPK2 to accrue in the cytoplasm [Engel et al., 1998].

Functionally, MAPKAPK2 has been implicated in a wide variety of roles within the cell. These are located both within the nucleus and within the cytoplasm, such as post-transcriptional regulation, actin remodelling, cell migration and cell cycle regulation. When activated MAPKAPK2 is situated in the nucleus it is believed to play a role in post-transcriptional regulation. There, MAPKAPK2 is thought to be responsible for stabilisation of the AU-rich elements through phosphorylation of mRNA binding proteins such as tristetraprolin (TTP), K homology-type splicing regulatory protein (KSRP) and heterogeneous nuclear ribonucleoprotein (hnRNP). This regulation leads to gene expression of cytokines such as IL-6, IL-8 and TNFα [Gaestal, 2006]. Another MAPKAPK2 phosphorylation target in the nucleus is considered to be the transcription factor CREB (cAMP Responsive Element Binding protein), although this action is not unequivocal and it is has been suggested that MSK1 may actually be the kinase responsible for CREB phosphorylation and activation under conditions of activation of the p38 MAPK pathway [Delghandi et al., 2005; Tan et al., 1996]. Once MAPKAPK2 is translocated out of the nucleus, following activation, it is able to act on a plethora of phosphorylation targets. One notable group of substrates are small heat shock proteins (Hsps), with Hsp25 and Hsp27 being identified as major targets for MAPKAPK2. In the case of Hsp25, MAPKAPK2 has been identified as the main kinase responsible for its activation. Phosphorylation of Hsp25, by MAPKAPK2, results in release from its role as a chaperone inhibiting actin polymerisation and thus acts to trigger actin remodelling and for actin polymerisation to occur [Benndorf et al., 1994]. Hsp27 exists as oligomers that act as ATP-independent chaperones and keep unfolded proteins in a "folding-ready" state in preparation for processes such as actin remodelling. MAPKAPK2 phosphorylation of Hsp27 is thought to be responsible for the heat shock protein's oligomerisation and may also regulate its chaperone properties [Rogalla et al., 1999].

Recently a new role for MAPKAPK2 has been identified as a checkpoint protein in the cell cycle [Reinhardt et al., 2009]. The phosphatase family Cdc25 removes inhibitory phosphate residues from the cyclic dependent kinases (Cdks), a major driving force in the cell cycle, thereby controlling progression of the cell cycle [Strausfeld et al., 1991]. All three Cdc25 isoforms, Cdc25A, Cdc25B and Cdc25C have recently been shown to be substrates for MAPKAPK2. Within the cell cycle Cdc25A plays a role in the G1-S checkpoint, with Cdc25B and Cdc25C having a role in G2 phase. During DNA damage, MAPKAPK2 is activated; it then phosphorylates Cdc25B and Cdc25C causing arrest of the cell cycle [Lammer et al., 1998]. In addition to this, MAPKAPK2 can phosphorylate and activate the ubiquitin ligase HDM2, which degrades the tumour suppressor protein p53 [Weber et al., 2005]. p53 is responsible for cell cycle regulation at G1/S and entry into apoptosis therefore through this MAPKAPK2 may play another role in cell cycle regulation. All of these roles of MAPKAPK2 throughout the cell show how multifaceted and important a downstream effector of p38 MAPK it is.

The biological functions of both MAPKAPK3 and MAPKAPK5 are poorly understood compared to MAPKAPK2. MAPKAPK3 is structurally most similar to MAPKAPK2 and may have its nuclear localisation regulated in a similar way [Zakowski 2004]. Little is known about its functionality, however it is thought to play a role in chromatin remodelling through phosphorylation of polycomb group protein BMI1 [Voncken et al., 2005]. MAPKAPK5 lacks the proline rich N-terminal region present in both MAPKAPK2 and MAPKAPK3. Again, little is known about its cellular function, however MAPKAPK5 knockout mice are more susceptible to skin cancer than wild type mice and thus it has been suggested that MAPKAPK5 may have a role as a tumour suppressor [Sun et al., 2007].

Two other families of kinases that are downstream effectors of the p38 MAPK pathway, and less well understood, are the serine threonine kinases, MAPK interacting kinases (MNKs) and the mitogen and stress-activated protein kinases (MSKs). In the case of MNKs there are two isoforms, MNK1 and MNK2, and stimulation of either the p38 MAPK pathway or the ERK pathway can lead to their activation thus, possibly,

providing an example of a source of convergence for these two key pathways. Structurally these kinases are similar to MAPKAPK1, MAPKAPK2 and MAPKAPK3 proteins but with an additional basic N-terminal structure designed to determine their intracellular targeting [Waskiewicz et al., 1997]. Although these kinases have not been widely studied, recent investigations of these proteins has shown that they are auto-inhibited in the absence of p38 and ERK phosphorylation [Jauch et al., 2006] and that, when activated, they provide the only kinases to phosphorylate Ser209 of eIF4E, the cap-binding protein, which increases translation [Mahalingam and Cooper, 2001]. They have also been implied in regulation of the innate immune response in macrophages through TNFα control [Andersson and Sundler, 2006].

In the MSK family there are two isoforms; MSK1 and MSK2. These enzymes share approximately 50% homology with MAPKAPK1 and, of the two, MSK1 is most widely studied [Arthur and Cohen, 2000]. MSK1 plays a role in phosphorylation and activation of the transcription factors CREB and, closely related, activating transcription factor 1, ATF1 [Deak et al., 1998]. Recent research has indicated that both MSK1 and MSK2 could play an important role in limiting the production of pro-inflammatory cytokines in response to stimulation of primary macrophages. This provides a negative feedback system that is able to limit toll-like receptor-mediated inflammation [Ananieva et al., 2008].

3.1.3 The Immune and Inflammatory Role of p38 MAP Kinase.

p38 MAPK plays a key role in regulation of the immune and inflammatory response to pathogens. p38α was the first p38 MAPK to be shown to play a role in inflammation. When pyridinyl imidazoles were first discovered it was thought that they had their anti-inflammatory effect through inhibition of 5-lipoxygenase and cyclooxygenase [Han et al., 1994]. However, further studies using the acute monocytic leukaemia cell line, THP-1, identified two 38 kDa protein kinases, namely p38α and p38β, as being responsible for cytokine suppression and loss of inflammation [Lee et al.,

1994]. Since then the p38 MAPK signalling cascade has been shown to play a pivotal role in the activation and production of several pro-inflammatory cytokines such as TNFα, interleukin 1, interleukin 6 and interleukin 8 [Lee at al., 1994]. In addition to its role in pro-inflammatory cytokine production it has also been established that p38 MAPK plays a key role in inducing enzymes such as COX2, which trigger eicosanoid production at sites of inflammation, and also iNOS, which triggers nitric oxide production at the site of inflammation [Dean et al., 1999].

To establish the roles of the different p38 MAPK isoforms in inflammation, knockout mice systems have been used. This approach showed that when p38A knockout mice were produced they had very low cytokine production [Beardmore et al., 2005]. It has also been reported that T helper cells, Th1, deficient in p38α did not produce interferon-γ when stimulated by interleukins 12 and 18, causing a lack of inflammatory response [Berenson et al., 2006]. However when a knockout mouse system of p38β was produced these mice were found to have normal LPS induced cytokine production and, counter-intuitively, there was even an increase in inflammation in some systems such and the bowels and joints [Beardmore et al., 2005]. Nevertheless, these knockout studies clearly show that p38α MAPK is the main p38 isoform involved in control of inflammatory system. However as the roles of p38δ and p38γ are not fully established, no firm conclusion can be made about their overall importance to immune system function. It should also be noted that knockout mice studies have also been carried out to ablate the key downstream effector of the p38 MAPK pathway, namely MAPKAPK2 [Kotlyarov et al., 1999]. Mice generated in this way exhibited a marked decreases in Il-6 and TNFα in response to LPS showing that this downstream kinase obviously plays a role in p38α MAPKs control of inflammation.

The control of pro-inflammatory cytokines is particularly important therapeutically as their over-production is seen in many disease states such as asthma, Crohns disease and rheumatoid arthritis [Russo and Polosa, 2005]. They are also implicated in playing roles in other diseases like heart failure and insulin resistant diabetes [Pomerantz et al., 2001, Takeda et al., 2005]. Due to this, blockage of their

production and/or actions is obviously a key target for therapeutic development and because of this several pharmaceutical companies have developed a series of p38α MAPK and MAPKAPK2 inhibitors. In the case of the p38α MAPK inhibitors only a few inhibitors have made it to the advanced stages of clinical trials. For example, Scios and Johnson and Johnson have the p38α MAPK inhibitor, SCIO 323 in phase II clinical trials to treat rheumatoid arthritis [Lee and Dominguez, 2005]. Somewhat less successfully, BIRB 796, developed by Boeringer Ingelheim, although it gave promising results in initial trials it was subsequently found to have limited effect in Crohn's disease and caused dangerously high increases in liver enzyme synthesis [Schreiber et al., 2006]. Similarly Amgen produced AMG 548, which exhibited a high rate of inhibition of pro-inflammatory cytokines in healthy males, however these trials had to be suspended as it was also shown to elevate the levels of liver enzyme synthesis [Lee and Dominguez, 2005]. Due to these liver complications, and the tendency of p38α MAPK inhibitors to put the patient at risk of infection, the focus of many companies has shifted from inhibitors of p38α MAPK to development of inhibitors of downstream effectors of the pathway such as MAPKAPK2. Development of these inhibitors is still in the very early stages and it was originally thought that the lack of availability of the crystal structure of the enzyme has precluded rational drug design. However since the crystal structure of unphosphorylated MAPKAPK2 was discovered in 2002, and showed that the kinase domain existed in an exposed, semi-activated state, and a selective inhibitor has still not been developed [Meng et al., 2002].

3.1.4 Phosphorylation of PDE4 enzymes by MAPKAPK2

Phosphodiesterase-4 enzymes are subject to phosphorylation at distinct sites with subsequent catalytic activity regulation by ERK1/2 [Hoffmann et al., 1999; MacKenzie et al., 2000; Baillie et al., 2001], PKA [Sette and Conti, 1996; MacKenzie et al., 2002], and an unknown protein kinase thought to be part of the PI-3K signalling pathway and activated by reactive oxygen species (ROS) [MacKenzie et al., 1998]. These phosphorylation events have been discussed previously in detail in Chapter 1.

The p38 MAPK signalling pathway plays a fundamental role in the immune and inflammatory response. Previous unpublished work from the Houslay lab suggested that PDE4 may be a phosphorylation target for a downstream effector of this pathway, namely MAPKAPK2. The aim of this chapter was to corroborate this and so identify whether PDE4 enzymes could indeed be phosphorylated and regulated through activation of MAPKAPK2 and elucidate the functional significance of the integration of cross talk between p38 MAPK and cAMP signalling.

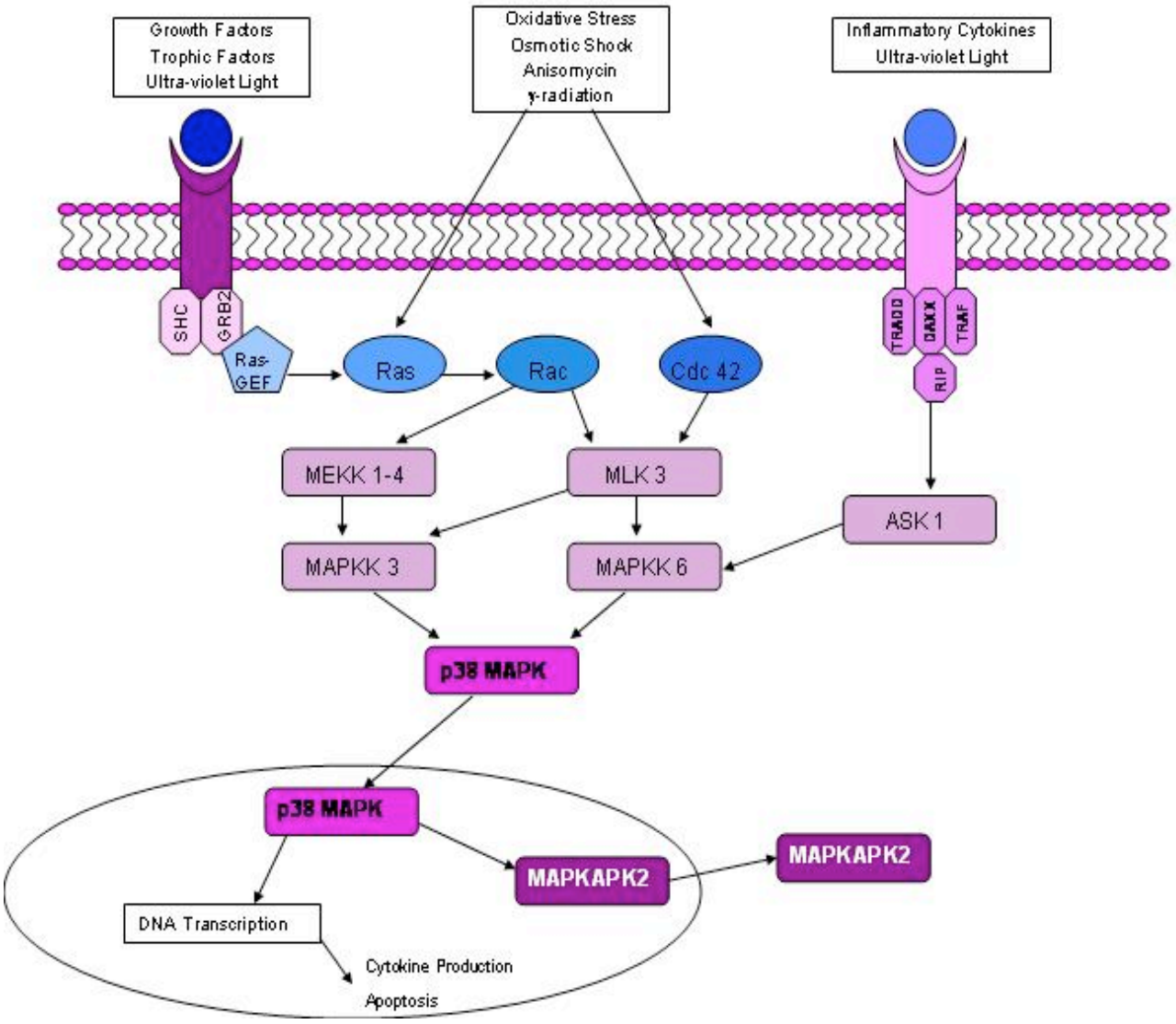

Figure 3.1 – Schematic representation of the p38 MAPK signalling pathway.

3.2 Results

Analysis of the amino acid sequence for PDE4A5 reveals two putative MAPKAPK2 phosphorylation sites with the consensus motif of Ø-X-Arg-X-X-Ser-Ø, where Ø are hydrophobic amino acids and X is any amino acid. [Stokoe et al., 1993; Rousseau et al., 2005]. Both of these regions are found within Upstream Conserved Region 1 as shown in Figure 3.2. The first potential site is serine 147, which lies within the sequence Leu-Tyr-Arg-Ser-Asp-Ser-Asp, and the second site is serine 161, within the motif Val-Ser-Arg-Ser-Ser-Ser-Val.

Unpublished work from the Houslay laboratory by Dr Elaine Hill and Dr Derek Wallace has shown that a purified PDE4A5 MBP fusion protein, generated by expression in *E.coli*, could be phosphorylated *in vitro* by recombinant MAPKAPK2, but not by recombinant p38 MAP Kinase [E.V. Hill, D.A. Wallace and M.D. Houslay, unpublished observations].

3.2.1 In vivo phosphorylation of PDE4A5 by MAPKAPK2

Previous phosphorylation experiments were carried out *in vitro* and so it is important to determine whether MAPKAPK2 could phosphorylate PDE4A5 in vivo in living cells. In order to achieve this a cell system had to be used where the p38 MAP Kinase cascade could be successfully activated and PDE4A5 manipulated. To achieve this COS1 cells were treated with either the p38 MAP Kinase activator anisomycin, the structure of which is shown in Figure 3.3 or the inflammatory cytokine, TNFα.

Figure 3.4(a) (work performed by Dr Derek Wallace) shows that endogenous p38 MAPK activity, indicated as dual phosphorylation of the kinase at Thr-180 and Tyr-182, was low in the basal state, and that it was activated in a potent, time dependent manner by anisomycin. The activation of p38 MAPK reached at maximum at 20min and

was sustained up to at least 60 min. Figure 3.4(b) shows that anisomycin also activated MAPKAPK2, indicated by phosphorylation at Thr-334, in a time dependent manner reaching a maximum at 30min and was sustained up to at least 60min. Figure 3.5 shows that TNFα also activates both p38 MAPK and MAPKAPK2 in a time dependent manner with p38 MAPK activation reaching a maximum at 5min and is sustained until 10 min where activity decreases but has still not returned to basal activity over a period of 25 min studied here.MAPKAPK2 activation reaches a maximum at 5min and an activated state is sustained up until at least 25 min albeit at a lower level (Figure 3.5). As a routine, I chose to use anisomycin for activation of p38 MAPK and MAPKAPK2 in the majority of experiments as it provided consistent and substantial levels of activation over an experimentally accessible time course.

In previous work performed by Dr Elaine Hill and Dr Derek Wallace PDE4A5 was transiently over-expressed in COS1 cells, which were grown in phosphate-free cell media that was supplemented with [^{32}P]-orthophosphate. The cells were treated with anisomycin or anisomycin plus the p38 MAPK inhibitor SB203580 (structure shown in Figure 3.3). Lysates were produced, PDE4A5 was immuno-precipitated and phosphorylation levels analysed as shown in Figure 3.6(a). This showed that anisomycin treatment resulted in increased phosphorylation of PDE4A5 to 172 +/- 8% and SB203580 ablated this phosphorylation to 124 +/- 4%, which proves that anisomycin is induction phosphorylation of PDE4A5 through the p38 MAP Kinase pathway.

However as it has been previously shown (unpublished work from the Houslay lab; E.V. Hill, D.A. Wallace) that PDE4A5 has two putative p38 MAPK phosphorylation sites it is important to establish if this phosphorylation is due to MAPKAPK2 phosphorylation or p38 MAPK phosphorylation of the PDE. To do this the two putative phosphorylation sites for MAPKAPK2 on PDE4A5 were mutated to alanine giving the two mutant PDE4A5 constructs S147A and S161A. These were transfected into COS1 cells grown in phosphate-free cell media that was supplemented with [^{32}P]-orthophosphate and were treated with anisomycin. Again, lysates were produced, PDE4A5 was immuno-precipitated and phosphorylation levels analysed as

shown in Figure 3.6(b). This showed that anisomycin is indeed phosphorylating PDE4A5 through MAPKAPK2 as it is acting at the phosphorylation site S147A. PDE4A5 was used as a standard and density of phosphorylation on the phospho-blot marked as 100%. When compared to this S161A gives a phosphorylation level of 90% +/- 2%, whereas S147A gives a phosphorylation level of 40% +/- 2%. Successful generation of a custom made antibody that targets this specific serine 147 phosphorylation site of PDE4A5 allowed cell lysates of COS1 cells, grown in normal cell media and transiently transfected with PDE4A5 treated with an anisomycin time course, to be probed for MAPKAPK2 specific phosphorylation as shown in Figure 3.6(c).These results confirmed that PDE4A5 is phosphorylated at serine 147 by MAPKAPK2.

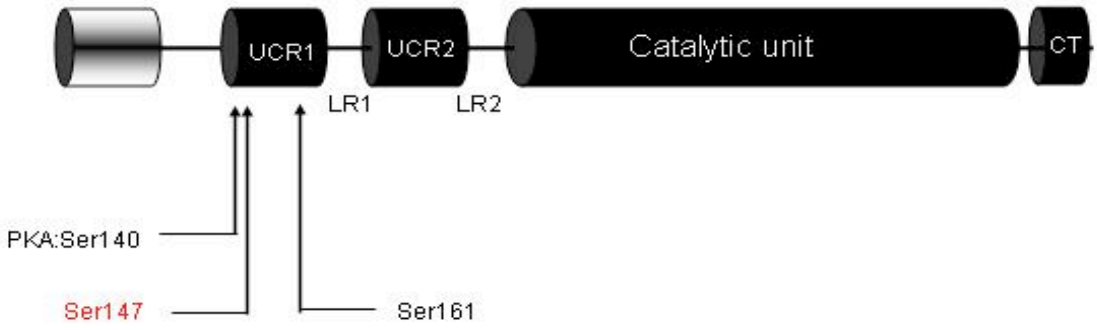

Figure 3.2 – Schematic representation of the basic structure of PDE4A5.

Schematic representation of the basic structure of PDE4A5. UCR = Upstream Conserved Region, LR = Linker Region and CT= C-Terminus. The PKA phosphorylation site (Ser 140) and the two potential MAPKAPK2 phosphorylation sites (Ser 147 and Ser 161) highlighted in the Upstream Conserved Region 1.

Anisomycin

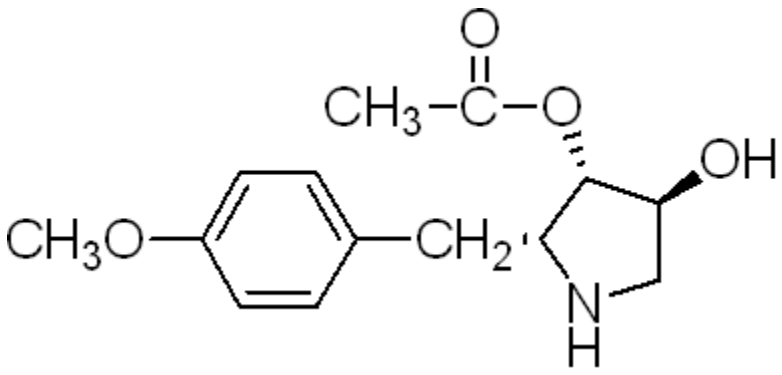

SB203580

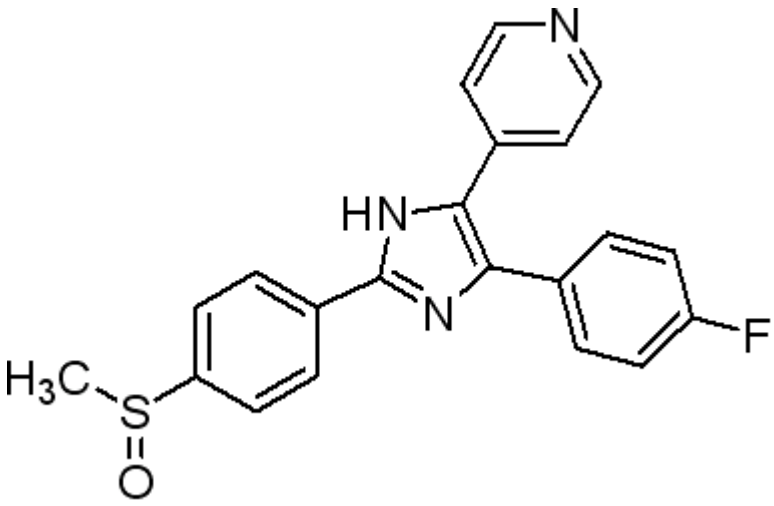

Figure 3.3 - Chemical structures of anisomycin and SB203580.

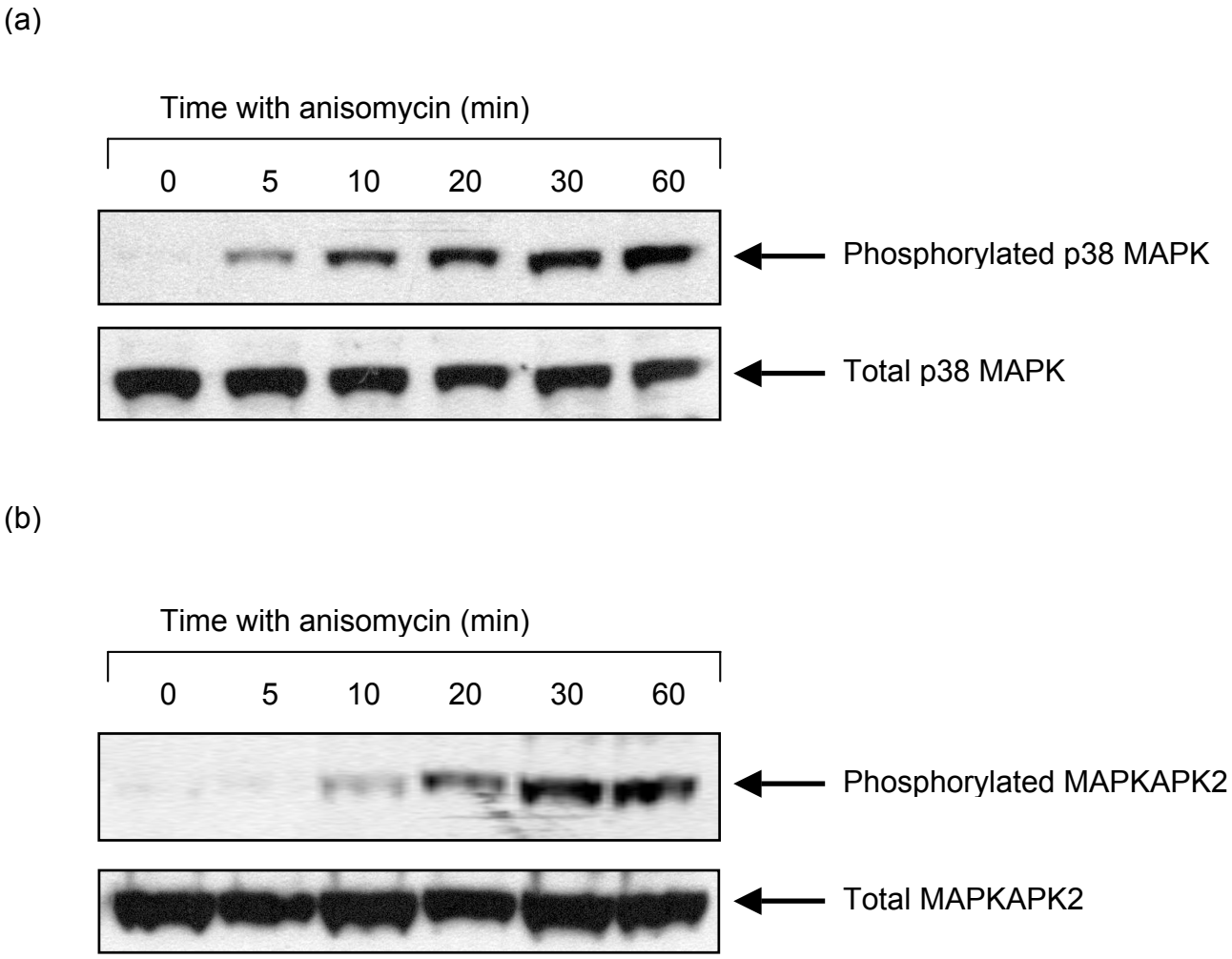

Figure 3.4 – Anisomycin time course of p38 MAPK and MAPKAPK2 activation in COS1 cells.

COS1 cells were treated with anisomycin (10μg/ml) at the indicated time points (0-60min). Total cell extract was produced and the lysates immuno-probed with anti-sera specific for the respective kinase activation. (a), top panel, is a Western blot probed with anti-sera able to detect endogenous levels of the dual phosphorylated (Thr-180 and Tyr-182), and activated, p38 MAPK. (a), bottom panel, is the same Western blot re-probed with an anti-serum to detect total endogenous p38 MAPK. (b), top panel, is a Western blot of phosphorylated, and activated, MAPKAPK2, as indicated by the detection of the mono phosphorylated (Thr-334) form. (b), bottom panel, is the same

Western blot re-probed for total endogenous MAPKAPK2, using a specific anti-serum. All Western blots are representative blots of at least three separate experiments.

This work was performed by Dr Derek Wallace.

(a)

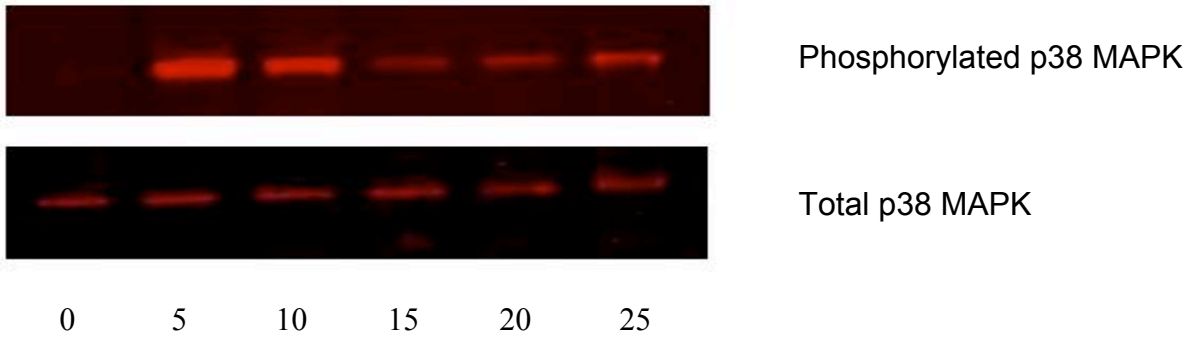

(b)

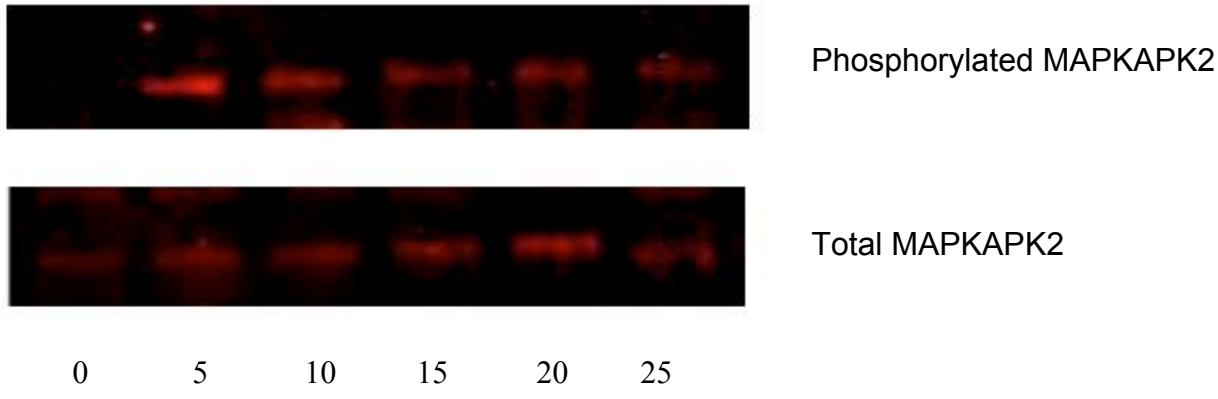

Figure 3.5 – TNFα time course of p38 MAPK and MAPKAPK2 activation in COS1 cells.

COS1 cells were treated with TNFα (10μM) at the indicated time points (0-25min). Total cell extract was produced and the lysates immuno-probed with anti-sera specific for the respective kinase activation. (a), top panel, is a Western blot probed with anti-sera able to detect endogenous levels of the dual phosphorylated (Thr-180 and Tyr-182), and activated, p38 MAPK. (a), bottom panel, is the same Western blot re-probed with an anti-serum to detect total endogenous p38 MAPK. (b), top panel, is a Western blot of phosphorylated, and activated, MAPKAPK2, as indicated by the detection of the mono phosphorylated (Thr-334) form. (b), bottom panel, is the same Western blot re-probed for total endogenous MAPKAPK2, using a specific anti-serum. All Western blots are representative blots of at least three separate experiments.

(a)

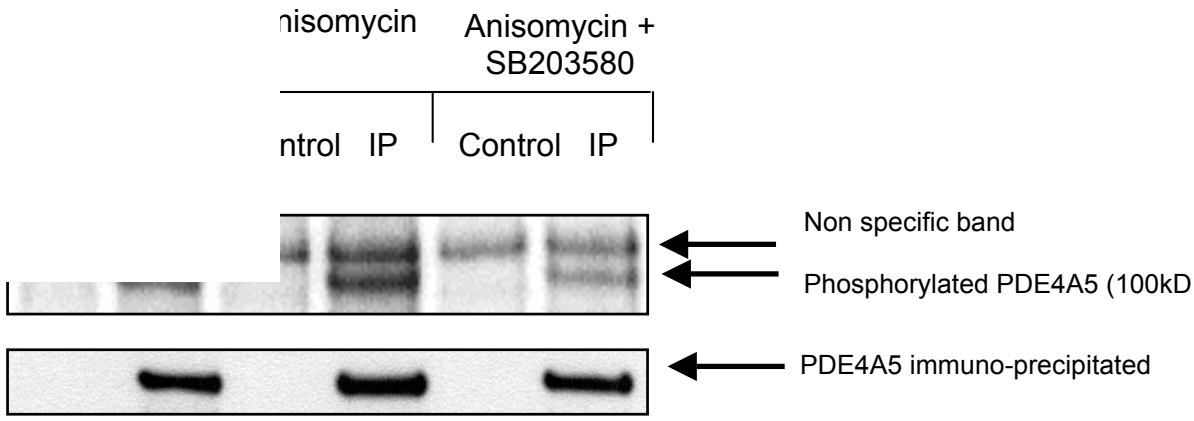

(b)

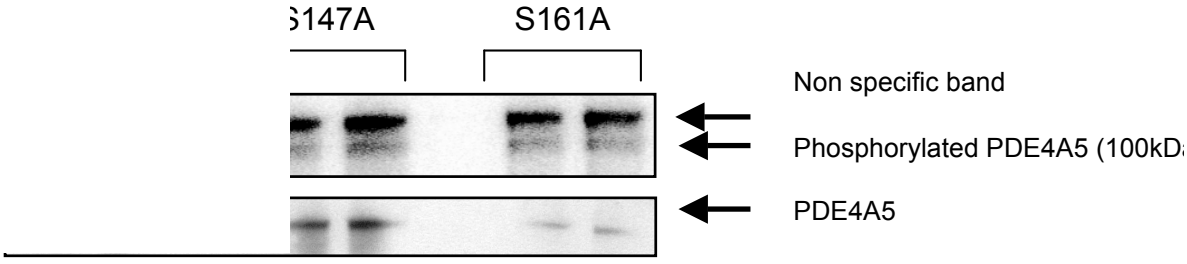

(c)

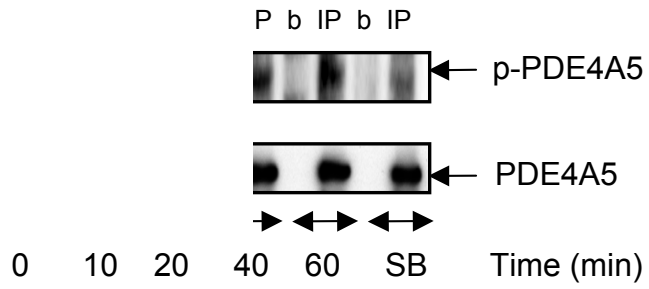

Figure 3.6 – PDE4A5 is phosphorylated by MAPKAPK2 at Serine 147.

COS1 cells were transiently transfected to over-express PDE4A5. The cells were grown in phosphate-free cell media that was supplemented with [^{32}P]-orthophosphate overnight. The cells were treated with anisomycin (10μg/ml) for 60min, to activate the p38 MAPK phosphorylation cascade, or anisomycin plus the p38 MAPK inhibitor SB203580 (10μM) for 60min respectively. Total cell lysate was produced. PDE4A5 was immuno-precipitated using an anti-PDE4A antibody conjugated to Protein G agarose with un-conjugated Protein G agarose used as a control immuno-precipitation. The immuno-precipitated proteins were separated by SDS-PAGE and transferred to a nitrocellulose membrane where the radioactive proteins were resolved using phosphor image screen technology. (a), top panel, is a scanned phosphor image screen of the phosphorylated PDE4A5 immuno-precipitated following treatment with anisomycin plus or minus SB203580. (a), bottom panel, is a Western blot of the same nitrocellulose membrane probed with the anti-PDE4A antibody to determine the relative immuno-precipitation of PDE4A5 from the three samples. COS1 cells were then transiently transfected to over-express either PDE4A5, Ser147Ala-PDE4A5 mutant or Ser161Ala-PDE4A5 mutant. The cells were grown in phosphate-free cell media that was supplemented with [^{32}P]-orthophosphate overnight. The cells were treated with

anisomycin (10μg/ml) for 60min, to activate the p38 MAPK phosphorylation cascade. Total cell lysate was produced. PDE4A5 was immuno-precipitated using an anti-PDE4A antibody conjugated to Protein G agarose with un-conjugated Protein G agarose used as a control immuno-precipitation. The immuno-precipitated proteins were separated by SDS-PAGE and transferred to a nitrocellulose membrane where the radioactive proteins were resolved using phosphor image screen technology. (b), top panel, is a scanned phosphor image screen of the phosphorylated PDE4A5, Ser147Ala-PDE4A5 mutant and Ser161Ala-PDE4A5 mutant forms were immuno-precipitated following treatment with anisomycin. (b), bottom panel, is a Western blot of the same nitrocellulose membrane probed with the anti-PDE4A antibody to determine the relative immuno-precipitation of PDE4A5 from the three samples. Immuno-precipitation of PDE4A5 was then carried out after various time points of treatment with anisomycin (10μg/ml) over a 60 min time course and the IP products produced were probed with a PDE4A4 Phospho-Ser147 specific antibody, (c). **This work was performed by Dr Elaine Hill and Dr Derek Wallace.**

3.2.2 Functional Effects of PDE4A5 Phosphorylation

PDE4 enzymes are known to be subject to regulation by three different kinases; PKA, ERK1/2 and an unknown kinase downstream of PI3 Kinase, as discussed previously. All long form PDE4 enzymes contain a conserved PKA phosphorylation site within the UCR1 region that upon phosphorylation induces a 2-fold increase in PDE4 activity [Houslay, 2001]. ERK has a conserved docking site on all PDE4 isoforms in the catalytic domain however it only has a functional effect on PDE4B, 4C and 4D isoforms as PDE4A isoforms lack the phosphorylation site for ERK [Baillie et al., 2000]. In long form PDE4B, 4C and 4D ERK2 phosphorylation leads to an inhibition of PDE activity, which can be overcome by PKA phosphorylation. PDE4A4/5 can also be phosphorylated by an unidentified downstream component of the PI3K pathway [MacKenzie et al., 1998; MacKenzie and Houslay, 2000] although the specific kinase responsible is yet to be identified.

3.2.2.1 Phosphorylation of PDE4A5

As stated above, PDE4A5 is able to be phosphorylated by PKA. A model system was set up to demonstrate this using COS1 cells transiently transfected to over-express PDE4A5. PKA was first activated by increasing intracellular cAMP levels. This was done using treatment with both IBMX, to block all PDE determined cAMP degradation, and the direct activator of adenylyl cyclase, the diterpene forskolin. This treatment induced PKA phosphorylation of PDE4A5, which was detected using a custom made antibody targeted to Ser140, the PKA phosphorylation site in UCR1 [MacKenzie et al., 2002] as shown in Figure 3.7(a). Quantification of the phosphorylation showed that the level of PKA phosphorylation of PDE4A5 gradually increased, reaching a maximum some 10-20min after forskolin challenge Figure 3.7(b).

As the identified site for MAPKAPK2 phosphorylation on PDE4A5 and the PKA phosphorylation site (Ser 147 for MAPKAPK2 and Ser 140 for PKA) are

extremely close together within UCR1 it was important to establish whether MAPKAPK2 phosphorylation was having an effect on the phosphorylation status of the PKA site. Again using the cell model of COS1 cells transiently transfected to over-express PDE4A5, anisomycin treatment was used to activate the p38 MAPK cascade and therefore activate MAPKAPK2. In this case, using the PKA phosphorylation site antibody, no PKA phosphorylation of PDE4A5 was detected, above the basal rate as shown in Figure 3.8(a). The level of phosphorylation was quantified using densitometry and it was confirmed that PKA phosphorylation levels remained at a low basal rate throughout treatment, Figure 3.8(b). This shows that MAPKAPK2 phosphorylation of PDE4A5 does not directly affect Ser140 of PDE4A5. It was, however, also important to establish whether MAPKAPK2 phosphorylation was altering PKA's ability to act at its target site within the long PDE4A5 isoform. As this site is in close proximity to the MAPKAPK2 site it is possible that steric hindrance caused by a conformational might prevent one kinase phosphorylate its target sites subsequent to the action of the other. Certainly the close proximity of these sites would prevent simultaneous phosphorylation by these two kinases due to steric hindrance, so phosphorylation by one kinase would always be expected to precede phosphorylation by the other. Using the model system with COS1 cells transfected to transiently express PDE4A5, these cells were pre-treated with anisomycin to activate MAPKAPK2 and this treatment was followed by activating PKA by treatment with forskolin together with IBMX. Doing this I noted that PKA phosphorylation of PDE4A5 ensued with similar kinetics and magnitude to that observed when cells were challenged with IBMX and forskolin and no pre-treatment with anisomycin (Fig. 3.9). Thus Ser140 phosphorylation levels gradually increased from 0-10 min reaching a sustained maximum at 10-20 min, Figure 3.9. This, therefore, shows that despite the close proximity of the phosphorylation sites of PKA and MAPKAPK2 on UCR1 there is no steric interference between the two kinases in the process of phosphorylation.

The phosphorylation studies were then repeated with the PDE4A5 Ser147Ala mutant for the MAPKAPK2 phosphorylation site, transiently over-expressed in COS1 cells, to establish whether mutation of the MAPKAPK2 target site had any effect on

PKA phosphorylation. As with the wild type PDE4A5 it was shown that increasing PKA phosphorylation occurred in a time dependent manner after PKA activation, Figure 3.10. No PKA phosphorylation above basal level was observed after activation of the p38 MAPK cascade. Figure 3.11, and lastly that activation of the p38 MAPK cascade did not affect the ability of PKA to phosphorylate PDE4A5 upon stimulation of adenylyl cyclase, Figure 3.12.

(a) Wild Type PDE4A5

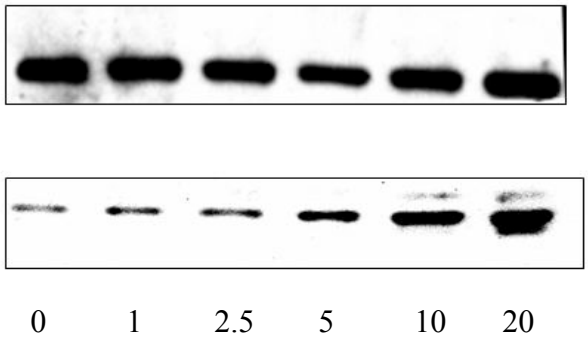

(b)

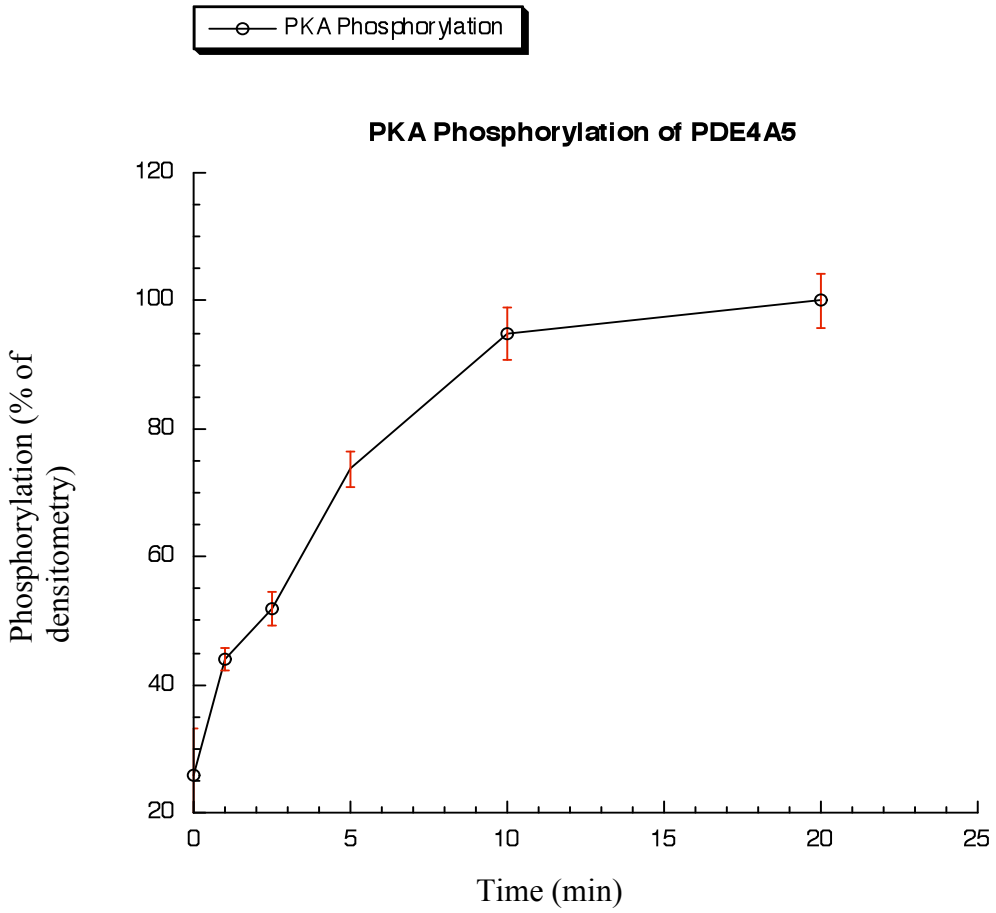

Figure 3.7 – Phosphorylation and act

COS1 cells were transfected to transiently express wild type rat PDE4A5. The transfected cells were pre-treated for 10min with the non-specific PDE inhibitor, IBMX (100μM) before challenge, 0-20min, with the adenylyl cyclase activator, forskolin (100μM). (a), top panel, is a Western blot probed with a rat PDE4A C-terminal specific anti-serum to provide both loading and PDE4A5 expression controls. (a), bottom panel, is the same Western blot re-probed with the phospho-UCR1 specific anti-serum to the PKA phosphorylated serine (S*) residue within the RRES*F consensus motif [MacKenzie et al., 2002]. (b) shows the densitometry of the phospho-UCR1 time course, corrected for PDE4A5 expression. All data shown are representative Western blots of three separate transfections and experiments +/- standard deviation.

(a) Wild Type PDE4A5

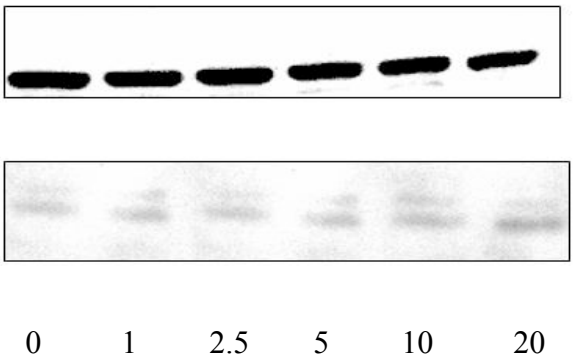

(b)

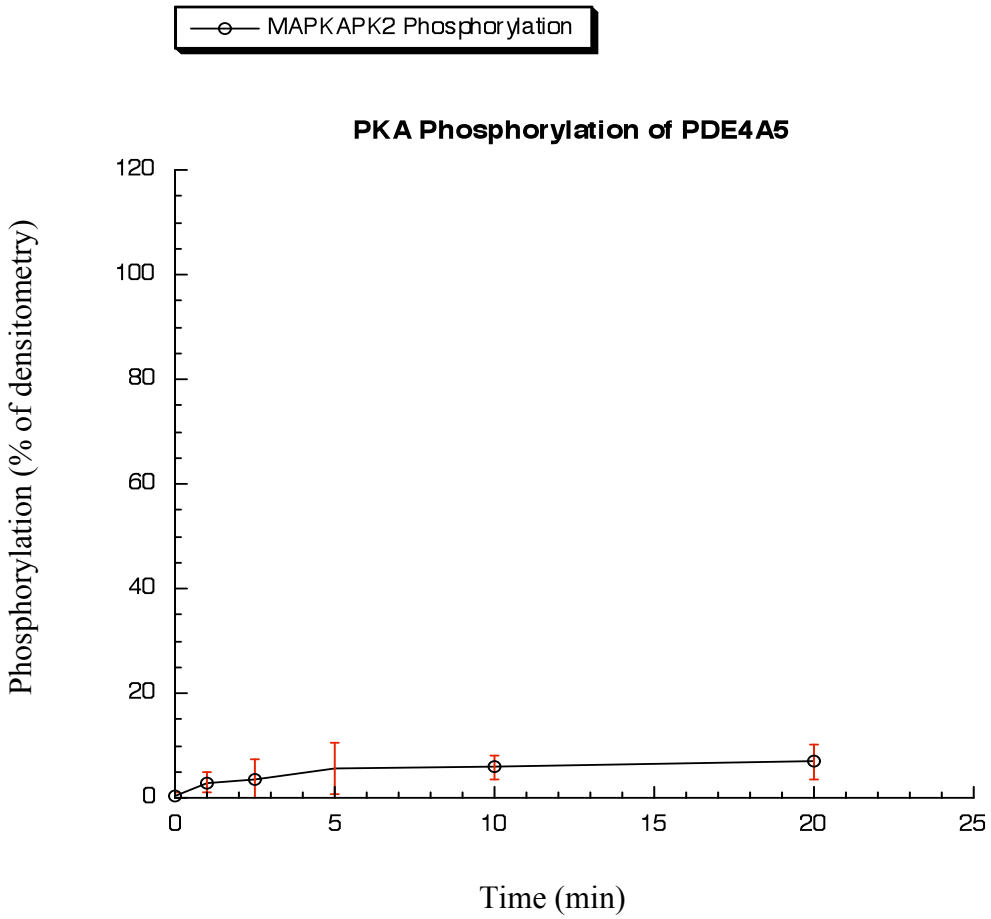

Figure 3.8 – Phosphorylation and activ .PK2.

COS1 cells were transfected to transiently express wild type rat PDE4A5. The transfected cells were treated for 60min with the p38 MAP Kinase activator, anisomycin (10μg/ml). (a), top panel, is a Western blot probed with a rat PDE4A C-terminal specific anti-serum to provide both loading and PDE4A5 expression controls. (a), bottom panel, is the same Western blot re-probed with the phospho-UCR1 specific anti-serum to the PKA phosphorylated serine (S*) residue within the RRES*F consensus motif [MacKenzie et al., 2002]. (b) shows the densitometry of the phospho-UCR1 time course, corrected for PDE4A5 expression. All data shown are representative Western blots of three separate transfections and experiments +/- standard deviation.

(a) Wild Type PDE4A5

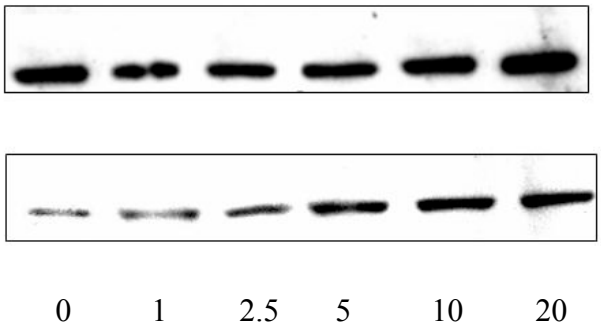

Time with Fsk (min) after Anisomycin and IBMX pre-treatment

(b)

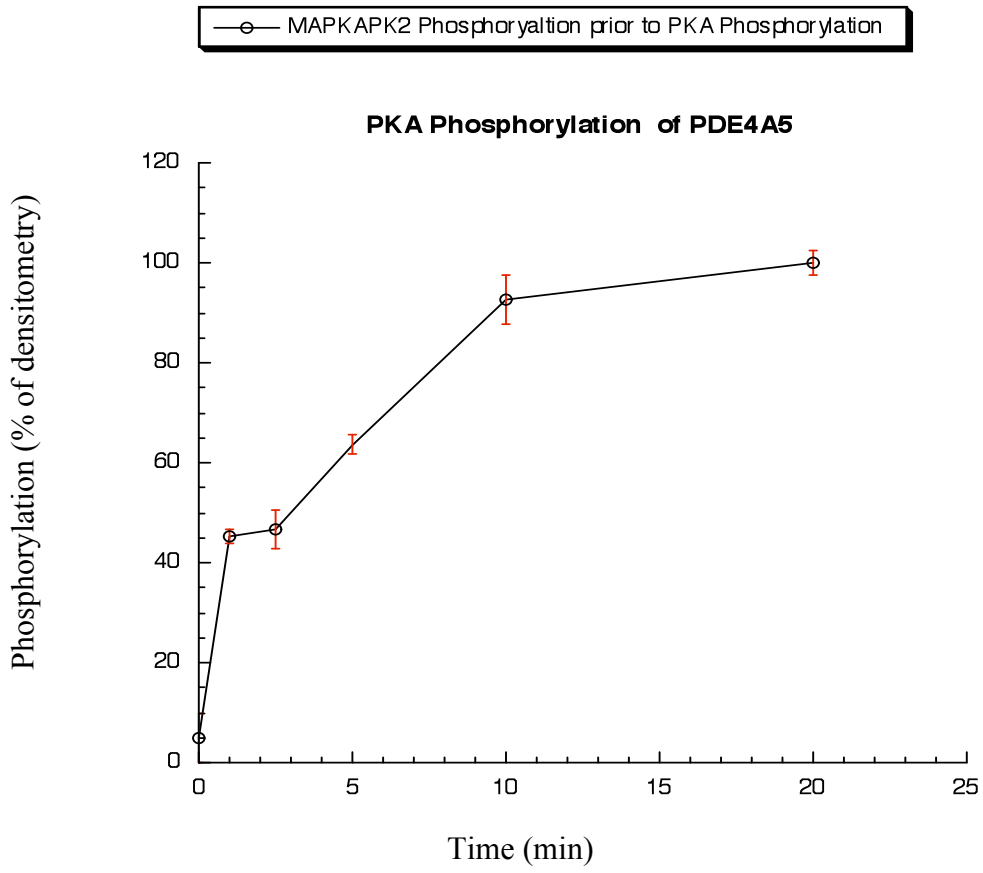

Figure 3.9 – Phosphorylation and A and MAPKAPK2.

COS1 cells were transfected to transiently express wild type rat PDE4A5. The transfected cells were pre-treated for 30min with the p38 MAP Kinase activator, anisomycin (10μg/ml), then treated with 10min with the non-specific PDE inhibitor, IBMX (100μM) before challenge, 0-20min, with the adenylyl cyclase activator, forskolin (100μM). (a), top panel, is a Western blot probed with a rat PDE4A C-terminal specific anti-serum to provide both loading and PDE4A5 expression controls. (a), bottom panel, is the same Western blot re-probed with the phospho-UCR1 specific anti-serum to the PKA phosphorylated serine (S*) residue within the RRES*F consensus motif [MacKenzie et al., 2002]. (b) shows the densitometry of the phospho-UCR1 time course, corrected for PDE4A5 expression. All data shown are representative Western blots of three separate transfections and experiments +/- standard deviation.

(a) PDE4A5 S147A mutant

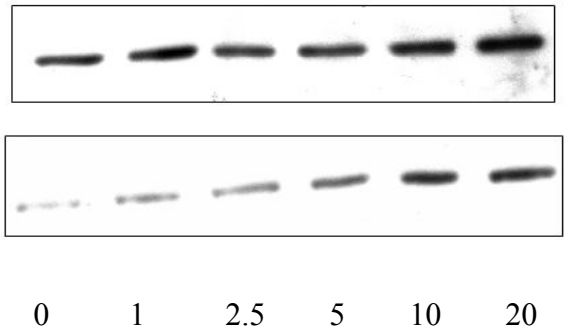

(b)

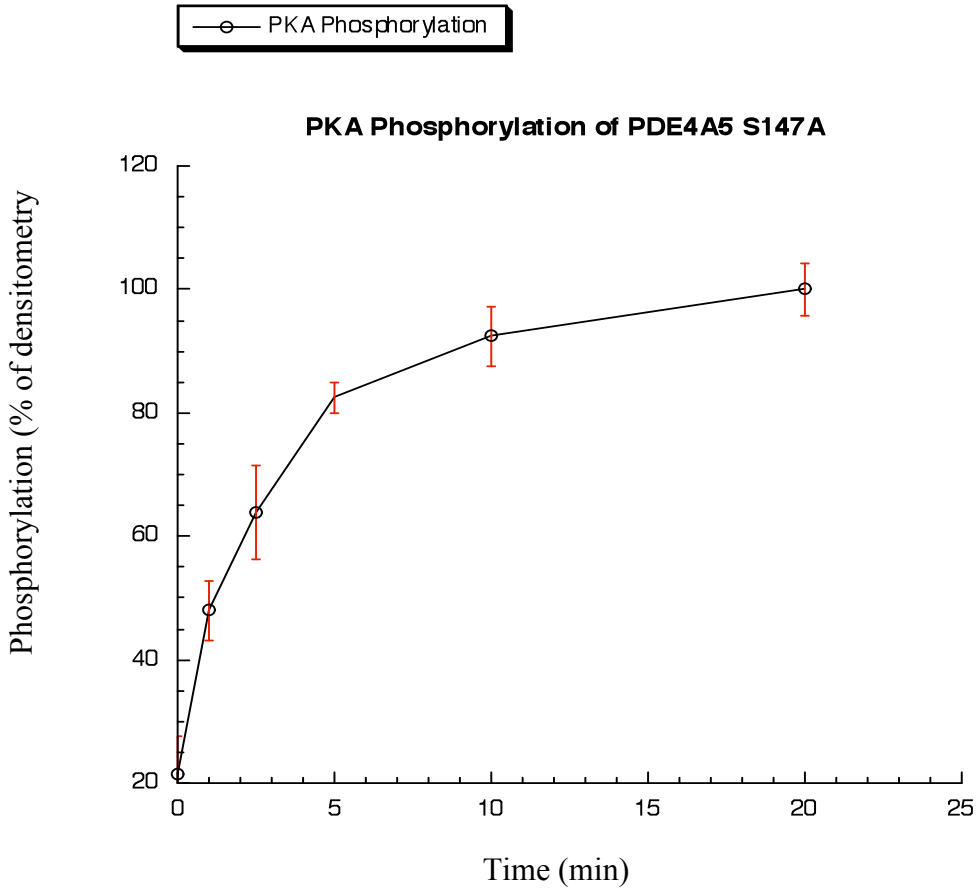

Figure 3.10 – Phosphorylation and act PKA.

COS1 cells were transfected to transiently express rat PDE4A5 with a mutation to alanine at serine 147, the predicted MAPKAPK2 phosphorylation site. The transfected cells were pre-treated for 10min with the non-specific PDE inhibitor, IBMX (100μM) before challenge, 0-20min, with the adenylyl cyclase activator, forskolin (100μM). (a), top panel, is a Western blot probed with a rat PDE4A C-terminal specific anti-serum to provide both loading and PDE4A5 expression controls. (a), bottom panel, is the same Western blot re-probed with the phospho-UCR1 specific anti-serum to the PKA phosphorylated serine (S*) residue within the RRES*F consensus motif [MacKenzie et al., 2002]. (b) shows the densitometry of the phospho-UCR1 time course, corrected for PDE4A5 expression. All data shown are representative Western blots of three separate transfections and experiments +/- standard deviation.

(a) PDE4A5 S147A mutant

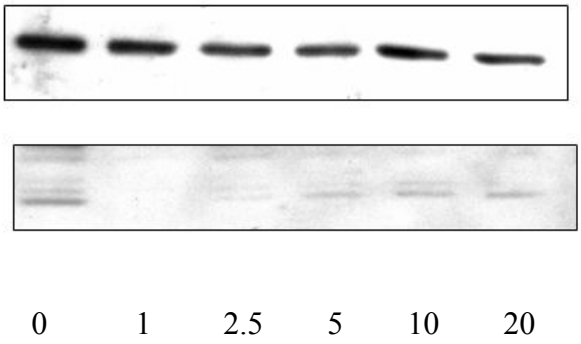

PDE 4A5 expression 100 kDa

PKA Phosphorylated PDE4A5 100 kDa

0 1 2.5 5 10 20

Time with Anisomycin (min)

(b)

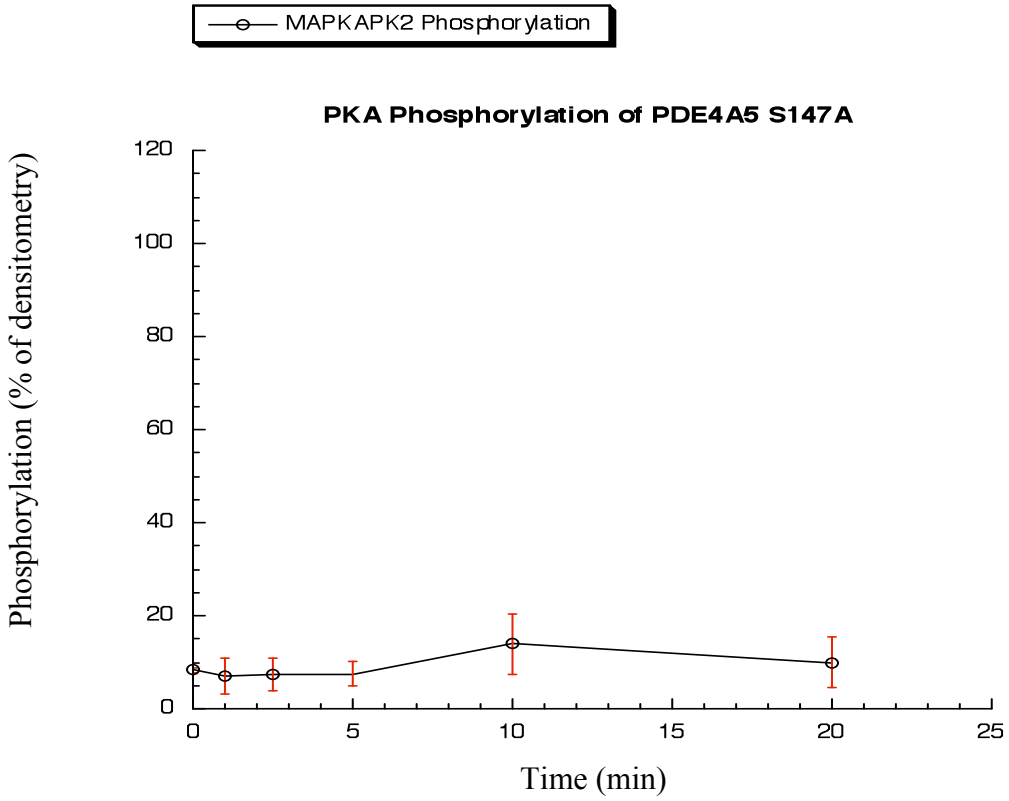

Figure 3.11 – Phosphorylation and activ

MAPKAPK2.

COS1 cells were transfected to transiently express rat PDE4A5 with a mutation to alanine at serine 147, the predicted MAPKAPK2 phosphorylation site. The transfected cells were treated for 60min with the p38 MAP Kinase activator, anisomycin (10μg/ml). (a), top panel, is a Western blot probed with a rat PDE4A C-terminal specific anti-serum to provide both loading and PDE4A5 expression controls. (a), bottom panel, is the same Western blot re-probed with the phospho-UCR1 specific anti-serum to the PKA phosphorylated serine (S*) residue within the RRES*F consensus motif [MacKenzie et al., 2002]. (b) shows the densitometry of the phospho-UCR1 time course, corrected for PDE4A5 expression. All data shown are representative Western blots of three separate transfections and experiments +/- standard deviation.

(a) PDE4A5 S147A mutant

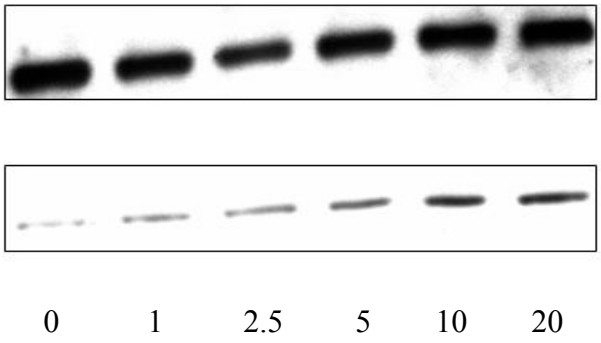

Time with Fsk (min) after Anisomycin and IBMX pre-treatment

(b)

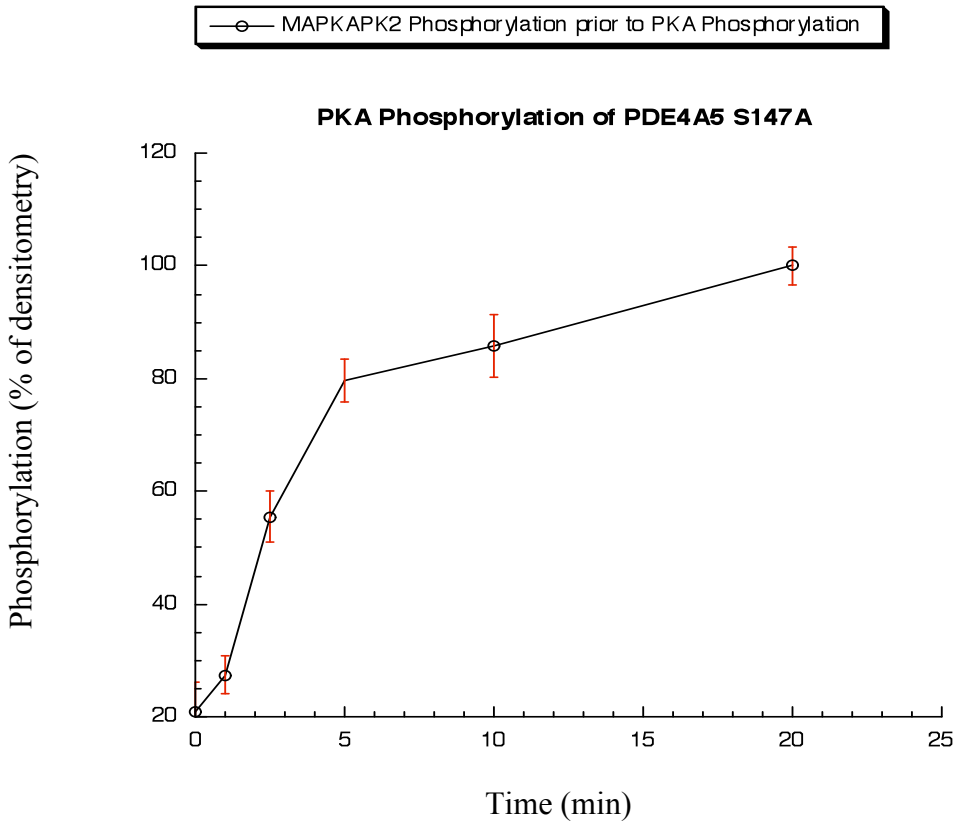

Figure 3.12 – Phosphorylation and a y PKA and MAPKAPK2.

COS1 cells were transfected to transiently express rat PDE4A5 with a mutation to alanine at serine 147, the predicted MAPKAPK2 phosphorylation site. The transfected cells were pre-treated for 30min with the p38 MAP Kinase activator, anisomycin (10μg/ml), then treated with 10min with the non-specific PDE inhibitor, IBMX (100μM) before challenge, 0-20min, with the adenylyl cyclase activator, forskolin (100μM). (a), top panel, is a Western blot probed with a rat PDE4A C-terminal specific anti-serum to provide both loading and PDE4A5 expression controls. (a), bottom panel, is the same Western blot re-probed with the phospho-UCR1 specific anti-serum to the PKA phosphorylated serine (S*) residue within the RRES*F consensus motif [MacKenzie et al., 2002]. (b) shows the densitometry of the phospho-UCR1 time course, corrected for PDE4A5 expression. All data shown are representative Western blots of three separate transfections and experiments +/- standard deviation.

3.2.2.2 Enzymatic Effect of MAPKAPK2 phosphorylation of PDE4A5.

As it has been established above that MAPKAPK2 phosphorylation of PDE4A5 has no effect on PKA phosphorylation of the enzyme it was then essential to establish whether phosphorylation had an effect on the function of the enzyme. To establish functionality of PDE4A5 the cell model of PDE4A5 transiently over expressed in COS1 cells was utilised again. Basal PDE4A5 enzymatic activity was established in unstimulated (resting) cells and taken as an activity level of 100% for further analysis, Figure 3.13. PKA was activated by pre-treatment with both IBMX, to block all PDE controlled cAMP degradation, plus the adenylyl cyclase activator, forskolin. PKA phosphorylation of PDE4A5 resulted in an increase in its enzymatic activity which, in a similar manner to that seen for the phosphorylation of PDE4A5, reached a plateau some 10-20 min after forskolin challenge with activity after 10 min challenge being some 266 +/- 5% above the control basal level and, at 20 min, some 280 +/- 4 % above the control basal level (mean ± SD; n= 3).

Phosphorylation of PDE4A5 by MAPKAPK2 was elicited by anisomycin treatment of transfected COS1 cells. This phosphorylation of PDE4A5 caused no change in PDE4A5 enzymatic activity above the basal level of 100%. However, perhaps most interestingly, when MAPKAPK2 phosphorylation of PDE4A5 was followed by PKA phosphorylation, the enzymatic activity was increased, showing that PKA phosphorylation can activate the MAPKAPK2-phosphorylated PDE4A5. However, the magnitude of activation by PKA was at a much lower level that seen with PKA phosphorylation alone, only ever reaching levels of 160 +/- 2% at 10 min and 174 +/- 4% at 20 min (mean ± SD; n=3) compared to the activity of non-PKA phosphorylated PDE4A5. This is significantly different to PKA phosphorylation alone with a p value of 0.021. These data suggest that, while MAPKAPK2 phosphorylation alone does not affect PDE4A5 activity, it acts to ablate the PKA phosphorylation induced increase in PDE4A5 activity.

Once again to establish that the effect of MAPKAPK2 was due to phosphorylation at Ser147 of PDE4A5 the Ser147Ala mutant and, additionally, a phosphorylation mimetic Ser147Asp mutant, were each transiently over expressed in COS1 cells and their enzymatic activity determined, Figure 3.14. Both mutants had a similar basal level of enzymatic activity to PDE4A5 wild type at 97 +/- 5% and 97 +/- 5% (mean ± SD; n=3) compared to wild-type PDE4A5. For subsequent comparative analyses then note that these were set to a relative activity level of 100%.

PKA phosphorylation of PDE4A5 Ser147Ala resulted in an increase in enzymatic activity, which reached a plateau at 10-20 min with activity at 20 min being 290 +/- 6% above the control (mean ± SD; n=3), untreated basal level. MAPKAPK2 phosphorylation of PDE4A5 Ser147Ala, like the wild type, showed no difference in enzymatic activity from the basal rate. However, in the case of prior MAPKAPK2 phosphorylation followed by PKA phosphorylation, the enzymatic activity was increased in a similar manner to that observed with PKA phosphorylation alone, attaining the same high rate of 287 +/- 4% at 20 min (mean ± SD; n=3), Figure 3.14(a).

Conversely PKA phosphorylation of PDE4A5 Ser147Asp resulted in a much slower increase in enzymatic activity, which reached plateau at the much lower level of 190 +/- 4% (mean ± SD; n=3) compared to the non-PKA phosphorylated form of this mutant enzyme. Strikingly, this reduction level of activation was similar to that observed upon PKA phosphorylation of the wild-type PDE4A5 that had been prior phosphorylated by MAPKAPK2 phosphorylation, which reached a plateau of activation at 183 +/- 7% (mean ± SD; n=3). Again no effect on the activity of the wild-type PDE4A5 was seen with MAPKAPK2 phosphorylation alone, Figure 3.14(b). These data suggest that, MAPKAPK2 is indeed phosphorylating PDE4A5 through Ser147, as when this site is mutated to alanine, which cannot be phosphorylated, then even when MAPKAPK2 and PKA are both activated in cells, PDE4A5 activity was increased to its maximal PKA phosphorylated state. Conversely, if Ser147 was mutated to the phosphorylation mimetic aspartate then, under conditions of PKA activation alone, PDE4A5 activity never rose to its full activation rate (Figure 3.14 (b)). Instead it rose to

only to approximately half of this, thereby mimicking the affect of pre-treatment of cells expressing wild-type PDE4A5 with anisomycin so as to MAPKAPK2 phosphorylate PDE4A5 prior to its phosphorylation by PKA.

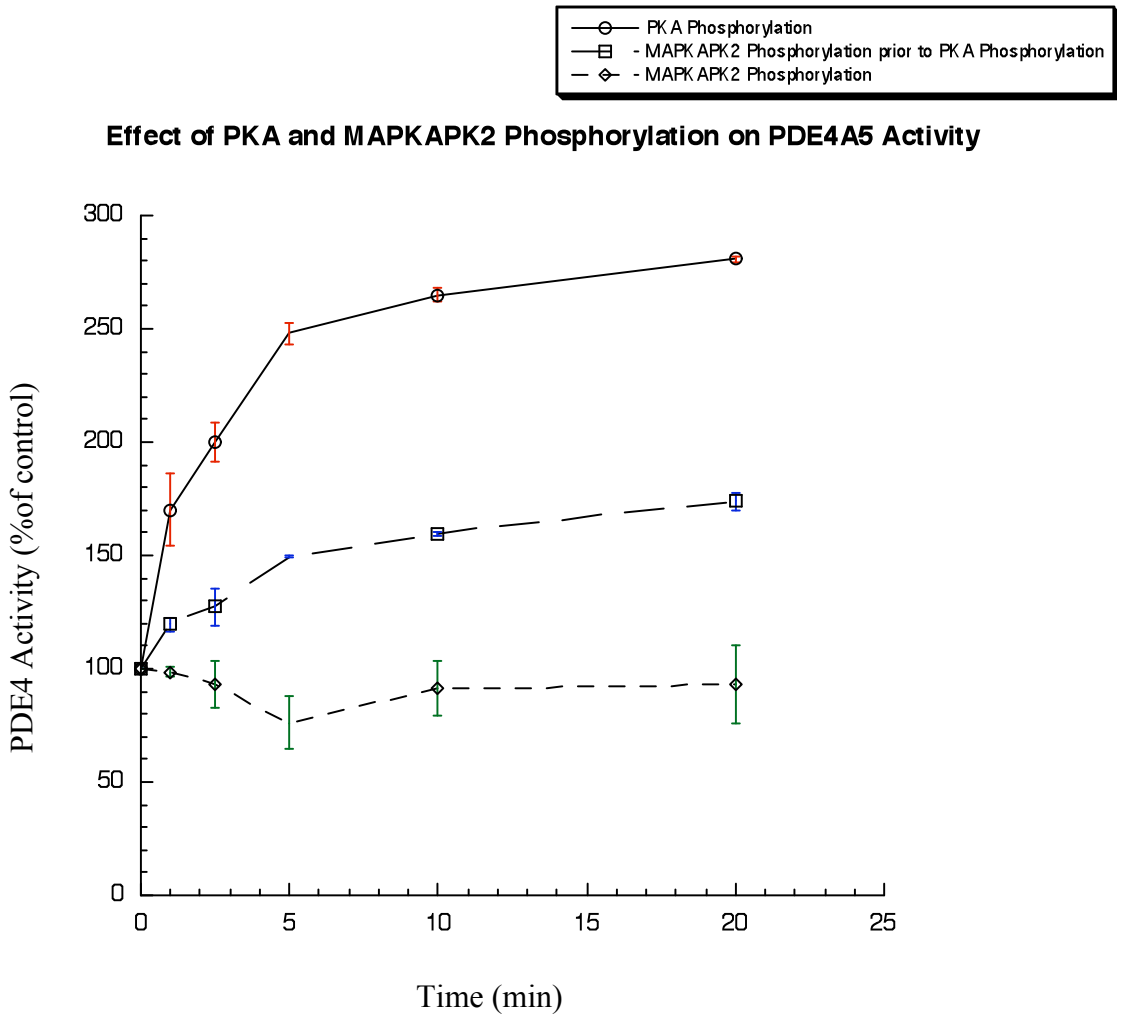

Figure 3.13 – Phosphoryla E4A5 by PKA and MAPKAPK2.

COS1 cells were transfected e rat PDE4A5. The transfected cells were subjected to three different treatments. They were either pre-treated for 10 min with the non-specific PDE inhibitor, IBMX (100µM) before challenge, 0-20 min, with the adenylyl cyclase activator, forskolin (100µM). Or they

were treated for 60 min with the p38 MAP Kinase pathway activator, anisomycin (10µg/ml). Or they were pre-treated for 30 min with anisomycin (10µg/ml), and then treated for 10 min with IBMX (100µM) before challenge, 0-20 min, with forskolin (100µM). The figure above shows the effect of PKA phosphorylation, MAPKAPK2 phosphorylation and MAPKAPK2 phosphorylation prior to PKA phosphorylation on PDE4A5 enzymatic activity. Assays were done using 1µM cAMP as substrate with COS1 cell lysates expressing equal immuno-reactive amounts of PDE4A5, as determined by the quantification of PDE4A5 expression. All data shown are mean data +/- standard deviation of the three separate transfections and experiments.

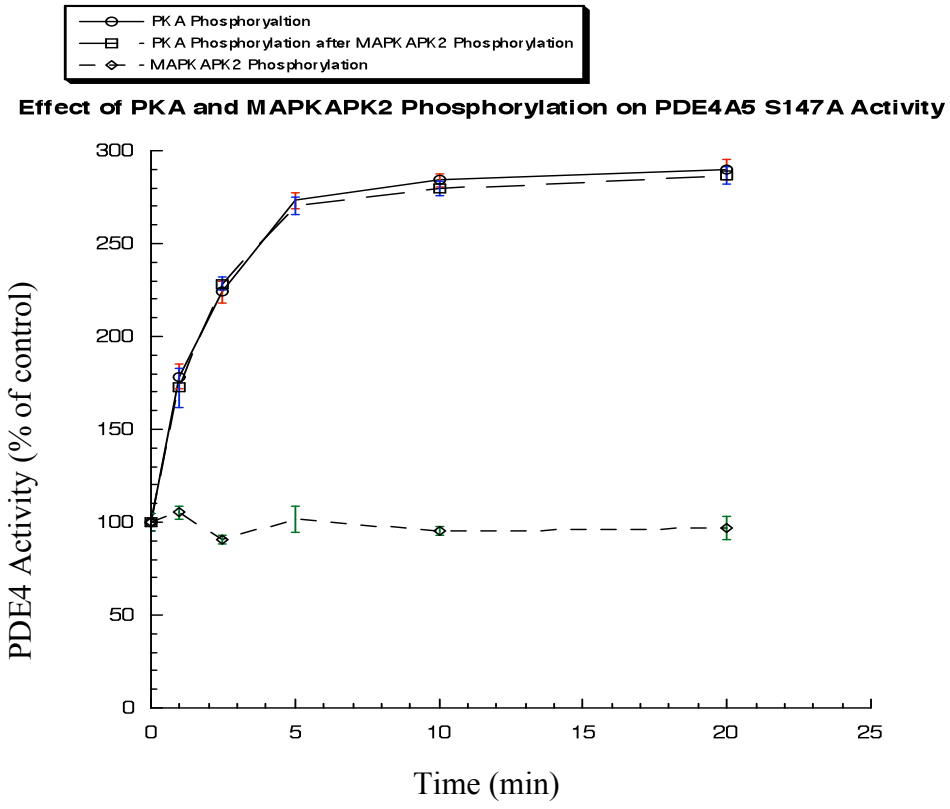

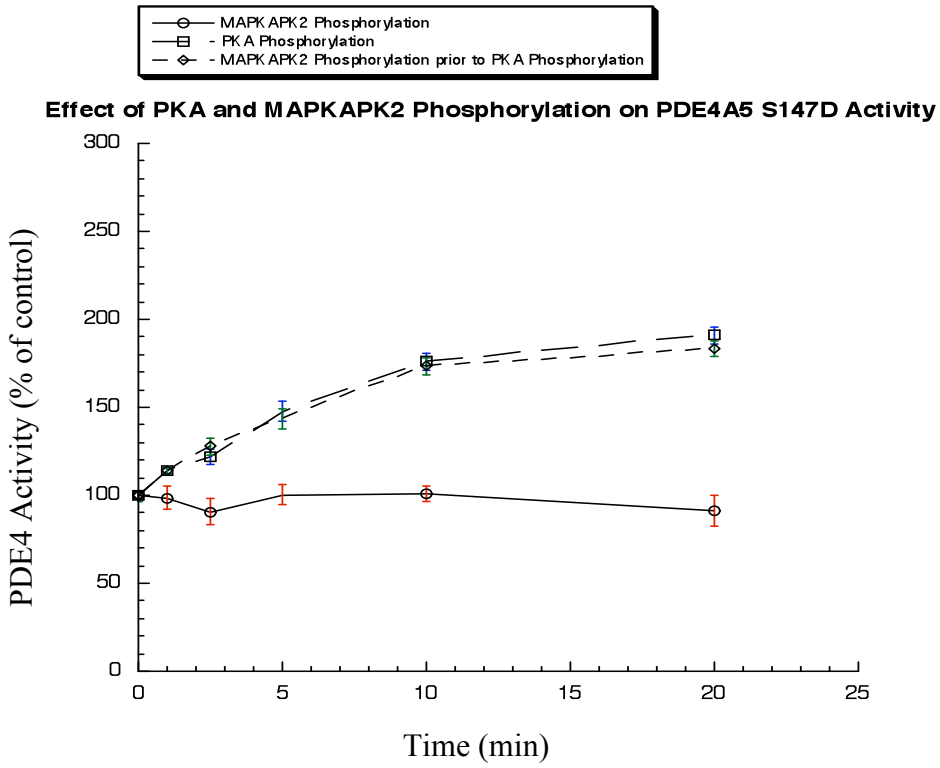

Figure 3.14 – Phosphorylation an A and S147D by PKA and MAPKAPK2.

COS1 cells were transfected to tran mutation to either alanine or aspartate at serine 147, tl rylation site. The transfected cells were subjected to three different treatments. They were either pre-treated for 10 min with the non-specific PDE inhibitor, IBMX (100 µM) before challenge, 0-20 min, with the adenylyl cyclase activator, forskolin (100 µM). Or they were treated for 60 min with the p38 MAP Kinase pathway activator, anisomycin (10 µg/ml). Or they were pre-treated for 30min with anisomycin (10 µg/ml), and then treated for 10min with IBMX (100uM) before challenge, 0-20min, with forskolin (100 µM). (a) shows the effect of PKA phosphorylation, MAPKAPK2 phosphorylation and MAPKAPK2 phosphorylation prior to PKA phosphorylation on PDE4A5 S147A enzymatic activity. Assays were done using 1µM cAMP as substrate with COS1 cell lysates expressing equal immuno-reactive amounts of PDE4A5 S147A, as determined by the quantification of PDE4A5 S147A expression. (b) shows the effect of PKA

phosphorylation, MAPKAPK2 phosphorylation and MAPKAPK2 phosphorylation prior to PKA phosphorylation on PDE4A5 S147D enzymatic activity. Assays were done using 1 μM cAMP as substrate with COS1 cell lysates expressing equal immuno-reactive amounts of PDE4A5 S147D, as determined by the quantification of PDE4A5 S147D expression. All data shown are mean data +/- standard deviation of the three separate transfections and experiments.

3.2.3 Cellular Response to MAPKAPK2 Phosphorylation of PDE4A5.

After establishing the effect of MAPKAPK2 phosphorylation on PDE4A5 it was important to understand how this might affect cellular metabolism of cAMP in the cell as a whole. This was done by measuring whole cell cAMP concentration in COS1 cells transiently over-expressing PDE4A5; a system that was used as a paradigm (Figure 3.15). In these experiments the diterpene, forskolin was used to activate adenylyl cyclase directly and, to allow comparison, cAMP levels within cells expressed as a percentage of resting cell level (taken as 100%). Doing this, intracellular cAMP reached a maximum of 236 +/- 9% at 5 min and returned to resting levels, 96 +/- 3%, by 15 min (mean ± SD; n=3). The transient nature of this rise is thought to be due to cAMP levels being raised in the cell and causing the activation of PKA which then phosphorylates and activates PDE4A5, leading to increased cAMP breakdown and a subsequent decrease in intracellular cAMP levels. To confirm that PKA activation plays a major factor influencing the transience fo this effect and so stimulating a decrease in cAMP concentration back to a basal level experiment were then performed with addition of the PKA inhibitor, KT5720 that was added prior to forskolin treatment. KT5720 pre-treatment resulted in a peak cAMP concentration of 246 +/- 2% occurring at 5 minutes however this level remained sustained for up to 15 min where it was 221 +/- 6% (mean ± SD; n=3). This shows that PKA activation plays a vital role in the regulation of cellular cAMP concentration after a period of 5 min, working as negative feedback regulator through activation of PDE4A5.

With this basic model of cellular cAMP concentration ascertained it was then crucial to discover if MAPKAPK2 phosphorylation plays a role regulating intracellular cAMP levels. Using the same cell model, anisomycin pre-treatment was carried out to activate the p38 MAPK cascade and cause PDE4A5 phosphorylation; this was followed by adenylyl cyclase activation through forskolin. Again cAMP concentration reached a peak level of 240 +/- 7% at 5 minutes however after 15 min, despite some lowering of cellular cAMP levels, the overall cAMP level only fell to 153 +/- 4% and not back to the basal steady-state level (mean ± SD; n=3). To confirm that this effect was due to activation of the p38 MAPK cascade an additional pre-treatment was done, in this case with SB203580, a specific p38 MAPK inhibitor. When this was carried out, forskolin challenge now showed peak cAMP concentration of 243 +/- 5% at 5 min and a return to basal rate of 97% +/- 7% after 15 min, mimicking the effect seen by simply challenging with forskolin alone (mean ± SD; n=3). These data show that activation of the p38 MAPK cascade within this cell system leads to a profound attenuation of the transient nature of cAMP accumulation subsequent to adenylyl cyclase activation. This appears to be achieved by it re-mapping the nature of the feed-back inhibition process driven by PKA activation of PDE4A5. It was then important to confirm if this was occurring through MAPKAPK2 phosphorylation of PDE4A5 as the experimental work above would imply.

Two cell models were created using COS1 cells, one transiently over-expressing the Ser147Ala-PDE4A5 MAPKAPK2 phosphorylation null mutant, Figure 3.16(a), and one transiently over-expressing the Ser147Asp-PDE4A5 MAPKAPK2 phosphorylation mimetic mutant, Figure 3.16(b). These models were both subjected to (i) forskolin treatment alone, to activate adenylyl cyclase and raise cAMP levels; (ii) KT5720 pre-treatment followed by forskolin treatment, to inhibit PKA activation and raise cellular cAMP and (iii) anisomycin pre-treatment followed by forskolin treatment, to activate the p38 MAPK cascade and raise cAMP levels.

In the case of the Ser147Ala-PDE4A5 mutant, when adenylyl cyclase was activated cAMP concentration in the cell reached a maximum of 256 +/- 5% at 5 min

and returned fully to resting rate 93 +/- 7% by 15 min (mean ± SD; n=3) . Then using the PKA inhibitor KT5720 before forskolin treatment, peak cAMP concentration of 260 +/- 2% occurs at 5 min and this level remained sustained up to 15 min where it was 230 +/- 3% (mean ± SD; n=3). This implies that in cell model expressing Ser147Ala-PDE4A5 cAMP concentration is controlled similarly to the wild type PDE4A5 in that adenylyl cyclase raises cellular cAMP concentration and PKA operates a negative feedback loop of this through Ser147Ala-PDE4A5. However when the p38 MAPK cascade was activated prior to raising cAMP levels cellular cAMP level rose to 248 +/- 8% at 5 min and fell back to basal rate of 87 +/- 7% after 15 min (mean ± SD; n=3) . This lack of effect implies that in the wild type PDE4A5 system the p38 MAPK cascade is exhibiting its effect through MAPKAPK2 phosphorylation of PDE4A5. This concept is confirmed using the Ser147Asp-PDE4A5 phosphorylation mimetic mutant where under adenylyl cyclase activation alone cAMP concentration rises to 251 +/- 2% but after 15 min only falls to 157 +/- 7%, not the basal level (mean ± SD; n=3).

These data show that MAPKAPK2 phosphorylation of PDE4A5 acts to attenuate the PKA phosphorylation induced activation of PDE4A5. This has a functional consequence in cells in re-mapping the functionality of the feedback cycle focused on PDE4A5 and mediated by PKA. This changes the profound transience of cAMP accumulation to one where a sustained increase in cellular cAMP levels is evident.

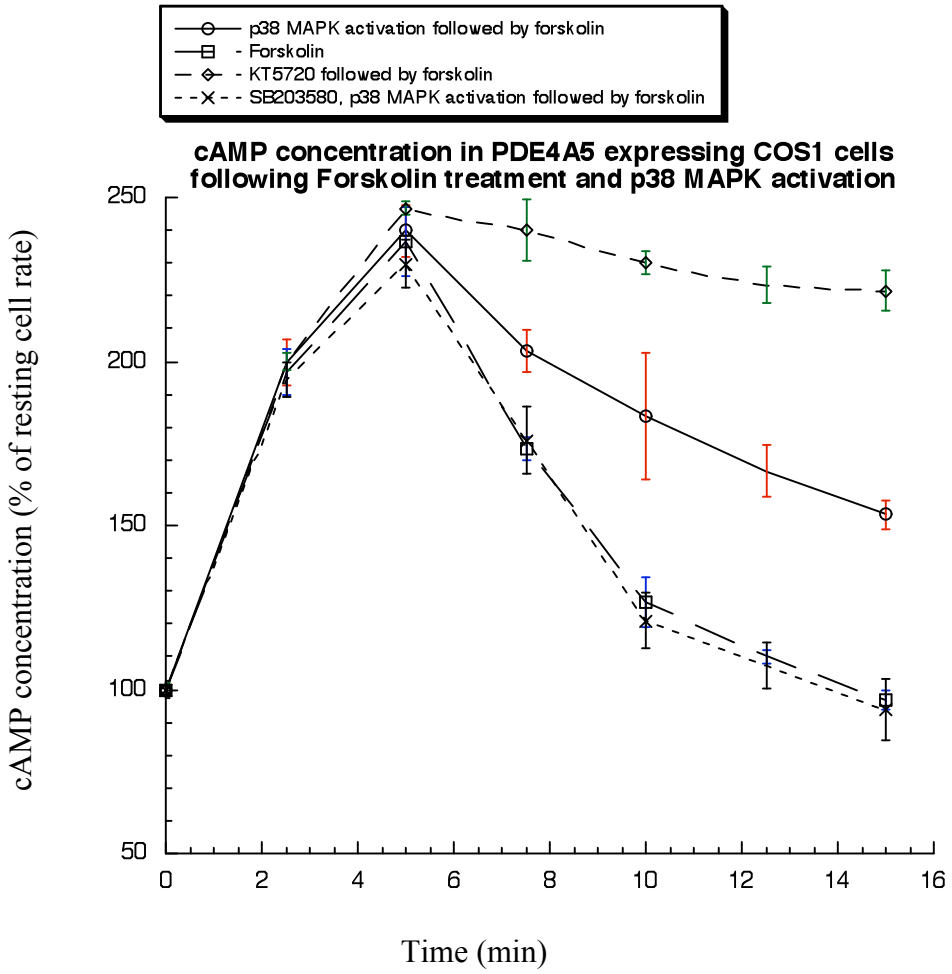

Figure 3.15 – Cellular cyclic expressing cells following Phosphorylation by PK

COS1 cells were transfected to at PDE4A5. The transfected cells were subjected to one of four pre-treatments: pre-treated with anisomycin (10 µg/ml) for 30 min to activate MAPKAPK2. Pre-treated with KT5720 (10 µM) for 30 min to block PKA activation. Pre-treated with SB203580 (25 µM) to inhibit the p38 MAP kinase pathway for 30 min followed by anisomycin (10µg/ml) treatment for 30 min to activate MAPKAPK2. And lastly, without pre-treatment. The cells were then subjected to a 0-15 min time course with Forskolin (100 µM) to activate PKA. The figure above shows cAMP concentration in cells following these treatments. cAMP concentration within the cell was measured using a commercial cAMP

competitive ELISA assay kit. cAMP concentration is measured as a percentage of resting cell cAMP concentration. All data shown are mean data +/- standard deviation of three separate transfections and experiments.

(a)

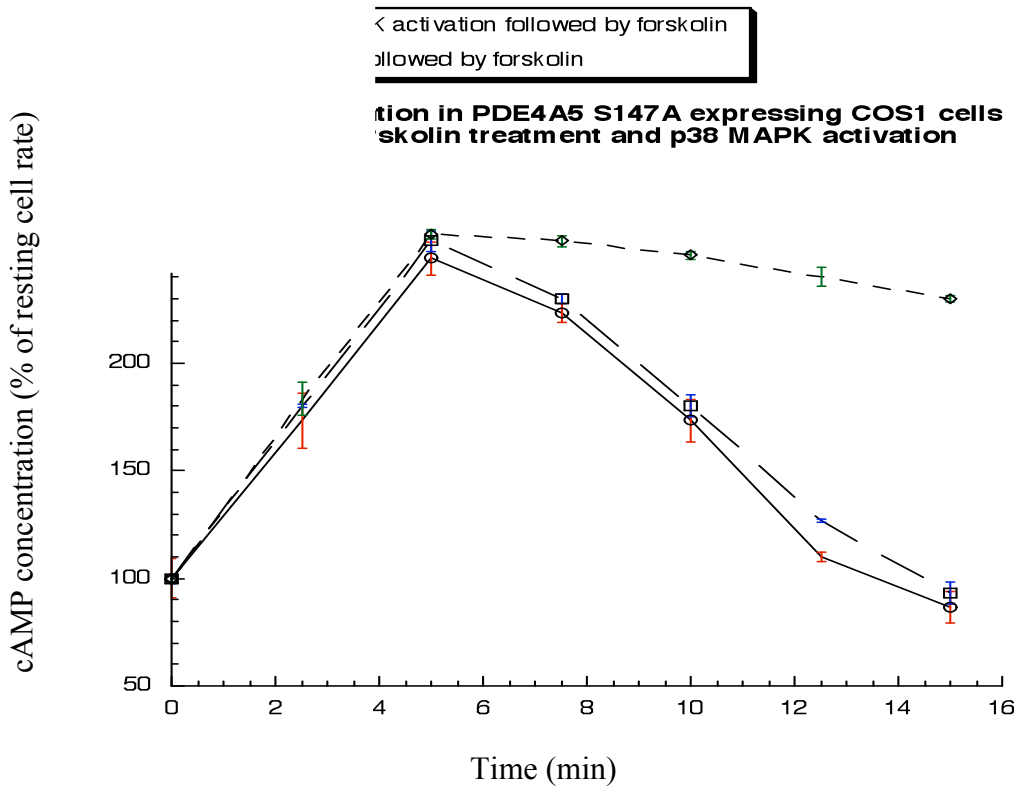

(b)

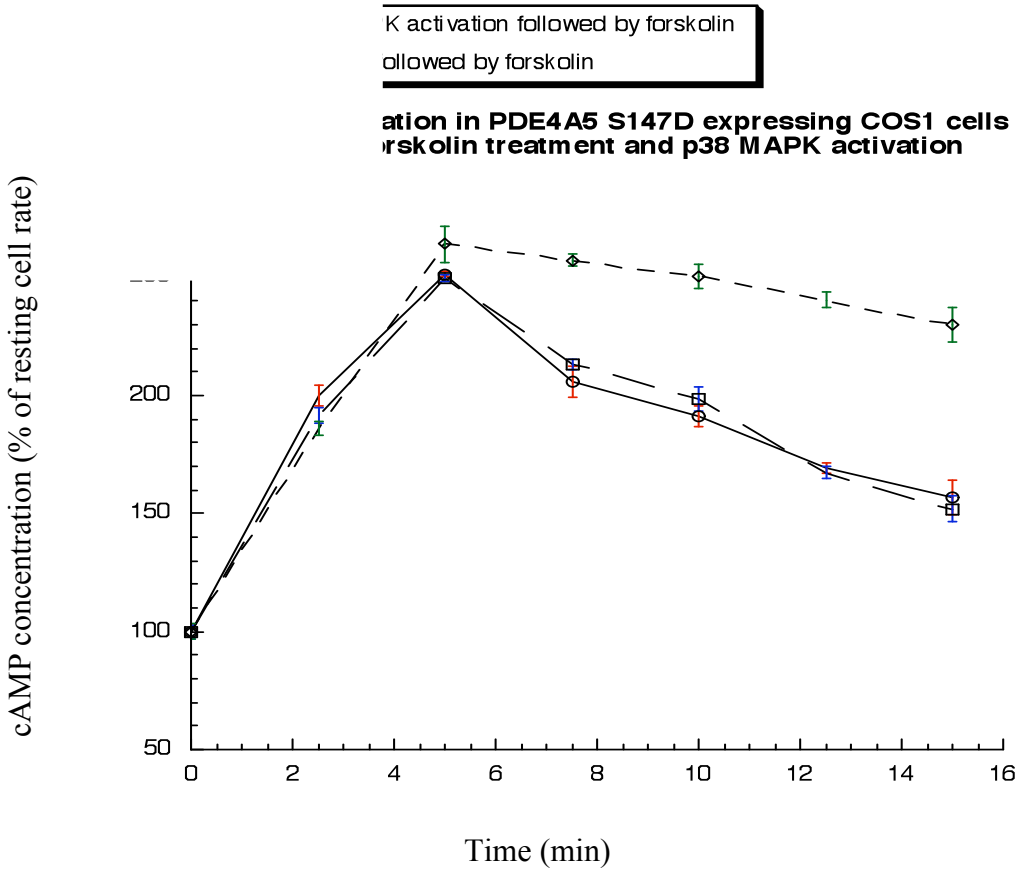

Figure 3.16 – Cellular cyclic AMP cc nd S147D expressing cells following Phosphory

COS1 cells were transfected to transie tation to either (a) alanine or (b) aspartate at Ser147, the predicted MAPKAPK2 phosphorylation site. The transfected cells were subjected to one of three pre-treatments: pre-treated with anisomycin (10 µg/ml) for 30 min, pre-treated with KT5720 (10 µM) for 30 min or without pre-treatment. The cells were then subjected to a 0-15 min time course with Forskolin (100 µM). The figure above shows cAMP concentration in cells following these treatments. cAMP concentration within the cell was measured using a commercial cAMP competitive ELISA assay kit. cAMP concentration is measured as a percentage of resting cell cAMP concentration. All data shown are mean data +/- standard deviation of three separate transfections and experiments.

3.2.4 Rolipram Inhibition of MAPKAPK2 Phosphorylated PDE4A5

As previously mentioned PDE4A5 can exhibit two binding states for rolipram [Jacobitz et al., 1996], the normal Low Affinity Rolipram Binding State (LARBS) and the higher sensitivity state, High Affinity Rolipram Binding State (HARBS). It was therefore important to establish if MAPKAPK2 phosphorylation of PDE4A5 altered its level of inhibition, and therefore binding affinity, of the PDE4 inhibitor rolipram. A cell model of COS1 cells transiently transfected to express PDE4A5 was exposed to MAPKAPK2 phosphorylation alone, PKA phosphorylation alone and MAPKAPK2 phosphorylation prior to PKA phosphorylation (all treatments as described previously), Figure 3.17(a). PDE enzymatic activity was then measured in a basal state and in the presence of rolipram. This showed that using 10 μM of rolipram for non-phosphorylated PDE4A5, PDE activity was inhibited by 50 +- 5% (mean ± SD; n=3). Similarly this was the case for MAPKAPK2 phosphorylated PDE4A5 where PDE activity at the basal rate was 99 +/- 3% and 47 +/- 7% in the rolipram inhibited state, PKA phosphorylated PDE4A5 where PDE activity at the basal rate was 265 +/- 4% and 137 +/- 3% in the rolipram inhibited state and MAPKAPK2 and PKA phosphorylated PDE4A5 where PDE activity at the basal rate was 160 +/- 2% and 85 +/- 4% in the rolipram inhibited state. These data show that PKA phosphorylation, MAPKAPK2 phosphorylation and a combination of both do not affect the ability of rolipram to inhibit PDE4A5. To confirm mutations at the MAPKAPK2 mutation site Ser147 had no affect on rolipram inhibition either the above experiment was repeated with COS1 cells transiently expressing Ser147Ala-PDE4A5 (Figure 3.17(b)) and Ser147Asp-PDE4A5 (Figure 3.17(c)) respectively. This showed that using the optimal EC_{50} concentration of rolipram for non-phosphorylated PDE4A5, PDE activity was inhibited by 50 +- 5%. Similarly this was the case for MAPKAPK2 phosphorylated Ser147Ala-PDE4A5 and Ser147Asp-PDE4A5, where PDE activity at the basal rate was 94 +/- 4% and 41 +/- 4%; and 102 +/- 4% and 48 +/- 2% respectively in the rolipram inhibited state, PKA phosphorylated Ser147Ala-PDE4A5 and Ser147Asp-PDE4A5, where PDE activity at the basal rate was 275 +/- 6% and 143 +/- 4%; and 162 +/- 5% and 79 +/- 7%, respectively, in the rolipram inhibited state and MAPKAPK2 and PKA phosphorylated Ser147Ala-PDE4A5 and

Ser147Asp-PDE4A5, where PDE activity at the basal rate was 275 +/- 6% and 136 +/- 4%; and 164 +/- 3% and 81+/- 4% respectively in the rolipram inhibited state. These data show that mutation of PDE4A5 at Ser147 to either alanine or aspartate does not affect the ability of rolipram to inhibit the enzyme. All data are mean ± SD; n=3.

(a)

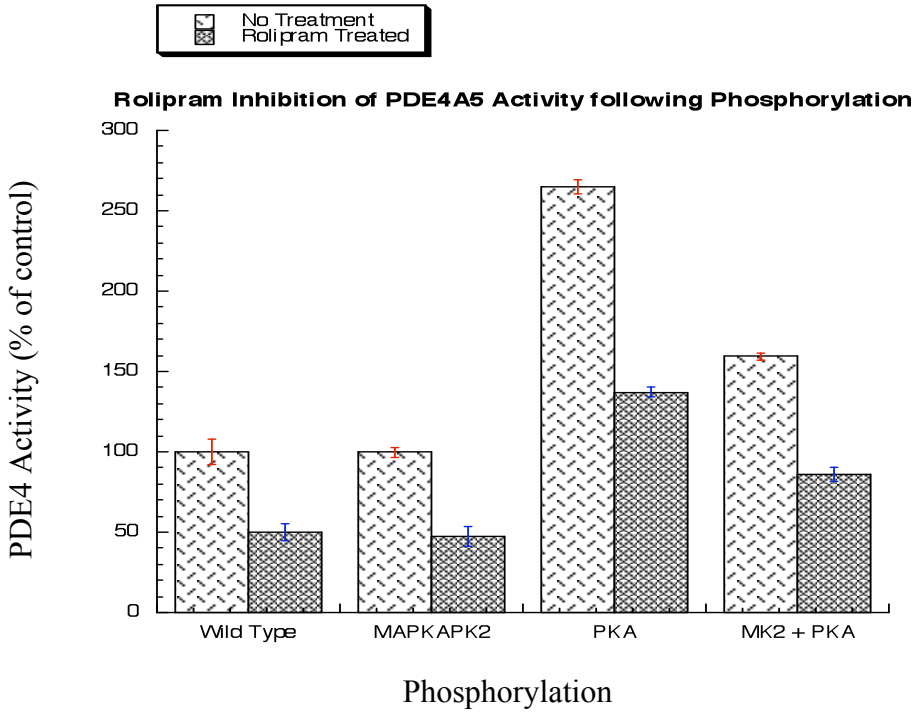

(b)

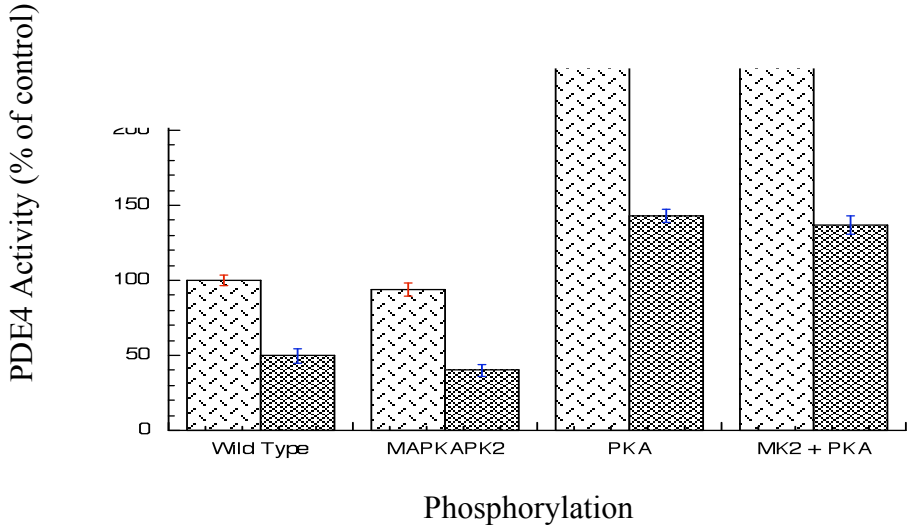

(c)

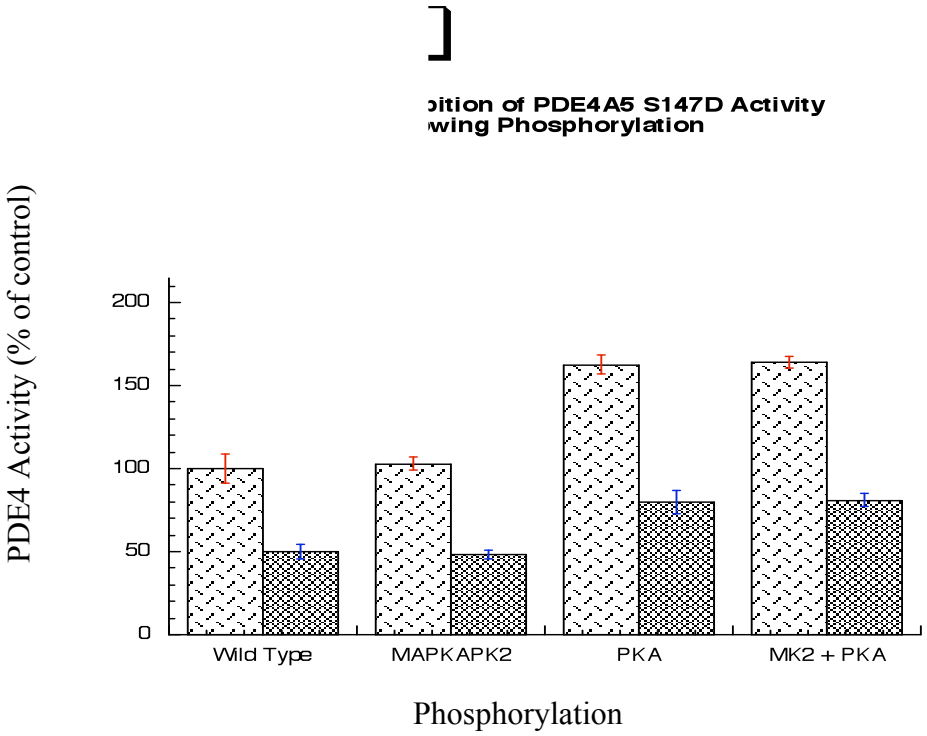

Figure 3.17 – Inhibition of rat S147D mutants activity by rolipram, following pl KAPK2.

COS1 cells were transfected to transiently express either (a) wild type rat PDE4A5, (b) PDE4A5 with a mutation to alanine at Ser147, or (c) PDE4A5 with a mutation to aspartate at Ser147. The transfected cells were subjected to three different treatments. They were either pre-treated for 10min with the non-specific PDE inhibitor, IBMX (100 µM) before 20 min challenge with the adenylyl cyclase activator, forskolin (100 µM), treated for 60 min with the p38 MAP Kinase pathway activator, anisomycin (10 µg/ml). Or they were pre-treated for 30min with anisomycin (10 µg/ml), and then treated for 10min with IBMX (100 µM) before 20min challenge with forskolin (100 µM). Phosphodiesterase activity assays were carried out under resting cell conditions and in presence of the PDE4 inhibitor Rolipram (10uM). Assays were done using 1µM cAMP as substrate with COS1 cell lysates expressing equal immuno-reactive amounts of (a) PDE4A5 wild type, (b) PDE4A5 Ser147Ala or (c) PDE4A5 Ser147Asp as determined

by the quantification of expression. All data shown are mean data +/- standard deviation of the three separate transfections and experiments.

3.2.5 Thermo-stability of PDE4A5 after Phosphorylation

At this juncture I wished to try and gain evidence that MAPKAPK2 phosphorylation of PDE4A5 caused a conformational change in PDE4A5 that might be consistent with my observation that it caused a decrease in the ability of PKA to activate PDE4A5. As shown previously this was not due to hindrance of PKA phosphorylation. Thus as far as activity changes occur, any such conformational change caused by MAPKAPK2 phosphorylation is effectively silent until the enzyme is PKA phosphorylated. Conformational changes can, however, be expected to affect the stability of proteins. This can very simply be assessed using a thermal inactivation procedure. The denaturation of proteins by heat occurs as a first-order process that, in the case of enzymes, can be followed by analysis of the exponential decay in their catalytic activity. A semi-log plot of the log % activity remaining against time thus allows for a determination of the half-life of inactivation ($t_{1/2}$).

Using a cell model of COS1 cells over-expressing PDE4A5 subjected to the various conditions described previously, treatment at 55°C causes the inactivation of PDE4A5 as a single exponential, Figure 3.18. From the data it is shown that wild type PDE4A5 reaches a half-life of inactivation at approximately 7.5 min. However if cells expressing PDE4A5 are subjected to forskolin treatment to increase intracellular cAMP levels and activate PKA and PDE4A5 taken for thermal inactivation studies then a half-life of inactivation is not reached until approximately 12 minutes. This shows that PKA phosphorylation of PDE4A5 results in an increase in structural stability of the enzyme. When MAPKAPK2 phosphorylation of PDE4A5 using the p38 MAPK activator was elicited then the half-life of inactivation of the enzyme decreased slightly from the wild-type non-phosphorylated enzyme, to a level of approximately 6.5 min implying that

MAPKAPK2 phosphorylation of PDE4A5 is responsible for decreased structural stability of the enzyme. This result was confirmed to be due to the p38 MAPK pathway through use of the p38 MAPK inhibitor SB203580, which took the half-life of inactivation back to approximately 7.5 min, a similar rate to that of wild type non-phosphorylated PDE4A5.

I then set out to see how MAPKAPK2 phosphorylation in combination with PKA phosphorylation affected the stability of PDE4A5. Pre-treatment with anisomycin followed by adenylyl cyclase activation by forskolin resulted in the half-life of inactivation of approximately 4.5 min. This is significantly lower than the half-lives seen for the non-phosphorylated wild type PDE4A5, for PKA phosphorylated PDE4A5 and for MAPKAPK2 phosphorylated PDE4A5. This implies that dual phosphorylation of PDE4A5 by PKA and MAPKAPK2 leads to a distinct change in structure, seen here as a loss of thermal stability. This is consistent with my data showing that after these phosphorylation events, MAPKAPK2 phosphorylation has a functional effect on PDE4A5 in attenuating its ability to be activated by PKA.

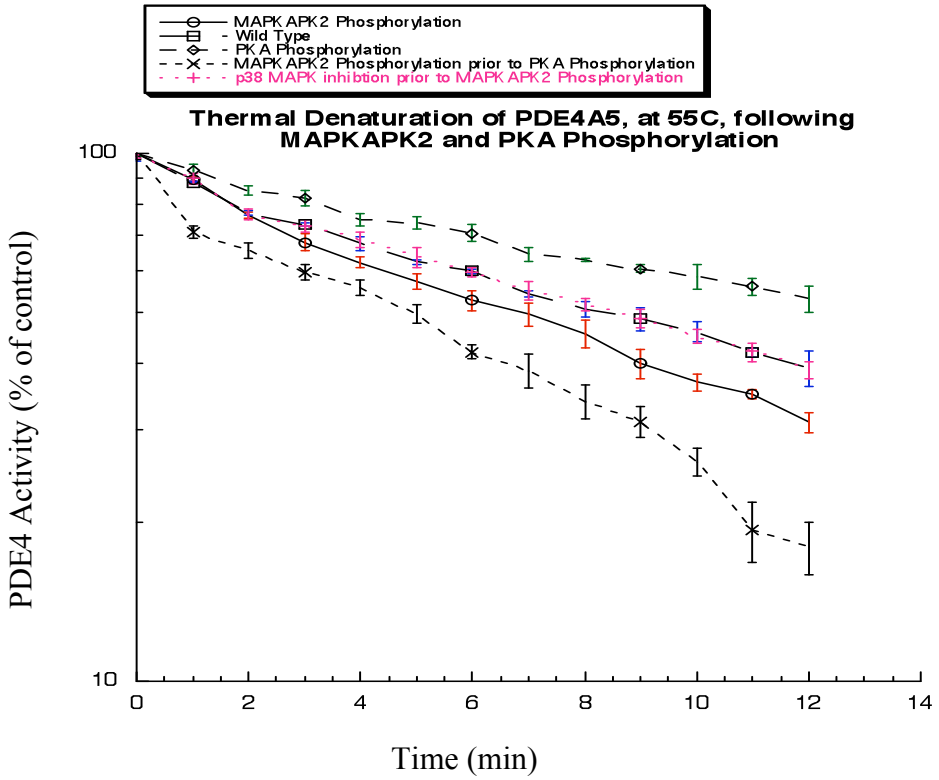

Figure 3.18 – Thermo-stability of l

Recombinant PDE4A5 was transier transfected cells were subjected to one of four treatm g/ml) for 60 min to activate MAPKAPK2, treated for 10min with IBMX (100 µM) before 20 min Forskolin (100 µM) challenge to activate PKA, pre-treated with anisomycin (10 µg/ml) for 30min then treated for 10min with IBMX (100 µM) before 20min Forskolin (100µM) challenge to activated MAPKAPK2 prior to PKA activation, or pre-treated with SB203580 (25 µM) to 30 min followed by anisomycin (10 µg/ml) treatment for 30 min, to block them stimulate activation of MAPKAPK2 through the p38 MAPK cascade. Total cell lysate was produced. Lysates were incubated at 55°C for the indicated times and then assayed for PDE4 activity using 1 µM cAMP as substrate. The log% residual activity was calculated and plotted as a function of increasing time. The half-life ($t_{1/2}$) was determined as the time at which 50% of the total PDE4 activity at time zero remained. Data shown are from three separate experiments using fractions

from three separate transfections and are expressed as mean values +/- standard deviation.

3.2.6 PDE4D3 is Phosphorylated by MAPKAPK2.

Now that the role of MAPKAPK2 phosphorylation in PDE4A5 function and activity has been established it raises question as to whether PDE4A5 is the only long form PDE4 that undergoes these phosphorylation events. As stated previously PDE4A5 plays an important role in inflammation along with the p38 MAP Kinase cascade [Schieven, 2005] but its expression levels are low in most cell systems where the PDE4D family are the largest expressed PDE4 group. Under analysis of sequence line ups of PDE4A5 and all other long form PDE4 isoforms consensus is seen between the UCR1 phosphorylation sites of the enzymes. Indeed PDE4D3 contains a consensus MAPKAPK2 phosphorylation site identical to that found in PDE4A5, namely Leu-Tyr-Arg-Ser-Asp-Ser-Asp. This sequence fits exactly the MAPKAPK2 phosphorylation consensus motif previously discovered: Ø-X-Arg-X-X-Ser-Ø, where Ø are hydrophobic amino acids and X is any amino acid. [Stokoe et al., 1993; Rousseau et al., 2005]. To confirm if PDE4D3 is phosphorylated by MAPKAPK2 enzymatic activity studies were carried out, similar to those shown above with PDE4A5. To establish functionality of PDE4D3 the cell model of PDE4D3 transiently over expressed in COS1 cells was utilised again. Basal PDE4D3 enzymatic activity was established in unstimulated cells and taken as an activity level of 100% for further analysis, Figure 3.19(a). PKA phosphorylation of the enzyme resulted in an increase in enzymatic activity of PDE4D3, which reaches a plateau at 10-20 min with activity at 10min being 240 +/- 7% and at 20 min being 269 +/- 15%, above the control basal level. MAPKAPK2 phosphorylation of PDE4D3 showed no altering in enzymatic activity above the basal level of 100%. Then when MAPKAPK2 phosphorylation of PDE4D3 was followed by PKA phosphorylation, the enzymatic activity was increased, as with PKA phosphorylation alone, but the increase occurred at a slower rate and plateaus at a much lower level only

ever reaching levels of 174 +/- 3% at 10 min and 182 +/- 4% at 20 min. These data suggest that PDE4D3 undergoes phosphorylation by MAPKAPK2 resulting in similar enzymatic effects in that, while MAPKAPK2 phosphorylation alone does not affect PDE4D3 activity, it acts to ablate the PKA phosphorylation induced increase in PDE4D3 activity. (mean ± SD; n=3)

To confirm this effect of MAPKAPK2 was due to its phosphorylation of PDE4D3 mutants of the potential MAPKAPK2 phosphorylation site on PDE4D3 were made. This site was, from the sequence line up data, Ser61 on PDE4D3 and mutations were made at this site to alanine, to act as a MAPKAPK2 phosphorylation null mutant and to aspartate a phosphorylation mimetic mutant. These were separately transiently over expressed in COS1 cells and their enzymatic activity established, Figure 3.19(b) and (c). Both mutants had a similar basal level of enzymatic activity to PDE4D3 wild type (80 +/- 5 %; n= 3) and were set to activity level of 100% for comparative analyses. PKA phosphorylation of Ser61Ala-PDE4D3 resulted in an increase in enzymatic activity, which reaches a plateau at 10-20 min with activity at 20 min being 264 +/- 6% above the control basal level. MAPKAPK2 phosphorylation of Ser61Ala-PDE4D3, like the wild type, showed no difference in enzymatic activity from the basal rate but in the case of MAPKAPK2 phosphorylation followed by PKA phosphorylation, the enzymatic activity was increased, as with PKA phosphorylation alone, to the same high rate of 257 +/- 5% at 20 min, Figure 3.19(b). Conversely PKA phosphorylation of Ser61Asp-PDE4D3 resulted it was at a slower increase in enzymatic activity, which reaches plateau at the much lower level of 186 +/- 3%. This level was similar to MAPKAPK2 phosphorylation followed by PKA phosphorylation of Ser61Asp-PDE4D3, which reaches its plateau at 190 +/- 2%. Again no effect on activity was seen with MAPKAPK2 phosphorylation alone, Figure 3.19(c). These data suggest that, MAPKAPK2 is indeed phosphorylating PDE4D3 through Ser61 giving highly similar results to those shown with PDE4A5 Ser147 mutants. These data indicate that some otherPDE4 long forms can be phosphorylated by MAPKAPK2 resulting in ablation of PKA phosphorylation induced increase in PDE4 activity. (mean ± SD; n=3)

(a)

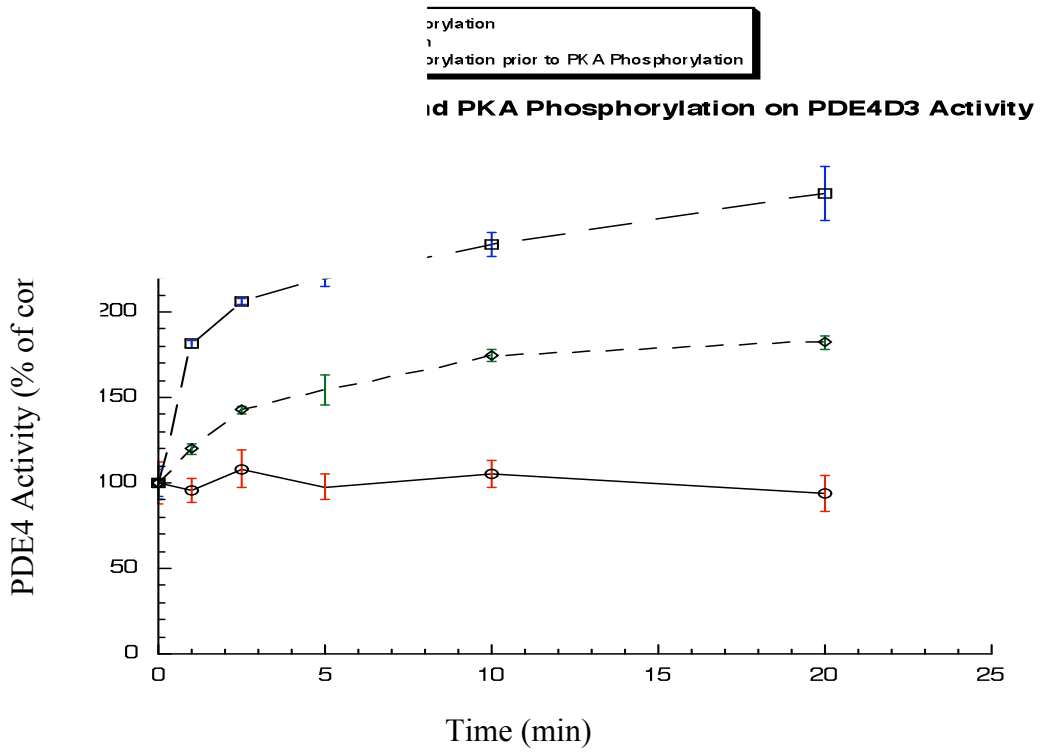
orylation
orylation prior to PKA Phosphorylation
d PKA Phosphorylation on PDE4D3 Activity
PDE4 Activity (% of cor
200
150
100
50
0
0
5
10
15
20
25
Time (min)

(b)

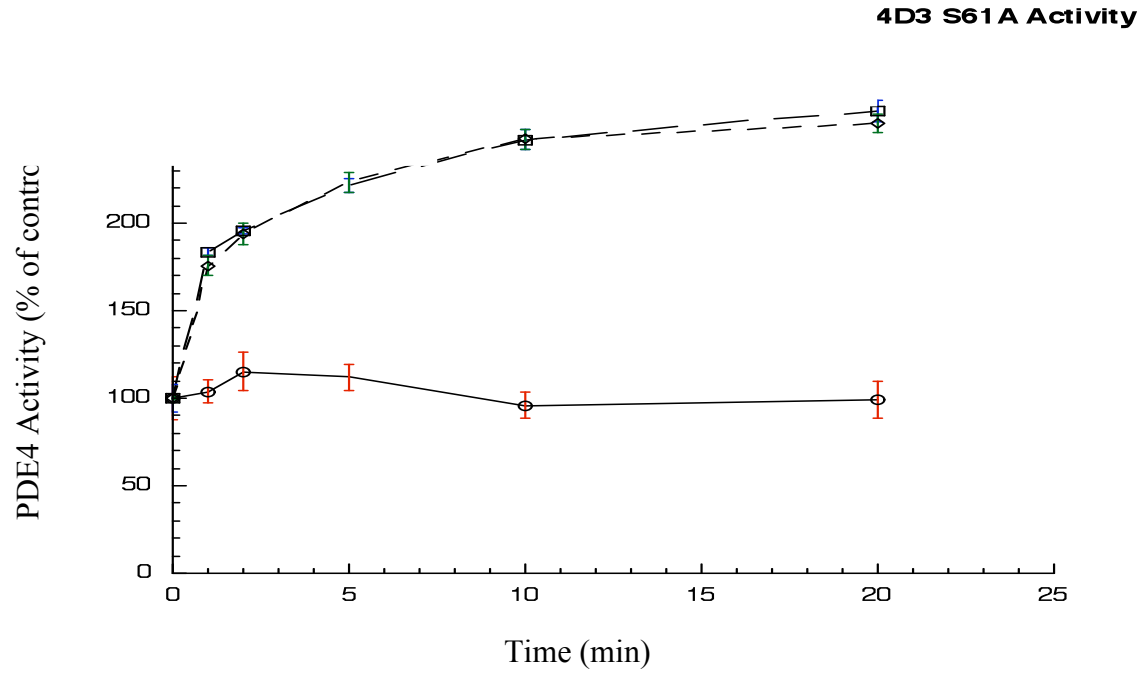
4D3 S61A Activity
PDE4 Activity (% of contrc
200
150
100
50
0
0
5
10
15
20
25
Time (min)

(c)

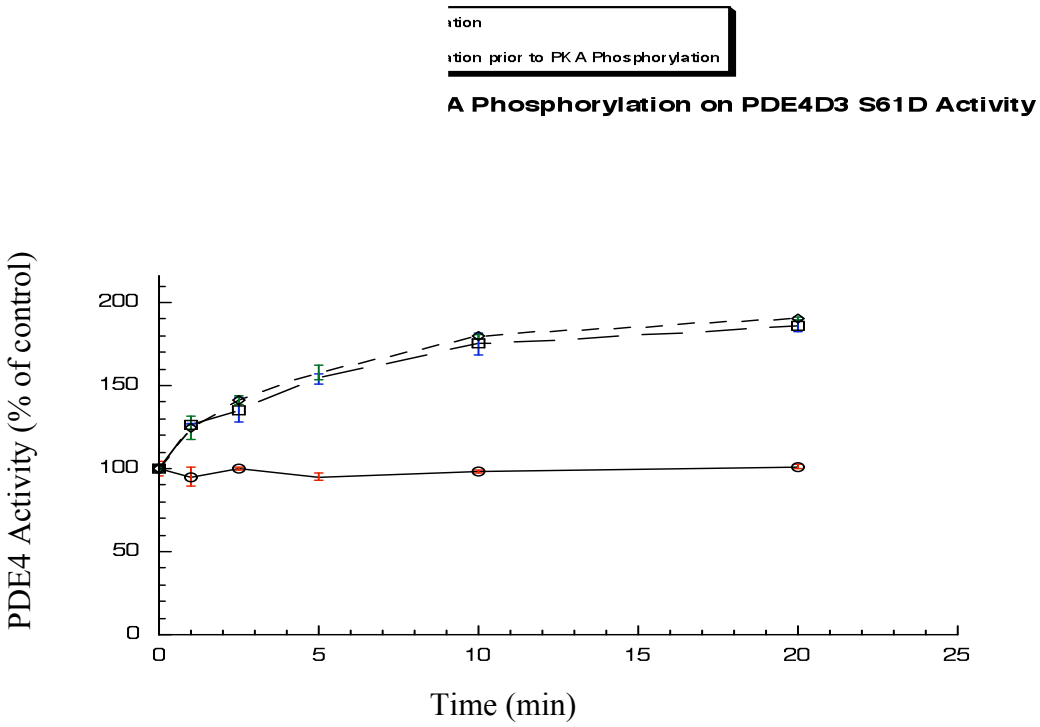

Figure 3.19 – Phosphorylation and ype, S61A and S61D by PKA and MAPKAPK2.

COS1 cells were transfected to trans ype, or with a mutation to either alanine or aspartate at Ser61, the predicted MAPKAPK2 phosphorylation site. The transfected cells were subjected to three different treatments. They were either pre-treated for 10 min with the non-specific PDE inhibitor, IBMX (100 µM) before challenge, 0-20 min, with the adenylyl cyclase activator, forskolin (100 µM). Or they were treated for 60min with the p38 MAP Kinase pathway activator, anisomycin (10 µg/ml). Or they were pre-treated for 30min with anisomycin (10 µg/ml), and then treated for 10 min with IBMX (100 µM) before challenge, 0-20 min, with forskolin (100 µM). (a) shows the effect of PKA phosphorylation, MAPKAPK2 phosphorylation and MAPKAPK2 phosphorylation prior to PKA phosphorylation on PDE4D3 enzymatic activity. Assays were done using 1µM cAMP as substrate with COS1 cell lysates expressing equal immuno-reactive amounts of PDE4D3, as determined by the quantification of PDE4D3 expression. (b) shows the effect of PKA

phosphorylation, MAPKAPK2 phosphorylation and MAPKAPK2 phosphorylation prior to PKA phosphorylation on PDE4D3 Ser61Ala enzymatic activity. Assays were done using 1μM cAMP as substrate with COS1 cell lysates expressing equal immuno-reactive amounts of PDE4D3 Ser61Ala, as determined by the quantification of PDE4D3 S61A expression. (c) shows the effect of PKA phosphorylation, MAPKAPK2 phosphorylation and MAPKAPK2 phosphorylation prior to PKA phosphorylation on PDE4D3 S61D enzymatic activity. Assays were done using 1μM cAMP as substrate with COS1 cell lysates expressing equal immuno-reactive amounts of PDE4D3 Ser61Asp, as determined by the quantification of PDE4D3 S61D expression. All data shown are mean data +/- standard deviation of the three separate transfections and experiments.

3.3 Discussion

The p38 MAP Kinase phosphorylation cascade plays an important role in regulation of immune and inflammatory systems in response to injury, infection and tissue damage [Schindler, 2007]. p38 MAPK has this effect by regulating the function of many immune and inflammatory cells including macrophages, monocytes, T-lymphocytes and mast cells, as well as regulating cell cytokine expression, adhesion and migration [Dong et al., 2002]. It has therefore been hypothesized that inhibition of the p38 MAPK cascade may be useful therapeutically in diseases of excessive immune of inflammatory reactions, such as COPD, asthma and rheumatoid arthritis [Cuenda and Rousseau, 2007].

Activation of p38 MAPK and subsequently MAPKAPK2 in most cells can be induced with anisomycin or TNFα. Anisomycin activates the cascade by synergistically acting with growth factors through stimulation of the G-proteins, Rac and Cdc42 (Figures 3.1 and 3.4) [Cahill et al., 1996]. It should be noted that anisomycin leads to delayed onset of MAPKAPK2 activation. For faster activation the pro-inflammatory cytokine TNFα could be used for p38 MAPK and MAPKAPK2 activation (Figure 3.5). TNFα has its affect through the TNF receptor, recruitment of TRAF2, and activation of ASK (Figure 3.4) [Ichijo et al., 1997 and Nishitoh et al., 1998]. Initial work from the Houslay laboratory has shown that there may be potential signalling cross talk between the p38 MAPK cascade and the regulation of intra-cellular cAMP concentrations [MacKenzie and Houslay, 2000]. These effects are consistent with the wealth of published data that implicates both PDE4 [Jin and Conti, 2002, Houslay et al., 2005 and Zhang et al., 2005] and p38 MAPK inhibition as potential ways of lowering pro-inflammatory cytokine production and the overall inflammatory response.

Analysis of the primary amino acid sequence of phosphodiesterase 4A5 shows that it contains two potential MAPKAPK2 phosphorylation consensus sequences. The consensus sequence, Ø-Xaa-Arg-Xaa-Xaa-Ser*-Ø where Ø represents a hydrophobic

amino acid, was seen at serine 147 and serine 161 within PDE4A5. Serine 161 (Val-Ser-Arg-Ser-Ser-Ser*-Val) is surrounded by optimal residues for MAPKAPK2 phosphorylation, whereas serine 147 (Leu-Tyr-Arg-Ser-Asp-Ser*-Asp) contains a hydrophilic C-terminal aspartic acid residue at a site indicated to be hydrophobic in the consensus sequence [Rousseau et al., 2005]. However the requirement for a C-terminal hydrophobic residue, and indeed even the requirement for an optimal consensus motif, has been recently questioned so both Ser147 and Ser161 are possible MAPKAPK2 phosphorylation target sites based on our current knowledge [Stokoe et al., 1993, Rousseau et al., 2005].

Previous unpublished work from the Houslay lab showed that recombinant MBP fusion protein of PDE4A5 could undergo in vitro phosphorylation with recombinant, active MAPKAPK2. This provided initial evidence that PDE4A5 was substrate of MAPKAPK2. These initial experiments alluded to PDE4A5 being phosphorylated at Ser147 by MAPKAPK2. This study was followed on using an *in vivo* phosphorylation system in which COS1 cells over-expressing PDE4A5, in the presence of [^{32}P]-orthophosphate were treated with anisomycin to trigger the p38 MAPK cascade. This confirmed that PDE4A5 undergoes phosphorylation by MAPKAPK2 in a cell system. Additionally it was shown that phosphorylation did occur at Ser147 but other sites may also be available because the level of phosphorylation was not completely ablated with the Ser147Ala mutant form of PDE4A5. However, as with all in vivo protein kinase phosphorylation assays there is a tendency for background or indiscriminate phosphorylation to occur [Berwick and Tavaré, 2004].

Proving that proteins are genuine substrates for specific protein kinases is very difficult given the promiscuous nature of in vitro phosphorylation assays, and the complexity and integration of cell signalling pathways. To address such concerns certain criteria should be satisfied to formally identify protein kinase substrates [Berwick and Tavaré, 2004]. The work previously done in the Houslay lab satisfied these criteria by showing that (1) the recombinant *in vitro* phosphorylation of the proposed substrate and reduction of phosphorylation using site-specific alanine

mutant(s), (2) proving that the phosphorylation can occur in intact cells to a stimuli that activates the protein kinase in a stimulus and concentration-dependent time course (Figure 3.4), (3) matching the phosphorylation site *in vivo* to the phosphorylation site *in vitro* (Figures 3.2 and 3.6) and (4) ablating, or at least attenuating, the phosphorylation using specific inhibitors (Figures 3.6) [Berwick and Tavaré, 2004]. As PDE4A5 satisfies each of these criteria for MAPKAPK2 phosphorylation it was concluded that PDE4A5 is a bone fide substrate of MAPKAPK2 in cells, with phosphorylation occurring at a single serine residue (Serine 147).

As described previously PDE4 enzymes are phosphorylated by a cAMP-dependent protein kinase, known to as PKA [Sette et al., 1994]. Further work identified a conserved single serine residue (Ser54 in PDE4D3 and Ser140 in PDE4A5) within the Upstream Conserved Region 1 (UCR1) as the phosphorylation target for PKA and showed that phosphorylation at this site conferred enzyme activation [Sette and Conti, 1996, Hoffman et al., 1998 and MacKenzie et al., 2002]. This was the first evidence that the UCR1 domain participates in the regulation of catalytic activity, and therefore must interact with the catalytic unit in some way. PKA phosphorylation is proposed to stop an inhibitory constraint placed upon the catalytic machinery by Upstream Conserved Region 2 through disruption of the intra-molecular interactions between UCR1 and UCR2 [Lim et al., 1999 and Beard et al., 2000]. It is thought that resolution of the crystal structure of the UCR domains of full-length PDE4 isoforms may provide insight into how these domains regulate the catalytic unit and the effect of PKA phosphorylation on this but, unfortunately, this structure has yet to be solved.

PDE4A5 enzyme activity is greatly enhanced following PKA phosphorylation (Figure 3.7) [MacKenzie et al., 2002 and Bolger et al., 2003]. Conversely, MAPKAPK2 phosphorylation of PDE4A5 has no overt functional effect upon catalytic activity (Figure 3.8). As UCR1 is conserved across the PDE4 gene families, it might be expected that MAPKAPK2 phosphorylates all PDE4 long isoforms. The MAPKAPK2 phosphorylation site (Ser147) is located 7 amino acid residues upstream of the PKA phosphorylation site (Ser140). It was hypothesised that phosphorylation by

MAPKAPK2 may not confer an overt functional effect on its own but may play a role in controlling the effect of PKA on PDE4A5. It was shown that MAPKAPK2 phosphorylation did not alter the ability of PKA to phosphorylated PDE4A5 (Figure 3.9), however it did delay both the onset and amplitude of PKA induced activity of the phosphodiesterase (Figure 3.10). This was confirmed through mutation of the Ser147 phosphorylation site to alanine (Figures 3.11, 3.12, 3.13 and 3.14), which exhibited full PDE4A5 activation despite activation of the p38 MAPK-MAPKAPK2 pathway and through use of a phospho-mimetic mutant where Ser147 was mutated to aspartate (Figure 3.14), which exhibited delay in onset and attenuated level of enzyme activation. This study was repeated using the long form phosphodiesterase, PDE4D3 to see if this result was specific to PDE4A5 or likely to be a pan PDE4 long isoform phenomenon. The results seen for PDE4D3 followed the same trend as PDE4A5 (Figure 3.19) indicating that this effect is likely to be a pan PDE4 long isoform wide effect with a MAPKAPK2 consensus phosphorylation site conserved in all long form PDE4s.

This indicates that in cells where the p38 MAPK-MAPKAPK2 signalling pathway is active, activation of PKA in a negative feedback system to control local cAMP concentrations through PDE4 long isoforms is likely to be attenuated due to active MAPKAPK2. To demonstrate this intracellular cAMP levels were monitored following p38 MAPK-MAPKAPK2 activation in a system containing over-expressed PDE4A5, (Figure 3.15). The normal response of this system to raising cAMP, using an activator such as forskolin, is activation of PKA that, in turn, leads phosphorylation and activation of the long PDE4 leading to a decrease in cAMP levels back to resting rate. This effect can most easily be captured experimentally in transfected systems where a PDE4 long isoforms is over-expressed and provides the dominant (>98%) cAMP PDE activity in these cells. However, this serves as a paradigm for compartments in cells where PDE4 long isoforms are sequestered and similarly provide the dominant PDE activity in that locality.

When PKA activity was pharmacologically inhibited prior to increasing intracellular cAMP levels with forskolin then such a feedback loop is cancelled out as

there is no mechanism to phosphorylate and activate PDE4. Under such circumstances the transient nature of the rise in intracellular cAMP to forskolin challenge is lost and a sustained increase in cAMP occurs due to a new steady state rate of cAMP generation and hydrolysis being reached due to the combined action of forskolin-activated adenylyl cyclase and active, but not activated, PDE4. While activation of the p38 MAPK-MAPKAPK2 pathway alone has no effect of steady state, resting intracellular cAMP levels due to its inability to affect PDE4 activity per se it now in attenuating activation of PDE4 by PKA, reprograms the negative feedback effect and thus severely compromises the transient nature of the cAMP increase, allowing for a sustained increase in cAMP levels, which do not returning to basal levels within a 20 min time frame.

As with treatment with SB203580, mutation of the MAPKAPK2 phosphorylation site in PDE4A5, namely Ser147 to alanine, ablated this effect of anisomycin, confirming that MAPKAPK2 phosphorylation at this site is the responsible phosphorylation site for this reaction (Figure 3.16).

These experiments fully support the hypothesis that when PKA is activated in a negative feedback system to control local cAMP concentration, activation of the p38 MAPK-MAPKAPK2 signalling pathway attenuates phosphodiesterase activation by PKA through MAPKAPK2 phosphorylation at a site in UCR1.

Phosphorylation of PDE4D3 by PKA conferred both activation of phosphodiesterase activity and increased sensitivity to rolipram inhibition [Hoffmann et al., 1998]. In all other long PDE4 isoforms the activation is exhibited but no altered rolipram inhibition is presented [MacKenzie et al., 2002]. In addition to this PDE4A4, the human homolog of PDE4A5 has been shown previously to exhibit altered rolipram inhibition states, thought to be due to protein interaction with the phosphodiesterase [Jacobitz et al., 1996]. However use of the MAPKAPK2 phosphorylation site mutant Ser147Ala and Ser147Asp in PDE4A5, along with in cell p38 MAPK-MAPKAPK2 activation shows that MAPKAPK2 phosphorylation did not alter PDE4A5 sensitivity to

rolipram inhibition (Figure 3.17). This, however, may not be the case for PDE4D3 and the application of a MAPKAPK2 phospho-mimetic mutant may yield different results and would have to be fully studied before any conclusions about its activity could be made.

Although it had been successfully concluded that the attenuating effect of MAPKAPK2 phosphorylation on PDE4A5 is not due to hindrance of PKA acting at its phosphorylation site or affecting its inhibition state, it is still unclear how MAPKAPK2 phosphorylation is altering PDE4A5's activity. To resolve this the full 3D structure of the PDE enzyme would have to be considered. In the case of the PKA phosphorylated PDE4A5 when the conformational status of the enzyme was evaluated using a thermostability assay it was shown that the PKA phosphorylated and activated enzyme was more structurally stable and less easily denatured by thermal inactivation than the non-phosphorylated enzyme (Figure 3.18). MAPKAPK2 phosphorylation of PDE4A5 alone slightly lowered the stability of the enzyme to below the level seen in the unactivated (basal state) enzyme, as evident from its faster thermal inactivation. It should, however, be noted that this decrease appears to be stimuli dependent as this effect is seen more prominently when anisomycin was used to activate the p38 MAPK-MAPKAPK2 pathway than when TNFα was used (Figure 3.18). This may be due to the two treatments acting through different signalling pathways or may be purely due to the fact that anisomycin is used for a prolonged period of time so with 1h treatment optimal phosphorylation will be reached. However with TNFα activation of the signalling pathway the window for activation is much shorter, being between 5 and 10 min so it would be easy for the optimal phosphorylation of PDE4A5 to be missed. This effect needs to be investigated in more detail before a full conclusion can be made. Interestingly, when phosphorylation of PDE4A5 occurs by both PKA and MAPKAPK2 stability of the enzyme is drastically altered with enzyme being denatured at a much faster rate than the non-activated enzyme (Figure 3.18). This implied that MAPKAPK2 phosphorylation is causing a dominant conformational change as evidenced by the decrease stability of the enzyme in its PKA activated state. This result explains the dominant functional effect that MAPKAPK2 phosphorylation exerts on PDE4A5

activity seen as an attenuated, PKA mediated, activation state of PDE4A5 under MAPKAPK2 phosphorylation.

This alteration in activation state may be playing a role in modifying the negative feedback loop usually controlled by PKA. In this loop in response to rising cAMP levels PKA is activated, this phosphorylates and activates a long PDE4 phosphodiesterase, which, in turn, lowers the cellular levels of cAMP back to basal. However when the p38 MAPK-MAPKAPK2 pathway is activated MAPKAPK2 phosphorylates the long PDE4, lowering its ability to be activated by PKA, leading it into reduced activation, and therefore not allowing cAMP levels to return as quickly to basal. As has been previously described MAPKAPK2 is thought to play a vital role in increasing TNFα and Il-6 production upon inflammatory stimulus. Conversely, cAMP is known to block the action of pro-inflammatory mediators [Barber et al., 2004]. Inhibition of PDE4 leads to elevation in intracellular cAMP concentration and a reduction in inflammatory response. Therefore it is proposed that MAPKAPK2 may be phosphorylating long PDE4 isoforms, attenuating their activation by PKA, as a protective feedback system to prevent over-load of the inflammatory system. This would mean that when the p38 MAPK-MAPKAPK2 signalling pathway was activated and causing release of pro-inflammatory cytokines, if cAMP levels were raised its PKA dependent feedback system would not be fully activated, due to MAPKAPK2 phosphorylation of PDE4, keeping cAMP from returning to its basal levels. Subsequently this would mean that inflammatory responses would not be activated by low cAMP levels, and there would not be two separate pathways invoking an inflammatory response causing the system to become overloaded.

This may be interesting therapeutically as it raises the question of whether inhibiting PDE4 fully during this process would prevent an excessive inflammatory response as is seen in diseases such as asthma and rheumatoid arthritis. This may also explain why p38α MAPK and MAPKAPK2 inhibition has had limited success as although inhibiting these kinases blocks pro-inflammatory cytokine release it leaves the

cyclic AMP pathway uncontrolled, allowing cAMP levels to be kept at a low rate through PDE4 action and creating another inflammatory response.

In conclusion MAPKAPK2 phosphorylated PDE4A5, and possibly other PDE4 isoforms, leading to attenuation of PKA mediated activation following an increase in intracellular cAMP concentration.

Chapter 4 Interaction of PDE4 with p75NTR and their role in Fibrinolysis

4.1 Introduction

4.1.1 Neurotrophins

The family of growth factor proteins, neurotrophins play an important role in influencing several important cellular activities such as proliferation, differentiation and cell growth [Levi-Montalcini et al., 1995]. The neurotrophin family consists of four members in humans: brain-derived neurotrophic factor (BDNF), neurotrophin 3, neurotrophin 4/5 together with the most commonly occurring and the most commonly investigated species, namely nerve growth factor (NGF) [Dechant & Neumann, 2002]. Structurally these important proteins are all similar, existing as homodimers and having a duplicate site for binding to receptors [Cowan et al., 2001]. Occasionally a fifth protein is included in this family, namely novel neurotrophin 1 (NNT-1). However NNT-1 is, technically, a cytokine and as it bears no structural resemblance to the other family members [Senaldi et al., 1999] it will not be discussed here.

Nerve growth factor was the first of the neurotrophins to be identified. It is composed of 2 chains of 118 amino acids containing 3 disulfide bonds arranged in a cysteine knot, which is essential for its activity [Silverman & Bradshaw, 1982; Wiesmann & de Vos, 2001]. Functionally NGF was originally established as playing a vital role as a growth factor in nerve proliferation and survival [Levi-Montaclcini et al., 2005]. However it was then also found to play an important role as a mediator in airway inflammation [Frossard et al., 2004]. A precursor to NGF has also been reported, namely proNGF [Ibanez, 2002]. ProNGF is an important component of mature NGF folding, production and secretion. ProNGF has been shown to be the dominant form of NGF in the brain [Rattenholl et al., 2001; Fahnestock et al., 2001].

Originally identified in the brain, brain derived neurotrophic factor was the second neurotrophin to be discovered [Leibrock et al., 1989]. It was initially thought to only be expressed in nerve tissue but has since been shown to be produced in a wide variety of immune cells such as macrophages, T cells and B cells [Kerschensteiner et al., 1999].

The next neurotrophin to be discovered was neurotrophin 3. This neurotrophin acts on certain neurons in the peripheral and central nervous system to help support survival and differentiation of neurons [Maisonpierre et al., 1990].

The last, and most recently discovered neurotrophin in this family is neurotrophin 4/5. This neurotrophin has not been studied as widely as the others. However it is considered to act similarly to BDNF [Patapoutian & Reichardt, 2001].

4.1.2 Neurotrophin Receptors

There are four different types of known receptors for neurotrophins [Chao, 2003]. Three of these belong to the tyrosine kinase receptor family (Trk receptors) and bind neurotrophins with high affinity. In marked contrast to this, the fourth receptor for neurotrophins is a low affinity receptor that is known as the p75 neurotrophin receptor (p75NTR) [Rodriguez-Tebar et al., 1990].

4.1.2.1 TrkA

The TrkA receptor is expressed throughout the central and peripheral nervous systems, as well as being expressed in non-neuronal cells such as immune and structural cells [Muragaki et al., 1995; Levi-Montalcini et al., 1995]. Each of the Trk receptors has a preferred ligand and in the case of TrkA receptor it is NGF, which it binds with high (picomolar) affinity, however it also shows some interaction with neurotrophin 3 [Sutter et al., 1979; Clary and Reichardt., 1994].

Structurally TrkA is a 140kDa glycoprotein [Weier et al., 1995]. Several isoforms have been identified, all of which consist of an extracellular neurotrophin binding region, a unique transmembrane helix and an intracellular domain with tyrosine kinase activity [Wiesmann & de Vos., 2001; Windisch et al., 1995]. The model of ligand binding and subsequent autophosphorylation of the receptor occurs in a conserved manner throughout all of the Trk receptor isoforms [Heldin. 1995]. In the case of TrkA, NGF binds to the D5 extracellular domain of the receptor through two areas [Wiesmann & de Vos, 2001]: a specificity patch that confers ligand specificity, and a conserved binding patch that is found in all Trk receptors [Wiesmann et al., 1999; McInnes & Sykes, 1997]. NGF binding leads to dimerisation of the receptor, resulting in activation of its intrinsic tyrosyl kinase activity through trans-phosphorylation of tyrosine residues 670, 674, 675 (in the activation loop of the kinase domain) and, subsequently, tyrosines 490, 751, 785 (outside the kinase domain), which result in activation of downstream signalling pathways [Jing et al., 1992; Heldin, 1995;].

Taking a more in-depth look at the phosphorylation sites outside the kinase domain gives an insight into how downstream signalling pathways are triggered. In the case of tyrosine 490, when this tyrosine becomes phosphorylated it interacts with the src homology 2 (SH2) domain of the adaptor protein shc2, resulting in its phosphorylation and subsequent binding and phosphorylation of Grb2. Grb2 can then go on to bind Sos leading to activation of the Ras/Raf pathway resulting in downstream processes such as proliferation and survival [McCormick, 1995, Nimnual et al., 1998; Stephens et al., 1994]. Similarly, phosphorylated tyrosine 785 confers binding to the SH2 domain of phospholipase C-γ which then becomes tyrosine phosphorylated and activated, leading to PIP2 breakdown and the generation of DAG and IP3. The generated DAG allows for activation of protein kinase C and the MKK pathways that play a role in cell proliferation and survival [Stephens et al., 1994; York et al., 2000]. The phosphorylation of tyrosine 751 allows binding to the SH2 domain of PI3 Kinase, activating the Akt and MKK pathways, resulting in neuroprotective downstream effects [Ohmichi et al., 1992].

4.1.2.2 TrkB

The TrkB receptor is ubiquitously expressed throughout both the central and peripheral nervous system as well as playing an important role in other areas such as the respiratory system [Klein et al., 1990; Nassenstein et al., 2006]. The main ligand for this receptor is BDNF. However it has also been shown to interact with neurotrophin 4, which may be a result of this protein having similarity to BDNF [Klein et al., 1991; Klein et al., 1992].

Structurally TrkB is similar to TrkA in that, despite there being three known isoforms, these all consist of a basic set structure: an extracellular BDNF (or NT-4) binding domain, a transmembrane domain and an intracellular domain [Barbacid, 1995; Strohmaier et al., 1996]. The intracellular domains differ between different isoforms with one isoform having tyrosine kinase activity while the other two, lesser known and little understood, isoforms tightly bind the Rho displacement factor Rho-GDI and facilitates the release of prenylated RhoA [Fryer et al., 1996; Yamashita et al., 2003]. Activation of the TrkB receptor occurs in a similar manner to activation of TrkA as described previously in that BDNF binds to the D5 extracellular domain of the TrkB receptor leading to dimerisation and resulting in activation of kinase activity through phosphorylation of tyrosine residues in the activation loop of kinase domain and also tyrosine residues outside the kinase domain that recruit proteins (e.g. PLC-γ, PI3K) that subsequently allow activation of various downstream signalling pathways [Jing et al., 1992; Heldin, 1995].

The “long”, tyrosine kinase form of the TrkB receptor signals cell survival and synaptic plasticity downstream through tyrosine phosphorylation in a similar manner as TrkA [Nonomura et al., 1996; Zirrgiebel et al., 1995; Glass et al., 1991]. While the “short” Rho-GDI form is found mostly located in the human brain and while its function is not fully understood, it is thought to play a role in signalling that regulates cell morphology and calcium influx [Fryer et al., 1996; Kryl & Barker, 2000].

4.1.2.3 TrkC

The TrkC receptor is the least studied of the Trk family of receptors. It is ubiquitously expressed throughout the brain, with its mRNA levels being highest in the hippocampus, an area important for learning and memory processes [Lamballe et al., 1994]. The ligand for this receptor is neurotrophin 3 [Lamballe et al., 1994].

Structurally it is similar to both TrkA and Trk B in that it consists of an extracellular NT-3 binding domain, a transmembrane domain and an intracellular domain. The intracellular domain has tyrosine kinase activity similar to that described in TrkA, playing a role in cell survival and synaptic plasticity. However it has also been shown to have potentially important role in cellular stress response [Faure et al., 2006].

4.1.3 p75NTR

4.1.3.1 Ligands, Structure and Activation

p75NTR was the first of the neurotrophin receptors to be identified and was originally shown to act as a low affinity receptor for NGF. Since then it has been shown to be able to bind all members of neurotrophin family and it is generally accepted that all neurotrophins are bound with similar (low) affinity with a fast dissociation rate [Barker, 2007].

Structurally, like the Trk receptors, p75NTR is a 75 kDa, highly conserved, type I transmembrane protein. It consists of four extracellular cysteine rich domains (CRDs), a transmembrane domain and an intracellular region (ICD) containing a death domain (DD). Unusually the receptor itself does not contain a catalytic region, such as the SH1 tyrosyl kinase domain found in members of the Trk receptor family, but instead is thought to sequester other signalling molecules to elicit downstream effects. Ligands for p75NTR bind electrostatically through interaction between the negative amino acids on to specific regions of the receptor (site 1: in the junction of the CRD1-CRD2 regions

and site 2: in the junction of the CRD3-CRD4 regions) and positive amino acids on the neurotrophins. Interestingly the p75NTR receptor can also bind pro-neurotrophins and this is thought to occur with a higher affinity than mature neurotrophin binding [Lee at al., 2001].

4.1.4 p75NTR Signalling Pathways

Classically p75NTR is thought to have four main downstream phenotypic actions: these are effects on cell survival, cell death, neurite outgrowth and fibrinolysis [Dechant & Barde, 2002; Sachs et al., 2007].

4.1.4.1 Cell Survival

In the case of cell survival, the binding of a neurotrophin, such as NGF, to p75NTR results in activation of NF-κB, which, in turn, induces activation of inhibitors of apoptosis (IAPs) through three separate pathways. The first of these is through recruitment of the receptor interacting protein 2 (RIP-2) to the intracellular portion (ICD) of the p75NTR receptor [Khursigara et al., 2001]. The second is through recruitment of TRAF and activation of the Il-1 receptor associated kinase (IRAK) and atypical PKC [Khursigara et al., 1999]. The third is through activation of PI3 Kinase and, subsequently, Akt/PKB [Roux et al., 2001].

It has also been suggested that p75NTR may play a role in cell survival through p75NTR directly interacting with TrkA with TrkA/p75NTR acting as co-receptors for NGF [Yoon et al., 1998; Lachyankar et al., 2003]. The precise mechanism of this interaction is, as yet, unknown but it has been suggested that this occurs through interaction of all 3 domains of each receptors (i.e., the extracellular, juxtamembrane and intracellular domains of TrkA and p75NTR all interact with their counterparts). However this hypothesis remains controversial as other studies have not confirmed this view. It has, however, been suggested that the nucleoporin p62, the TNF Receptor Associated Factor, TRAF6 and/or the neurotrophin receptor homologue NRH2 may be

working as adaptor proteins, binding the 2 receptors into a complex [Chao, 2003; Wehrman et al., 2007]. The downstream effect of the interaction between these receptors has been proposed to prevent any apoptotic signal via the DD of p75NTR and redirect p75NTR signalling towards those allowing for cell survival such as the MAPK pathways. This suggests that the NF-κB pathway controlled by the p75NTR receptor and the MAPK pathways controlled by the Trk receptors could be working synergistically to promote survival [Chao, 2003; Yoon et al., 1998].

4.1.4.2 Cell Death

p75NTR has also been shown to play a role in cell death. It is thought that the receptor can influence programmed cell death through several routes. The two principal routes are, firstly p75NTR interaction with adaptor proteins and secondly ceramide synthesis [Roux & Barker, 2002].

In the case of adaptor protein interaction, several different potential interacting adaptor proteins have been identified. These include the neurotrophin receptor interacting factor (NRIF) that binds to the death and juxtamembrane domains of p75NTR, resulting in downstream JNK MAPK pathway activation [Casademunt et al., 1999]. Neurotrophin receptor associated cell death executor (NADE) works in a similar manner, interacting with p75NTR and promoting activation of the JNK MAPK pathway [Mukai et al., 2000]. In both of these cases activated JNK then goes on to phosphorylate the pro-apoptotic proteins p53, Bad and Bax leading to release of cytochrome C and caspase activation, resulting in apoptotic cell death [Roux & Barker, 2002].

In ceramide synthesis-mediated apoptosis, p75NTR seemingly induces activation of the sphingomyelinase group of enzymes. These cleave sphingomyelin into ceramides, which then go on to activate JNK that, in turn, results in apoptotic cell death in the way described above [Blochl & Blochl, 2007].

One other proposed way in which p75NTR is thought to lead to apoptosis is through interaction with its co-receptor, Sortilin. However, this mechanism is not yet fully understood. It has been suggested, however, that the role of TrkA and role or sortilin as co-receptors may be mutually exclusive with one co-receptor controlling cell death and one controlling cell survival [Bronfman & Fainzilber, 2004].

4.1.4.3 Functional Regulation

p75NTR has also been shown to play a role in functional regulation outside of cell survival and cell death. In one example of this, the Nogo receptor forms a complex with p75NTR, which results in neurite outgrowth [Wang et al., 2002]. This works through activation of the p75NTR/NOGO-R complex by growth inhibitor proteins allowing p75NTR to bind Rho-GDI (Rho-GDP Dissociation Inhibitor) and act as a displacement factor for RhoA release triggering concomitant neurite outgrowth [Yamashita & Tohyama, 2003]. Another example is the functional role p75NTR plays in fibrinolysis, which will be described in more detail later in section 4.1.6.

4.1.5 The role of p75NTR in respiratory inflammation

Although p75NTR is most commonly known for its role in the nervous system it has also been shown to play a role in inflammation of the respiratory system [Freund-Michel & Frossard, 2008].

For this to be fully appreciated then the expression pattern of p75NTR and its regulation throughout the respiratory system must be fully understood. The first, and most obvious site of p75NTR expression in this system is in the sensory neurons that innervate the lungs [Levi-Montaclini, 1987]. In mice with excess NGF it has been shown that there is hyper-innervation of these nerves, which increases neuronal growth and survival [Hoyle et al., 1998] and leads to inflammation. B lymphocytes have also been shown to express p75NTR [Torcia et al., 1996]. In these cells the neurotrophin, NGF is thought to have an autocrine effect [Lambiase et al., 1997] with activation of

p75NTR resulting in release of immunoglobins and differentiation and proliferation of B lymphocytes [Ehrhard et al., 1994] enhancing inflammation.

p75NTR is also expressed in eosinphils in the lungs of asthma patients following allergen attack [Nassenstein et al., 2003] but not in peripheral systems. This again implies that p75NTR plays a role in airway inflammation, in this instance possibly through promoting the survival of eosinophila and of their ability to release Il-1 and Il-3 [Chevalier et al., 1994].

Basophils have also been shown to express p75NTR and activation of the receptor in these cells causes IL-13 and histamine release. Interestingly Il-13 levels have been shown to be up-regulated in asthmatic patients [Burgi et al., 1996], suggesting a potential role of p75NTR. Finally, structural cells such as human pulmonary fibroblasts have also been shown to express p75NTR with a potential role in fibrosis and this will be discussed in detail later [Olgart & Frossard, 2001].

With the details of p75NTR expression throughout this system now beginning to be understood, several studies have been carried out looking at the overall effect of p75NTR in inflammation. Initial studies into this showed that NGF induces inflammation of the respiratory system largely through its binding to p75NTR. These studies were carried out using p75NTR knock-out mice and p75NTR antibodies in asthmatic inflammation model systems and showed that in the absence of p75NTR inflammation was reduced [Kerzel et al., 2003; Tokuoka et al., 2001]. However, studies using p75NTR knock-out mice showed that bronchial hyper-responsiveness does not occur in response to irritant stimuli like capsaicin [Kerzel et al., 2003]. From this it would seem that p75NTR plays an important role in the response of the bronchii to irritation.

4.1.6 The role of p75NTR in fibrinolysis and its potential role in inflammation

In spinal cord injury models it has been shown that p75NTR expression is increased at the site of injury with an increase in fibrin deposition also observed [Stark el al., 2001]. In work carried out in collaboration between the Houslay laboratory in the University of Glasgow and the Akassoglou laboratory at University of California San Diego, USA (now at the Gladstone Institute in San Francisco, USA) the role of p75NTR in fibrinolysis and importance of cAMP signalling to this has been uncovered. This research showed that p75NTR plays an important role in proteolytic activity and results in a decrease in fibrin degradation. The pathway in which this was shown to work is shown in Figure 4.1. This shows that when p75NTR interacts with cAMP phosphodiesterase, PDE4A5, this confers a localised decrease in cyclic AMP around p75NTR. This localised decrease in cAMP negates inhibitory regulation of p75NTR by cAMP and leads to its activation causing a reduction in expression of tissue Plasminogen Activator and an increase in Plasminogen Activator Inhibitor-1. This results in a reduction of plasmin and plasmin-dependent extracellular proteolysis and, therefore, promotes reduced fibrin degradation and ECM remodelling. Some of work that elucidated this is shown here. This discovery is likely to be of physiological significance as defects in fibrinolysis have been seen in lung inflammation [Renz et al., 2004] and PDE4A isoforms are also known to play a very important role in respiratory disorders as PDE4A4, the human homologue of rodent PDE4A5 is up-regulated in the lungs of COPD patients [Barber et al., 2004] and also binds to p75NTR.

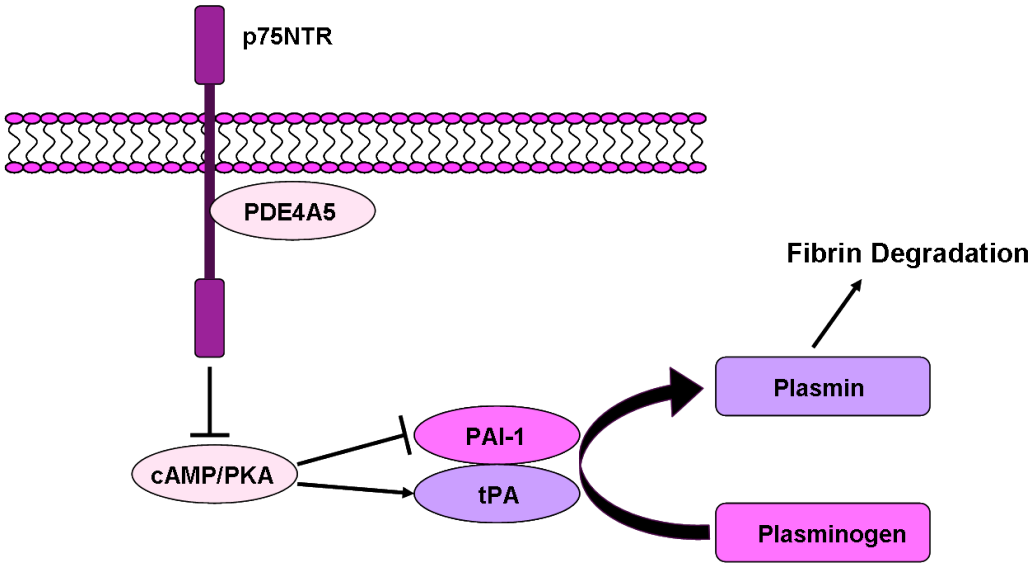

Figure 4.1 – Schematic model of the role of p75NTR in cAMP-mediated plasminogen activation.

The proposed model is that PDE4A5 interacts with the p75 Neurotrophin Receptor resulting in degradation of cAMP. Decrease in cAMP reduces expression of tissue Plasminogen Activator and increases Plasminogen Activator Inhibitor-1. This results in reduction of plasmin and plasmin-dependent extracellular proteolysis, resulting in reduced fibrin degradation and ECM remodelling.

4.2 Results

4.2.1 The p75 neurotrophin receptor interacts with Phosphodiesterase 4A

In a previous study in which I was a co-author [Sachs et al, 2007] it has been demonstrated that p75NTR can interact with the long PDE4A isoforms, PDE4A5. Figure 4.1 is modified from this publication. In this work our collaborators showed that when p75NTR was co-immunoprecipitated from NIH3T3 fibroblast cells stably expressing p75NTR, then probing this immunoprecipitate with anti-PDE4A antisera identified an endogenous PDE4A species migrating at approximately 100 kDa, the size of PDE4A5, figure 4.2(a). The afore mentioned stably transfected NIH3T3 cell line was used as a model from then on and referred to here as NIH3T3-p75NTR. The next logical step was to establish the functional consequence of this interaction. This was done by our collaborators who generated a genetically modified A-kinase activity reporter (AKAR2) to contain a membrane-targeted fluorescence reporter of PKA activity (pm-AKAR2.2), allowing for measurement of fluorescence resonance energy transfer (FRET) measurement of PKA phosphorylation in living cells. In wild type NIH3T3 cells there is a dramatic emission ratio change for pm-AKAR2.2 in response to forskolin, figure 4.2(b). However in NIH3T3-p75NTR cells there was an attenuated response to forskolin compared to in the wild type. These results seemed to indicate that there was reduced PKA activity at the plasma membrane upon expression of p75NTR. This implies that p75NTR targets cAMP degradation to the membrane, which is consistent with the notion that p75NTR sequesters a cAMP-degrading phosphodiesterase.

It was then important to establish the specificity of the interaction of p75NTR with phosphodiesterase-4. A series of mapping studies were carried out using truncated mutants of p75NTR. The forms used were full length (FL) p75NTR, and mutants missing the distal 3 amino acids, Δ3, the distal 62 amino acids Δ62, the distal 83 amino acids, Δ83 and finally missing the distal 151 amino acids, Δ151 (figure 4.2(c)). Of these five forms only Δ151 did not co-immunoprecipitate with PDE4A, suggesting that

interaction between p75NTR and PDE4A must occur somewhere in the juxtamembrane region of p75NTR, with the required amino acid regions being between amino acids 275 and 343, figure 4.2(c). Now that the region of interaction of the PDE4A on p75NTR had been shown the next logical step was to establish the region of interaction on the phosphodiesterase.

This work then lead to our laboratory's role in the collaboration. As the PDE4 family contains several consensus sites in its difference isoforms it had to be elucidated whether interaction between PDE4 and p75NTR was specific to one family. To establish this, Dr George Baillie purified recombinant proteins of typical long form phosphodiesterases, namely PDE4A4, PDE4A5 and PDE4D5. These were individually incubated with purified recombinant p75NTR and examined for the ability to be co-immunoprecipitated. Both PDE4A4 and PDE4A5 were shown to interact with p75NTR in this way, however PDE4D5 did not (Figure 4.2(d)). At this point the publication states that interaction between p75NTR and PDE4A4/5 is specific to those isoforms. However although these data may imply that this is a PDE4A specific effect, it does not actually show that it is specific to the PDE4A4/5 isoforms rather than the PDE4A family as a whole. Following on from this I began my role in this collaboration. I transfected PDE4A isoforms into NIH3T3-p75NTR cells for co-immunoprecipitation studies to be carried out. This showed that various PDE4A long form isoforms, namely PDE4A5, PDE4A5, PDE4A10 and PDE4A11, as well as the PDE4A1 short isoform, interact with p75NTR within the cell. This indicates that p75NTR interaction is not specific to PDE4A4/5 as originally thought [Sachs et al., 2007] but is a 'pan' PDE4A isoform interaction, figure 4.3. It should, however, be noted that studies using an isoform-specific antisera have shown that the PDE immuno-precipitated endogenously with p75NTR in NIH3T3 cells is indeed PDE4A5. However, my studies indicate that PDE4A isoforms other than just PDE4A4/5 may interact endogenously with p75NTR in various other cell types.

My preliminary peptide array mapping technology was then used to try and elucidate specific regions of PDE4A5 where p75NTR binds, figure 4.4. These data

showed that there are five potential binding regions for p75NTR on PDE4A5. One is located in the N-terminal at amino acids 16-60, one in UCR2 at amino acids 251-276, two in the catalytic region at amino acids 396-420 and 666-700 and one in the C-terminus at amino acids 801-830. It should be noted, however, that extensive mutation studies and peptide competition studies need to be carried out for the involvement of such possible interaction sites to be confirmed.

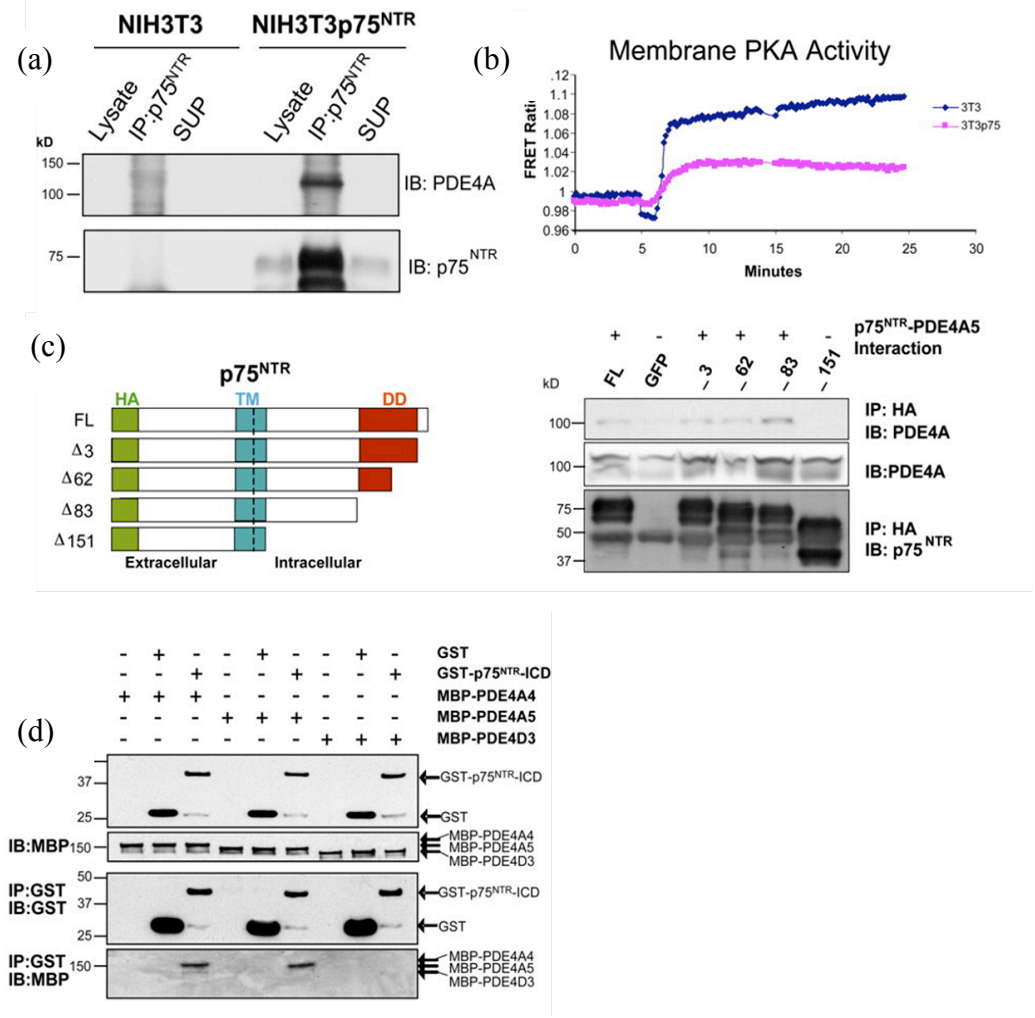

Figure 4.2 - p75NTR interacts with PDE4A5 [Sachs et al, 2007].

This figure is modified from Sachs et al, 2007, an article in which I am a co-author. (a) Co-immunoprecipitation of p75NTR with endogenous PDE4A5 in NIH3T3 fibroblast cells that stably express p75NTR. Immunoprecipitation was carried out with anti-p75NTR and probed with anti-PDE4A or anti-p75NTR. (b) FRET emission ratio change of NIH3T3 and NIH3T3 p75NTR stable cells for the cytoplasmic FRET PKA sensor (pm-AKAR2.2) in response to forskolin. FRET change represents membrane activation of PKA (c) Mapping of the p75NTR sites required for interaction with PDE4A5 using truncation of p75NTR. Schematic diagram of HA-tagged p75NTR

intracellular deletions. *TM,* transmembrane domain; *DD,* death domain. Truncates were transiently transfected into NIH3T3 cells. Lysates were immunoprecipitated with an anti-HA antibody and probed with anti-PDE4A or anti-p75NTR. (d) Co-immunoprecipitation of purified, recombinant p75NTR with purified, recombinant PDE4A4, PDE4A5 and PDE4D3. Immunoprecipitation was carried out with Glutathione Sepharose beads and probed with anti-GST or anti-MBP.

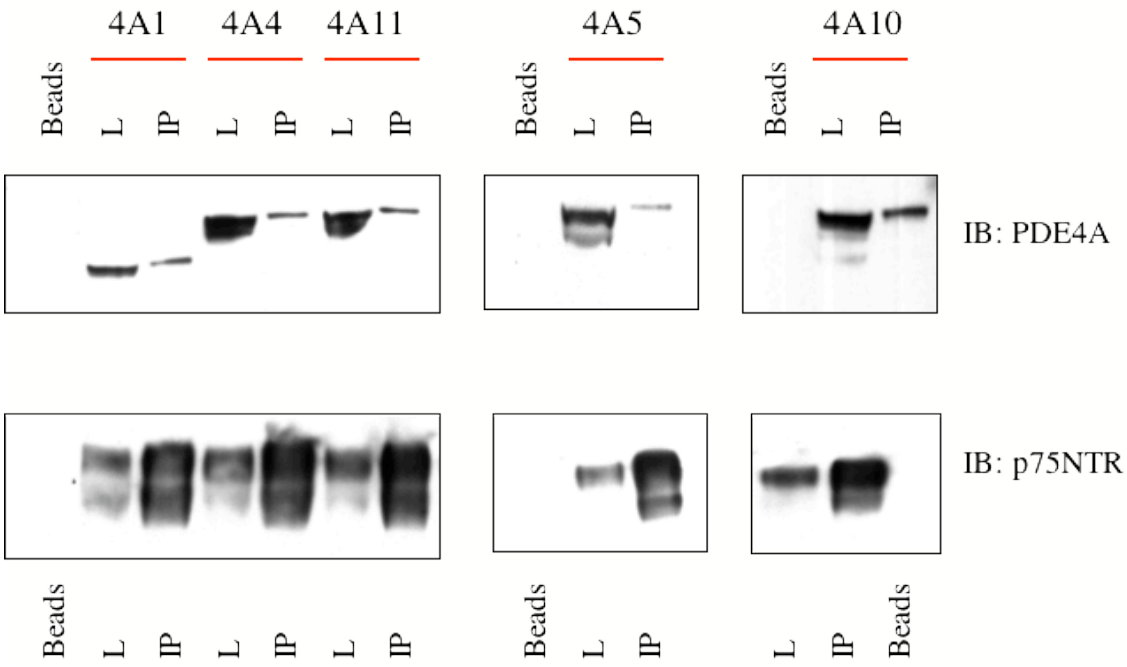

Figure 4.3 – p75NTR co-immunoprecipitates with long form PDE4A isoforms in transiently transfected NIH3T3 cells.

NIH3T3 cells were transiently transfected with HA-tagged p75NTR and long form PDE4A isoforms, PDE4A1, PDE4A4, PDE4A5 and PDE4A11. BEADS = beads alone, L = lysate input control, IP = immunoprecipitate output. Total cell extract was produced and the lysates immunoprecipitated with HA anti-sera conjugated agarose beads. These IPs were then probed with anti-PDE4A (top panel) and anti-p75NTR (bottom panel) anti-sera. All Western blots are representative blots of at least three separate experiments.

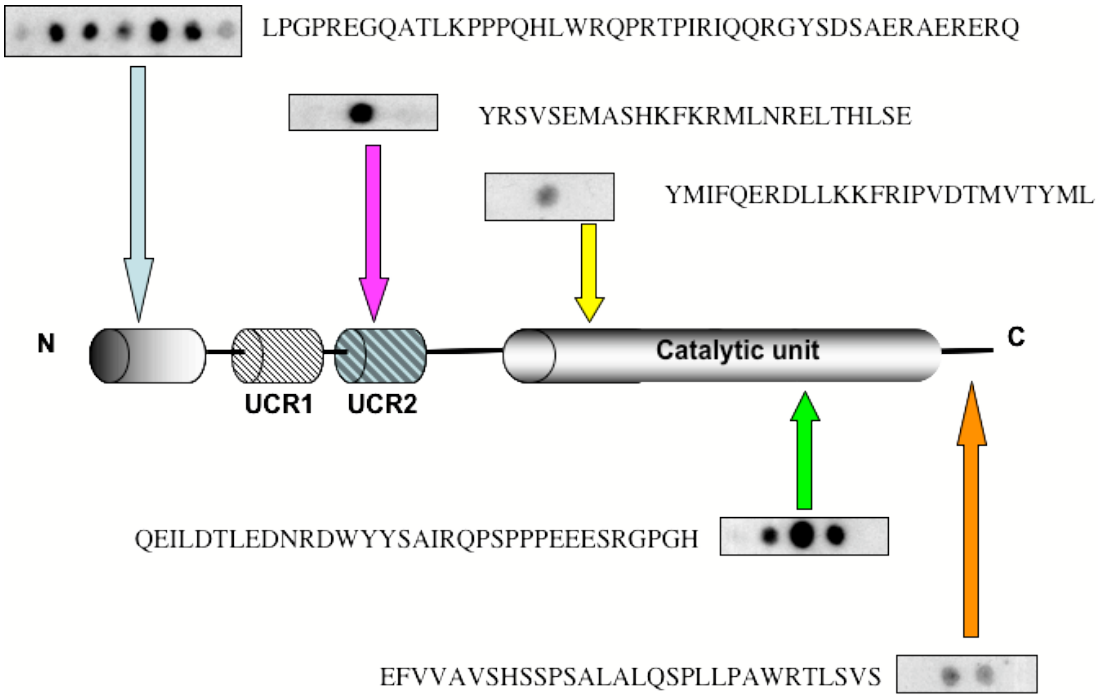

Figure 4.4 – Peptide Array mapping of p75NTR's binding sites on PDE4A5.

Five amino acid overlapping 25mer peptides representing the sequence of PDE4A5 were spotted onto nitrocellulose membrane. Purified, recombinant His-tagged p75NTR was overlaid onto this and anti-His anti-sera was used to detect binding. The schematic shows structural areas of binding along with their sequence. All peptide array blots are representative of at least three separate experiments.

4.2.2 Functional effect of p75NTR interaction with PDE4A5.

As previously mentioned, there was reduced PKA activity (thought to be a result of lowered cAMP levels) at the plasma membrane upon expression of p75NTR. This indicates that p75NTR, through binding of the cAMP hydrolysing enzyme PDE4, may lead to compartmentalised cAMP degradation to the membrane. It was important to attain whether this effect was purely due to the location of PDE4 at the membrane, due

to an overall increase in PDE levels or if the PDE interaction with p75NTR is somehow making the enzyme more basally active leading to increased levels of hydrolysis. The protein expression level of PDE4A was not different when I compared levels in wild type NIH3T3 cells and NIH3T3-p75NTR (Fig. 4.5 (a)). These data indicate that expression levels of PDE4A are not affected by expression of p75NTR in these cells. This disproves the notion that p75NTR increases local cAMP degradation by altering PDE4A expression level and, instead is consistent with it sequestering PDE4A5. To study whether PDE4 interaction with p75NTR increases the basal activity levels of the PDE4 enzyme wild type NIH3T3 cells were transiently transfected to over-express PDE4A5, lysates were collected and these were incubated with varying concentrations of purified recombinant p75NTR before cAMP PDE activity assays were carried out. This showed that p75NTR interaction with PDE4A5 did not alter the activity of this enzyme and also did not alter its ability to be inhibited by the PDE4 inhibitor rolipram, figure 4.5 (b). This disproves the notion that interaction of p75NTR with PDE4A5 is increasing its enzymatic activity therefore showing that the decrease in PKA activity at the plasma membrane is not due to increased enzymatic activity of PDE4A5 but is rather due to the increased presence of PDE4A5 located to p75NTR.

(a)

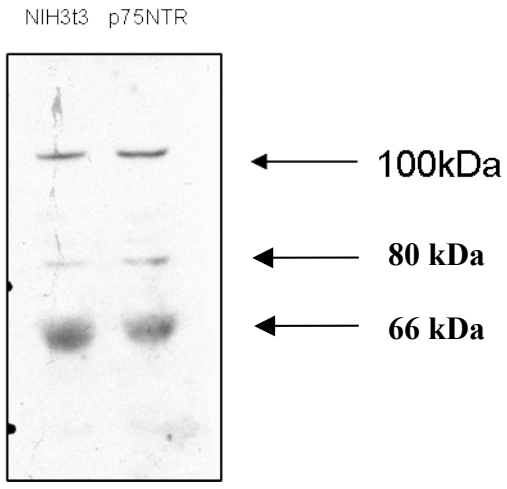

(b)

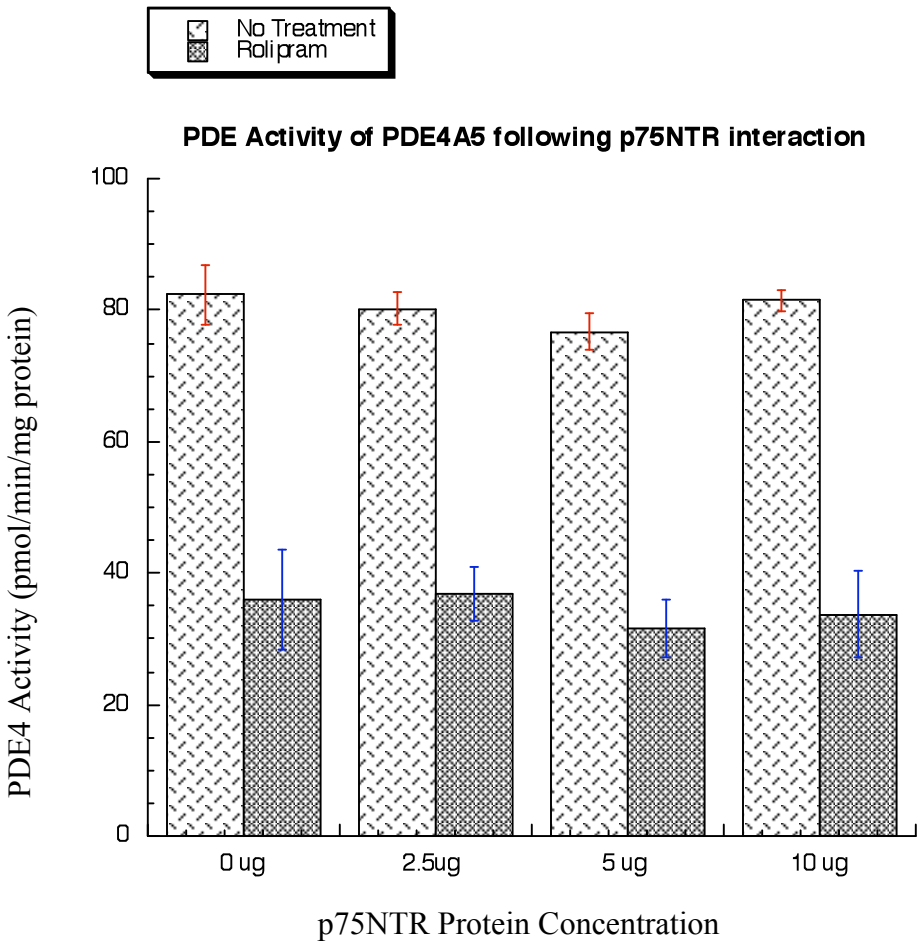

Figure 4.5 – PDE4 express odiesterase activity of PDE4A5 following p75NTR

(a) Total cell extract of NIH3 ble cells were collected and immuno-blotted for PDE4A expression levels using an anti-PDE4A specific anti-sera. The band at approximately 100 kDa corresponds to PDE4A5 whereas the lower to bands at approximately 80 and 66 kDa correspond to lower forms such at PDE4A1 and PDE4A7. (b) NIH3T3 cells were transfected to transiently express rat PDE4A5. Total cell lysate was collected and incubated at 4^{o}C with three different concentrations of

p75NTR (2.5 μg, 5 μg and 10 μg) for 3 hours. An enzymatic activity assay was then carried out on the samples along with a PDE4A5 alone control lysate. A second enzymatic activity assay was carried out on the same samples with the PDE4-specific inhibitor, Rolipram (10 μM). Assays were done using 1 μM cAMP as substrate with NIH3T3 cell lysates expressing equal immuno-reactive amounts of PDE4A5, as determined by the quantification of PDE4A5 expression. All data shown are mean data +/- standard deviation of the three separate transfection experiments.

4.2.3 PDE4A5 controls p75NTRs role in fibrinolysis and this is in turn mediated by MAPKAPK2.

p75NTR is known to play a role in the control of fibrin degradation. In the presence of p75NTR the process of fibrinolysis is inhibited. This is evident in figure 4.6 where I compared wild type NIH3T3 cells to NIH3T3-p75NTR cells in a 3D fibrin gel model, used to assess quantitatively fibrin breakdown. In this system, after 9 days, the wild type cells exhibited 58 % +/- 3 % fibrin degradation whereas the cells stably expressing p75NTR only exhibited 19 % +/- 2 % fibrin degradation, this was a significant difference with a p value of 0.002. Interestingly, when this experiment was repeated in the presence of the PDE4 inhibitor rolipram (10 μM) fibrin degradation in the wild type cells was unaffected with degradation being 60 % +/- 3 % whereas in the NIH3T3-p75NTR cells fibrin degradation dramatically increased to 51 % +/- 9 % with a p value of 0.02 when compared to untreated cells.

This implies that PDE4 plays an important role in p75NTR's control of fibrinolysis and that disruption of this interaction results in alteration of fibrin degradation. Indeed in Sachs et al., 2007 it is described how this interaction is thought to play a role in fibrin degradation and Figure 4.1 provides a modified description of this. In short, p75NTR interacts with PDE4A, this interaction leads to reduced local cyclic AMP levels and therefore low levels of PKA activation. This decreased level of

cAMP/PKA reduces expression of tissue Plasminogen Activator and increases Plasminogen Activator Inhibitor-1. This results in reduction of plasmin and plasmin-dependent extracellular proteolysis, leading to reduction in fibrin degradation. It should be noted that it is not known how, presumably, locally activated PKA inhibits p75NTR functioning and allows fibrin breakdown. One possibility is that p75NTR is thought to signal through Rho [Yamashita et al., 2003] and as PKA can phosphorylate and inhibit the functioning of Rho-GTPases then this might be one possible route [Qiao et al., 2003].

In previous chapters it has been mentioned that PDE4 can be phosphorylated by MAPKAPK2 and I set out to see if this might affect the interaction of PDE4A5 with p75NTR and the role of this receptor in fibrinolysis. Co-immunoprecipitation studies in NIH3T3-p75NTR showed that after stimulation of MAPKAPK2 through activation of p38MAPK using either anisomycin or TNFα, then an increased amount of endogenous PDE4A5 is pulled down with p75NTR (figure 4.7). When MAPKAPK2 activation is inhibited using SB203580 this increase was negated. It is known that p75NTR does not contain a phosphorylation site for MAPKAPK2 so, presumably, this increase in interaction was occurring through the MAPKAPK2 phosphorylation of PDE4A5. To gain insight into this, NIH3T3-p75NTR cells were transiently transfected to over-express PDE4A5 S147A, a mutant form of PDE4A5 that cannot be phosphorylated by MAPKAPK2. In co-immunoprecipitation studies using this mutant it was shown that upon MAPKAPK2 stimulation there was no longer an increase in interaction between p75NTR and PDE4A5, implying that the previous increase in interaction seen was indeed due to MAPKAPK2 phosphorylation of PDE4A5.

However what still remained unclear was what, if any, role this increased interaction would play in p75NTR and PDE4 mediated fibrinolysis. To test this, as previously, wild type NIH3T3 cells were compared to NIH3T3-p75NTR cells both of which had been seeded into 3D fibrin gel matrices. The cell-matrices were exposed to treatment with anisomycin (10 mg/ml) and fibrin degradation was studied after 9 days, figure 4.8. In the wild type NIH3T3 cells no significant difference was seen when

comparing fibrin degradation of no treatment 58 % +/- 4 % to anisomycin treatment 57 % +/- 3 % with a p value of 0.43. However when comparing the two treatments in the NIH3T3-p75NTR cells a significant difference is seen with no treatment giving 19 % +/- 2 % fibrin degradation whereas anisomycin treatment resulted in 1.4 % +/- 1.1 % degradation with a p value of 0.004.

This profound loss of fibrin degradation in anisomycin-treated NIH3T3-p75NTR cells was hypothesised to be due to the increased sequestration of PDE4A by p75NTR, further lowering local cAMP levels and thereby further inhibiting the fibrinolysis pathway through the pathway elucidated by Sachs et al 2007. To confirm that this effect was due to activation of the p38MAPK pathway, and not due to anisomycin having any other 'off-target' cellular effect, the experiment was repeated with the p38 MAPK inhibitor SB203580 along with anisomycin. Results for these treatments of NIH3T3-p75NTR show a marked difference between the anisomycin plus SB203580 treated cells, at 18 % +/- 2 % fibrin degradation compared to anisomycin treatment alone at 1.4 % +/- 1.1 %, with a p value of 0.005. This shows that the loss of fibrin degradation is due to activation of the p38MAPK pathway. In addition to this, I also carried out a treatment with both anisomycin and rolipram added together in the NIH3T3-p75NTR cells. This led to a level of fibrin degradation of 35 % +/- 3 %, which is a level of degradation that lies between that observed upon treatment with rolipram alone and with anisomycin alone. This suggests that the effects of p38MAPK pathway activation and PDE4 inhibition are competing with each other.

(a)

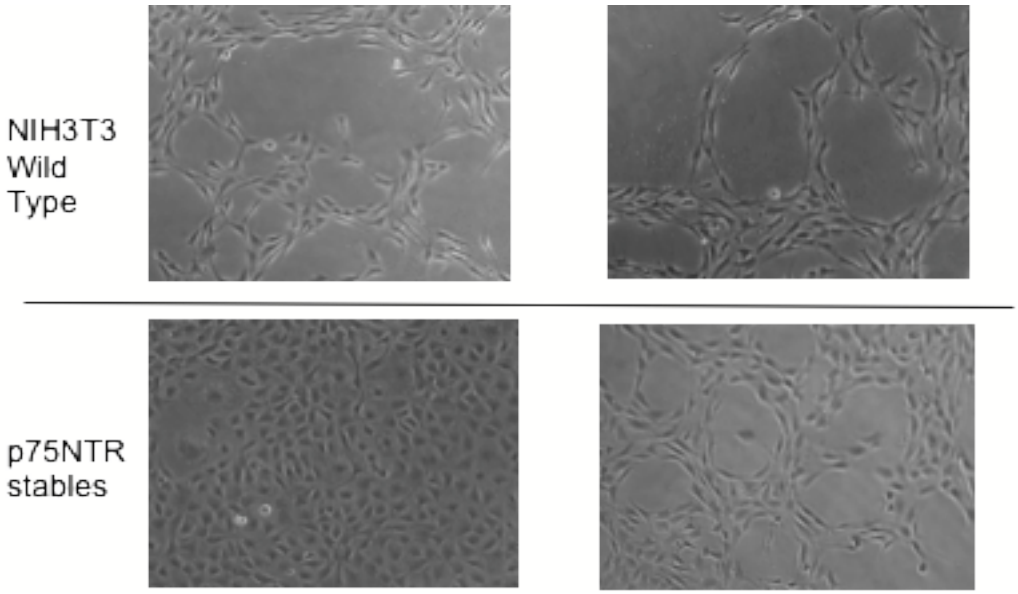

(b)

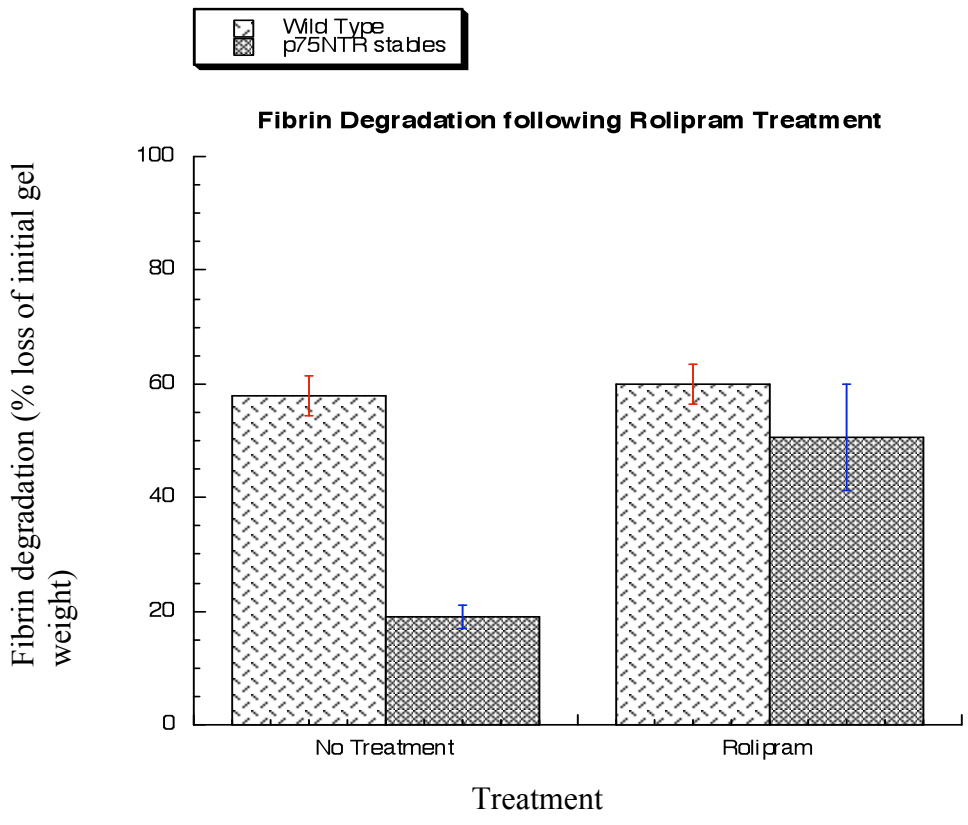

Figure 4.6 – Expression of p75NTR regulates fibrinolysis in NIH3T3 fibroblasts and is PDE4 dependent.

NIH3T3 cells and NIH3T3 p75NTR stable cells were seeded into 3-Dimensional fibrin gels and incubated at 37^{o}C for 9 days. Cells were either left untreated or subjected to prolonged treatment with the PDE4-specific inhibitor, rolipram (10 μM) for 8 days. (a) is 10X magnification images of fibrin gels and lytic zones. (b) is quantification of degradation of the 3D fibrin gels calculated by weighing after 9 days. All data shown are representative mean data +/- standard deviation of three separate experiments.

(a)

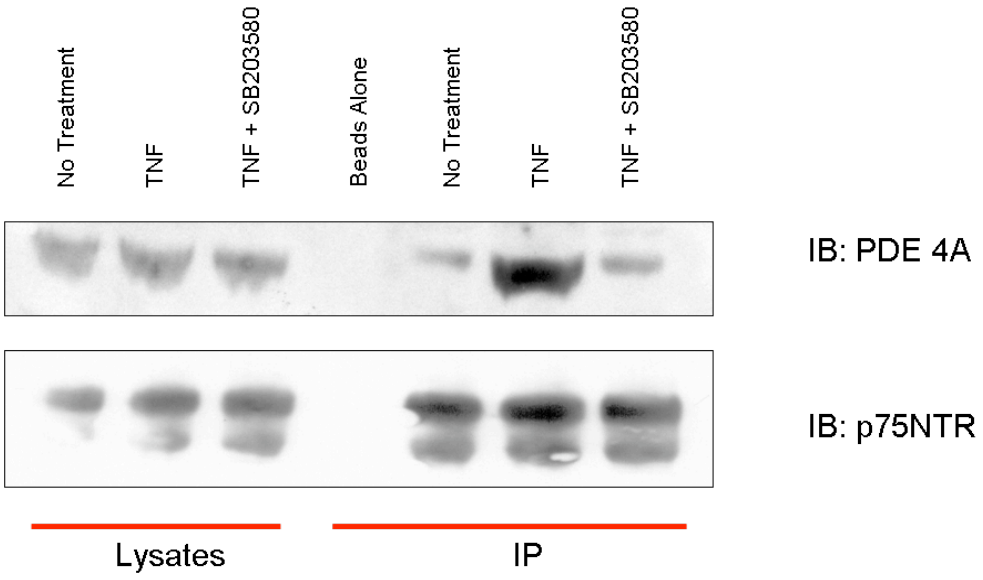

(b)

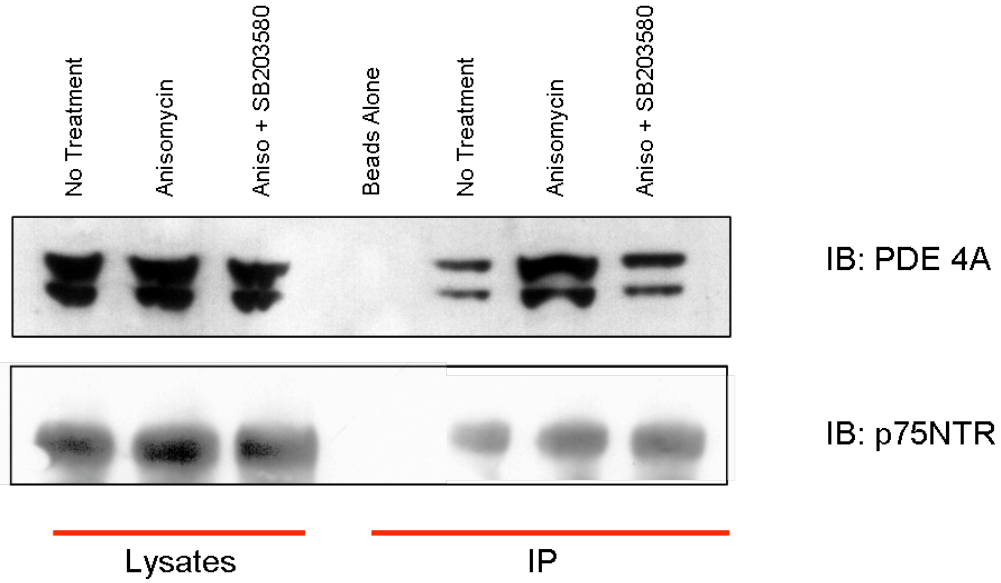

(c)

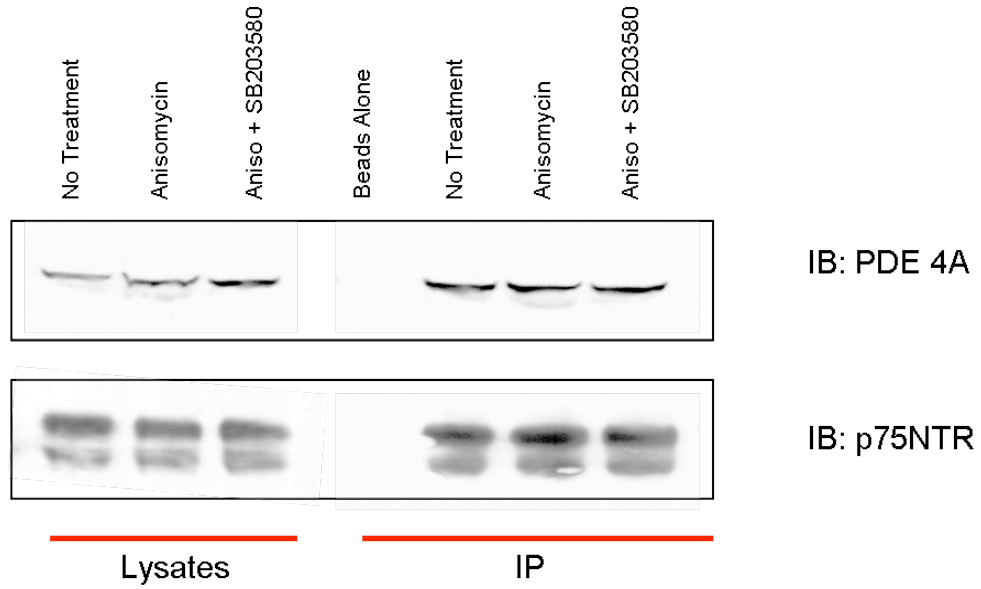

Figure 4.7 – MAPKAPK2 phosphorylation of PDE4A5 increases the level of PDE4A5 that co-immunoprecipitates with p75NTR.

(a) NIH3T3 p75NTR stable cells were either; left untreated, challenged for 10min with the p38 MAP Kinase activator, TNFα (10 µg/ml), or pre-treated with SB203580 (25

μM) to inhibit the p38 MAP kinase pathway for 30min followed by 10min TNFα (10 μg/ml) challenge. Total cell extract was produced and the lysates immunoprecipitated with anti-p75NTR anti-sera bound to agarose beads. These IPs were then probed with anti-PDE4A for endogenous PDE4A (top panel) and anti-p75NTR (bottom panel) anti-sera. (b) NIH3T3 p75NTR stable cells were transitently transfected to express rat PDE4A5. The transfected cells were either; left untreated, challenged for 60min with the p38 MAP Kinase activator, anisomycin (10 μg/ml), or pre-treated with the p38 MAP Kinase inhibitor, SB203580 (25 μM) for 30min followed by 60min anisomycin (10 μg/ml) challenge. Total cell extract was produced and the lysates immunoprecipitated with anti-p75NTR anti-sera bound to agarose beads. These IPs were then probed with anti-PDE4A (top panel) (NB transfection was done using a PDE4A5-VSV construct here however immuno-blotting was carried out with PDE4A specific antisera, it is assumed that the doublet band seen represents endogenous PDE4A5 as well as the PDE4A5-VSV transfected construct) and anti-p75NTR (bottom panel) anti-sera. (c) NIH3T3 p75NTR stable cells were transiently transfected to express the null MAPKAPK2 phosphorylation mutant of rat PDE4A5 (S147A). The transfected cells were either; left untreated, challenged for 60min with the p38 MAP Kinase activator, anisomycin (10 μg/ml), or pre-treated with SB203580 (25 μM) to inhibit the p38 MAP kinase pathway for 30min followed by 60min anisomycin (10 μg/ml) challenge. Total cell extract was produced and the lysates immunoprecipitated with anti-p75NTR anti-sera bound to agarose beads. These IPs were then probed with anti-PDE4A (top panel) and anti-p75NTR (bottom panel) anti-sera. All Western blots are representative blots of at least three separate experiments.

(a)

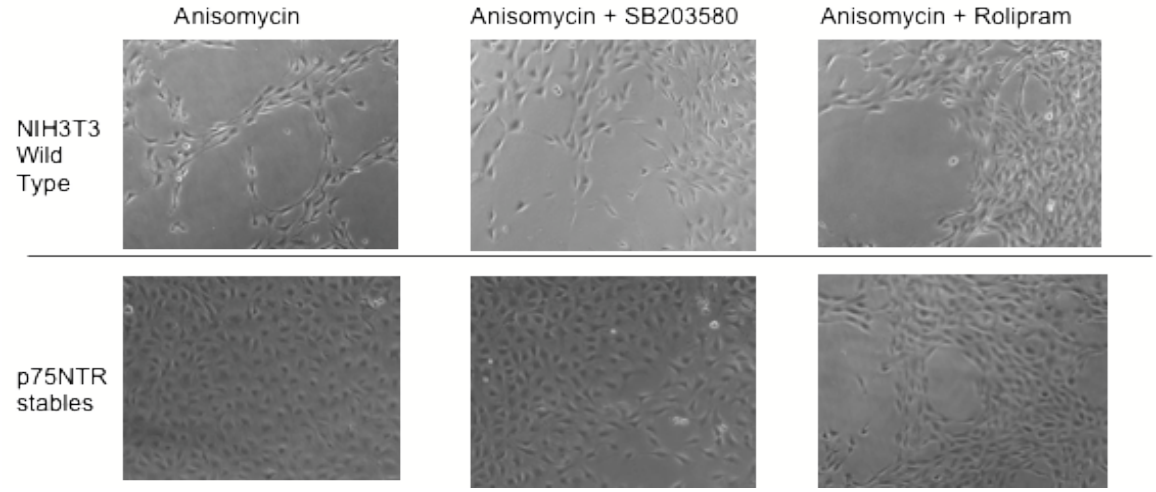

(b)

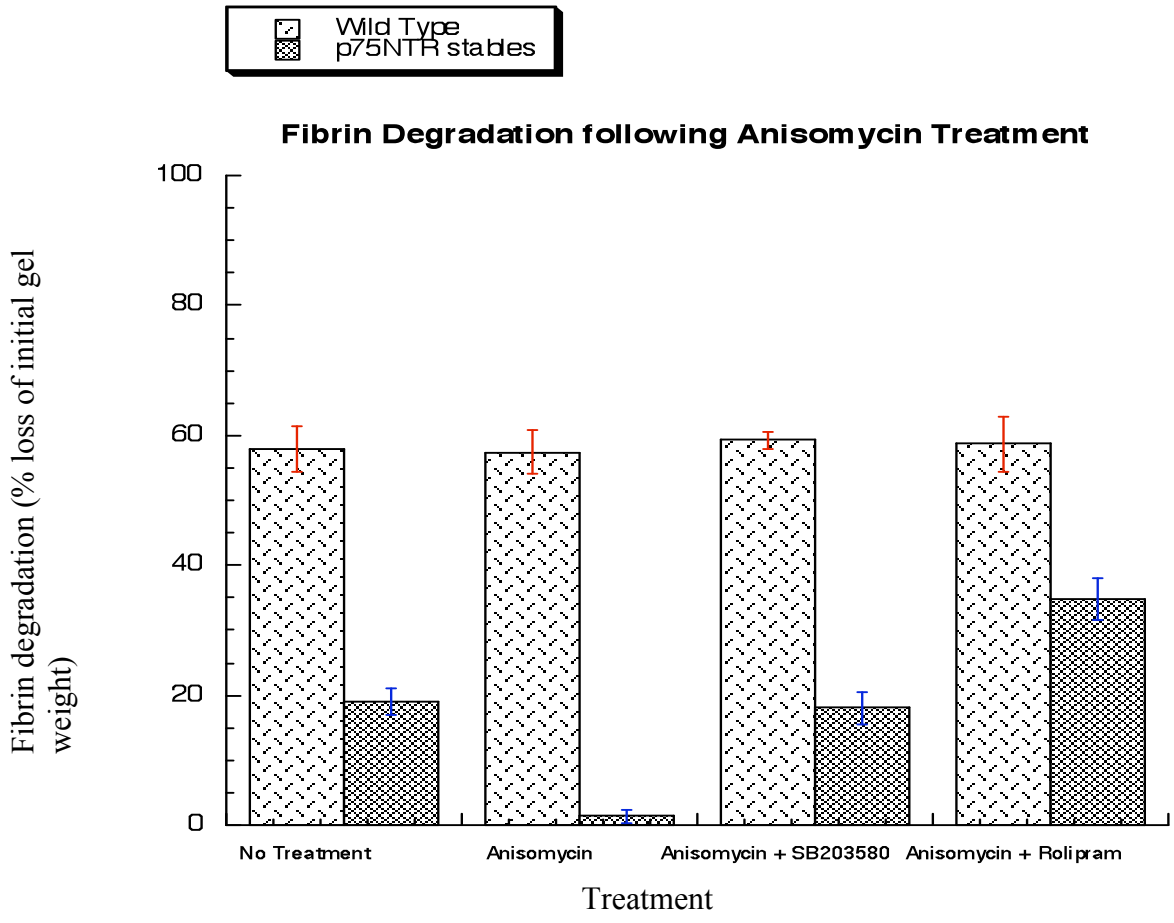

Figure 4.8 – MAPKAPK2 Phosphorylation regulates p75NTR mediated fibrinolysis in NIH3T3 fibroblasts and is PDE4 dependent.

NIH3T3 cells and NIH3T3 p75NTR stable cells were seeded into 3-Dimensional fibrin gels and incubated at 37^{o}C for 9 days. Cells were either; left untreated, subjected to prolonged treatment with the p38 MAP Kinase activator anisomycin (1 μg/ml) for 8 days, pre-treated with SB203580 (25 μM) to inhibit the p38 MAP kinase pathway for one day followed by prolonged treatment with both SB203580 and the p38 MAP Kinase activator anisomycin (1 μg/ml) for 8 days, or pre-treated with the PDE4-specific inhibitor, rolipram (10 μM) for one day followed by prolonged treatment with both rolipram and the p38 MAP Kinase activator anisomycin (1 μg/ml) for 8 days. (a) is 10X magnification images of fibrin gels and lytic zones. (b) is quantification of degradation of the 3D fibrin gels calculated by weighing after 9 days. All data shown are representative mean data +/- standard deviation of three separate experiments.

Having identified a novel role for the p38MAPK pathway in modulating regulation of fibrin breakdown through the p75NTR/PDE4A system in a model cell system it was important to establish whether this effect could be shown in a primary cell system. To do this Mouse embryonic Fibroblast cells (MEFs) were used. Wild type MEFs were obtained from both c57 black mice and, in addition, from c57 black mice developed by Prof Marco Conti's Laboratory (UCSF, San Francisco, USA) to have PDE4A knocked out by deletion of a catalytic unit encoding exon, referred to hereafter as PDE4A (-/-). Initial tests were performed on these MEFs to confirm that they expressed both p75NTR and PDE4A (in the wild type) and lacked PDE4A expression (in the PDE4A (-/-) knockout), data not shown. Phosphodiesterase activity assays were also performed to compare overall PDE and PDE4 activity levels in the wild type MEFs and those from the PDE4A-/- knockout. These results showed that knocking out PDE4A has only a very small effect on total cAMP phosphodiesterase activity. These data confirm what has been previously shown in the Houslay lab (unpublished) where PDE4A has very low expression level in many non-neuronal cell types.

I found that I could use this primary cell system to perform fibrin degradation assays as described above. Thus both wild type MEFs and PDE4A (-/-) MEFs were seeded into 3D fibrin gel matrices and degradation studied after 9 days, figure 4.9. Comparison between the wild type and the PDE4A (-/-) cells showed that while wild type cells had a level of fibrin degradation of 20 % +/- 1.7 %, the PDE4A (-/-) MEFs cells showed a significantly higher level of degradation at 66 % +/- 9 % with a p value of 0.009. This is consistent with a role for PDE4A in regulating p75NTR functioning in inhibiting fibrin degradation [Sachs et al., 2007]. It also is consistent with my studies showing that pan PDE4 inhibition with rolipram treatment potentiating fibrin breakdown in the NIH3T3-p75NTR cell model.

Consistent with this finding, I noted that when wild type MEFs were treated with the PDE4 inhibitor rolipram (10 μM) then fibrin degradation rose to 57 % +/- 3 %, showing that loss of 'pan' PDE4 activity in the fibrin degradation pathway leads to an increase in fibrinolysis. However, I was able to show that loss of PDE4A alone is responsible for this change of fibrinolysis in that when the PDE4A (-/-) MEFs were treated with rolipram then fibrin degradation was unchanged from untreated cells, being some 60 % +/- 6 % after 9 days. These results show no significant difference to that of untreated PDE4A (-/-) MEFs, with a p value of 0.23, figure 4.9. This shows that inhibition of the PDE4B and PDE4D isoforms still present in PDE4A (-/-) MEF cells does not affect fibrin degradation indicating the regulatory effect of p75NTR involves purely PDE4A, presumably through its specific sequestration to the p75NTR.

The next stage in investigating the role of PDE4A in the inhibitory effect of p75NTR on fibrin degradation in MEFs was to establish if MAPKAPK2 phosphorylation of PDE4A5 due to activation of the p38MAPK pathway played a role in alteration of fibrinolysis, figure 4.9. Comparison of the wild type MEF cells and the PDE4A-/- MEF cells, in fibrin degradation assays, showed that prolonged exposure to anisomycin (10mg/ml) resulted in 3 % +/- 2 % degradation in the wild type, whereas 59 % +/- 5 % was shown in the PDE4A (-/-) cells. When these data were compared to the results for degradation in the absence of added anisomycin, the PDE4A (-/-) cells

showed no significant difference %, p value of 0.25, to the untreated degradation level of 66 % +/- 10 observed. However, in marked contrast to this when using the wild type MEFs a significant difference was seen, in that under anisomycin challenge fibrin degradation in wild type MEFs is fully ablated. The anisomycin experiment was then repeated in the presence of the p38 MAP Kinase inhibitor SB203580, which is shown to have no effect on the level of fibrin degradation in the PDE4A (-/-) MEFs but, in the case of the wild type MEFs, it returns the degradation level back to ones that are similar to the level seen upon no treatment, namely 20 % +/- 5 %, confirming that this effect was indeed due to activation of the p38 MAP Kinase signalling cascade and not any off-target effect of anisomycin on these cells.

Although this confirmed that the p38 MAP Kinase pathway seems to play a role in loss of fibrin degradation I needed to design experiments to determine whether the observed effects were due to PDE4A phosphorylation by MAPKAPK2 or not, figure 4.10. To do this PDE4A (-/-) MEFs were efficiently transfected (> 65-80%) using Amaxa® technology to express either PDE4A5 or the MAPKAPK2 phosphorylation null mutant of PDE4A5, namely S147A-PDE4A5, figure 4.10. Such transfected cells were seeded into 3D fibrin gel matrices and exposed to a series of treatments, as was done previously. Re-introduction of PDE4A5 into the knockout MEFs was shown to "rescue" (recapitulate) the effect seen in wild type cells with degradation levels of 22 % +/- 9 % under no stimulation and, indeed, a similar level of degradation (23 % +/- 7 %) was seen in the cells re-expressing the MAPKAPK2 phosphorylation null S147A-PDE4A5 mutant, which I have shown previously (Chapter 3) to have similar cAMP-degrading PDE activity to wild-type PDE4A5. Cells transfected with either of these two constructs showed a similar increase in fibrin degradation upon rolipram challenge with wild-type PDE4A5 transfected cells having a level of 58 % +/- 10 % and S147A-PDE4A5 transfected cells having a level of 62 % +/- 9 %. However a significant difference is seen between the MEFs transfected with these two cell constructs in the case of anisomycin challenge where wild-type PDE4A5 transfected cells show reduced fibrin degradation, 4 % +/- 3 % (p value of 0.031) when compared to untreated cells whereas the S147A-PDE4A5 transfected cells do not show any significant difference

compared to untreated cells, with degradation remaining at a level of 25 % +/- 4 % (p value of 0.37). Challenge with the p38 MAPK inhibitor SB203580 ablated the effect of anisomycin in wild-type PDE4A5 transfected cells (Figure 4.10 c). These data indicate that the loss of fibrin degradation seen in wild type MEFs upon anisomycin stimulation is likely to be due to the MAPKAPK2 phosphorylation of PDE4A5.

To confirm the role of functionality of PDE4A5 in this system the PDE4A (-/-) MEF cells were transfected to express a catalytically inactive form of PDE4A5, figure 4.11. This construct D591A-PDE4A5 has a single alanine mutation of an essential Asp591 that is located deep in the catalytic pocket which renders it catalytically inactive [McCahill et al., 2005]. In the case of PDE4A (-/-) MEFs transfected with this construct, then in the fibrin degradation assay, fibrinolysis levels were unchanged by transfection, being at a high level of 65 % +/- 5 %. Additionally there was no significant difference seen in this level upon challenge with either rolipram alone, anisomycin alone or anisomycin + SB203580. This shows that catalytically active PDE4A must be transfected in for it to have an effect on p75NTR-mediated inhibition of fibrinolysis.

These data all indicate that PDE4A plays a critical role in the ability of p75NTR to inhibit fibrin degradation. In order to explore this further I set out to investigate whether removing an isoform PDE4 from a different sub-family would an effect of fibrin degradation. To do this PDE4B (-/-) MEFs were seeded into 3D fibrin gel matrices and degradation was compared with that of wild-type MEFs, figure 4.12. This showed that both wild type and PDE4B (-/-) MEFs had a similar level of fibrin degradation of 20 % +/- 2 % and 17 % +/- 5 %, respectively, with a p value of 0.18. This shows that loss of PDE4B does not affect p75NTR mediated inhibition of fibrin degradation. I also showed that under challenge with either rolipram alone or anisomycin alone or anisomycin + SB203580 there was no significant difference between the data obtained using wild type MEFs compared to the PDE4B (-/-) MEFS.

(|a)

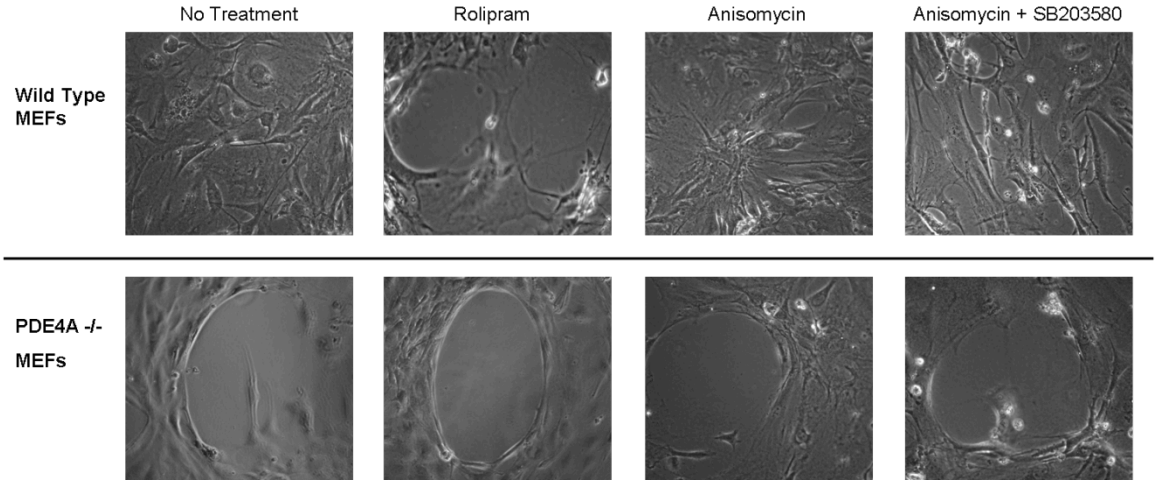

(b)

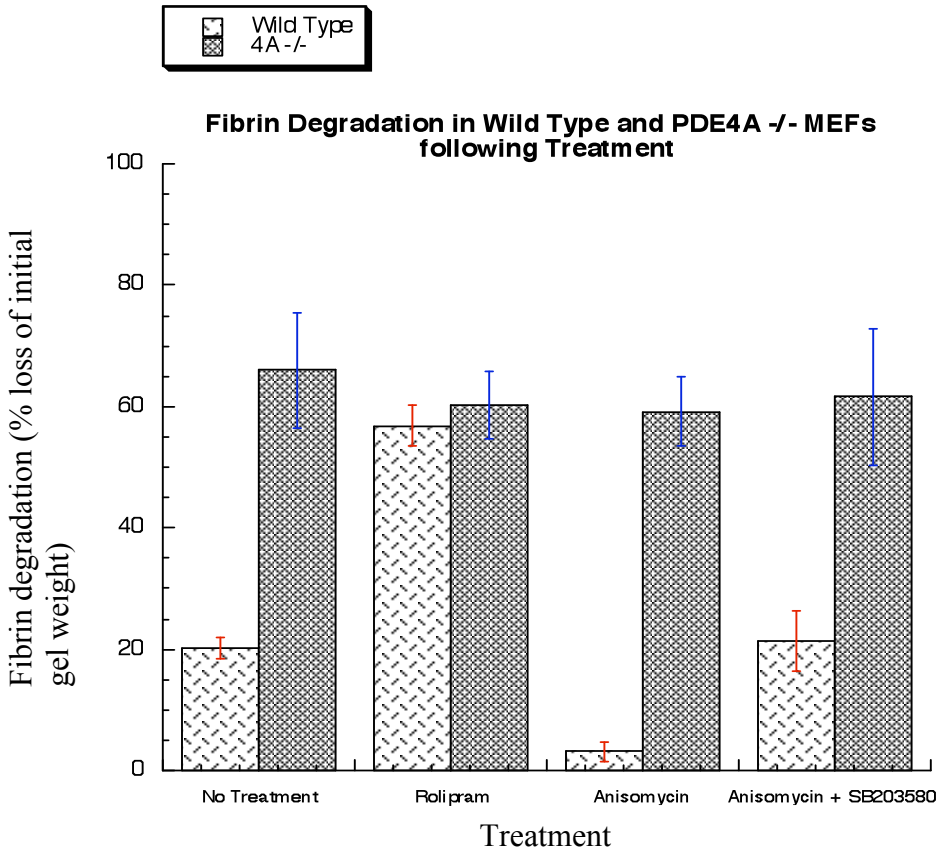

Figure 4.9 – MAPKAPK2 Phosphorylation regulates p75NTR mediated fibrinolysis in Mouse Embryonic Fibroblasts and is PDE4A dependent.

Mouse Embryonic Fibroblasts (MEFs) and PDE4A knock-out (4A-/-) mouse embryonic fibroblasts were seeded into 3-Dimensional fibrin gels and incubated at 37^{o}C for 9 days. Cells were either; left untreated, subjected to prolonged treatment with the PDE4-specific inhibitor, rolipram (10 μM) for 8 days, subjected to prolonged treatment with the p38 MAP Kinase activator anisomycin (1 μg/ml) for 8 days, or pre-treated with SB203580 (25 μM) to inhibit the p38 MAP kinase pathway for one day followed by prolonged treatment with both SB203580 and the p38 MAP Kinase activator anisomycin (1 μg/ml) for 8 days. (a) is 10X magnification images of fibrin gels and lytic zones. (b) is quantification of degradation of the 3D fibrin gels calculated by weighing after 9 days. All data shown are representative mean data +/- standard deviation of three separate experiments.

(a)

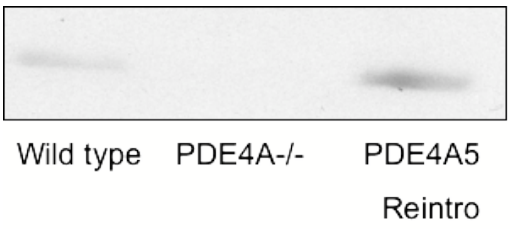
Wild type
PDE4A-/-
PDE4A5
Reintro

(b)

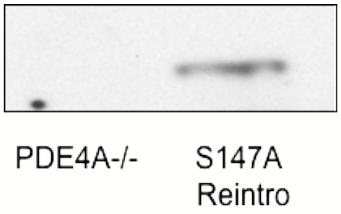
PDE4A-/-
S147A
Reintro

(c)

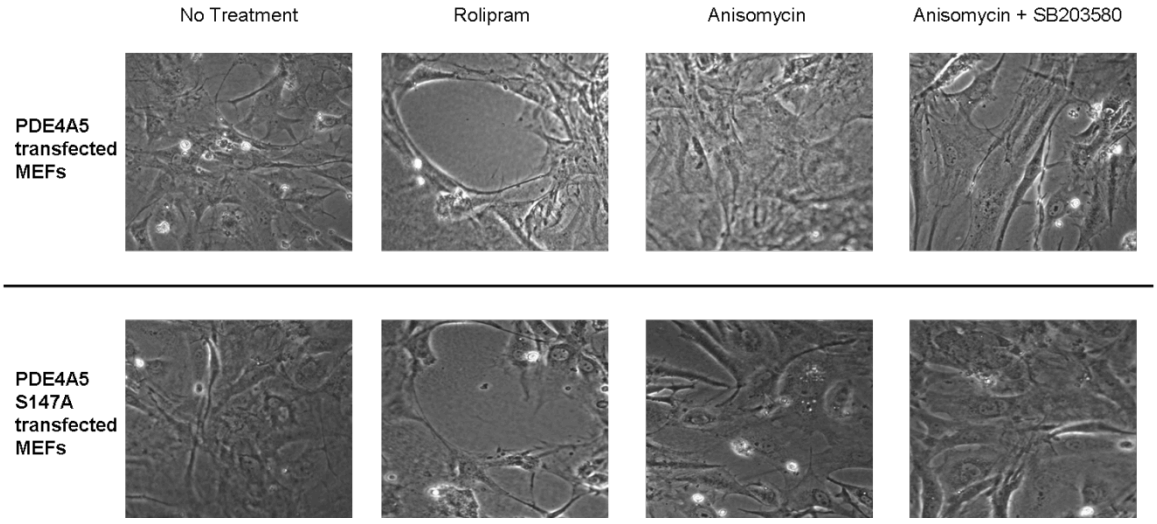
No Treatment
Rolipram
Anisomycin
Anisomycin + SB203580
PDE4A5 transfected MEFs
PDE4A5 S147A transfected MEFs

(d)

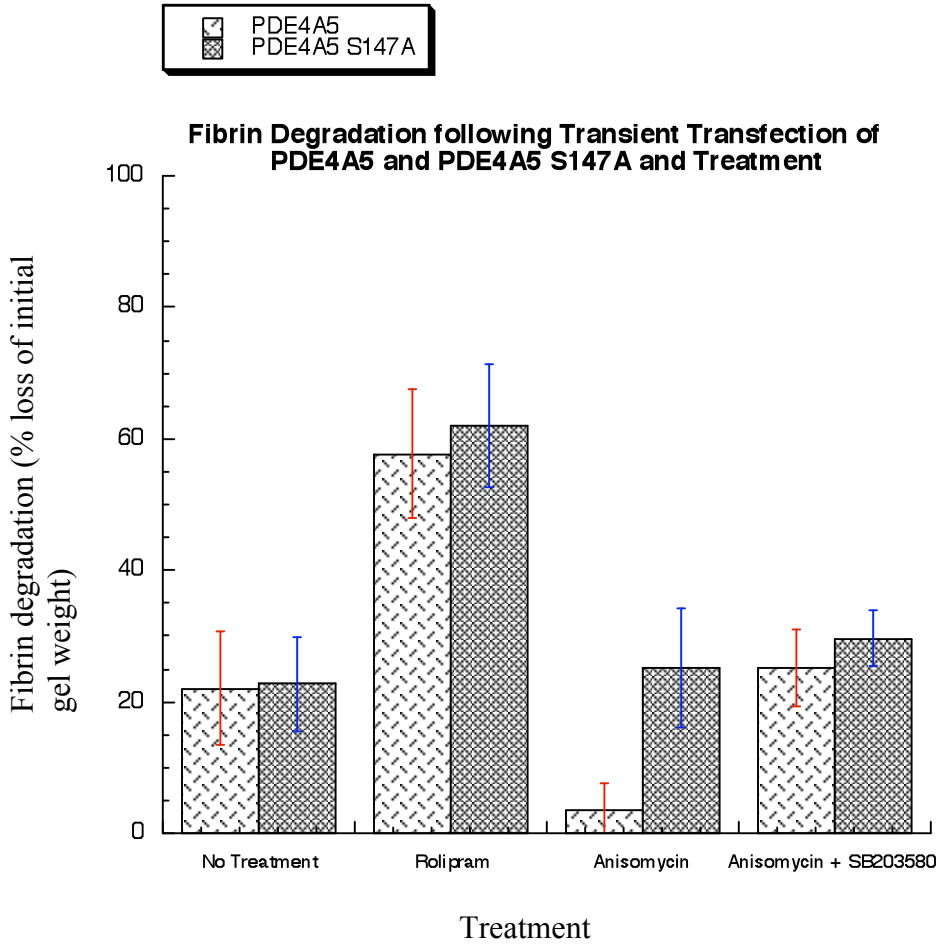

Figure 4.10 – MAPKAPK2 Phosphorylation of PDE4A5 regulates p75NTR mediated fibrinolysis in Mouse Embryonic Fibroblasts.

PDE4A knock-out, PDE4A (-/-), mouse embryonic fibroblasts were transiently transfected to express PDE4A5 and the null MAPKAPK2 phosphorylation mutant of rat PDE4A5 (S147A). (a) and (b) shows western blots of lysates of these cells, immuno-probed with a PDE4A specific antibody. They were then seeded into 3-Dimensional fibrin gels and incubated at 37^{o}C for 9 days. Cells were either; left untreated, subjected to prolonged treatment with the PDE4-specific inhibitor, rolipram (10 μM) for 8 days, subjected to prolonged treatment with the p38 MAP Kinase activator anisomycin (1 μg/ml) for 8 days, or pre-treated with SB203580 (25 μM) to inhibit the p38 MAP kinase pathway for one day followed by prolonged treatment with both SB203580 and the p38

MAP Kinase activator anisomycin (1 μg/ml) for 8 days. (c) is 10X magnification images of fibrin gels and lytic zones. (d) is quantification of degradation of the 3D fibrin gels calculated by weighing after 9 days. All data shown are representative mean data +/- standard deviation of three separate experiments.

(a)

PDE4A-/- PDE4A5 DN Reintro

(b)

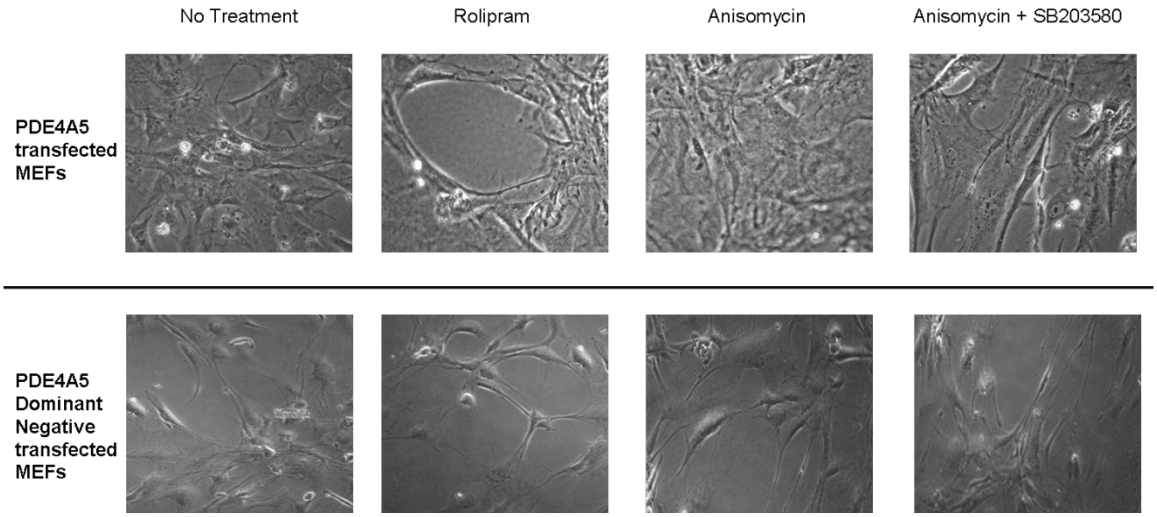

(c)

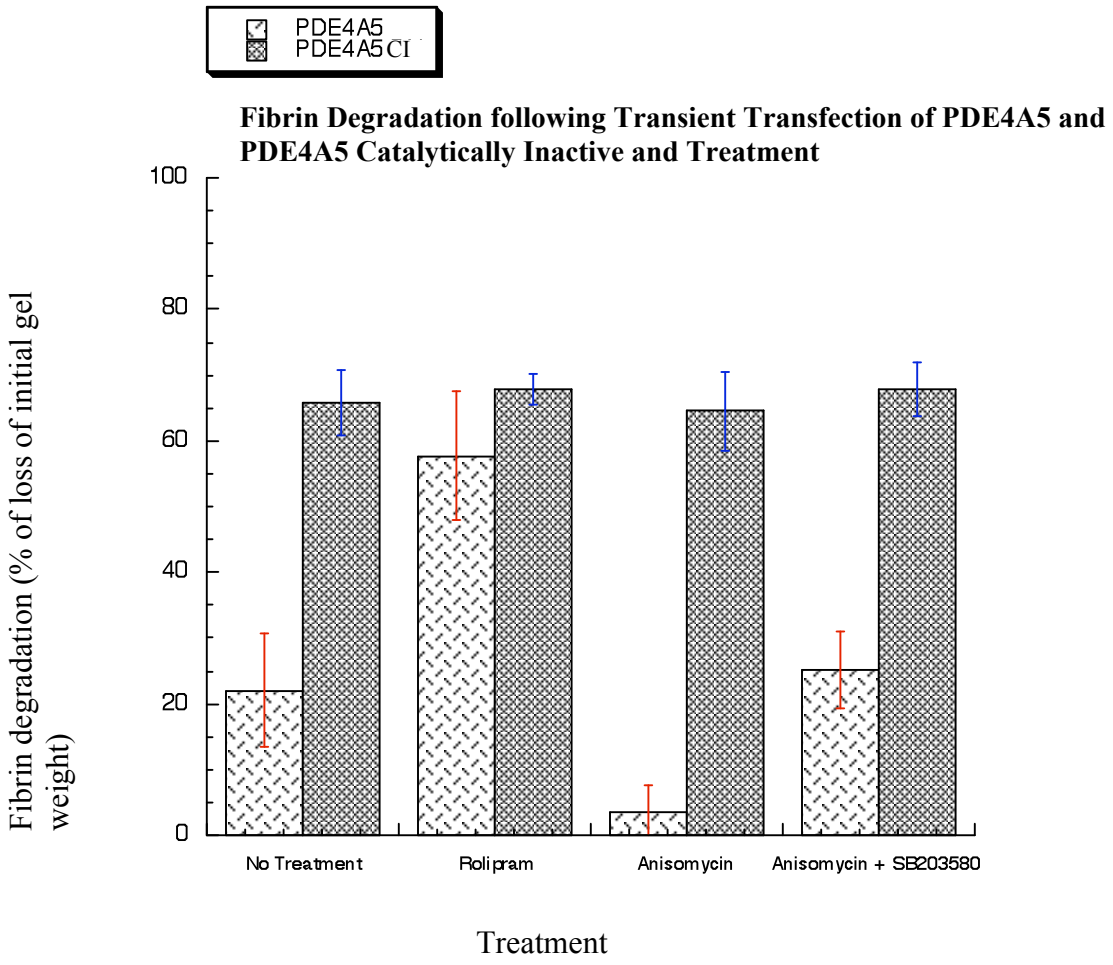

Figure 4.11 – PDE4A5 function regulates p75NTR mediated fibrinolysis in Mouse Embryonic Fibroblasts.

PDE4A knock-out PDE4A (-/-) mouse embryonic fibroblasts were transiently transfected to express PDE4A5 and catalytically inactive mutant of rat PDE4A5 (PDE4A5-CI), western blot of PDE4A5 catalytically inactive reintroduction is shown in (a), blots were probed with a PDE4A specific antibody. They were then seeded into 3-Dimensional fibrin gels and incubated at 37^{o}C for 9 days. Cells were either; left untreated, subjected to prolonged treatment with the PDE4-specific inhibitor, rolipram (10 μM) for 8 days, subjected to prolonged treatment with the p38 MAP Kinase activator anisomycin (1 μg/ml) for 8 days, or pre-treated with SB203580 (25 μM) to inhibit the p38 MAP kinase pathway for one day followed by prolonged treatment with

both SB203580 and the p38 MAP Kinase activator anisomycin (1 μg/ml) for 8 days. (b) is 10X magnification images of fibrin gels and lytic zones. (c) is quantification of degradation of the 3D fibrin gels calculated by weighing after 9 days. All data shown are representative mean data +/- standard deviation of three separate experiments.

(a)

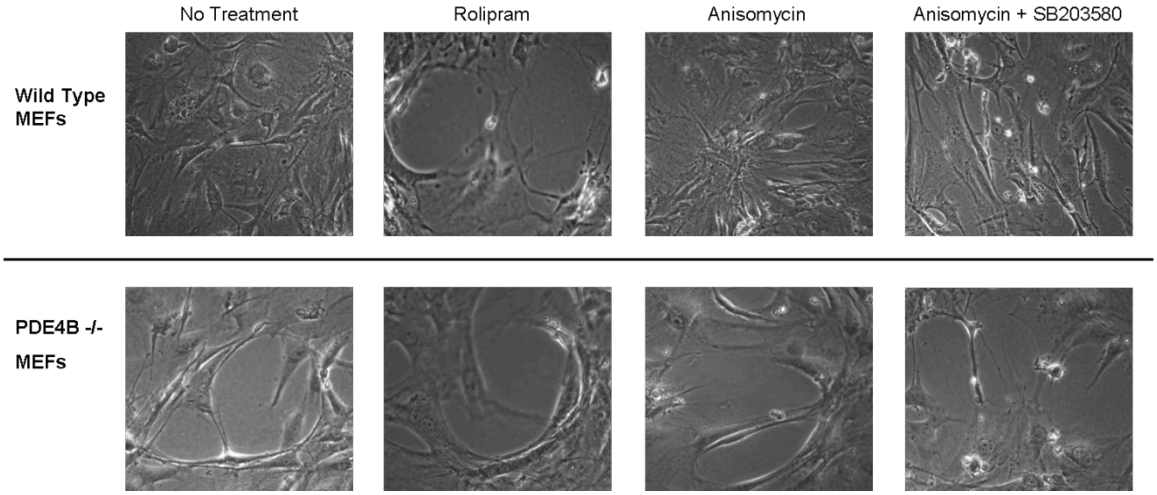

(b)

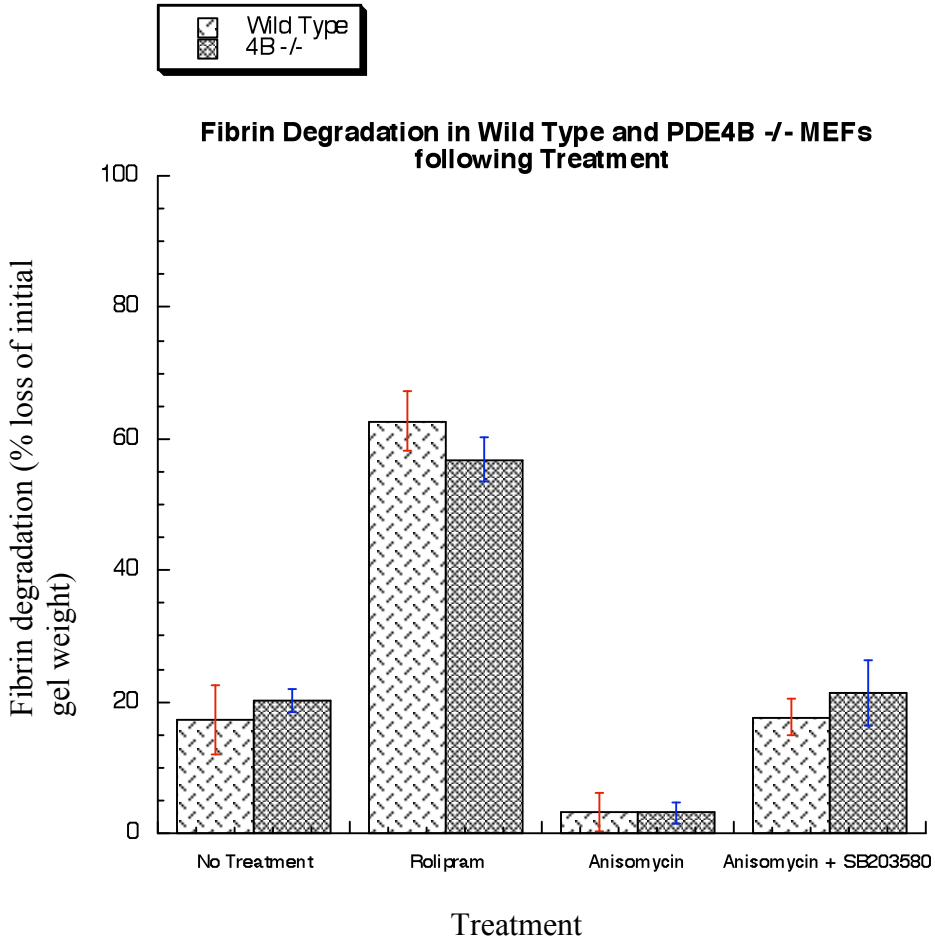

Figure 4.12 – Fibrinolysis in mouse embryonic fibroblasts and is not PDE4B dependent.

Mouse Embryonic Fibroblasts (MEFs) and PDE4B knock-out, PDE4B (-/-) mouse embryonic fibroblasts were seeded into 3-Dimensional fibrin gels and incubated at 37^{o}C for 9 days. Cells were either; left untreated, subjected to prolonged treatment with the PDE4-specific inhibitor, rolipram (10 μM) for 8 days, subjected to prolonged treatment with the p38 MAP Kinase activator anisomycin (1 μg/ml) for 8 days, or pre-treated with SB203580 (25 μM) to inhibit the p38 MAP kinase pathway for one day followed by prolonged treatment with both SB203580 and the p38 MAP Kinase activator anisomycin (1 μg/ml) for 8 days. (a) is 10X magnification images of fibrin gels and lytic zones. (b) is quantification of degradation of the 3D fibrin gels calculated by weighing after 9 days. All data shown are representative mean data +/- standard deviation of three separate experiments.

4.3 Discussion

Inappropriate fibrin deposition after injury and in disease states is a major pathological condition which is largely untreatable clinically [Adams et al., 2004]. Understanding the molecular means through which fibrin breakdown is inhibited is important in understanding molecular pathologies and identifying new therapeutic targets. The p75 neurotrophin receptor is up-regulated in injury and many fibrotic disease states and can markedly inhibit fibrin breakdown. In this study and through collaboration with the Akassoglou lab at UCSD we have shown that to achieve this inhibitory action of p75NTR, it needs to sequester PDE4A5 [Sachs et al., 2007]. Interestingly many PDE4 selective inhibitors have already been developed to treat inflammatory lung disease, where fibrosis is a major issue. A key part of the efficacy of these drugs relates to their being potent inhibitors of the action of TNFα [Houslay et al., 2005; Spina, 2008]. TNFα is already known to have potent pro-fibrotic actions, the molecular basis of this is poorly understood. It is however known that a key signalling

pathway activated by TNF– α [Itatsu et al., 2009] is the stress-activated, p38 MAP kinase cascade [Dent et al., 2003; Uhlik et al., 2003; Xu et al., 2006], which plays a fundamental role in regulating the immune and inflammatory response to infection and tissue injury [Dong et al., 2002].

MAPKAPK2 is an important downstream protein kinase in the p38 MAPK pathways. It is phosphorylated and activated by p38 MAPK [Ben-Levy et al., 1998; Meng et al., 2002; Stokoe et al. 1992]. Relatively few substrates for MAPKAPK2 have been identified to date limiting the understanding of the consequences of its activation. In chapter 3 it was shown that MAPKAPK2 can phosphorylate PDE4A5, leading to attenuation of its activation through PKA phosphorylation.

Using NIH3T3 cells as a model system and MEFs as a primary cell system, I have shown that in cells containing both p75NTR and PDE4A5 there was only a very low level of fibrin degradation, consistent with the hypothesis that PDE4A5 activity and p75NTR play a role in inhibiting fibrin breakdown. This is further proved through the use of the PDE4 specific inhibitor, Rolipram and MEF 4A (-/-) knockout cells where I showed that fibrin degradation is greatly enhanced. However, I also observed that anisomycin treatment, and therefore activation of MAPKAPK2, profoundly decreases fibrin breakdown in wild-type cells whilst it fails to inhibit the enhanced fibrin breakdown seen in PDE4A (-/-) knockout MEFs. This indicates that anisomycin is exerting its inhibitory effect through PDE4A5, which is confirmed by anisomycins inability to inhibit the amplified rate of fibrin breakdown seen in wild-type MEFs treated with rolipram to pharmacologically ablate PDE4 activity. These results were recapitulated through transfection of PDE4A5 back in to the PDE4A (-/-) knockout MEFs, with this experiment resulting in restoration of the loss of fibrin degradation seen in wild type MEFs. Demonstration of a role for MAPKAPK2 in this regulatory system was shown by transfection of the MAPKAPK2 phosphorylation-defective Ser147Ala-PDE4A5 mutant into PDE4A (-/-) knockout MEFs. Whilst this mutant PDE4A5, which has identical activity to wild-type PDE4A5 led to a similar decrease in fibrin breakdown as seen with the wild-type PDE4A5, now anisomycin failed to cause any inhibition of

fibrin breakdown in cells transfected with this MAPKAPK2-phosphorylation defective mutant PDE4A5.

I propose that phosphorylation of PDE4A5 by MAPKAPK2 causes a conformational change in PDE4A5 of which one functional, phenotypic output is an enhanced ability to interact with p75NTR and consequent decrease in fibrin breakdown in fibroblasts expressing these species. This novel regulatory mechanism may provide an important contributor to the pro-inflammatory and pro-fibrotic actions associated with activation of the p38 MAPK/MAPKAPK2 phosphorylation cascade by TNFα and other inflammatory activating species. It may also provide and explanation as to why PDE4 inhibitors can reduce not only the progression of fibrosis but also aid remodelling by facilitating fibrin breakdown [Cortijo et al., 2009; de Visser et al., 2008; Videla et al., 2006].

Chapter 5 Multi-functional Docking Domains On PDE4A5

5.1 Introduction

With completion of the human genome project giving us a greater insight into disease the requirement for a quick, effective method of peptide screening, for the development of new peptide therapeutics (biologics), has become of increasing importance. Several high throughput techniques for doing this have been developed recently. One interesting technique for high throughput analysis of potential therapeutic targets is the SPOT-synthesis peptide library method. This method uses combinatorial chemistry to simultaneously create a number of different peptides in a library for use in screening specific targets for defining protein-protein interaction surfaces, peptide agonists/antagonists and peptides binding to enzymes as substrates, inhibitors and regulators [Frank, 2002].

In this technique short peptide chains are synthesized on a cellulose membrane where, for example, they can be overlaid with a tagged purified recombinant protein to elucidate whether interaction of the peptide and protein can occur or treated with an enzyme, such as a protein kinase to determine if they act as either a substrate or inhibitor [Kofler et al., 2005; Baillie et al., 2007; Sachs et al., 2007]. In the case of the work done in the study described here, peptides 25 amino acids in length, each overlapping by 5 residues, were synthesized to span the entire sequence of proteins such as PDE4A5. This peptide array was then overlaid with the potential interacting protein of interest and, in combination with analysis of 3D protein structures, the putative location of interaction sites can be elucidated [Bolger et al., 2006]. The role of individual amino acids within these potential linear binding epitopes can then be investigated by the creation of scanning amino acid substitution arrays. In these, every amino acid in a 25mer sequence is replaced by alanine, in turn, to create a library of ‘mutant’ peptides from the parent interacting peptide. Using this one can establish if binding is altered with a particular

amino acid substitution and, therefore, identify the potential importance of specific amino acids in the native peptide sequence in binding of the interacting protein. Once potentially important individual amino acids are elucidated through this technique they can then, once more, be altered to various other amino acids to allow optimization of protein binding through increasing affinity and selectivity [Gold et al., 2006]. Following this, membrane permeable peptides can be made to try and disrupt specific protein-protein interactions within the cell. These offer the potential for developing smaller peptides and peptidomimetics for potential therapeutic use in particular instances.

Despite this technique providing a highly specific, detailed way to establish the nature of protein-protein interactions it should be noted that it must be used with caution. Using small length peptides does not take in to account the steric chemistry of the proteins and therefore could give false positive results or miss detecting binding involving a number of amino acids that are far separated in the linear sequence but coalesce to form a complex binding site within the 3-D protein structure. To eliminate false positive interactions other biological techniques, such as co-immunoprecipitation, site-directed mutagenesis and bioinformational analyses, must be used in parallel with this technique.

Through use of SPOT-synthesis technology binding sites on PDE4 isoforms for beta-arrestin, RACK1 [Bolger et al., 2006], DISC1 [Murdoch et al., 2007] and Nudel [Collins et al., 2008] have been identified. Here I have identified a potential multifunctional docking site on the conserved catalytic unit of PDE4 isoforms. In other systems it has been suggested that proteins can contain multifunctional docking sites that allow them to bind a host of rapidly exchanging signaling molecules and potentially act as a scaffold for signaling [Ponzetto et al., 1994]. Examples of this have been identified in c-Kit, a pro-oncogenic stem cell factor receptor that can associate with three different members of the Src family through two separate multifunctional docking sites [Wollberg et al., 2003] and in the hepatocyte growth factor receptor where a multifunctional binding site has been shown to interact with various SH2 containing signal transducers [Ponzetto et al., 1994].

The discovery of a multifunctional docking site on PDE4 enzymes may allow for a deeper understanding in the role of these enzymes in signal scaffolding, provide a means of fidelity that constrains the number of partner proteins that a PDE4 isoform can engage with at any one time, may help untangle the issue of complicated side effects associated with therapeutic PDE inhibitors and may offer a new means of designing therapeutics using agents that modulate interaction at such sites.

5.2 Results

With the discovery of peptide array mapping technology the identification of potential sites of interaction between proteins has become easier. Interestingly, the fidelity and efficiency of phosphorylation of proteins, including certain PDE4 species, by the MAPK signaling pathway-related kinase, ERK requires docking sites in addition to the consensus recognition site surrounding the target serine [Sharrocks et al., 2000]. These KIM and FQF sites greatly facilitate phosphorylation by allowing ERK to dock onto the target molecule. As stated in previous chapters (Chapter 3) the kinase, MAPKAPK2 has been shown to phosphorylate PDE4. Clearly MAPKAPK2 has to interact directly with PDE4A5 to phosphorylate it. Here I set out to see if PDE4A5 and MAPKAPK2 bind to each other and be co-immunoprecipated and also to see if interaction sites could be identified using scanning peptide array technology.

5.2.1 A Potential Multifunctional Docking Domain

Previous work has shown that long form PDE4s contain an FQF binding motif that has been observed to play a critical role in its ability to bind several important regulatory proteins, such as ERK and beta-arrestin [Bolger et al., 2006] for example. To confirm whether this region is also critical for the interaction of MAPKAPK2 and other binding partners to PDE4A5, 5-residue overlapping 25-mer peptide arrays were made

with amino acid sequences representing this area for both PDE4A5 and PDE4D5 (amino acids 667-716 on PDE4A5 and amino acids 651-700 on PDE4D5). The PDE4A5 arrays were probed with purified recombinant GST alone and purified recombinant versions of two interactors known to bind to PDE4A5, namely the Src family tyrosyl kinase Lyn and MAPKAPK2, figure 5.2(a). Previously it had been shown that the SH3 domain of Lyn binds to the unique N-terminal domain of PDE4A5 [Beard et al., 2002]. These results showed that both full-length Lyn and MAPKAPK2 bind at the general site of the FQF motif, whereas GST alone does not. This identifies then a new binding site for Lyn on PDE4A5, namely within the FQF region, adding it to the growing number of proteins that bind to PDE4 isoforms at >1 interaction site.

The PDE4D5 arrays were probed with purified recombinant GST alone and purified recombinant versions of the known interactors, the sumo-conjugating enzyme UBC9, ERK and beta-arrestin, figure 5.2(b). These results showed that UBC9, ERK and beta-arrestin all bind at the general site of the FQF motif, whereas again GST alone does not. To confirm that this was due to the FQF portion of this region alanine scans were produced of the FQF region and its surrounding amino acids in both PDE4A5, figure 5.3(a) and PDE4D5, figure 5.3(b). These were overlaid with the same proteins mentioned above and all five of the proteins showed decreased binding when either of the phenylalanines of the FQF motif were mutated to alanine.

Figure 5.1 – Sequence alignments of Phosphodiesterase 4 Long Isoforms

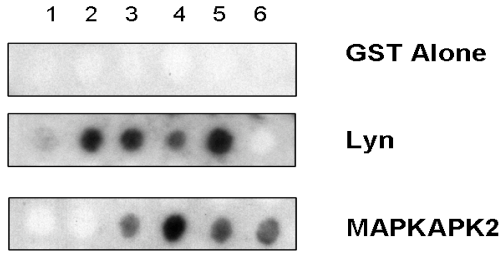

1 SAIRQSPSPPLEEEPGGLGHPSLPD
2 SPSPPLEEEPGGLGHPSLPDKFQFE
3 LEEEPGGLGHPSLPDKFQFELTLEE
4 GGLGHPSLPDKFQFELTLEEEEEED
5 PSLPDKFQFELTLEEEEEEDSLEVP
6 KFQFELTLEEEEEEDSLEVPGLPTT

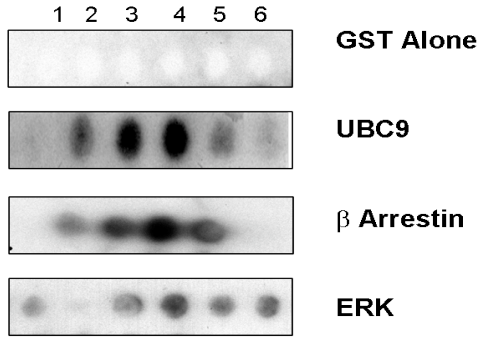

1 SPSPAPDDPEEGRQGQTEKFQFELT
2 PDDPEEGRQGQTEKFQFELTLEEDG
3 EGRQGQTEKFQFELTLEEDGESDTE
4 QTEKFQFELTLEEDGESDTEKDSGS
5 QFELTLEEDGESDTEKDSGSQVEED
6 LEEDGESDTEKDSGSQVEEDTSCSD

Figure 5.2 – Various proteins bind to a conserved region in the catalytic domain of long form PDE4s.

Peptide arrays were generated for the catalytic domain sequence of A.A. 667-716 on PDE4A5 and A.A. 651-700 on PDE4D5. These were probed with different purified recombinant proteins. (a) PDE4A5 was overlaid with GST alone, GST tagged Lyn

which is a protein tyrosine kinase and GST tagged MAPKAPK2. GST-specific anti-sera was then used to detect the areas of binding to the membrane. (b) PDE4D5 was overlaid with GST alone, GST tagged UBC9 which is an E2 ligase enzyme, GST tagged β-arrestin which is a signal scaffold protein and GST tagged extracellular regulated kinase (ERK). GST-specific anti-sera was then used to detect the areas of binding to the membrane. All peptide arrays are representative arrays of at least three separate experiments.

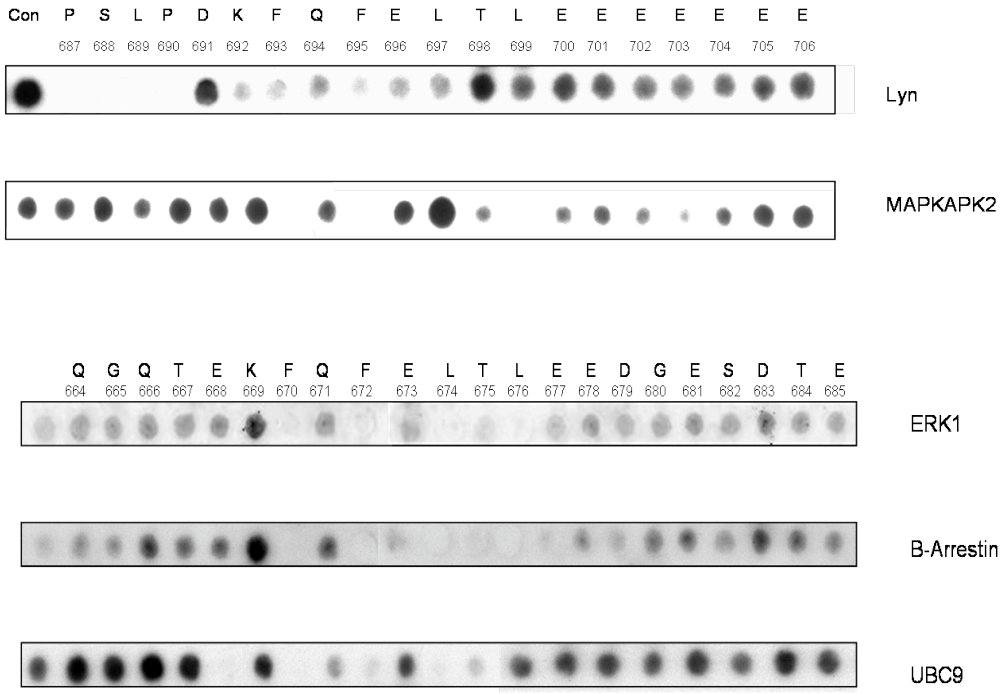

Figure 5.3 – Alanine Scanning of PDE4A5 and PDE4D5 sequences surrounding the FQF motif.

Peptide array technology was used to synthesise alanine scanning arrays of PDE4A5 and PDE4D5 on a Whatman 50 membrane. This was done using specific sequences highlighted in Figure 5.6. These are amino acids 687-706, in PDE4A5 and amino acids 664-685 in PDE4D5. A control spot was created with each sequence the each amino acid in turn was mutated to alanine. The membrane was probed with purified recombinant GST-tagged Lyn or MAPKAPK2 for PDE4A5 or GST-tagged ERK, B-

Arrestin or UBC9. GST-specific anti-sera was then used to detect the areas of protein binding to the membrane. Highlighted are the main amino acids where conversion to alanine ablates binding. All peptide arrays are representative arrays of at least three separate experiments.

5.2.2 Phosphodiesterase-4 may interact with MAPKAPK2

To further test the hypothesis that PDE4 isoforms might sequester MAPKAPK2 co-immunoprecipitation studies were carried out. These experiments were performed using HEK293 cells, figure 5.4(b), (c) and (d), for PDE4B, PDE4C and PDE4D isoforms and using COS1 cells transiently transfected to express PDE4A5, as PDE4A isoforms exist in such low levels endogenously they cannot be easily detected, figure 5.4(a). Lysates were made and endogenous MAPKAPK2 was immunoprecipitated using Protein G beads coupled to a commercially available MAPKAPK2 antibody. Western blots were then run and probed with antibodies specific for PDE4A, PDE4B, PDE4C and PDE4D. These results showed that long form versions from all PDE4 subtypes could co-immunoprecipitate with MAPKAPK2.

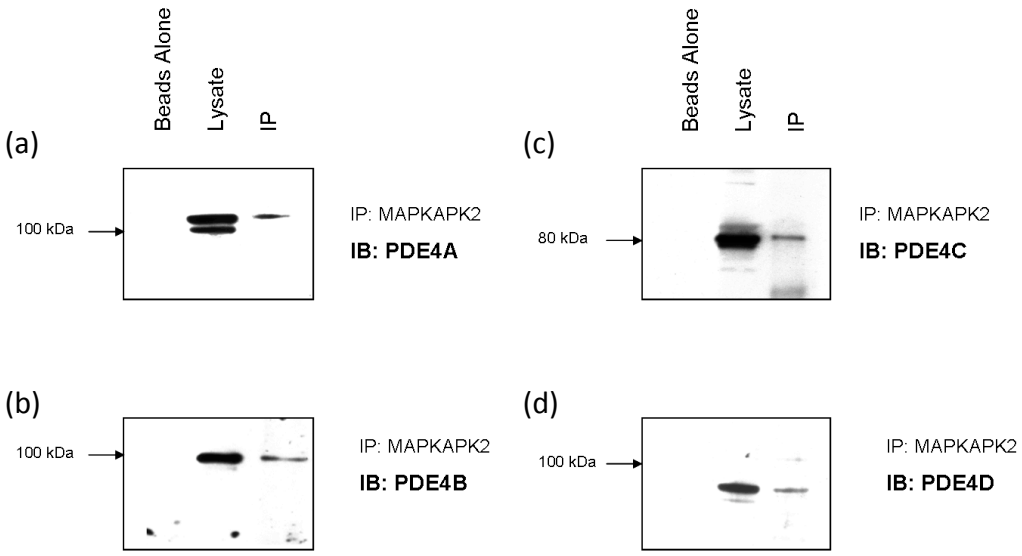

Figure 5.4 – MAPKAPK2 interacts with PDE4 long form isoforms in HEK293 cells.

HEK293 cells were transiently transfected with PDE4A5, (a). Total cell extract was produced and the lysates immunoprecipitated with MAPKAPK2 anti-sera conjugated to Protein G agarose beads. This IP was then probed with anti-PDE4A anti-sera and MAPKAPK2 anti-sera (data not shown). (b), (c) and (d) Total cell extract was produced from untransfected wild type HEK293 cells. The lysates were immunoprecipitated with MAPKAPK2 conjugated to Protein G agarose beads and resultant IPs probed with PDE4B, PDE4C and PDE4D anti-sera respectively and MAPKAPK2 anti-sera (data not shown). All Western blots are representative blots of at least three separate experiments.

5.2.3 Phosphodiesterase 4A5 directly interacts with MAPKAPK2 at four specific sites

Further studies into the interaction of PDE4 with MAPKAPK2 were focused on PDE4A5 as this has been the focus of my studies as described in previous chapters. In these I showed that MAPKAPK2 has a functional link in regulating PDE4A5.

A full-length peptide array of PDE4A5 was made. This consisted of peptide "spots" of 25 amino acids that overlapped by five amino acids, making up the entire PDE4A5 sequence. This array was then overlaid with purified recombinant GST tagged MAPKAPK2 and the location of binding sites established by probing with GST specific anti-sera and processed in a similar fashion to a western blot. The results showed that when spots previously shown to bind GST alone were discounted; four potential binding sites for MAPKAPK2 on PDE4A5 were identifiable, figure 5.5. These sites were amino acids 131-155 within UCR1, amino acids 582-606 and 647-671 within the catalytic region and amino acids 682-702 within the C-terminal region.

To gain further insight into particular amino acids that were important in each of these regions and to confirm the fidelity of interaction at such sites, alanine scanning peptide arrays were created for each region. These alanine scan arrays were then probed with purified recombinant GST tagged MAPKAPK2 and probed as described previously, figure 5.6. These data show that in the first region identified, in UCR1, mutation of amino acids phenylalanine 141, leucine 142 and tyrosine 143 to alanine ablated binding. This suggests that such residues may play a crucial role in the interaction of PDE4A5 with MAPKAPK2. In the first catalytic region sequence, potentially important amino acids identified as required for binding were Trp 591, Thr 592, Ile 595, Glu 598 and Phe 599. In the second catalytic region sequence potentially important amino acids that were identified as required for binding were Ile 654, Leu 655, Asp 656, Trp 664, Tyr 665, His 666, Ser 667, Ile 669 and Gln 671. Finally in the C-terminal region the amino acids Phe 693, Gln 694, Phe 695, Thr 698, Leu 699, Glu 700, Glu 701, Glu 702 and Glu 703 were shown to be potentially important amino acids required for binding.

Surface exposure of these potentially important residues was then evaluated using molecular modeling on PDE4A4, the human orthologue of PDE4A5, as the structure of this human isoform is known [Terry et al., 20003] and the sequence of their catalytic units is highly conserved. This analysis showed that amino acids Phe 141, Leu 142 and Tyr 143; Ile 654, Leu 655 and Asp 656; Trp 664, Tyr 665, His 666 and Ser 667; Phe 693, Gln 694, Phe 695 and Thr 698, Leu 699, Glu 700, Glu 701, all were well exposed at surface and so could potential interact with MAPKAPK2, Figure 5.7.

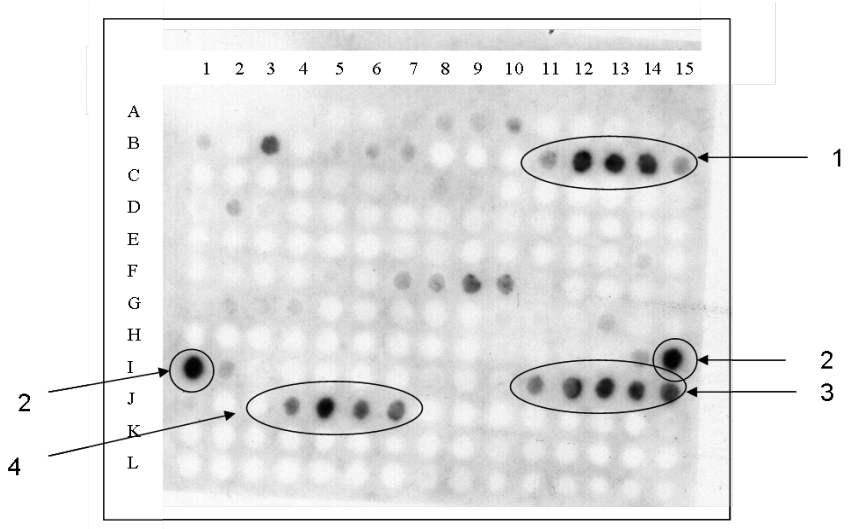

1. A.A. 121-165 QASPGLVLHAGATTSQRRESFLYRS
LVLHAGATTSQRRESFLYRSDSDYD
GATTSQRRESFLYRSDSDYDMSPKA
QRRESFLYRSDSDYDMSPKAVSRSS
LYRSDSDYDMSPKAVSRSSSVASE

2. A.A. 577-606 DLSNPTKPLELYRQWTDRIMAEFFQ
TKPLELYRQWTDRIMAEFFQQGDRE

3. A.A. 637-681 HPLWETWADLVHPDAQDILDTLEDN
TWADLVHPDAQDILDTLEDNRDWYH
VHPDAQDILDTLEDNRDWYHSAIRQ
QDILDTLEDNRDWYHSAIRQSPSPP
TLEDNRDWYHSAIRQSPSPPLEEEP

4. A.A. 677-716 LEEEPGGLGHPSLPDKFQFELTLEE
GGLGHPSLPDKFQFELTLEEEEEED
PSLPDKFQFELTLEEEEEEDSLEVP
KFQFELTLEEEEEEDSLEVPGLPTT

Figure 5.5 – MAPKAPK2 binds to specific regions of PDE4A5 on a full length overlapping Peptide Array.

Peptide array technology was used to synthesise a full-length array of PDE4A5 on a Whatman 50 membrane. This consisted of 25 amino acid spots that overlapped by 5

amino acids. The membrane was probed with purified recombinant GST-tagged MAPKAPK2. GST-specific anti-sera was then used to detect the areas of MAPKAPK2 binding to the membrane. Highlighted are the four main regions of most intense binding and their sequences. All peptide arrays are representative arrays of at least three separate experiments.

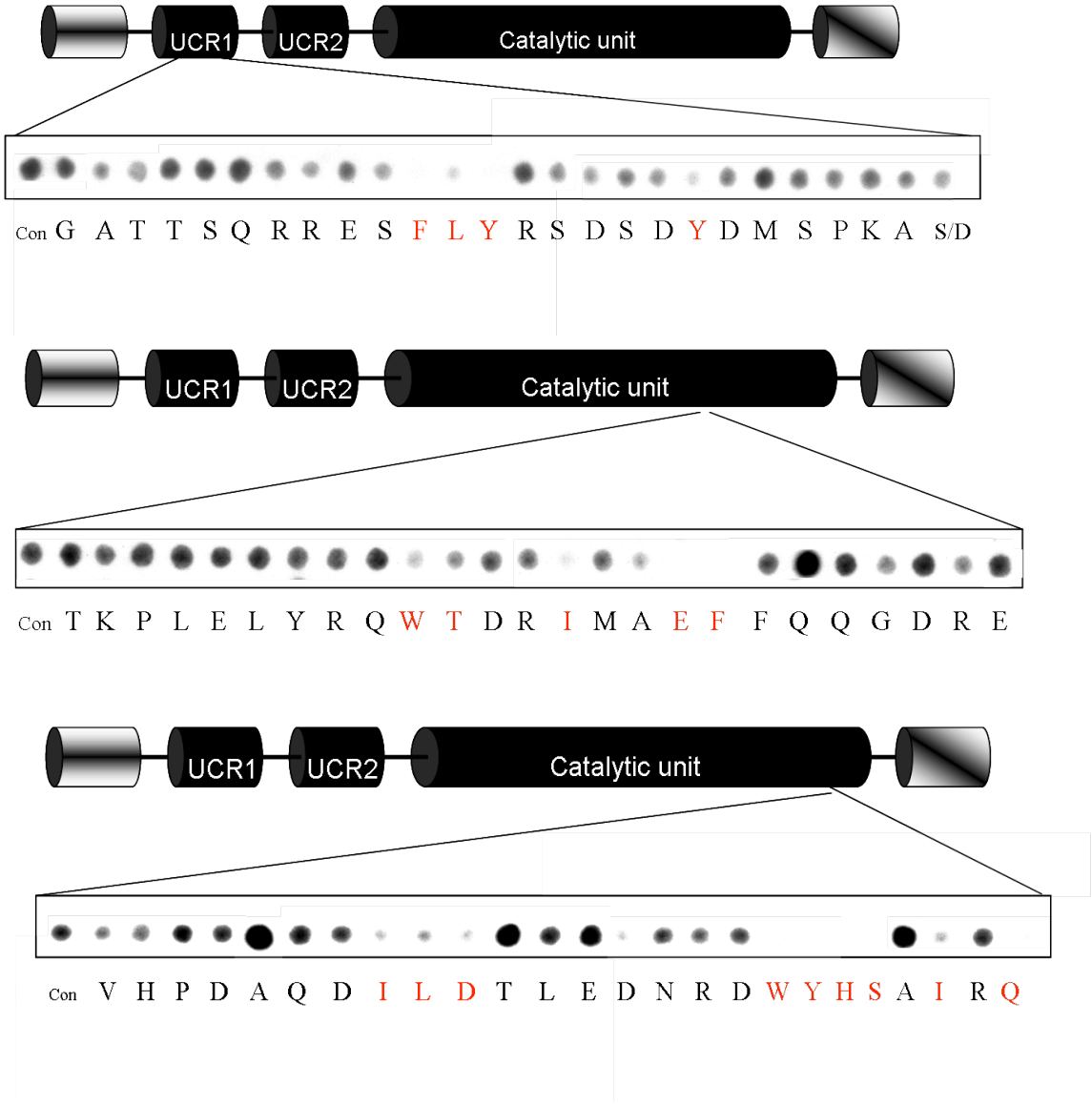

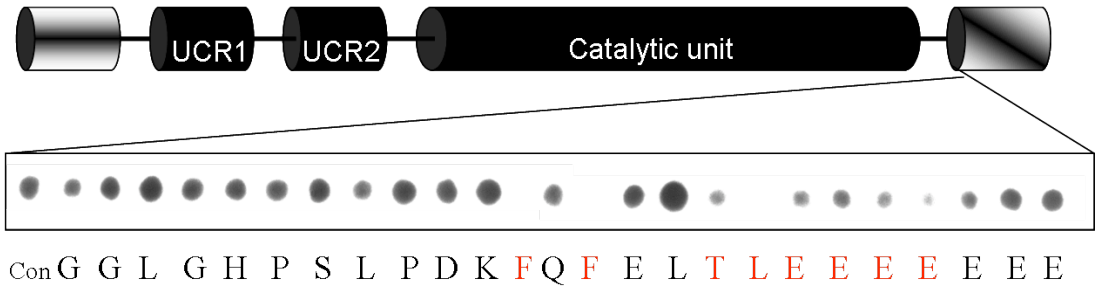

Figure 5.6 – Alanine Scanning of specific PDE4A5 sequences highlights regions of MAPKAPK2 binding.

Peptide array technology was used to synthesise alanine scanning arrays of PDE4A5 on a Whatman 50 membrane. This was done using specific sequences highlighted in Figure 5.5. These are amino acids 131-155, 582-606, 647-671, 682-702. A control spot was created with each sequence the each amino acid in turn was mutated to alanine. The membrane was probed with purified recombinant GST-tagged MAPKAPK2. GST-specific anti-sera was then used to detect the areas of MAPKAPK2 binding to the membrane. Highlighted are the main amino acids where conversion to alanine ablates binding. All peptide arrays are representative arrays of at least three separate experiments.

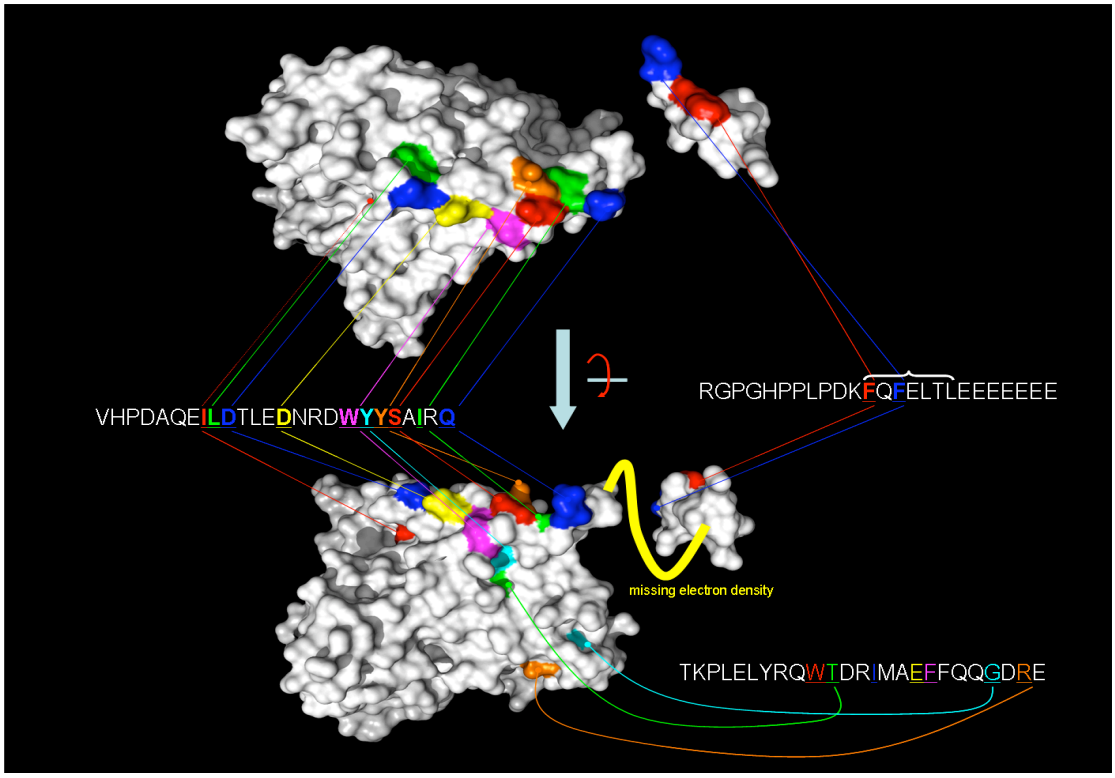
VHPDAQEILDTLEDNRDWYYSAIRQ
RGPGHPPLPDKFQFELTLEEEEEEE
missing electron density
TKPLELYRQWTDRIMAEFFQQGDRE

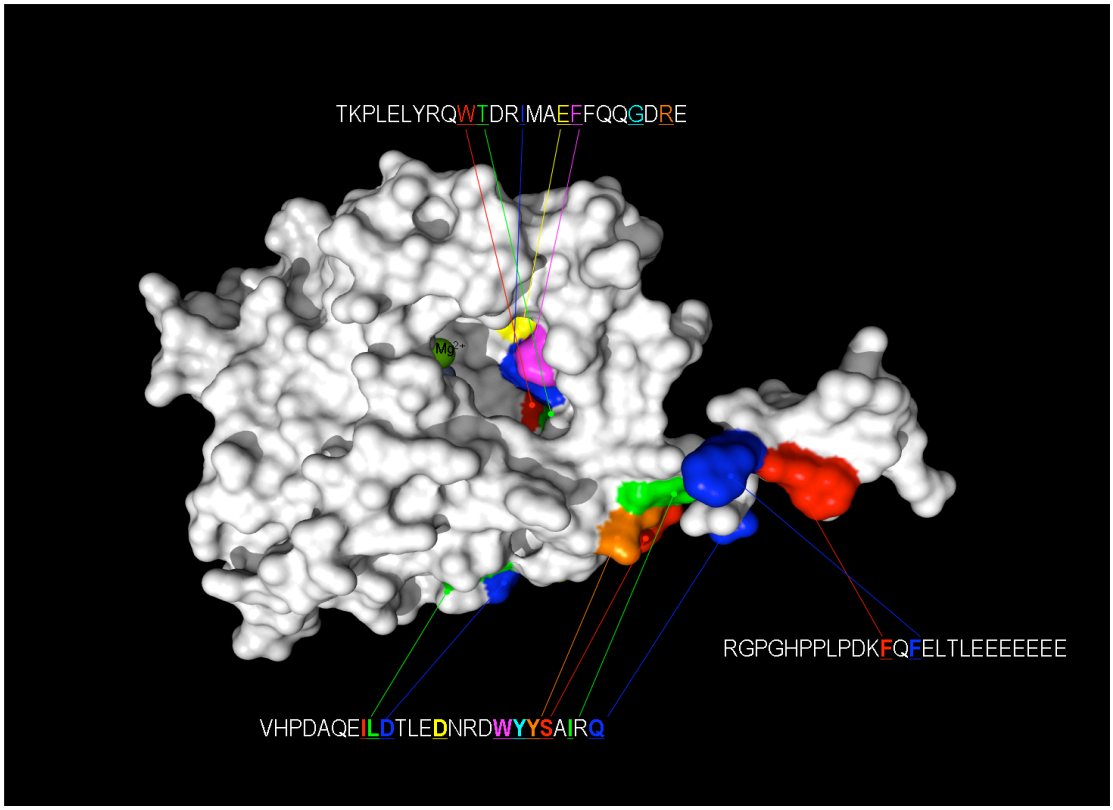
TKPLELYRQWTDRIMAEFFQQGDRE
Mg2+
RGPGHPPLPDKFQFELTLEEEEEEE
VHPDAQEILDTLEDNRDWYYSAIRQ

Figure 5.7 – Molecular model of PDE4A5 with potential MAPKAPK2 binding regions highlighted

This figure was generated in Rasmol by Dr David Adams, University of Strathclyde and is of the PDE4A catalytic unit [Wang et al., 2007]. It shows a molecular model of potential MAPKAPK2 binding regions, identified using peptide arrays, on the PDE4A catalytic unit and can be used to highlight whether they show surface exposure or not.

Site directed mutagenesis was then used to mutate groups of these amino acids to alanine in a mammalian expressing pcDNA vector of PDE4A5. Such mutated forms of PDE4A5 were then subjected to co-immunoprecipitation studies with MAPKAPK2 after over-expression of the mutants in COS1 cells, Figure 5.8. These data showed that mutation of the cluster of Phe 141, Leu 142 and Tyr 143, to alanine, in UCR1 almost completely disrupted binding to a level of 3.0 % +/- 3.8 % whereas mutations at the other sites did not elicit such a dramatic reduction in the interaction of with MAPKAPK2. Thus mutation of the cluster of Ile 654, Leu 655 and Asp 656 to alanine lowered interaction to 88 % +/- 5%, while mutation of the cluster of Trp 664, Tyr 665, His 666 and Ser 667 to alanine in PDE4A5 lowered interaction with MAPKAPK2 to 80 % +/- 7 %, and mutation of the cluster of Phe 693, Gln 694 and Phe 695 to alanine lowered interaction with MAPKAPK2 to 63 % +/- 2 % and mutation of the cluster of Tyr 698, Leu 699, Glu 700 and Glu 701 to alanine lowering interaction with MAPKAPK2 to 67 % +/- 4 %.

These data show that, to some extent, all of the areas predicted from the scanning peptide array analysis to be necessary for the interaction of PDE4A5 with MAPKAPK2 do indeed appear to play a contributory role, with the Phe-Leu-Tyr motif or, as I term it, the ‘FLY’ site in UCR1 region seemingly being most vital. It is also apparent that several of these sites are conserved between several species of long form PDE4 as shown in the line-up detailed in figure 5.1.

To confirm whether this ‘FLY’ site was indeed a real docking domain a full length overlapping 25mer peptide array was made for another known MAPKAPK2

substrate TSC2, (Tuberous Sclerosis 2) and this was overlaid with MAPKAPK2-GST, Figure 5.9. One main region of binding was shown on this array from amino acids 1236-1271. This contained amino acids 1248-Ala-Leu-Tyr-Lys-Ser-Leu-Ser-1255 somewhat similar to the binding site seen on PDE4.

(a)

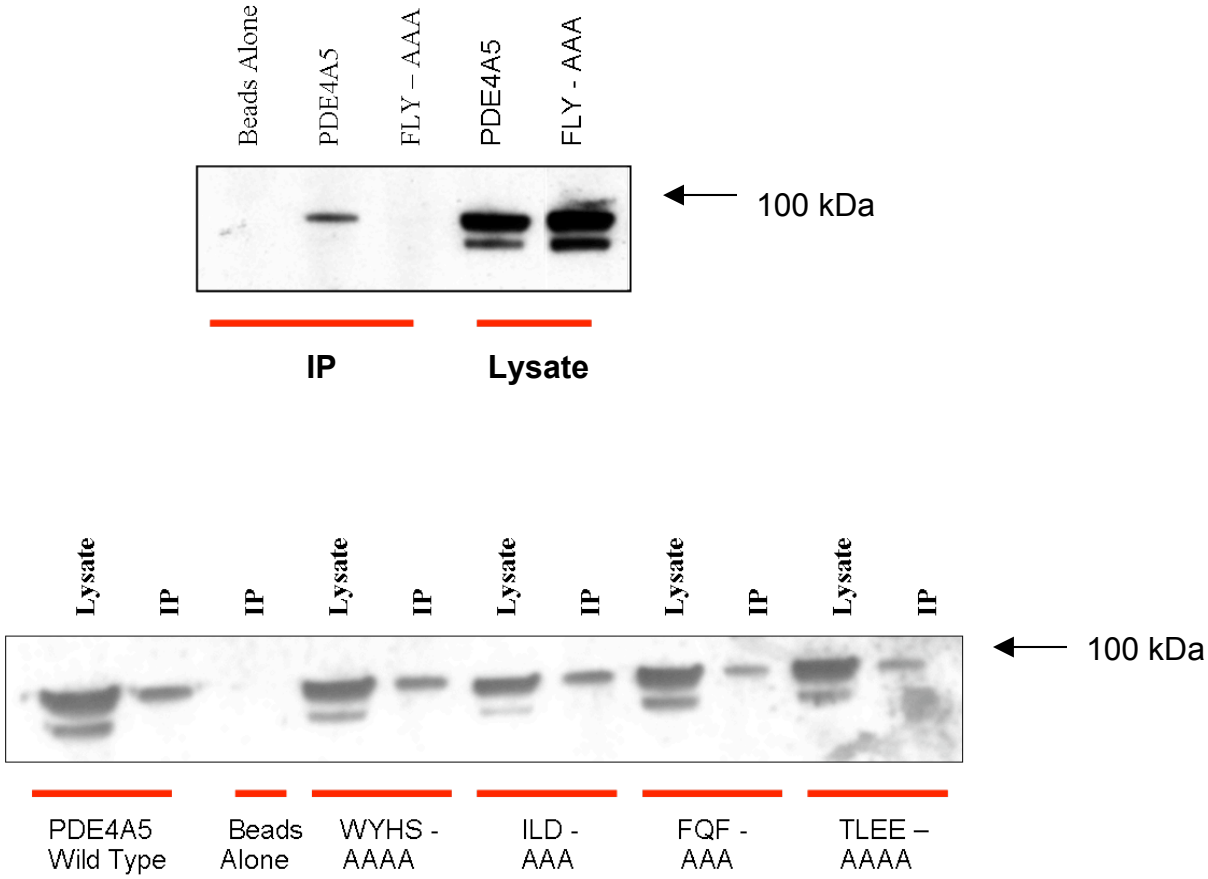

(b)

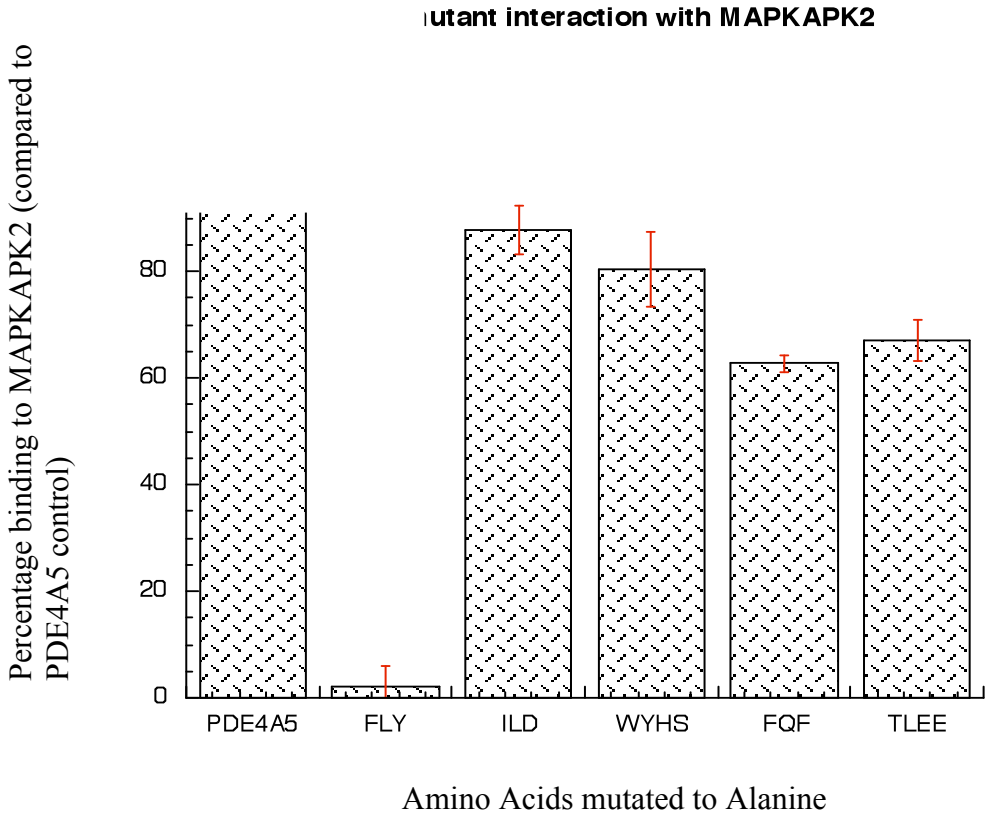

Figure 5.8 – MAPKAPK2 interа 3 cells.

Mutations of PDE4A5 were creat ed in peptide arrays were mutated to alanine. These were F141, L142 and Y143 to triple alanine, I654, L655 and D656 to triple alanine, W664, Y665, H666 and S667 to quadruple alanine, F693, Q694 and F695 to triple alanine and T698, L699, E700 and E701 to quadruple alanine. HEK293 cells were transiently transfected with PDE4A5. Total cell extract was produced and the lysates immunoprecipitated with MAPKAPK2 anti-sera conjugated to Protein G agarose beads. (a) This IP was then probed with anti-PDE4A anti-sera and MAPKAPK2 anti-sera (data not shown). (b) Percentage difference in binding compared to the control was then calculated using densitometry. All Western blots are representative blots of at least three separate experiments.

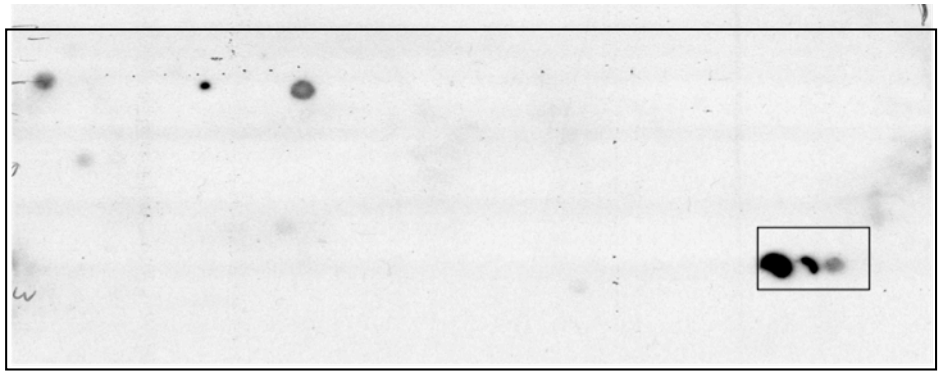

MAAERFKEHRDT ALYKSLSVPAAGTAKPPT

FKEHRDT ALYKSLSVPAAGTAKPPTLPRSN

DT ALYKSLSVPAAGTAKPPTLPRSNTDSAM

Figure 5.9 – MAPKAPK2 binds to specific regions of TSC2 on a full length overlapping Peptide Array.

Peptide array technology was used to synthesise a full-length array of TSC2 on a Whatman 50 membrane. This consisted of 25 amino acid spots that overlapped by 5 amino acids. The membrane was probed with purified recombinant GST-tagged MAPKAPK2. GST-specific anti-sera was then used to detect the areas of MAPKAPK2 binding to the membrane. Highlighted are the four main regions of most intense binding and their sequences. All peptide arrays are representative arrays of at least three separate experiments.

5.3 Discussion

There are many complex interactions in signaling pathways. However, in recent years it has become clear that signaling cascades do not work in isolation but, instead, many different signaling cascades can interact so as to functionally integrate their output. The fundamental question now being posed is not only the temporal control of such interactions but whether these may indeed be controlled spatially.

It has been hypothesized that signaling systems may be controlled spatially through the presence of protein recognition 'modules' or 'motifs' that control the targeting of specific proteins, such as kinases, phosphatases and phosphodiesterases, to distinct sites in cells [Sharrocks et al., 2000; Scott and Pawson, 2009; Houslay, 2010]. The ERK signaling cascade provides an exemplar of this notion as aberrant activation of this pathway can lead to uncontrolled proliferation and, thereby, cancer. One way of controlling this pathway is to keep critical components spatially separate in the cell and control functional interactions. Additionally, interactions between proteins in this pathway are used to enhance signaling, ensuring fidelity of action and potential for maximizing action. This latter point is particularly pertinent for the action of protein kinases to be defined to specific substrates for not only can there be consensus substrate motifs that direct phosphorylation to target amino acids but it appears that fidelity and efficiency of action of certain kinases can be driven by additional docking and substrate specificity motifs that are spatially discrete from the site of phosphorylation. The exemplar of this is the interaction between the ERK and JNK kinases with authentic substrates where two such binding motifs have been identified in addition to the proline-directed substrate motif that surrounds the phosphorylation target. These are the kinase interacting motif (KIM docking motif) that has been shown to act as a target site for both ERK and JNK with the consensus motif Val-Xaa-Xaa-Lys-Lys-Xaa6-Leu-Leu-Leu-Xaa122-phosphoSer and the Phe-Xaa-Phe specificity site (FxF docking motif) that until now was thought to only confer specificity with regards to ERK action [Sharrocks et al., 2000].

5.3.1 Kinase Interaction Motif

The presence of these KIM and FxF docking sites have been described on a small number of signaling proteins. The KIM docking motif has been shown to be present on the p90 ribosomal S6 protein kinase (RSK), where it targets ERK to the kinase allowing for kinase activation via ERK phosphorylation [Smith et al., 1998]. It is

also present on the protein tyrosine phosphatase PTP-SL where it allows for ERK targeting to the enzyme and also confers ERK phosphorylation of this enzyme [Pulido et al., 1998]. It should be noted, however, that ERK is not the only MAP kinase which can be targeted to the KIM docking motif, indeed JNK can also be targeted here. In the case of the transcription factor c-Jun, JNK is targeted to its KIM motif, binds, phosphorylates and allows for transcriptional activity to occur [Karin, 1995].

5.3.2 Phe-Xaa-Phe docking motif

The FxF docking site is similar in function to the KIM site in that originally it was thought to target for ERK specifically. Its presence was originally identified in the transcription factor LIN-1 where it was shown to target for ERK to allow for efficient phosphorylation of the factor and for transcriptional activity to occur [Jacobs et al., 1998]. The transcription factor Elk-1 also has an FxF motif where ERK interacts [Jacobs et al., 1999]. It has been hypothesized that this motif contributes to the binding affinity of ERK although it is unclear whether this docking motif actually works in a 'classical' direct binding manner like the KIM motif or if it works through some other mechanism [Jacobs et al., 1999]. Indeed here it has been shown that ERK is not the only protein that can bind to this site in certain cases (other protein binders include RACK1 and DISC1 for examples [Bolger et al., 2006; Murdoch et al., 2007] implying that this site works in a much more complicated multi-functional manner which will be discussed further later.

5.3.3 Docking motifs on Phosphodiesterase PDE4D

Phosphodiesterases are a prime example of signaling proteins that are involved in signaling cascade cross-talk indeed some 'docking motifs' on these have already been identified [Houslay and Adams, 2003; Houslay 2010].

The phosphodiesterase isoform, PDE4D3 was the first PDE4D long form to be isolated and, as such, has been routinely studied by many investigators. Studies on this enzyme looking for binding motifs have shown that PDE4D3 contains both a KIM

binding motif, on the β-hairpin loop of its catalytic domain and an FxF binding motif on an exposed α-helix of the catalytic domain [MacKenzie et al., 2000; Houslay and Adams, 2003]. In the case of this long form phosphodiesterase, the targeted binding of ERK to these two motifs allows for phosphorylation of the enzyme at Ser579, leading to inhibition of enzymatic activity [Hoffmann et al., 1999]. The importance of these docking/specificity sites was shown through mutation studies where mutation of the key binding residues to alanine in either the KIM or the FxF motif led to a loss of ERK interaction and a loss of ERK regulated inhibition of the enzyme in intact cells [MacKenzie et al., 2000].

5.3.4 Phe-Xaa-Phe is a binding domain for many proteins on PDE4

During the binding motif studies on PDE4D3 it was highlighted [MacKenzie et al., 2000] that both the KIM and FxF binding sites were not only present on this isoform of PDE4 but are conserved throughout all of the long form family members as shown here in the sequence alignment in Figure 5.1.

To my surprise, peptide array mapping studies of the kinase MAPKAPK2 on the PDE4A isoform PDE4A5 identified, for the first time, that this MAPK kinase family member can also bind at the same FxF site where ERK is able to bind (Figure 5.2). Indeed, subsequent to this, we set out to determine whether other known interacting partners of PDE4 might also interact with PDE4D3 at this site (Figure 5.3). The results of this identified that the Src tyrosyl kinase Lyn, the sumo-conjugating enzyme UBC9 and the signaling scaffolding protein b-arrestin can all also potentially bind at this motif. This work implies that instead of the FxF being an ERK specific, or even MAP Kinase specific binding site it may instead provide a multi-functional docking domain for several partner proteins of PDE4.

Functionally it is not yet fully clear what effect this may have *in vivo* but it can by hypothesized that the presence of a multi-functional docking site like this may lead aid in the fidelity of compartmentalization of signaling through PDE4 species in the cell.

In doing this such a site may confer fidelity of functionality by only allowing one partner from such a pool using this multi-functional docking site to be engaged with a PDE4 enzyme at any one specific time. This would serve to prevent several conflicting signaling events to be triggered simultaneously and might also minimize any potential for forming aggregates. For example, it could be surmised that, targeting of MAPKAPK2 to the motif, allowing for MAPKAPK2 phosphorylation of the PDE enzyme would prevent binding of other protein interactors of the enzyme, such as β-Arrestin, which may cause a conformational change in the enzyme or ERK which may inhibit the enzymes activity. Indeed the purpose of this docking motif may be to provide a simple mechanism for spatial regulation of PDE4 isoform function throughout the cell.

5.3.5 Does MAPKAPK2 have a docking motif?

Discovery of this apparent multi-functional docking motif in the catalytic region of PDE4 highlighted the potential for further docking motifs in this enzyme. Using MAPKAPK2, the functional interaction of which is discussed in Chapter 3, as a model then potential binding sites for this kinase on PDE4 were mapped using peptide arrays and mutagenesis, Figure 5.5. Through this study it was shown that mutagenesis of only one of the five potential binding sites for MAPKAPK2 on PDE4 fully ablated interaction between these two proteins. This site was Phe-Leu-Tyr referred to here as the FLY domain. While, functionally, the significance of this is not yet known, it provides interest as a potential docking domain for MAPKAPK2 due to its obvious crucial role in determining PDE4:MAPKAPK2 interaction. However, might other MAPKAPK2 substrates exhibit this motif? Indeed when further MAPKAPK2 substrates were studied some key substrates were shown to contain a similar motif. The well-established MAPKAPK2 substrate TSC2 [Li et al., 2003] appears to contain a similar sequence to this that lies between amino acids 1236-1271 (Figure 5.9). However in this sequence the phenylalanine is replaced with alanine, giving a sequence of Ala-Leu-Tyr. While at first sight this sequence may not immediately seem similar to the docking site of MAPKAPK2 on PDE4 on closer inspection, and with expansion to look at the sequence

surrounding this binding site, similarities become more apparent. While in PDE4, MAPKAPK2 binding involves a region with the sequence 141-Phe-Leu-Tyr-Arg-Ser-Asp-Ser-147, in the case of TSC2 binding is seen at the sequence 1248-Ala-Leu-Tyr-Lys-Ser-Leu-Ser-1255.This seems to suggest that while it was initially thought that a FLY domain was responsible for the interaction of MAPKAPK2 with its targets perhaps it would be more accurate to suggest that MAPKAP2 requires a Xaa-Leu-Tyr-Xaa-Ser-Xaa-Ser motif for catalytic binding. It would thus be interesting to see if mutating this sequence in TSC2 altered its interaction with, and ability to be phosphorylated by, MAPKAPK2.

5.3.6 Significance of Binding Motifs

Here it is clearly demonstrated that there are potential multi-functional docking motifs present on Phosphodiesterase-4 enzymes. This discovery, together with the identification of potential docking motifs on other signaling proteins [Holland and Cooper, 1999], may imply that multi-functional docking domains have an important undiscovered role in cell signaling. However it still remains unclear the precise functional importance of these domains and a great deal of work needs to be down to elucidate what control these sites may have. Indeed it would be interesting to uncover whether the sites play a functional role themselves or if they may play a larger scaffolding role in compartmentalization of cellular signaling. Certainly in the case of MAPKAPK2 it would be very interesting to discover the real function of this site as this kinase plays a wide-ranging role in a number of cells and it would be interesting to ascertain whether its role could be controlled through manipulation of these sites.

Chapter 6 Final Discussion

Phosphodiesterase-4 enzymes hydrolyse the second messenger cyclic 3'5' AMP to 5'-AMP and so inactivate this critical second messenger. As PDEs provide the only way the cell has to break down cAMP, therefore members of the ubiquitously expressed PDE4 family are set to play an important role in cell signaling. In the worked described in this thesis I have investigated the phosphorylation and protein-protein interactions of the cAMP phosphodiesterase isoform, PDE4A4/5. Here I showed that PDE4A4/5 can be phosphorylated by the p38 downstream kinase, MAPKAPK2. This phosphorylation attenuates the activation of this phosphodiesterase through Protein Kinase A phosphorylation. I then went on to show that PDE4A4/5 interacts with the low affinity neurotrophin receptor, p75NTR and that this interaction inhibits normal fibrin breakdown in an *in vitro* model. I also show that phosphorylation of PDE4A5 by MAPKAPK2 enhances the inhibition of fibrin breakdown. In the final section of this thesis I have also shown that long form PDE4 isoforms contain a potential multi-functional docking site where several partner proteins can bind. The implications of this body of work are wide ranging and here I set out to discuss why these may have a significant impact on the development of PDE4A directed therapeutics, particularly in the case of inflammatory disease directed therapeutics.

6.1 The Role of Phosphodiesterase-4 in Inflammatory Disease

One of the main focuses of the role of PDE4s in a disease state has been the investigation of its role in inflammatory diseases [Spina, 2008]. PDE4 provides the primary means of cAMP degradation in cells of inflammatory response, such as macrophages, eosinophils, neutrophils, T cells and B cells [Saetta et al., 1993; Riise et al., 1995; Vassallo et al., 2008]. Due to this, inflammatory diseases such as chronic obstructive pulmonary disease (COPD), asthma, multiple sclerosis and rheumatoid arthritis all are thought to have PDE4 isoenzymes playing a key role in their pathology [Houslay et al., 2005].

cAMP plays a crucial part in the regulation of primary activating pathways such as the cytokine release pathway in T cells and macrophages [Kanda & Watanabe, 2001; Duan et al., 2010]. It is therefore thought that if PDE4 is inhibited, leading to an increase in intracellular cAMP levels, an attenuation of the pro-inflammatory response in the cells may occur. Indeed in macrophages it has been shown that increased intracellular cAMP levels, in combination with stimulation of the Toll Like Receptor pathways, leads to suppression of the generation and release of the pro-inflammatory cytokine, TNFα and the induction of the anti-inflammatory cytokine interleukin 10 [Wall et al., 2009].

Interestingly, different PDE4 isoforms appear to have different actions in airway function. Thus, the specific inhibition of PDE4B has been shown to reduce the release of pro-inflammatory cytokines such as TNFα in primary macrophages in response to toll like receptor signalling [Jin et al., 2005], whereas PDE4D inhibition has been shown to promote airway smooth muscle relaxation [Mehats et al., 2003 and Jin and Conti, 2002]. It would therefore appear that inhibition of both PDE4 isoforms leads to relief of some of the symptoms of COPD in different cell types.

In a clinical context it has been shown that PDE4A4 is up-regulated in BAL macrophages from patients suffering from Chronic Obstructive Pulmonary Disease (COPD), and PDE4B2 has been shown to be up-regulated in peripheral blood monocytes of smokers [Barber et al., 2004]. These findings, in combination with the *in vitro* discoveries described above, would seem to indicate that PDE4 targeted inhibitors might indeed provide therapeutic relief of COPD. Interestingly it has also been shown that PDE4A4/5 is also up-regulated in sleep deprivation and can cause cognitive defects [Vecsey et al., 2009] and, indeed, in inflammatory conditions such as COPD patients exhibit sleep deprivation due to constriction of the airways. It would be interesting to see if there is a link between these levels of up-regulation within the two conditions and perhaps to see if any of the other, non-lung targeted effects of COPD also may be occurring as a result of up-regulated PDE4A. Indeed certain forms of heart disease have been found to be more prominent in patients suffering from COPD [Rabe et al., 2007]. Could it be that use of phosphodiesterase 4 inhibitors in a condition such as COPD

might provide a multi-faceted therapeutic, relieving not just the obvious prominent lung-centred symptoms of the disease but also exert beneficial actions elsewhere in the body at the same time?

6.2 PDE4 Inhibitors

Due to the obvious role of phosphodiesterase 4 in inflammatory disease a lot of work has been carried out in the pharmaceutical industry to develop successful PDE4 inhibitors as therapeutics for inflammatory diseases. However until now there has been limited success in this research until recently [Spina, 2008; Pages et al., 2009; Houslay et al., 2005].

Non-selective phosphodiesterase inhibitors such as theophylline have been used for decades to treat bronchial asthma but have always presented problems with major side effects like cardiac dysrhythmmia and nausea [Page, 1999]. The PDE4 selective inhibitor Rolipram was originally developed as an anti-depressant [Wachtel, 1982] and, subsequently, for the treatment of COPD [Barnette & Underwood, 2000]. However, major side effects, namely nausea, vomiting and enhanced gastric acid secretion precluded its clinical use for either indication [Hebenstreit et al., 1989].

It therefore became necessary to develop more specific drugs that did not exhibit such severe side effects. So following on from these developments a second generation of PDE4 inhibitors was created that included Cilomilast and Roflumilast [Spina, 2009] that have shown reduced side effects in animal models. Cilomilast, developed by GlaxoSmithKline, underwent extensive Phase III clinical trials [Houslay et al., 2005; Rennard et al., 2006]. Despite strong initial results this drug failed to show any significant improvements in a final clinical trial of COPD patients and was therefore denied approval by the Food and Drug Administration (FDA) in the USA [Rennard et al., 2008]. Roflumilast is one of the most potent oral PDE4 inhibitors with a longer half life than Cilomilast [Houslay et al., 2005]. It was also recently denied approval by the FDA although, excitingly, it has very recently been approved within Europe as a once-a-

day treatment for COPD patients with chronic bronchitis under the trade name Daxas [Rabe, 2010; Pages et al., 2009; http://www.nycomed.com/en/Menu/Media/News+releases/ Nycomed press release].

Several other generations of isoform specific PDE4 inhibitors are also in development , although phase 3 clinical trials have either yet to be performed for these or they have not given clinically significant results in phase 2 studies [Spina, 2008; Pages et al., 2009]. One 'new' generation PDE4 inhibitor which is currently being passed through Phase 2 clinical trials is Apremilast which, unlike many other PDE4 inhibitors, is being developed for the treatment of psoriasis and arthritis, where it shows potential therapeutic efficacy [Schafer et al., 2010; McCann et al., 2010]. Indeed development, and the so far success, of PDE4 inhibitors like Apremilast may imply that the pharmaceutical industry has been putting too much emphasis on the development of PDE4 inhibitors for COPD alone. This emphasis is understandable because COPD is the sixth leading cause of death in the world and is proposed to move up to the fourth leading cause of death worldwide by 2030 [Mather and Loncar, 2006]. However with advances in PDE4 inhibitors for the treatment of COPD being limited perhaps it is time that the development of these therapeutics shifted to focus on other disease states where PDE4 is implicated to play an important role, such as the inflammatory disorders just mentioned (arthritis and psoriasis) and even CNS diseases whether PDE4s have been shown to have a role [Sachs et al., 2007; Millar et al., 2007].

6.3 A potential Role for My Findings in the Development of Novel Therapeutics

As the development of PDE4 inhibitors has been a complicated and challenging task perhaps a better understand of the enzymes phosphorylation states and protein interaction may open up new opportunities for therapeutic development.

6.3.1 PDE4 and MAPKAPK2 in therapeutic development

As I have shown in Chapter 3 of this thesis PDE4A5 can be phosphorylated by MAPKAPK2, a downstream kinase of the p38 MAP Kinase pathway. This phosphorylation leads to attenuation of activation of the PDE through PKA phosphorylation. Therefore in the presence of p38 MAP Kinase signaling pathway activation I have shown that there is a sustained, instead of transient, increase in intracellular cyclic AMP levels.

Interestingly inhibition of the p38 MAPK pathway, like PDE4, has also been investigated as a potential therapeutic target for inflammatory diseases as it plays a fundamental role in the inflammatory response (see Chapter 3.1.3). Thus, it may be that activation of the p38 MAPK-MK2 pathway in the inflammatory response will not only promote the expression of pro-inflammatory mediators but may simultaneously also increase cAMP levels through PDE4 phosphorylation, which creates a form of negative feedback leading to suppression of this pro-inflammatory response and increased induction of anti-inflammatory cytokines such as interleukin 10. Indeed this would be in-keeping with previous studies mentioned above which showed that stimulation of the cAMP pathway in combination with the Toll Like Receptor pathways (that have been shown to activate p38 MAPK downstream), leads to negative feedback of the pro-inflammatory cytokine response in macrophages and promotion of the anti-inflammatory response [Wall et al., 2009].

This discovery poses interesting questions about the development of current therapeutics p38 MAPK inhibitors [Cohen, 2009]. While it is thought that blocking the p38 MAPK pathway or MAPKAPK2 should lead to loss of pro-inflammatory response [Cohen, 2009; Duraisamy et al., 2008], the influence of these inhibitors on cAMP response may now have to be taken into account. Indeed if MAPKAPK2 is inhibited and therefore is no longer available to phosphorylate PDE, this may allow for full activation of the phosphodiesterase enzyme, leading to a decrease in intracellular cAMP levels and

a loss of the anti-inflammatory response seen in response to TLR stimulation. Indeed in these circumstances the most logical therapeutic to be developed would be a selective PDE4 inhibitor as this would allow for promotion of the anti-inflammatory response. Therefore, while the discovery of the interaction between PDE4 and MAPKAPK2 may not directly aid in the development of more specific, effective PDE4 inhibitors therapeutically, it may provide a valuable insight into understanding the downfall of p38 MAPK pathway-based inhibitor studies [Cohen, 2010; Hendriks et al., 2010].

6.3.2 PDE4 and p75NTR in therapeutic development

p75NTR has also been shown to play a role in inflammatory disease (see Chapter 4.1.5) with it being recently proposed that it may, particularly, have a role in fibrosis in inflammatory conditions [Sachs et al., 2007]. Indeed p75NTR can markedly inhibit fibrin breakdown (leading to tissue scarring). However here I have shown in Chapter 4 that for this to occur it needs to sequester PDE4A5. As stated above PDE4 selective inhibitors have been developed to treat inflammatory diseases, where fibrosis is a major issue and as stated previously a key part of the efficacy of these inhibitors relates to their ability to inhibit TNFα [Houslay et al., 2005; Spina, 2008; Wall et al., 2009]. TNFα is thought to have a potent pro-fibrotic action [Zhang et al., 2007]. The molecular basis of this is not fully understood but it is known that the key signaling cascade activated by TNFα is the p38 MAPK pathway [Dent et al., 2003; Uhlik et al., 2003; Xu et al., 2006]. Here I have shown that MAPKAPK2 can phosphorylate PDE4A5 which in a fibrin model system leads to an almost total loss of fibrin breakdown.

Inappropriate fibrin build up may be responsible for tissue scarring of the lungs in COPD and asthma [Nakstad et al., 1990]. From what I have shown in this thesis it could be implied that disruption of the interaction of PDE4A5 and p75NTR may decrease this inappropriate loss of fibrin breakdown. Indeed small molecules targeted to disrupt this interaction may provide a more specific therapeutic for the treatment of certain aspects of COPD, without the potential side effects seen in PDE4 inhibitors. However a great deal of research into this still needs to be carried out as disruption of

this interaction may have significant effects elsewhere in the body. In this context it may also be appropriate for inhibitors of the p38 MAPK pathway to be employed as they may also help enhance fibrin breakdown through loss of PDE4 phosphorylation.

6.3.3 The effect of a multifunctional docking domain on therapeutic development

In the final study described within this thesis I discovered a potential multifunctional docking domain on PDE4 long isoforms. The significance of this still remains unclear and much more research is needed into this before full conclusions can be made. It may be however that the presence of a multi-docking site like this plays some role in the adverse effects of PDE4 inhibitors as such inhibitors may be affecting the interaction of PDE4 with several partner proteins, not just ones involved in target reactions. Indeed it may also be altering compartmentalization of the PDE4 enzymes allowing for uncontrolled, unregulated distribution throughout the cell.

In the context of the work I have done here, and with the development of peptide array mapping technology, it would be interesting to speculate what small molecule disruption of the complexes described throughout this thesis would result in functionally. Small molecule disruption targeting MAPKAPK2s interaction with the FLY domain of PDE4A5 may not be an ideal therapeutic target as it would appear that disruption of this interaction would lead to increased PDE4 activity, decreased cAMP levels and therefore a loss of anti-inflammatory action. However, small molecular disruption of the specific interaction sites for p75NTR with PDE4A5 may have more potential as a therapeutic. Indeed it could be speculated that disruption of this complex would lead to increased fibrin breakdown, potentially relieving fibrin scarring exhibited in conditions such as COPD and spinal cord injury where inappropriate fibrin deposition is an issue [Beattie et al., 2002; Sachs et al., 2007].

6.4 Final Conclusion

In conclusion, here I have identified new aspects of Phosphodiesterase-4 interaction and regulation. This gives an insight into how this enzyme may function in the inflammatory system however its precise mechanism of action appears to be very complicated and further research is required to decode its precise role throughout this system.

Issues that I think need to be addressed globally, how my work can help solve these and how I would continue this research:

- In my opinion the development of PDE4 inhibitors as a therapeutic target is currently too broad ranging. Focusing on PDE4 as one single target is clearly not working as this research has been ongoing for many years and still too many side effects are observed with these inhibitors. Instead perhaps a better option would be to focus on very specific PDE4 isoforms and their partner proteins in specific disease states. Disruption of individual interactions like these may provide highly specific therapeutics lacking adverse side effects. For example, here I have shown that interaction between PDE4A4/5 and p75NTR occurs at specific sites. If I had more time to further this work it would be interesting to see if these sites could be manipulated to produce a small disruptor molecule to stop this interaction. This could then be used in cell system models to see how it affects fibrin breakdown and, with ethical approval, could then be used in whole animal studies to see the effects that this molecule would have on COPD animal models and spinal cord injury animal models.
- I also think progression of the work on PDE4 and MAPKAPK2 phosphorylation may give an interesting insight into the complex inflammatory feedback system in the immune system. Indeed if I had time to further this work I would use a primary cell system such as Bone Marrow Derived Macrophages (BMDMs) to observe how loss of PDE4A (through knock-out) affects the inflammatory response of these cells in response to activation of the p38 MAPK pathway. Indeed PDE4A, MAPKAPK2 double knockout mice could also be engineered to study the effects on inflammation upon loss of both of these signaling pathways. I would hypothesise that in PDE4A (-/-) BMDMs there would be an increase in the anti-inflammatory response from these cells, counteracting the pro-

inflammatory surge and indeed in a MAPKAPK2/PDE 4A double knock-out system the anti-inflammatory response would be increased as well as the pro-inflammatory response decreasing. This process could however be complicated as knock-out of two important signaling enzymes such as PDE4A and MAPKAPK2 in one mouse model may not be viable.

Chapter 7 Bibliography

ADAMS, R.A., PASSINO, M., SACHS, B.D., NURIEL, T. & AKASSOGLOU, K. (2004). Fibrin mechanisms and functions in nervous system pathology. *Mol Interv*, **4,** 163-76.

ANANIEVA, O., DARRAGH, J., JOHANSEN, C., CARR, J.M., MCILRATH, J., PARK, J.M., WINGATE, A., MONK, C.E., TOTH, R., SANTOS, S.G., IVERSEN, L. & ARTHUR, J.S. (2008). The kinases MSK1 and MSK2 act as negative regulators of Toll-like receptor signaling. *Nat Immunol*, **9,** 1028-36.

ANDERSSON, K. & SUNDLER, R. (2006). Posttranscriptional regulation of TNFalpha expression via eukaryotic initiation factor 4E (eIF4E) phosphorylation in mouse macrophages. *Cytokine*, **33,** 52-7.

ARAVIND, L. & PONTING, C.P. (1997). The GAF domain: an evolutionary link between diverse phototransducing proteins. *Trends Biochem Sci*, **22,** 458-9.

ARIGA, M., NEITZERT, B., NAKAE, S., MOTTIN, G., BERTRAND, C., PRUNIAUX, M.P., JIN, S.L. & CONTI, M. (2004). Nonredundant function of phosphodiesterases 4D and 4B in neutrophil recruitment to the site of inflammation. *J Immunol*, **173,** 7531-8.

ARTEMYEV, N.O., SURENDRAN, R., LEE, J.C. & HAMM, H.E. (1996). Subunit structure of rod cGMP-phosphodiesterase. *J Biol Chem*, **271,** 25382-8.

ARTHUR, J.S. (2008). MSK activation and physiological roles. *Front Biosci*, **13,** 5866-79.

ARTHUR, J.S. & COHEN, P. (2000). MSK1 is required for CREB phosphorylation in response to mitogens in mouse embryonic stem cells. *FEBS Lett*, **482,** 44-8.

ASIRVATHAM, A.L., GALLIGAN, S.G., SCHILLACE, R.V., DAVEY, M.P., VASTA, V., BEAVO, J.A. & CARR, D.W. (2004). A-kinase anchoring proteins interact with phosphodiesterases in T lymphocyte cell lines. *J Immunol*, **173,** 4806-14.

AVRUCH, J. (2007). MAP kinase pathways: the first twenty years. *Biochim Biophys Acta*, **1773,** 1150-60.

BAILLIE, G.S. (2009). Compartmentalized signalling: spatial regulation of cAMP by the action of compartmentalized phosphodiesterases. *Febs J*, **276,** 1790-9.

BAILLIE, G.S., ADAMS, D.R., BHARI, N., HOUSLAY, T.M., VADREVU, S., MENG, D., LI, X., DUNLOP, A., MILLIGAN, G., BOLGER, G.B., KLUSSMANN, E. & HOUSLAY, M.D. (2007). Mapping binding sites for the PDE4D5 cAMP-specific phosphodiesterase to the N- and C-domains of beta-arrestin using spot-immobilized peptide arrays. *Biochem J*, **404,** 71-80.

BAILLIE, G.S., MACKENZIE, S.J., MCPHEE, I. & HOUSLAY, M.D. (2000). Sub-family selective actions in the ability of Erk2 MAP kinase to phosphorylate and regulate the activity of PDE4 cyclic AMP-specific phosphodiesterases. *Br J Pharmacol*, **131,** 811-9.

BARBACID, M. (1995). Structural and functional properties of the TRK family of neurotrophin receptors. *Ann N Y Acad Sci*, **766,** 442-58.

BARBER, R., BAILLIE, G.S., BERGMANN, R., SHEPHERD, M.C., SEPPER, R., HOUSLAY, M.D. & HEEKE, G.V. (2004). Differential expression of PDE4 cAMP phosphodiesterase isoforms in inflammatory cells of smokers with

COPD, smokers without COPD, and nonsmokers. *Am J Physiol Lung Cell Mol Physiol*, **287,** L332-43.

BARKER, P.A. (2007). High affinity not in the vicinity? *Neuron*, **53,** 1-4.

BARKER, P.A. (2009). A p75(NTR) pivoting paradigm propels perspicacity. *Neuron*, **62,** 3-5.

BARNETTE, M.S. & UNDERWOOD, D.C. (2000). New phosphodiesterase inhibitors as therapeutics for the treatment of chronic lung disease. *Curr Opin Pulm Med*, **6,** 164-9.

BAZHIN, A.V., TAMBOR, V., DIKOV, B., PHILIPPOV, P.P., SCHADENDORF, D. & EICHMULLER, S.B. cGMP-phosphodiesterase 6, transducin and Wnt5a/Frizzled-2-signaling control cGMP and Ca(2+) homeostasis in melanoma cells. *Cell Mol Life Sci*, **67,** 817-28.

BEARD, M.B., OLSEN, A.E., JONES, R.E., ERDOGAN, S., HOUSLAY, M.D. & BOLGER, G.B. (2000). UCR1 and UCR2 domains unique to the cAMP-specific phosphodiesterase family form a discrete module via electrostatic interactions. *J Biol Chem*, **275,** 10349-58.

BEARDMORE, V.A., HINTON, H.J., EFTYCHI, C., APOSTOLAKI, M., ARMAKA, M., DARRAGH, J., MCILRATH, J., CARR, J.M., ARMIT, L.J., CLACHER, C., MALONE, L., KOLLIAS, G. & ARTHUR, J.S. (2005). Generation and characterization of p38beta (MAPK11) gene-targeted mice. *Mol Cell Biol*, **25,** 10454-64.

BEATTIE, M.S., HARRINGTON, A.W., LEE, R., KIM, J.Y., BOYCE, S.L., LONGO, F.M., BRESNAHAN, J.C., HEMPSTEAD, B.L. & YOON, S.O. (2002). ProNGF induces p75-mediated death of oligodendrocytes following spinal cord injury. *Neuron*, **36,** 375-86.

BEAVO, J.A. (1995). Cyclic nucleotide phosphodiesterases: functional implications of multiple isoforms. *Physiol Rev*, **75,** 725-48.

BEAVO, J.A. & BRUNTON, L.L. (2002). Cyclic nucleotide research -- still expanding after half a century. *Nat Rev Mol Cell Biol*, **3,** 710-8.

BEN-LEVY, R., HOOPER, S., WILSON, R., PATERSON, H.F. & MARSHALL, C.J. (1998). Nuclear export of the stress-activated protein kinase p38 mediated by its substrate MAPKAP kinase-2. *Curr Biol*, **8,** 1049-57.

BENNDORF, R., HAYESS, K., RYAZANTSEV, S., WIESKE, M., BEHLKE, J. & LUTSCH, G. (1994). Phosphorylation and supramolecular organization of murine small heat shock protein HSP25 abolish its actin polymerization-inhibiting activity. *J Biol Chem*, **269,** 20780-4.

BERENSON, L.S., YANG, J., SLECKMAN, B.P., MURPHY, T.L. & MURPHY, K.M. (2006). Selective requirement of p38alpha MAPK in cytokine-dependent, but not antigen receptor-dependent, Th1 responses. *J Immunol*, **176,** 4616-21.

BERWICK, D.C. & TAVARE, J.M. (2004). Identifying protein kinase substrates: hunting for the organ-grinder's monkeys. *Trends Biochem Sci*, **29,** 227-32.

BLACKWOOD, D.H., FORDYCE, A., WALKER, M.T., ST CLAIR, D.M., PORTEOUS, D.J. & MUIR, W.J. (2001). Schizophrenia and affective disorders--cosegregation with a translocation at chromosome 1q42 that directly disrupts brain-expressed genes: clinical and P300 findings in a family. *Am J Hum Genet*, **69,** 428-33.

BLOCHL, A. & BLOCHL, R. (2007). A cell-biological model of p75NTR signaling. *J Neurochem*, **102,** 289-305.

BOLGER, G., MICHAELI, T., MARTINS, T., ST JOHN, T., STEINER, B., RODGERS, L., RIGGS, M., WIGLER, M. & FERGUSON, K. (1993). A family of human phosphodiesterases homologous to the dunce learning and memory gene product of Drosophila melanogaster are potential targets for antidepressant drugs. *Mol Cell Biol*, **13,** 6558-71.

BOLGER, G.B., BAILLIE, G.S., LI, X., LYNCH, M.J., HERZYK, P., MOHAMED, A., MITCHELL, L.H., MCCAHILL, A., HUNDSRUCKER, C., KLUSSMANN, E., ADAMS, D.R. & HOUSLAY, M.D. (2006). Scanning peptide array analyses identify overlapping binding sites for the signalling scaffold proteins, beta-arrestin and RACK1, in cAMP-specific phosphodiesterase PDE4D5. *Biochem J*, **398,** 23-36.

BOLGER, G.B., ERDOGAN, S., JONES, R.E., LOUGHNEY, K., SCOTLAND, G., HOFFMANN, R., WILKINSON, I., FARRELL, C. & HOUSLAY, M.D. (1997). Characterization of five different proteins produced by alternatively spliced mRNAs from the human cAMP-specific phosphodiesterase PDE4D gene. *Biochem J*, **328 (Pt 2),** 539-48.

BOLGER, G.B., MCCAHILL, A., HUSTON, E., CHEUNG, Y.F., MCSORLEY, T., BAILLIE, G.S. & HOUSLAY, M.D. (2003). The unique amino-terminal region of the PDE4D5 cAMP phosphodiesterase isoform confers preferential interaction with beta-arrestins. *J Biol Chem*, **278,** 49230-8.

BOLGER, G.B., PEDEN, A.H., STEELE, M.R., MACKENZIE, C., MCEWAN, D.G., WALLACE, D.A., HUSTON, E., BAILLIE, G.S. & HOUSLAY, M.D. (2003). Attenuation of the activity of the cAMP-specific phosphodiesterase PDE4A5 by interaction with the immunophilin XAP2. *J Biol Chem*, **278,** 33351-63.

BOLGER, G.B., RODGERS, L. & RIGGS, M. (1994). Differential CNS expression of alternative mRNA isoforms of the mammalian genes encoding cAMP-specific

phosphodiesterases. *Gene*, **149,** 237-44.

BOOLELL, M., GEPI-ATTEE, S., GINGELL, J.C. & ALLEN, M.J. (1996). Sildenafil, a novel effective oral therapy for male erectile dysfunction. *Br J Urol*, **78,** 257-61.

BRADFORD, M.M. (1976). A rapid and sensitive method for the quantitation of microgram quantities of protein utilizing the principle of protein-dye binding. *Anal Biochem*, **72,** 248-54.

BRANCHO, D., TANAKA, N., JAESCHKE, A., VENTURA, J.J., KELKAR, N., TANAKA, Y., KYUUMA, M., TAKESHITA, T., FLAVELL, R.A. & DAVIS, R.J. (2003). Mechanism of p38 MAP kinase activation in vivo. *Genes Dev*, **17,** 1969-78.

BRISTOL, J.A., SIRCAR, I., MOOS, W.H., EVANS, D.B. & WEISHAAR, R.E. (1984). Cardiotonic agents. 1. 4,5-Dihydro-6-[4-(1H-imidazol-1-yl)phenyl]-3 (2H)-pyridazinones: novel positive inotropic agents for the treatment of congestive heart failure. *J Med Chem*, **27,** 1099-101.

BRONFMAN, F.C. & FAINZILBER, M. (2004). Multi-tasking by the p75 neurotrophin receptor: sortilin things out? *EMBO Rep*, **5,** 867-71.

BURGI, B., OTTEN, U.H., OCHENSBERGER, B., RIHS, S., HEESE, K., EHRHARD, P.B., IBANEZ, C.F. & DAHINDEN, C.A. (1996). Basophil priming by neurotrophic factors. Activation through the trk receptor. *J Immunol*, **157,** 5582-8.

BURGIN, A.B., MAGNUSSON, O.T., SINGH, J., WITTE, P., STAKER, B.L., BJORNSSON,
J.M., THORSTEINSDOTTIR, M., HRAFNSDOTTIR, S., HAGEN, T.,

KISELYOV, A.S., STEWART, L.J. & GURNEY, M.E. Design of phosphodiesterase 4D (PDE4D) allosteric modulators for enhancing cognition with improved safety. *Nat Biotechnol*, **28,** 63-70.

CAHILL, M.A., JANKNECHT, R. & NORDHEIM, A. (1996). Signalling pathways: jack of all cascades. *Curr Biol*, **6,** 16-9.

CARD, G.L., BLASDEL, L., ENGLAND, B.P., ZHANG, C., SUZUKI, Y., GILLETTE, S., FONG, D., IBRAHIM, P.N., ARTIS, D.R., BOLLAG, G., MILBURN, M.V., KIM, S.H., SCHLESSINGER, J. & ZHANG, K.Y. (2005). A family of phosphodiesterase inhibitors discovered by cocrystallography and scaffold-based drug design. *Nat Biotechnol*, **23,** 201-7.

CARLISLE MICHEL, J.J., DODGE, K.L., WONG, W., MAYER, N.C., LANGEBERG, L.K. & SCOTT, J.D. (2004). PKA-phosphorylation of PDE4D3 facilitates recruitment of the mAKAP signalling complex. *Biochem J*, **381,** 587-92.

CARNEGIE, G.K., MEANS, C.K. & SCOTT, J.D. (2009). A-kinase anchoring proteins: from protein complexes to physiology and disease. *IUBMB Life*, **61,** 394-406.

CARR, D.W., STOFKO-HAHN, R.E., FRASER, I.D., CONE, R.D. & SCOTT, J.D. (1992). Localization of the cAMP-dependent protein kinase to the postsynaptic densities by A-kinase anchoring proteins. Characterization of AKAP 79. *J Biol Chem*, **267,** 16816-23.

CASADEMUNT, E., CARTER, B.D., BENZEL, I., FRADE, J.M., DECHANT, G. & BARDE, Y.A. (1999). The zinc finger protein NRIF interacts with the neurotrophin receptor p75(NTR) and participates in programmed cell death. *Embo J*, **18,** 6050-61.

CHABRE, M., BIGAY, J., BRUCKERT, F., BORNANCIN, F., DETERRE, P., PFISTER, C. & VUONG, T.M. (1988). Visual signal transduction: the cycle of transducin shuttling between rhodopsin and cGMP phosphodiesterase. *Cold Spring Harb Symp Quant Biol*, **53 Pt 1,** 313-24.

CHAO, M.V. (2003). Neurotrophins and their receptors: a convergence point for many signalling pathways. *Nat Rev Neurosci*, **4,** 299-309.

CHEVALIER, S., PRALORAN, V., SMITH, C., MACGROGAN, D., IP, N.Y., YANCOPOULOS, G.D., BRACHET, P., POUPLARD, A. & GASCAN, H. (1994). Expression and functionality of the trkA proto-oncogene product/NGF receptor in undifferentiated hematopoietic cells. *Blood*, **83,** 1479-85.

CHRISTIAN, F., ANTHONY, D.F., VADREVU, S., RIDDELL, T., DAY, J.P., MCLEOD, R., ADAMS, D.R., BAILLIE, G.S. & HOUSLAY, M.D. p62 (SQSTM1) and cyclic AMP phosphodiesterase-4A4 (PDE4A4) locate to a novel, reversible protein aggregate with links to autophagy and proteasome degradation pathways. *Cell Signal*, **22,** 1576-96.

CLARY, D.O. & REICHARDT, L.F. (1994). An alternatively spliced form of the nerve growth factor receptor TrkA confers an enhanced response to neurotrophin 3. *Proc Natl Acad Sci U S A*, **91,** 11133-7.

CLIFTON, A.D., YOUNG, P.R. & COHEN, P. (1996). A comparison of the substrate specificity of MAPKAP kinase-2 and MAPKAP kinase-3 and their activation by cytokines and cellular stress. *FEBS Lett*, **392,** 209-14.

COHEN, P. (2009). Targeting protein kinases for the development of anti-inflammatory drugs. *Curr Opin Cell Biol*, **21,** 317-24.

COHEN, S. & FLEISCHMANN, R. Kinase inhibitors: a new approach to rheumatoid arthritis treatment. *Curr Opin Rheumatol*, **22,** 330-5.

COLLINS, D.M., MURDOCH, H., DUNLOP, A.J., CHARYCH, E., BAILLIE, G.S., WANG, Q., HERBERG, F.W., BRANDON, N., PRINZ, A. & HOUSLAY, M.D. (2008). Ndel1 alters its conformation by sequestering cAMP-specific phosphodiesterase-4D3 (PDE4D3) in a manner that is dynamically regulated through Protein Kinase A (PKA). *Cell Signal*, **20,** 2356-69.

CONTI, M. & BEAVO, J. (2007). Biochemistry and physiology of cyclic nucleotide phosphodiesterases: essential components in cyclic nucleotide signaling. *Annu Rev Biochem*, **76,** 481-511.

COQUIL, J.F., FRANKS, D.J., WELLS, J.N., DUPUIS, M. & HAMET, P. (1980). Characteristics of a new binding protein distinct from the kinase for guanosine 3':5'-monophosphate in rat platelets. *Biochim Biophys Acta*, **631,** 148-65.

CORTIJO, J., IRANZO, A., MILARA, X., MATA, M., CERDA-NICOLAS, M., RUIZ-SAURI, A., TENOR, H., HATZELMANN, A. & MORCILLO, E.J. (2009). Roflumilast, a phosphodiesterase 4 inhibitor, alleviates bleomycin-induced lung injury. *Br J Pharmacol*, **156,** 534-44.

COUDRAY, C., CHARON, C., KOMAS, N., MORY, G., DIOT-DUPUY, F., MANGANIELLO, V., FERRE, P. & BAZIN, R. (1999). Evidence for the presence of several phosphodiesterase isoforms in brown adipose tissue of Zucker rats: modulation of PDE2 by the fa gene expression. *FEBS Lett*, **456,** 207-10.

COWAN, W.M. (2001). Viktor Hamburger and Rita Levi-Montalcini: the path to the discovery of nerve growth factor. *Annu Rev Neurosci*, **24,** 551-600.

CUENDA, A. & ROUSSEAU, S. (2007). p38 MAP-kinases pathway regulation, function and role in human diseases. *Biochim Biophys Acta*, **1773,** 1358-75.

DE OLIVEIRA, S.K., HOFFMEISTER, M., GAMBARYAN, S., MULLER-ESTERL, W., GUIMARAES, J.A. & SMOLENSKI, A.P. (2007). Phosphodiesterase 2A forms a complex with the co-chaperone XAP2 and regulates nuclear translocation of the aryl hydrocarbon receptor. *J Biol Chem*, **282,** 13656-63.

DE ROOIJ, J., REHMANN, H., VAN TRIEST, M., COOL, R.H., WITTINGHOFER, A. & BOS, J.L. (2000). Mechanism of regulation of the Epac family of cAMP-dependent RapGEFs. *J Biol Chem*, **275,** 20829-36.

DE ROOIJ, J., ZWARTKRUIS, F.J., VERHEIJEN, M.H., COOL, R.H., NIJMAN, S.M., WITTINGHOFER, A. & BOS, J.L. (1998). Epac is a Rap1 guanine-nucleotide-exchange factor directly activated by cyclic AMP. *Nature*, **396,** 474-7.

DE VISSER, Y.P., WALTHER, F.J., LAGHMANI, E.H., VAN WIJNGAARDEN, S., NIEUWLAND, K. & WAGENAAR, G.T. (2008). Phosphodiesterase-4 inhibition attenuates pulmonary inflammation in neonatal lung injury. *Eur Respir J*, **31,** 633-44.

DEAK, M., CLIFTON, A.D., LUCOCQ, L.M. & ALESSI, D.R. (1998). Mitogen- and stress-activated protein kinase-1 (MSK1) is directly activated by MAPK and SAPK2/p38, and may mediate activation of CREB. *Embo J*, **17,** 4426-41.

DEAN, J.L., BROOK, M., CLARK, A.R. & SAKLATVALA, J. (1999). p38 mitogen-activated protein kinase regulates cyclooxygenase-2 mRNA stability and transcription in lipopolysaccharide-treated human monocytes. *J Biol Chem*, **274,** 264-9.

DECHANT, G. & BARDE, Y.A. (2002). The neurotrophin receptor p75(NTR): novel functions and implications for diseases of the nervous system. *Nat Neurosci*, **5,** 1131-6.

DECHANT, G. & NEUMANN, H. (2002). Neurotrophins. *Adv Exp Med Biol*, **513,** 303-34.

DELGHANDI, M.P., JOHANNESSEN, M. & MOENS, U. (2005). The cAMP signalling pathway activates CREB through PKA, p38 and MSK1 in NIH 3T3 cells. *Cell Signal*, **17,** 1343-51.

DENINNO, M.P., ANDREWS, M., BELL, A.S., CHEN, Y., ELLER-ZARBO, C., ESHELBY, N., ETIENNE, J.B., MOORE, D.E., PALMER, M.J., VISSER, M.S., YU, L.J., ZAVADOSKI, W.J. & MICHAEL GIBBS, E. (2009). The discovery of potent, selective, and orally bioavailable PDE9 inhibitors as potential hypoglycemic agents. *Bioorg Med Chem Lett*, **19,** 2537-41.

DENT, P., YACOUB, A., CONTESSA, J., CARON, R., AMORINO, G., VALERIE, K., HAGAN, M.P., GRANT, S. & SCHMIDT-ULLRICH, R. (2003). Stress and radiation-induced activation of multiple intracellular signaling pathways. *Radiat Res*, **159,** 283-300.

DIEBOLD, I., DJORDJEVIC, T., PETRY, A., HATZELMANN, A., TENOR, H., HESS, J. & GORLACH, A. (2009). Phosphodiesterase 2 mediates redox-sensitive endothelial cell proliferation and angiogenesis by thrombin via Rac1

and NADPH oxidase 2. *Circ Res*, **104,** 1169-77.

DONG, C., DAVIS, R.J. & FLAVELL, R.A. (2002). MAP kinases in the immune response. *Annu Rev Immunol*, **20,** 55-72.

DONG, H., OSMANOVA, V., EPSTEIN, P.M. & BROCKE, S. (2006). Phosphodiesterase 8 (PDE8) regulates chemotaxis of activated lymphocytes. *Biochem Biophys Res Commun*, **345,** 713-9.

DUAN, B., DAVIS, R., SADAT, E.L., COLLINS, J., STERNWEIS, P.C., YUAN, D. & JIANG, L.I. Distinct roles of adenylyl cyclase VII in regulating the immune responses in mice. *J Immunol*, **185,** 335-44.

DURAISAMY, S., BAJPAI, M., BUGHANI, U., DASTIDAR, S.G., RAY, A. & CHOPRA, P. (2008). MK2: a novel molecular target for anti-inflammatory therapy. *Expert Opin Ther Targets*, **12,** 921-36.

EHRHARDT, A., DAVID, M.D., EHRHARDT, G.R. & SCHRADER, J.W. (2004). Distinct mechanisms determine the patterns of differential activation of H-Ras, N-Ras, K-Ras 4B, and M-Ras by receptors for growth factors or antigen. *Mol Cell Biol*, **24,** 6311-23.

ENGEL, K., KOTLYAROV, A. & GAESTEL, M. (1998). Leptomycin B-sensitive nuclear export of MAPKAP kinase 2 is regulated by phosphorylation. *Embo J*, **17,** 3363-71.

ENSLEN, H., BRANCHO, D.M. & DAVIS, R.J. (2000). Molecular determinants that mediate selective activation of p38 MAP kinase isoforms. *Embo J*, **19,** 1301-11.

ERNEUX, C., COUCHIE, D., DUMONT, J.E., BARANIAK, J., STEC, W.J., ABBAD,

E.G., PETRIDIS, G. & JASTORFF, B. (1981). Specificity of cyclic GMP activation of a multi-substrate cyclic nucleotide phosphodiesterase from rat liver. *Eur J Biochem*, **115,** 503-10.

ESPANEL, X. & HOOFT VAN HUIJSDUIJNEN, R. (2005). Applying the SPOT peptide synthesis procedure to the study of protein tyrosine phosphatase substrate specificity: probing for the heavenly match in vitro. *Methods*, **35,** 64-72.

FAHNESTOCK, M., MICHALSKI, B., XU, B. & COUGHLIN, M.D. (2001). The precursor pro-nerve growth factor is the predominant form of nerve growth factor in brain and is increased in Alzheimer's disease. *Mol Cell Neurosci*, **18,** 210-20.

FAURE, J., UYS, J.D., MARAIS, L., STEIN, D.J. & DANIELS, W.M. (2006). Early maternal separation followed by later stressors leads to dysregulation of the HPA-axis and increases in hippocampal NGF and NT-3 levels in a rat model. *Metab Brain Dis*, **21,** 181-88.

FISHER, D.A., SMITH, J.F., PILLAR, J.S., ST DENIS, S.H. & CHENG, J.B. (1998). Isolation and characterization of PDE8A, a novel human cAMP-specific phosphodiesterase. *Biochem Biophys Res Commun*, **246,** 570-7.

FRANCIS, S.H., BESSAY, E.P., KOTERA, J., GRIMES, K.A., LIU, L., THOMPSON, W.J. & CORBIN, J.D. (2002). Phosphorylation of isolated human phosphodiesterase-5 regulatory domain induces an apparent conformational change and increases cGMP binding affinity. *J Biol Chem*, **277,** 47581-7.

FRANCIS, S.H. & CORBIN, J.D. (2005). Phosphodiesterase-5 inhibition: the molecular biology of erectile function and dysfunction. *Urol Clin North Am*, **32,** 419-29, vi.

FRANCIS, S.H., TURKO, I.V. & CORBIN, J.D. (2001). Cyclic nucleotide phosphodiesterases: relating structure and function. *Prog Nucleic Acid Res Mol Biol*, **65,** 1-52.

FRANK, R. (2002). The SPOT-synthesis technique. Synthetic peptide arrays on membrane supports--principles and applications. *J Immunol Methods*, **267,** 13-26.

FREDHOLM, B.B., HOKFELT, T. & MILLIGAN, G. (2007). G-protein-coupled receptors: an update. *Acta Physiol (Oxf)*, **190,** 3-7.

FREUND-MICHEL, V. & FROSSARD, N. (2008). The nerve growth factor and its receptors in airway inflammatory diseases. *Pharmacol Ther*, **117,** 52-76.

FROSSARD, N., FREUND, V. & ADVENIER, C. (2004). Nerve growth factor and its receptors in asthma and inflammation. *Eur J Pharmacol*, **500,** 453-65.

FRYER, R.H., KAPLAN, D.R., FEINSTEIN, S.C., RADEKE, M.J., GRAYSON, D.R. & KROMER, L.F. (1996). Developmental and mature expression of full-length and truncated TrkB receptors in the rat forebrain. *J Comp Neurol*, **374,** 21-40.

GAESTEL, M. (2006). MAPKAP kinases - MKs - two's company, three's a crowd. *Nat Rev Mol Cell Biol*, **7,** 120-30.

GAESTEL, M. (2006). Molecular chaperones in signal transduction. *Handb Exp Pharmacol***,**
93-109.

GALPERIN, M.Y. (2006). Structural classification of bacterial response regulators: diversity of output domains and domain combinations. *J Bacteriol*, **188,** 4169-82.

GEOFFROY, V., FOUQUE, F., LUGNIER, C., DESBUQUOIS, B. & BENELLI, C. (2001). Characterization of an in vivo hormonally regulated phosphodiesterase 3 (PDE3) associated with a liver Golgi-endosomal fraction. *Arch Biochem Biophys*, **387,** 154-62.

GERITS, N., KOSTENKO, S., SHIRYAEV, A., JOHANNESSEN, M. & MOENS, U. (2008). Relations between the mitogen-activated protein kinase and the cAMP-dependent protein kinase pathways: comradeship and hostility. *Cell Signal*, **20,** 1592-607.

GILLESPIE, P.G. & BEAVO, J.A. (1989). cGMP is tightly bound to bovine retinal rod phosphodiesterase. *Proc Natl Acad Sci U S A*, **86,** 4311-5.

GILLESPIE, P.G. & BEAVO, J.A. (1989). Inhibition and stimulation of photoreceptor phosphodiesterases by dipyridamole and M&B 22,948. *Mol Pharmacol*, **36,** 773-81.

GIORDANO, D., DE STEFANO, M.E., CITRO, G., MODICA, A. & GIORGI, M. (2001). Expression of cGMP-binding cGMP-specific phosphodiesterase (PDE5) in mouse tissues and cell lines using an antibody against the enzyme amino-terminal domain. *Biochim Biophys Acta*, **1539,** 16-27.

GLASS, D.J., NYE, S.H., HANTZOPOULOS, P., MACCHI, M.J., SQUINTO, S.P., GOLDFARB, M. & YANCOPOULOS, G.D. (1991). TrkB mediates BDNF/NT-3-dependent survival and proliferation in fibroblasts lacking the low affinity NGF receptor. *Cell*, **66,** 405-13.

GLAVAS, N.A., OSTENSON, C., SCHAEFER, J.B., VASTA, V. & BEAVO, J.A. (2001). T cell activation up-regulates cyclic nucleotide phosphodiesterases 8A1

and 7A3. *Proc Natl Acad Sci U S A*, **98,** 6319-24.

GLOERICH, M. & BOS, J.L. Epac: defining a new mechanism for cAMP action. *Annu Rev Pharmacol Toxicol*, **50,** 355-75.

GOLD, N.D. & JACKSON, R.M. (2006). A searchable database for comparing protein-ligand binding sites for the analysis of structure-function relationships. *J Chem Inf Model*, **46,** 736-42.

GRAUER, S.M., PULITO, V.L., NAVARRA, R.L., KELLY, M.P., KELLEY, C., GRAF, R., LANGEN, B., LOGUE, S., BRENNAN, J., JIANG, L., CHARYCH, E., EGERLAND, U., LIU, F., MARQUIS, K.L., MALAMAS, M., HAGE, T., COMERY, T.A. & BRANDON, N.J. (2009). Phosphodiesterase 10A inhibitor activity in preclinical models of the positive, cognitive, and negative symptoms of schizophrenia. *J Pharmacol Exp Ther*, **331,** 574-90.

GROLLMAN, A.P. (1967). Inhibitors of protein biosynthesis. II. Mode of action of anisomycin. *J Biol Chem*, **242,** 3226-33.

GUO, J., WATSON, A., KEMPSON, J., CARLSEN, M., BARBOSA, J., STEBBINS, K., LEE, D., DODD, J., NADLER, S.G., MCKINNON, M., BARRISH, J. & PITTS, W.J. (2009). Identification of potent pyrimidine inhibitors of phosphodiesterase 7 (PDE7) and their ability to inhibit T cell proliferation. *Bioorg Med Chem Lett*, **19,** 1935-8.

HAN, J., LEE, J.D., BIBBS, L. & ULEVITCH, R.J. (1994). A MAP kinase targeted by endotoxin and hyperosmolarity in mammalian cells. *Science*, **265,** 808-11.

HAYASHI, M., MATSUSHIMA, K., OHASHI, H., TSUNODA, H., MURASE, S., KAWARADA, Y. & TANAKA, T. (1998). Molecular cloning and characterization of human PDE8B, a novel thyroid-specific isozyme of 3',5'-

cyclic nucleotide phosphodiesterase. *Biochem Biophys Res Commun*, **250,** 751-6.

HEBENSTREIT, G.F., FELLERER, K., FICHTE, K., FISCHER, G., GEYER, N., MEYA, U., SASTRE-Y-HERNANDEZ, M., SCHONY, W., SCHRATZER, M., SOUKOP, W. & ET AL. (1989). Rolipram in major depressive disorder: results of a double-blind comparative study with imipramine. *Pharmacopsychiatry*, **22,** 156-60.

HELDIN, C.H. (1995). Dimerization of cell surface receptors in signal transduction. *Cell*, **80,** 213-23.

HENDRIKS, B.S., SEIDL, K.M. & CHABOT, J.R. Two additive mechanisms impair the differentiation of 'substrate-selective' p38 inhibitors from classical p38 inhibitors in vitro. *BMC Syst Biol*, **4,** 23.

HETMAN, J.M., ROBAS, N., BAXENDALE, R., FIDOCK, M., PHILLIPS, S.C., SODERLING, S.H. & BEAVO, J.A. (2000). Cloning and characterization of two splice variants of human phosphodiesterase 11A. *Proc Natl Acad Sci U S A*, **97,** 12891-5.

HETMAN, J.M., SODERLING, S.H., GLAVAS, N.A. & BEAVO, J.A. (2000). Cloning and characterization of PDE7B, a cAMP-specific phosphodiesterase. *Proc Natl Acad Sci U S A*, **97,** 472-6.

HIMES, B.E., HUNNINGHAKE, G.M., BAURLEY, J.W., RAFAELS, N.M., SLEIMAN, P., STRACHAN, D.P., WILK, J.B., WILLIS-OWEN, S.A., KLANDERMAN, B., LASKY-SU, J., LAZARUS, R., MURPHY, A.J., SOTO-QUIROS, M.E., AVILA, L., BEATY, T., MATHIAS, R.A., RUCZINSKI, I., BARNES, K.C., CELEDON, J.C., COOKSON, W.O., GAUDERMAN, W.J., GILLILAND, F.D., HAKONARSON, H., LANGE, C., MOFFATT, M.F.,

O'CONNOR, G.T., RABY, B.A., SILVERMAN, E.K. & WEISS, S.T. (2009). Genome-wide association analysis identifies PDE4D as an asthma-susceptibility gene. *Am J Hum Genet*, **84,** 581-93.

HOLLAND, P.M. & COOPER, J.A. (1999). Protein modification: docking sites for kinases. *Curr Biol*, **9,** R329-31.

HOLLMANN, M.W., STRUMPER, D., HERROEDER, S. & DURIEUX, M.E. (2005). Receptors, G proteins, and their interactions. *Anesthesiology*, **103,** 1066-78.

HOMMES, D.W., PEPPELENBOSCH, M.P. & VAN DEVENTER, S.J. (2003). Mitogen activated protein (MAP) kinase signal transduction pathways and novel anti-inflammatory targets. *Gut*, **52,** 144-51.

HOUSLAY, M.D. (1998). Adaptation in cyclic AMP signalling processes: a central role for cyclic AMP phosphodiesterases. *Semin Cell Dev Biol*, **9,** 161-7.

HOUSLAY, M.D. (2005). The long and short of vascular smooth muscle phosphodiesterase-4 as a putative therapeutic target. *Mol Pharmacol*, **68,** 563-7.

HOUSLAY, M.D. (2001). PDE4 cAMP-specific phosphodiesterases. *Prog Nucleic Acid Res Mol Biol*, **69,** 249-315.

HOUSLAY, M.D. Underpinning compartmentalised cAMP signalling through targeted cAMP breakdown. *Trends Biochem Sci*, **35,** 91-100.

HOUSLAY, M.D. & ADAMS, D.R. (2003). PDE4 cAMP phosphodiesterases: modular enzymes that orchestrate signalling cross-talk, desensitization and compartmentalization. *Biochem J*, **370,** 1-18.

HOUSLAY, M.D. & ADAMS, D.R. Putting the lid on phosphodiesterase 4. *Nat*

Biotechnol, **28,** 38-40.

HOUSLAY, M.D., BAILLIE, G.S. & MAURICE, D.H. (2007). cAMP-Specific phosphodiesterase-4 enzymes in the cardiovascular system: a molecular toolbox for generating compartmentalized cAMP signaling. *Circ Res*, **100,** 950-66.

HOUSLAY, M.D. & KOLCH, W. (2000). Cell-type specific integration of cross-talk between extracellular signal-regulated kinase and cAMP signaling. *Mol Pharmacol*, **58,** 659-68.

HOUSLAY, M.D., SCHAFER, P. & ZHANG, K.Y. (2005). Keynote review: phosphodiesterase-4 as a therapeutic target. *Drug Discov Today*, **10,** 1503-19.

HOYLE, G.W., GRAHAM, R.M., FINKELSTEIN, J.B., NGUYEN, K.P., GOZAL, D. & FRIEDMAN, M. (1998). Hyperinnervation of the airways in transgenic mice overexpressing nerve growth factor. *Am J Respir Cell Mol Biol*, **18,** 149-57.

HUANG, C.Y., CHAU, V., CHOCK, P.B., WANG, J.H. & SHARMA, R.K. (1981). Mechanism of activation of cyclic nucleotide phosphodiesterase: requirement of the binding of four Ca2+ to calmodulin for activation. *Proc Natl Acad Sci U S A*, **78,** 871-4.

HUANG, L.J., DURICK, K., WEINER, J.A., CHUN, J. & TAYLOR, S.S. (1997). D-AKAP2, a novel protein kinase A anchoring protein with a putative RGS domain. *Proc Natl Acad Sci U S A*, **94,** 11184-9.

HUDDLESTON, A.J., KNODERER, C.A., MORRIS, J.L. & EBENROTH, E.S. (2009). Sildenafil for the treatment of pulmonary hypertension in pediatric patients. *Pediatr Cardiol*, **30,** 871-82.

HUSTON, E., BEARD, M., MCCALLUM, F., PYNE, N.J., VANDENABEELE, P., SCOTLAND, G. & HOUSLAY, M.D. (2000). The cAMP-specific phosphodiesterase PDE4A5 is cleaved downstream of its SH3 interaction domain by caspase-3. Consequences for altered intracellular distribution. *J Biol Chem*, **275,** 28063-74.

HUSTON, E., LUMB, S., RUSSELL, A., CATTERALL, C., ROSS, A.H., STEELE, M.R., BOLGER, G.B., PERRY, M.J., OWENS, R.J. & HOUSLAY, M.D. (1997). Molecular cloning and transient expression in COS7 cells of a novel human PDE4B cAMP-specific phosphodiesterase, HSPDE4B3. *Biochem J*, **328 (Pt 2),** 549-58.

HUSTON, E., POOLEY, L., JULIEN, P., SCOTLAND, G., MCPHEE, I., SULLIVAN, M., BOLGER, G. & HOUSLAY, M.D. (1996). The human cyclic AMP-specific phosphodiesterase PDE-46 (HSPDE4A4B) expressed in transfected COS7 cells occurs as both particulate and cytosolic species that exhibit distinct kinetics of inhibition by the antidepressant rolipram. *J Biol Chem*, **271,** 31334-44.

IBANEZ, C.F. (2002). Jekyll-Hyde neurotrophins: the story of proNGF. *Trends Neurosci*, **25,** 284-6.

ICHIJO, H., NISHIDA, E., IRIE, K., TEN DIJKE, P., SAITOH, M., MORIGUCHI, T., TAKAGI, M., MATSUMOTO, K., MIYAZONO, K. & GOTOH, Y. (1997). Induction of apoptosis by ASK1, a mammalian MAPKKK that activates SAPK/JNK and p38 signaling pathways. *Science*, **275,** 90-4.

ITATSU, K., SASAKI, M., HARADA, K., YAMAGUCHI, J., IKEDA, H., SATO, Y., OHTA, T., SATO, H., NAGINO, M., NIMURA, Y. & NAKANUMA, Y. (2009). Phosphorylation of extracellular signal-regulated kinase 1/2, p38 mitogen-activated protein kinase and nuclear translocation of nuclear factor-kappaB are involved in upregulation of matrix metalloproteinase-9 by tumour

necrosis factor-alpha. *Liver Int*, **29,** 291-8.

JACOBITZ, S., MCLAUGHLIN, M.M., LIVI, G.P., BURMAN, M. & TORPHY, T.J. (1996). Mapping the functional domains of human recombinant phosphodiesterase 4A: structural requirements for catalytic activity and rolipram binding. *Mol Pharmacol*, **50,** 891-9.

JACOBS, D., BEITEL, G.J., CLARK, S.G., HORVITZ, H.R. & KORNFELD, K. (1998). Gain-of-function mutations in the Caenorhabditis elegans lin-1 ETS gene identify a C-terminal regulatory domain phosphorylated by ERK MAP kinase. *Genetics*, **149,** 1809-22.

JACOBS, D., GLOSSIP, D., XING, H., MUSLIN, A.J. & KORNFELD, K. (1999). Multiple docking sites on substrate proteins form a modular system that mediates recognition by ERK MAP kinase. *Genes Dev*, **13,** 163-75.

JAUCH, R., CHO, M.K., JAKEL, S., NETTER, C., SCHREITER, K., AICHER, B., ZWECKSTETTER, M., JACKLE, H. & WAHL, M.C. (2006). Mitogen-activated protein kinases interacting kinases are autoinhibited by a reprogrammed activation segment. *Embo J*, **25,** 4020-32.

JIN, S.L. & CONTI, M. (2002). Induction of the cyclic nucleotide phosphodiesterase PDE4B is essential for LPS-activated TNF-alpha responses. *Proc Natl Acad Sci U S A*, **99,** 7628-33.

JIN, S.L., LAN, L., ZOUDILOVA, M. & CONTI, M. (2005). Specific role of phosphodiesterase 4B in lipopolysaccharide-induced signaling in mouse macrophages. *J Immunol*, **175,** 1523-31.

JIN, S.L., LATOUR, A.M. & CONTI, M. (2005). Generation of PDE4 knockout mice by gene targeting. *Methods Mol Biol*, **307,** 191-210.

JING, S., TAPLEY, P. & BARBACID, M. (1992). Nerve growth factor mediates signal transduction through trk homodimer receptors. *Neuron*, **9,** 1067-79.

JOHNSON, B.D., SCHEUER, T. & CATTERALL, W.A. (1994). Voltage-dependent potentiation of L-type Ca2+ channels in skeletal muscle cells requires anchored cAMP-dependent protein kinase. *Proc Natl Acad Sci U S A*, **91,** 11492-6.

JOHNSTON, L.A., ERDOGAN, S., CHEUNG, Y.F., SULLIVAN, M., BARBER, R., LYNCH, M.J., BAILLIE, G.S., VAN HEEKE, G., ADAMS, D.R., HUSTON, E. & HOUSLAY, M.D. (2004). Expression, intracellular distribution and basis for lack of catalytic activity of the PDE4A7 isoform encoded by the human PDE4A cAMP-specific phosphodiesterase gene. *Biochem J*, **380,** 371-84.

KADOSHIMA-YAMAOKA, K., MURAKAWA, M., GOTO, M., TANAKA, Y., INOUE, H., MURAFUJI, H., NAGAHIRA, A., HAYASHI, Y., NAGAHIRA, K., MIURA, K., NAKATSUKA, T., CHAMOTO, K., FUKUDA, Y. & NISHIMURA, T. (2009). ASB16165, a novel inhibitor for phosphodiesterase 7A (PDE7A), suppresses IL-12-induced IFN-gamma production by mouse activated T lymphocytes. *Immunol Lett*, **122,** 193-7.

KAKKAR, R., RAJU, R.V. & SHARMA, R.K. (1999). Calmodulin-dependent cyclic nucleotide phosphodiesterase (PDE1). *Cell Mol Life Sci*, **55,** 1164-86.

KANDA, N. & WATANABE, S. (2001). Regulatory roles of adenylate cyclase and cyclic nucleotide phosphodiesterases 1 and 4 in interleukin-13 production by activated human T cells. *Biochem Pharmacol*, **62,** 495-507.

KARIN, M. (1995). The regulation of AP-1 activity by mitogen-activated protein kinases. *J Biol Chem*, **270,** 16483-6.

KAWASAKI, H., SPRINGETT, G.M., MOCHIZUKI, N., TOKI, S., NAKAYA, M., MATSUDA, M., HOUSMAN, D.E. & GRAYBIEL, A.M. (1998). A family of cAMP-binding proteins that directly activate Rap1. *Science*, **282,** 2275-9.

KE, H. & WANG, H. (2007). Crystal structures of phosphodiesterases and implications on substrate specificity and inhibitor selectivity. *Curr Top Med Chem*, **7,** 391-403.

KELLY, M.P. & BRANDON, N.J. (2009). Differential function of phosphodiesterase families in the brain: gaining insights through the use of genetically modified animals. *Prog Brain Res*, **179,** 67-73.

KELLY, M.P., LOGUE, S.F., BRENNAN, J., DAY, J.P., LAKKARAJU, S., JIANG, L., ZHONG, X., TAM, M., SUKOFF RIZZO, S.J., PLATT, B.J., DWYER, J.M., NEAL, S., PULITO, V.L., AGOSTINO, M.J., GRAUER, S.M., NAVARRA, R.L., KELLEY, C., COMERY, T.A., MURRILLS, R.J., HOUSLAY, M.D. & BRANDON, N.J. Phosphodiesterase 11A in brain is enriched in ventral hippocampus and deletion causes psychiatric disease-related phenotypes. *Proc Natl Acad Sci U S A*, **107,** 8457-62.

KERSCHENSTEINER, M., GALLMEIER, E., BEHRENS, L., LEAL, V.V., MISGELD, T., KLINKERT, W.E., KOLBECK, R., HOPPE, E., OROPEZA-WEKERLE, R.L., BARTKE, I., STADELMANN, C., LASSMANN, H., WEKERLE, H. & HOHLFELD, R. (1999). Activated human T cells, B cells, and monocytes produce brain-derived neurotrophic factor in vitro and in inflammatory brain lesions: a neuroprotective role of inflammation? *J Exp Med*, **189,** 865-70.

KERZEL, S., PATH, G., NOCKHER, W.A., QUARCOO, D., RAAP, U., GRONEBERG, D.A., DINH, Q.T., FISCHER, A., BRAUN, A. & RENZ, H. (2003). Pan-neurotrophin receptor p75 contributes to neuronal hyperreactivity and airway inflammation in a murine model of experimental asthma. *Am J Respir Cell Mol Biol*, **28,** 170-8.

KHURSIGARA, G., BERTIN, J., YANO, H., MOFFETT, H., DISTEFANO, P.S. & CHAO, M.V. (2001). A prosurvival function for the p75 receptor death domain mediated via the caspase recruitment domain receptor-interacting protein 2. *J Neurosci*, **21,** 5854-63.

KHURSIGARA, G., ORLINICK, J.R. & CHAO, M.V. (1999). Association of the p75 neurotrophin receptor with TRAF6. *J Biol Chem*, **274,** 2597-600.

KLEIN, R., CONWAY, D., PARADA, L.F. & BARBACID, M. (1990). The trkB tyrosine protein kinase gene codes for a second neurogenic receptor that lacks the catalytic kinase domain. *Cell*, **61,** 647-56.

KLEIN, R., JING, S.Q., NANDURI, V., O'ROURKE, E. & BARBACID, M. (1991). The trk proto-oncogene encodes a receptor for nerve growth factor. *Cell*, **65,** 189-97.

KLEIN, R., NANDURI, V., JING, S.A., LAMBALLE, F., TAPLEY, P., BRYANT, S., CORDON-CARDO, C., JONES, K.R., REICHARDT, L.F. & BARBACID, M. (1991). The trkB tyrosine protein kinase is a receptor for brain-derived neurotrophic factor and neurotrophin-3. *Cell*, **66,** 395-403.

KOFLER, M., MOTZNY, K. & FREUND, C. (2005). GYF domain proteomics reveals interaction sites in known and novel target proteins. *Mol Cell Proteomics*, **4,** 1797-811.

KOHOUT, T.A. & LEFKOWITZ, R.J. (2003). Regulation of G protein-coupled receptor kinases and arrestins during receptor desensitization. *Mol Pharmacol*, **63,** 9-18.

KOTERA, J., FUJISHIGE, K., YUASA, K. & OMORI, K. (1999). Characterization and phosphorylation of PDE10A2, a novel alternative splice variant of human phosphodiesterase that hydrolyzes cAMP and cGMP. *Biochem Biophys Res Commun*, **261,** 551-7.

KOTLYAROV, A., NEININGER, A., SCHUBERT, C., ECKERT, R., BIRCHMEIER, C., VOLK, H.D. & GAESTEL, M. (1999). MAPKAP kinase 2 is essential for LPS-induced TNF-alpha biosynthesis. *Nat Cell Biol*, **1,** 94-7.

KRYL, D. & BARKER, P.A. (2000). TTIP is a novel protein that interacts with the truncated T1 TrkB neurotrophin receptor. *Biochem Biophys Res Commun*, **279,** 925-30.

KUZHANDAIVELU, N., CONG, Y.S., INOUYE, C., YANG, W.M. & SETO, E. (1996). XAP2, a novel hepatitis B virus X-associated protein that inhibits X transactivation. *Nucleic Acids Res*, **24,** 4741-50.

KYRIAKIS, J.M. & AVRUCH, J. (2001). Mammalian mitogen-activated protein kinase signal transduction pathways activated by stress and inflammation. *Physiol Rev*, **81,** 807-69.

LACHYANKAR, M.B., CONDON, P.J., DAOU, M.C., DE, A.K., LEVINE, J.B., OBERMEIER, A. & ROSS, A.H. (2003). Novel functional interactions between Trk kinase and p75 neurotrophin receptor in neuroblastoma cells. *J Neurosci Res*, **71,** 157-72.

LADDHA, S.S. & BHATNAGAR, S.P. (2009). A new therapeutic approach in Parkinson's disease: some novel quinazoline derivatives as dual selective phosphodiesterase 1 inhibitors and anti-inflammatory agents. *Bioorg Med Chem*, **17,** 6796-802.

LALIBERTE, F., LIU, S., GORSETH, E., BOBECHKO, B., BARTLETT, A., LARIO, P., GRESSER, M.J. & HUANG, Z. (2002). In vitro PKA phosphorylation-mediated human PDE4A4 activation. *FEBS Lett*, **512,** 205-8.

LAMBALLE, F., SMEYNE, R.J. & BARBACID, M. (1994). Developmental expression of trkC, the neurotrophin-3 receptor, in the mammalian nervous system. *J Neurosci*, **14,** 14-28.

LAMBIASE, A., CENTOFANTI, M., MICERA, A., MANNI, G.L., MATTEI, E., DE GREGORIO, A., DE FEO, G., BUCCI, M.G. & ALOE, L. (1997). Nerve growth factor (NGF) reduces and NGF antibody exacerbates retinal damage induced in rabbit by experimental ocular hypertension. *Graefes Arch Clin Exp Ophthalmol*, **235,** 780-5.

LAMMER, C., WAGERER, S., SAFFRICH, R., MERTENS, D., ANSORGE, W. & HOFFMANN, I. (1998). The cdc25B phosphatase is essential for the G2/M phase transition in human cells. *J Cell Sci*, **111 (Pt 16),** 2445-53.

LANG, R., HAMMER, M. & MAGES, J. (2006). DUSP meet immunology: dual specificity MAPK phosphatases in control of the inflammatory response. *J Immunol*, **177,** 7497-504.

LANGEBERG, L.K. & SCOTT, J.D. (2005). A-kinase-anchoring proteins. *J Cell Sci*, **118,** 3217-20.

LAVAN, B.E., LAKEY, T. & HOUSLAY, M.D. (1989). Resolution of soluble cyclic nucleotide phosphodiesterase isoenzymes, from liver and hepatocytes, identifies a novel IBMX-insensitive form. *Biochem Pharmacol*, **38,** 4123-36.

LEE, J.C., LAYDON, J.T., MCDONNELL, P.C., GALLAGHER, T.F., KUMAR, S., GREEN, D., MCNULTY, D., BLUMENTHAL, M.J., HEYS, J.R., LANDVATTER, S.W. & ET AL. (1994). A protein kinase involved in the regulation of inflammatory cytokine biosynthesis. *Nature*, **372,** 739-46.

LEE, M.R. & DOMINGUEZ, C. (2005). MAP kinase p38 inhibitors: clinical results and an intimate look at their interactions with p38alpha protein. *Curr Med Chem*, **12,** 2979-94.

LEE, R., KERMANI, P., TENG, K.K. & HEMPSTEAD, B.L. (2001). Regulation of cell survival by secreted proneurotrophins. *Science*, **294,** 1945-8.

LEFIEVRE, L., DE LAMIRANDE, E. & GAGNON, C. (2002). Presence of cyclic nucleotide phosphodiesterases PDE1A, existing as a stable complex with calmodulin, and PDE3A in human spermatozoa. *Biol Reprod*, **67,** 423-30.

LEFKOWITZ, R.J. & SHENOY, S.K. (2005). Transduction of receptor signals by beta-arrestins. *Science*, **308,** 512-7.

LEIBROCK, J., LOTTSPEICH, F., HOHN, A., HOFER, M., HENGERER, B., MASIAKOWSKI, P., THOENEN, H. & BARDE, Y.A. (1989). Molecular cloning and expression of brain-derived neurotrophic factor. *Nature*, **341,** 149-52.

LEVI-MONTALCINI, R., DAL TOSO, R., DELLA VALLE, F., SKAPER, S.D. & LEON, A. (1995). Update of the NGF saga. *J Neurol Sci*, **130,** 119-27.

LI, L., YEE, C. & BEAVO, J.A. (1999). CD3- and CD28-dependent induction of PDE7 required for T cell activation. *Science*, **283,** 848-51.

LI, X., BAILLIE, G.S. & HOUSLAY, M.D. (2009). Mdm2 directs the ubiquitination of beta-arrestin-sequestered cAMP phosphodiesterase-4D5. *J Biol Chem*, **284,** 16170-82.

LI, X., HUSTON, E., LYNCH, M.J., HOUSLAY, M.D. & BAILLIE, G.S. (2006). Phosphodiesterase-4 influences the PKA phosphorylation status and membrane translocation of G-protein receptor kinase 2 (GRK2) in HEK-293beta2 cells and cardiac myocytes. *Biochem J*, **394,** 427-35.

LIM, J., PAHLKE, G. & CONTI, M. (1999). Activation of the cAMP-specific phosphodiesterase PDE4D3 by phosphorylation. Identification and function of an inhibitory domain. *J Biol Chem*, **274,** 19677-85.

LIN, C.S., CHOW, S., LAU, A., TU, R. & LUE, T.F. (2002). Human PDE5A gene encodes three PDE5 isoforms from two alternate promoters. *Int J Impot Res*, **14,** 15-24.

LIN, C.S., LIN, G. & LUE, T.F. (2003). Isolation of two isoforms of phosphodiesterase 5 from rat penis. *Int J Impot Res*, **15,** 129-36.

LIU, Y., SHAKUR, Y., YOSHITAKE, M. & KAMBAYASHI JI, J. (2001). Cilostazol (pletal): a dual inhibitor of cyclic nucleotide phosphodiesterase type 3 and adenosine uptake. *Cardiovasc Drug Rev*, **19,** 369-86.

LUGNIER, C. (2006). Cyclic nucleotide phosphodiesterase (PDE) superfamily: a new target for the development of specific therapeutic agents. *Pharmacol Ther*, **109,** 366-98.

LUKAS, S.M., KROE, R.R., WILDESON, J., PEET, G.W., FREGO, L., DAVIDSON, W., INGRAHAM, R.H., PARGELLIS, C.A., LABADIA, M.E. & WERNEBURG, B.G. (2004). Catalysis and function of the p38 alpha.MK2a signaling complex. *Biochemistry*, **43,** 9950-60.

LYNCH, M.J., BAILLIE, G.S., MOHAMED, A., LI, X., MAISONNEUVE, C., KLUSSMANN, E., VAN HEEKE, G. & HOUSLAY, M.D. (2005). RNA silencing identifies PDE4D5 as the functionally relevant cAMP phosphodiesterase interacting with beta arrestin to control the protein kinase A/AKAP79-mediated switching of the beta2-adrenergic receptor to activation of ERK in HEK293B2 cells. *J Biol Chem*, **280,** 33178-89.

MACKENZIE, K.F., TOPPING, E.C., BUGAJ-GAWEDA, B., DENG, C., CHEUNG, Y.F., OLSEN, A.E., STOCKARD, C.R., HIGH MITCHELL, L., BAILLIE, G.S., GRIZZLE, W.E., DE VIVO, M., HOUSLAY, M.D., WANG, D. & BOLGER, G.B. (2008). Human PDE4A8, a novel brain-expressed PDE4 cAMP-specific phosphodiesterase that has undergone rapid evolutionary change. *Biochem J*, **411,** 361-9.

MACKENZIE, S.J., BAILLIE, G.S., MCPHEE, I., BOLGER, G.B. & HOUSLAY, M.D. (2000). ERK2 mitogen-activated protein kinase binding, phosphorylation, and regulation of the PDE4D cAMP-specific phosphodiesterases. The involvement of COOH-terminal docking sites and NH2-terminal UCR regions. *J Biol Chem*, **275,** 16609-17.

MACKENZIE, S.J., BAILLIE, G.S., MCPHEE, I., MACKENZIE, C., SEAMONS, R.,

MCSORLEY, T., MILLEN, J., BEARD, M.B., VAN HEEKE, G. & HOUSLAY, M.D. (2002). Long PDE4 cAMP specific phosphodiesterases are activated by protein kinase A-mediated phosphorylation of a single serine residue in Upstream Conserved Region 1 (UCR1). *Br J Pharmacol*, **136,** 421-33.

MACKENZIE, S.J. & HOUSLAY, M.D. (2000). Action of rolipram on specific PDE4 cAMP phosphodiesterase isoforms and on the phosphorylation of cAMP-response-element-binding protein (CREB) and p38 mitogen-activated protein (MAP) kinase in U937 monocytic cells. *Biochem J*, **347,** 571-8.

MACKENZIE, S.J., YARWOOD, S.J., PEDEN, A.H., BOLGER, G.B., VERNON, R.G. & HOUSLAY, M.D. (1998). Stimulation of p70S6 kinase via a growth hormone-controlled phosphatidylinositol 3-kinase pathway leads to the activation of a PDE4A cyclic AMP-specific phosphodiesterase in 3T3-F442A preadipocytes. *Proc Natl Acad Sci U S A*, **95,** 3549-54.

MAHALINGAM, M. & COOPER, J.A. (2001). Phosphorylation of mammalian eIF4E by Mnk1 and Mnk2: tantalizing prospects for a role in translation. *Prog Mol Subcell Biol*, **27,** 132-42.

MAISONPIERRE, P.C., BELLUSCIO, L., SQUINTO, S., IP, N.Y., FURTH, M.E., LINDSAY, R.M. & YANCOPOULOS, G.D. (1990). Neurotrophin-3: a neurotrophic factor related to NGF and BDNF. *Science*, **247,** 1446-51.

MARCHMONT, R.J. & HOUSLAY, M.D. (1980). A peripheral and an intrinsic enzyme constitute the cyclic AMP phosphodiesterase activity of rat liver plasma membranes. *Biochem J*, **187,** 381-92.

MARTINEZ, S.E., WU, A.Y., GLAVAS, N.A., TANG, X.B., TURLEY, S., HOL, W.G. & BEAVO, J.A. (2002). The two GAF domains in phosphodiesterase 2A have distinct roles in dimerization and in cGMP binding. *Proc Natl Acad Sci U S A*, **99,** 13260-5.

MATHERS, C.D. & LONCAR, D. (2006). Projections of global mortality and burden of disease from 2002 to 2030. *PLoS Med*, **3,** e442.

MCCAHILL, A., MCSORLEY, T., HUSTON, E., HILL, E.V., LYNCH, M.J., GALL, I., KERYER, G., LYGREN, B., TASKEN, K., VAN HEEKE, G. & HOUSLAY, M.D. (2005). In resting COS1 cells a dominant negative approach shows that specific, anchored PDE4 cAMP phosphodiesterase isoforms gate the activation, by basal cyclic AMP production, of AKAP-tethered protein kinase A type II located in the centrosomal region. *Cell Signal*, **17,** 1158-73.

MCCAHILL, A., WARWICKER, J., BOLGER, G.B., HOUSLAY, M.D. & YARWOOD, S.J. (2002). The RACK1 scaffold protein: a dynamic cog in cell response mechanisms. *Mol Pharmacol*, **62,** 1261-73.

MCCANN, F.E., PALFREEMAN, A.C., ANDREWS, M., PEROCHEAU, D.P., INGLIS, J.J., SCHAFER, P., FELDMANN, M., WILLIAMS, R.O. & BRENNAN, F.M. Apremilast, a novel PDE4 inhibitor, inhibits spontaneous production of tumour necrosis factor-alpha from human rheumatoid synovial cells and ameliorates experimental arthritis. *Arthritis Res Ther*, **12,** R107.

MCCORMICK, F. (1995). Ras-related proteins in signal transduction and growth control. *Mol Reprod Dev*, **42,** 500-6.

MCINNES, C. & SYKES, B.D. (1997). Growth factor receptors: structure, mechanism, and drug discovery. *Biopolymers*, **43,** 339-66.

MCPHEE, I., COCHRAN, S. & HOUSLAY, M.D. (2001). The novel long PDE4A10

cyclic AMP phosphodiesterase shows a pattern of expression within brain that is distinct from the long PDE4A5 and short PDE4A1 isoforms. *Cell Signal*, **13,** 911-8.

MCPHEE, I., POOLEY, L., LOBBAN, M., BOLGER, G. & HOUSLAY, M.D. (1995). Identification, characterization and regional distribution in brain of RPDE-6 (RNPDE4A5), a novel splice variant of the PDE4A cyclic AMP phosphodiesterase family. *Biochem J*, **310 (Pt 3),** 965-74.

MCPHEE, I., YARWOOD, S.J., SCOTLAND, G., HUSTON, E., BEARD, M.B., ROSS, A.H., HOUSLAY, E.S. & HOUSLAY, M.D. (1999). Association with the SRC family tyrosyl kinase LYN triggers a conformational change in the catalytic region of human cAMP-specific phosphodiesterase HSPDE4A4B. Consequences for rolipram inhibition. *J Biol Chem*, **274,** 11796-810.

MEACCI, E., TAIRA, M., MOOS, M., JR., SMITH, C.J., MOVSESIAN, M.A., DEGERMAN, E., BELFRAGE, P. & MANGANIELLO, V. (1992). Molecular cloning and expression of human myocardial cGMP-inhibited cAMP phosphodiesterase. *Proc Natl Acad Sci U S A*, **89,** 3721-5.

MEHATS, C., JIN, S.L., WAHLSTROM, J., LAW, E., UMETSU, D.T. & CONTI, M. (2003). PDE4D plays a critical role in the control of airway smooth muscle contraction. *Faseb J*, **17,** 1831-41.

MENG, W., SWENSON, L.L., FITZGIBBON, M.J., HAYAKAWA, K., TER HAAR, E., BEHRENS, A.E., FULGHUM, J.R. & LIPPKE, J.A. (2002). Structure of mitogen-activated protein kinase-activated protein (MAPKAP) kinase 2 suggests a bifunctional switch that couples kinase activation with nuclear export. *J Biol Chem*, **277,** 37401-5.

MICHAELI, T., BLOOM, T.J., MARTINS, T., LOUGHNEY, K., FERGUSON, K.,

RIGGS, M., RODGERS, L., BEAVO, J.A. & WIGLER, M. (1993). Isolation and characterization of a previously undetected human cAMP phosphodiesterase by complementation of cAMP phosphodiesterase-deficient Saccharomyces cerevisiae. *J Biol Chem*, **268,** 12925-32.

MICHIE, A.M., LOBBAN, M., MULLER, T., HARNETT, M.M. & HOUSLAY, M.D. (1996). Rapid regulation of PDE-2 and PDE-4 cyclic AMP phosphodiesterase activity following ligation of the T cell antigen receptor on thymocytes: analysis using the selective inhibitors erythro-9-(2-hydroxy-3-nonyl)-adenine (EHNA) and rolipram. *Cell Signal*, **8,** 97-110.

MIKI, N., BARABAN, J.M., KEIRNS, J.J., BOYCE, J.J. & BITENSKY, M.W. (1975). Purification and properties of the light-activated cyclic nucleotide phosphodiesterase of rod outer segments. *J Biol Chem*, **250,** 6320-7.

MILATOVICH, A., BOLGER, G., MICHAELI, T. & FRANCKE, U. (1994). Chromosome localizations of genes for five cAMP-specific phosphodiesterases in man and mouse. *Somat Cell Mol Genet*, **20,** 75-86.

MILLAR, J.K., MACKIE, S., CLAPCOTE, S.J., MURDOCH, H., PICKARD, B.S., CHRISTIE, S., MUIR, W.J., BLACKWOOD, D.H., RODER, J.C., HOUSLAY, M.D. & PORTEOUS, D.J. (2007). Disrupted in schizophrenia 1 and phosphodiesterase 4B: towards an understanding of psychiatric illness. *J Physiol*, **584,** 401-5.

MILLAR, J.K., PICKARD, B.S., MACKIE, S., JAMES, R., CHRISTIE, S., BUCHANAN, S.R., MALLOY, M.P., CHUBB, J.E., HUSTON, E., BAILLIE, G.S., THOMSON, P.A., HILL, E.V., BRANDON, N.J., RAIN, J.C., CAMARGO, L.M., WHITING, P.J., HOUSLAY, M.D., BLACKWOOD, D.H.,

MUIR, W.J. & PORTEOUS, D.J. (2005). DISC1 and PDE4B are interacting genetic factors in schizophrenia that regulate cAMP signaling. *Science*, **310,** 1187-91.

MILLER, C.L., OIKAWA, M., CAI, Y., WOJTOVICH, A.P., NAGEL, D.J., XU, X., XU, H., FLORIO, V., RYBALKIN, S.D., BEAVO, J.A., CHEN, Y.F., LI, J.D., BLAXALL, B.C., ABE, J. & YAN, C. (2009). Role of Ca2+/calmodulin-stimulated cyclic nucleotide phosphodiesterase 1 in mediating cardiomyocyte hypertrophy. *Circ Res*, **105,** 956-64.

MILLIGAN, G. (2004). G protein-coupled receptor dimerization: function and ligand pharmacology. *Mol Pharmacol*, **66,** 1-7.

MONGILLO, M., MCSORLEY, T., EVELLIN, S., SOOD, A., LISSANDRON, V., TERRIN, A., HUSTON, E., HANNAWACKER, A., LOHSE, M.J., POZZAN, T., HOUSLAY, M.D. & ZACCOLO, M. (2004). Fluorescence resonance energy transfer-based analysis of cAMP dynamics in live neonatal rat cardiac myocytes reveals distinct functions of compartmentalized phosphodiesterases. *Circ Res*, **95,** 67-75.

MONGILLO, M., TOCCHETTI, C.G., TERRIN, A., LISSANDRON, V., CHEUNG, Y.F., DOSTMANN, W.R., POZZAN, T., KASS, D.A., PAOLOCCI, N., HOUSLAY, M.D. & ZACCOLO, M. (2006). Compartmentalized phosphodiesterase-2 activity blunts beta-adrenergic cardiac inotropy via an NO/cGMP-dependent pathway. *Circ Res*, **98,** 226-34.

MORIN, F., LUGNIER, C., KAMENI, J. & VOISIN, P. (2001). Expression and role of phosphodiesterase 6 in the chicken pineal gland. *J Neurochem*, **78,** 88-99.

MUKAI, J., HACHIYA, T., SHOJI-HOSHINO, S., KIMURA, M.T., NADANO, D.,

SUVANTO, P., HANAOKA, T., LI, Y., IRIE, S., GREENE, L.A. & SATO, T.A. (2000). NADE, a p75NTR-associated cell death executor, is involved in signal transduction mediated by the common neurotrophin receptor p75NTR. *J Biol Chem*, **275,** 17566-70.

MURAGAKI, Y., TIMOTHY, N., LEIGHT, S., HEMPSTEAD, B.L., CHAO, M.V., TROJANOWSKI, J.Q. & LEE, V.M. (1995). Expression of trk receptors in the developing and adult human central and peripheral nervous system. *J Comp Neurol*, **356,** 387-97.

MURDOCH, H., MACKIE, S., COLLINS, D.M., HILL, E.V., BOLGER, G.B., KLUSSMANN, E., PORTEOUS, D.J., MILLAR, J.K. & HOUSLAY, M.D. (2007). Isoform-selective susceptibility of DISC1/phosphodiesterase-4 complexes to dissociation by elevated intracellular cAMP levels. *J Neurosci*, **27,** 9513-24.

NAKSTAD, B., LYBERG, T., SKJONSBERG, O.H. & BOYE, N.P. (1990). Local activation of the coagulation and fibrinolysis systems in lung disease. *Thromb Res*, **57,** 827-38.

NASSENSTEIN, C., DAWBARN, D., POLLOCK, K., ALLEN, S.J., ERPENBECK, V.J., SPIES, E., KRUG, N. & BRAUN, A. (2006). Pulmonary distribution, regulation, and functional role of Trk receptors in a murine model of asthma. *J Allergy Clin Immunol*, **118,** 597-605.

NI, H., WANG, X.S., DIENER, K. & YAO, Z. (1998). MAPKAPK5, a novel mitogen-activated protein kinase (MAPK)-activated protein kinase, is a substrate of the extracellular-regulated kinase (ERK) and p38 kinase. *Biochem Biophys Res Commun*, **243,** 492-6.

NIMNUAL, A.S., YATSULA, B.A. & BAR-SAGI, D. (1998). Coupling of Ras and Rac guanosine triphosphatases through the Ras exchanger Sos. *Science*, **279,** 560-3.

NISHITOH, H., SAITOH, M., MOCHIDA, Y., TAKEDA, K., NAKANO, H., ROTHE, M., MIYAZONO, K. & ICHIJO, H. (1998). ASK1 is essential for JNK/SAPK activation by TRAF2. *Mol Cell*, **2,** 389-95.

NONOMURA, T., KUBO, T., OKA, T., SHIMOKE, K., YAMADA, M., ENOKIDO, Y. & HATANAKA, H. (1996). Signaling pathways and survival effects of BDNF and NT-3 on cultured cerebellar granule cells. *Brain Res Dev Brain Res*, **97,** 42-50.

O'CONNELL, J.C., MCCALLUM, J.F., MCPHEE, I., WAKEFIELD, J., HOUSLAY, E.S., WISHART, W., BOLGER, G., FRAME, M. & HOUSLAY, M.D. (1996). The SH3 domain of Src tyrosyl protein kinase interacts with the N-terminal splice region of the PDE4A cAMP-specific phosphodiesterase RPDE-6 (RNPDE4A5). *Biochem J*, **318 (Pt 1),** 255-61.

O'CONNOR, V., GENIN, A., DAVIS, S., KARISHMA, K.K., DOYERE, V., DE ZEEUW, C.I., SANGER, G., HUNT, S.P., RICHTER-LEVIN, G., MALLET, J., LAROCHE, S., BLISS, T.V. & FRENCH, P.J. (2004). Differential amplification of intron-containing transcripts reveals long term potentiation-associated up-regulation of specific Pde10A phosphodiesterase splice variants. *J Biol Chem*, **279,** 15841-9.

OHMICHI, M., DECKER, S.J. & SALTIEL, A.R. (1992). Nerve growth factor stimulates the tyrosine phosphorylation of a 38-kDa protein that specifically associates with the src homology domain of phospholipase C-gamma 1. *J Biol Chem*, **267,** 21601-6.

OKI, N., TAKAHASHI, S.I., HIDAKA, H. & CONTI, M. (2000). Short term feedback regulation of cAMP in FRTL-5 thyroid cells. Role of PDE4D3

phosphodiesterase activation. *J Biol Chem*, **275,** 10831-7.

OLGART, C. & FROSSARD, N. (2001). Human lung fibroblasts secrete nerve growth factor: effect of inflammatory cytokines and glucocorticoids. *Eur Respir J*, **18,** 115-21.

PAGE, C.P. (1999). Recent advances in our understanding of the use of theophylline in the treatment of asthma. *J Clin Pharmacol*, **39,** 237-40.

PAGES, L., GAVALDA, A. & LEHNER, M.D. (2009). PDE4 inhibitors: a review of current developments (2005 - 2009). *Expert Opin Ther Pat*, **19,** 1501-19.

PATAPOUTIAN, A. & REICHARDT, L.F. (2001). Trk receptors: mediators of neurotrophin action. *Curr Opin Neurobiol*, **11,** 272-80.

PAWSON, T. (1995). Protein-tyrosine kinases. Getting down to specifics. *Nature*, **373,** 477-8.

PEARSON, G., ROBINSON, F., BEERS GIBSON, T., XU, B.E., KARANDIKAR, M., BERMAN, K. & COBB, M.H. (2001). Mitogen-activated protein (MAP) kinase pathways: regulation and physiological functions. *Endocr Rev*, **22,** 153-83.

PEREZ-TORRES, S., CORTES, R., TOLNAY, M., PROBST, A., PALACIOS, J.M. & MENGOD, G. (2003). Alterations on phosphodiesterase type 7 and 8 isozyme mRNA expression in Alzheimer's disease brains examined by in situ hybridization. *Exp Neurol*, **182,** 322-34.

PEREZ-TORRES, S., MIRO, X., PALACIOS, J.M., CORTES, R., PUIGDOMENECH, P. & MENGOD, G. (2000). Phosphodiesterase type 4 isozymes expression in human brain examined by in situ hybridization histochemistry and[3H]rolipram binding autoradiography. Comparison with monkey and rat brain. *J Chem*

Neuroanat, **20,** 349-74.

PERRY, S.J., BAILLIE, G.S., KOHOUT, T.A., MCPHEE, I., MAGIERA, M.M., ANG, K.L., MILLER, W.E., MCLEAN, A.J., CONTI, M., HOUSLAY, M.D. & LEFKOWITZ, R.J. (2002). Targeting of cyclic AMP degradation to beta 2-adrenergic receptors by beta-arrestins. *Science*, **298,** 834-6.

POMERANTZ, B.J., REZNIKOV, L.L., HARKEN, A.H. & DINARELLO, C.A. (2001). Inhibition of caspase 1 reduces human myocardial ischemic dysfunction via inhibition of IL-18 and IL-1beta. *Proc Natl Acad Sci U S A*, **98,** 2871-6.

PONZETTO, C., BARDELLI, A., ZHEN, Z., MAINA, F., DALLA ZONCA, P., GIORDANO, S., GRAZIANI, A., PANAYOTOU, G. & COMOGLIO, P.M. (1994). A multifunctional docking site mediates signaling and transformation by the hepatocyte growth factor/scatter factor receptor family. *Cell*, **77,** 261-71.

PUGH, E.N., JR. & LAMB, T.D. (1990). Cyclic GMP and calcium: the internal messengers of excitation and adaptation in vertebrate photoreceptors. *Vision Res*, **30,** 1923-48.

PULIDO, R., ZUNIGA, A. & ULLRICH, A. (1998). PTP-SL and STEP protein tyrosine phosphatases regulate the activation of the extracellular signal-regulated kinases ERK1 and ERK2 by association through a kinase interaction motif. *Embo J*, **17,** 7337-50.

QIAO, J., HUANG, F. & LUM, H. (2003). PKA inhibits RhoA activation: a protection mechanism against endothelial barrier dysfunction. *Am J Physiol Lung Cell Mol Physiol*, **284,** L972-80.

RABE, K.F. Roflumilast for the treatment of chronic obstructive pulmonary disease. *Expert Rev Respir Med*.

RABE, K.F., HURD, S., ANZUETO, A., BARNES, P.J., BUIST, S.A., CALVERLEY, P., FUKUCHI, Y., JENKINS, C., RODRIGUEZ-ROISIN, R., VAN WEEL, C. & ZIELINSKI, J. (2007). Global strategy for the diagnosis, management, and prevention of chronic obstructive pulmonary disease: GOLD executive summary. *Am J Respir Crit Care Med*, **176,** 532-55.

RATTENHOLL, A., RUOPPOLO, M., FLAGIELLO, A., MONTI, M., VINCI, F., MARINO, G., LILIE, H., SCHWARZ, E. & RUDOLPH, R. (2001). Pro-sequence assisted folding and disulfide bond formation of human nerve growth factor. *J Mol Biol*, **305,** 523-33.

REINEKE, U., VOLKMER-ENGERT, R. & SCHNEIDER-MERGENER, J. (2001). Applications of peptide arrays prepared by the SPOT-technology. *Curr Opin Biotechnol*, **12,** 59-64.

REINHARDT, H.C. & YAFFE, M.B. (2009). Kinases that control the cell cycle in response to DNA damage: Chk1, Chk2, and MK2. *Curr Opin Cell Biol*, **21,** 245-55.

RENA, G., BEGG, F., ROSS, A., MACKENZIE, C., MCPHEE, I., CAMPBELL, L., HUSTON, E., SULLIVAN, M. & HOUSLAY, M.D. (2001). Molecular cloning, genomic positioning, promoter identification, and characterization of the novel cyclic amp-specific phosphodiesterase PDE4A10. *Mol Pharmacol*, **59,** 996-1011.

RENELAND, R.H., MAH, S., KAMMERER, S., HOYAL, C.R., MARNELLOS, G., WILSON, S.G., SAMBROOK, P.N., SPECTOR, T.D., NELSON, M.R. & BRAUN, A. (2005). Association between a variation in the phosphodiesterase

4D gene and bone mineral density. *BMC Med Genet*, **6,** 9.

RENNARD, S., KNOBIL, K., RABE, K.F., MORRIS, A., SCHACHTER, N., LOCANTORE, N., CANONICA, W.G., ZHU, Y. & BARNHART, F. (2008). The efficacy and safety of cilomilast in COPD. *Drugs*, **68 Suppl 2,** 3-57.

RENNARD, S.I., SCHACHTER, N., STREK, M., RICKARD, K. & AMIT, O. (2006). Cilomilast for COPD: results of a 6-month, placebo-controlled study of a potent, selective inhibitor of phosphodiesterase 4. *Chest*, **129,** 56-66.

RENTERO, C. & PUIGDOMENECH, P. (2006). Specific use of start codons and cellular localization of splice variants of human phosphodiesterase 9A gene. *BMC Mol Biol*, **7,** 39.

RENZ, H., KERZEL, S. & NOCKHER, W.A. (2004). The role of neurotrophins in bronchial asthma: contribution of the pan-neurotrophin receptor p75. *Prog Brain Res*, **146,** 325-33.

REYES-IRISARRI, E., MARKERINK-VAN ITTERSUM, M., MENGOD, G. & DE VENTE, J. (2007). Expression of the cGMP-specific phosphodiesterases 2 and 9 in normal and Alzheimer's disease human brains. *Eur J Neurosci*, **25,** 3332-8.

RIISE, G.C., LARSSON, S., LOWHAGEN, O. & ANDERSSON, B.A. (1995). Circulating leukocyte adhesion molecules in stable asthma and nonobstructive chronic bronchitis. *Allergy*, **50,** 693-8.

RODRIGUEZ-TEBAR, A., DECHANT, G. & BARDE, Y.A. (1990). Binding of brain-derived neurotrophic factor to the nerve growth factor receptor. *Neuron*, **4,** 487-92.

ROGALLA, T., EHRNSPERGER, M., PREVILLE, X., KOTLYAROV, A., LUTSCH, G., DUCASSE, C., PAUL, C., WIESKE, M., ARRIGO, A.P., BUCHNER, J. & GAESTEL, M. (1999). Regulation of Hsp27 oligomerization, chaperone function, and protective activity against oxidative stress/tumor necrosis factor alpha by phosphorylation. *J Biol Chem*, **274,** 18947-56.

ROUSSEAU, S., PEGGIE, M., CAMPBELL, D.G., NEBREDA, A.R. & COHEN, P. (2005). Nogo-B is a new physiological substrate for MAPKAP-K2. *Biochem J*, **391,** 433-40.

ROUX, P.P. & BARKER, P.A. (2002). Neurotrophin signaling through the p75 neurotrophin receptor. *Prog Neurobiol*, **67,** 203-33.

ROUX, P.P., BHAKAR, A.L., KENNEDY, T.E. & BARKER, P.A. (2001). The p75 neurotrophin receptor activates Akt (protein kinase B) through a phosphatidylinositol 3-kinase-dependent pathway. *J Biol Chem*, **276,** 23097-104.

ROUX, P.P. & BLENIS, J. (2004). ERK and p38 MAPK-activated protein kinases: a family of protein kinases with diverse biological functions. *Microbiol Mol Biol Rev*, **68,** 320-44.

RUSSO, C. & POLOSA, R. (2005). TNF-alpha as a promising therapeutic target in chronic asthma: a lesson from rheumatoid arthritis. *Clin Sci (Lond)*, **109,** 135-42.

RUTTEN, K., BASILE, J.L., PRICKAERTS, J., BLOKLAND, A. & VIVIAN, J.A. (2008). Selective PDE inhibitors rolipram and sildenafil improve object retrieval performance in adult cynomolgus macaques. *Psychopharmacology (Berl)*, **196,** 643-8.

SACHS, B.D., BAILLIE, G.S., MCCALL, J.R., PASSINO, M.A., SCHACHTRUP, C.,

WALLACE, D.A., DUNLOP, A.J., MACKENZIE, K.F., KLUSSMANN, E., LYNCH, M.J., SIKORSKI, S.L., NURIEL, T., TSIGELNY, I., ZHANG, J., HOUSLAY, M.D., CHAO, M.V. & AKASSOGLOU, K. (2007). p75 neurotrophin receptor regulates tissue fibrosis through inhibition of plasminogen activation via a PDE4/cAMP/PKA pathway. *J Cell Biol*, **177,** 1119-32.

SAETTA, M., DI STEFANO, A., MAESTRELLI, P., FERRARESSO, A., DRIGO, R., POTENA, A., CIACCIA, A. & FABBRI, L.M. (1993). Activated T-lymphocytes and macrophages in bronchial mucosa of subjects with chronic bronchitis. *Am Rev Respir Dis*, **147,** 301-6.

SCHAFER, P.H., PARTON, A., GANDHI, A.K., CAPONE, L., ADAMS, M., WU, L., BARTLETT, J.B., LOVELAND, M.A., GILHAR, A., CHEUNG, Y.F., BAILLIE, G.S., HOUSLAY, M.D., MAN, H.W., MULLER, G.W. & STIRLING, D.I. Apremilast, a cAMP phosphodiesterase-4 inhibitor, demonstrates anti-inflammatory activity in vitro and in a model of psoriasis. *Br J Pharmacol*, **159,** 842-55.

SCHIEVEN, G.L. (2005). The biology of p38 kinase: a central role in inflammation. *Curr Top Med Chem*, **5,** 921-8.

SCHINDLER, J.F., MONAHAN, J.B. & SMITH, W.G. (2007). p38 pathway kinases as anti-inflammatory drug targets. *J Dent Res*, **86,** 800-11.

SCHREIBER, S., FEAGAN, B., D'HAENS, G., COLOMBEL, J.F., GEBOES, K., YURCOV, M., ISAKOV, V., GOLOVENKO, O., BERNSTEIN, C.N., LUDWIG, D., WINTER, T., MEIER, U., YONG, C. & STEFFGEN, J. (2006). Oral p38 mitogen-activated protein kinase inhibition with BIRB 796 for active

Crohn's disease: a randomized, double-blind, placebo-controlled trial. *Clin Gastroenterol Hepatol*, **4,** 325-34.

SCOTT, J.D. & PAWSON, T. (2009). Cell signaling in space and time: where proteins come together and when they're apart. *Science*, **326,** 1220-4.

SENALDI, G., VARNUM, B.C., SARMIENTO, U., STARNES, C., LILE, J., SCULLY, S., GUO, J., ELLIOTT, G., MCNINCH, J., SHAKLEE, C.L., FREEMAN, D., MANU, F., SIMONET, W.S., BOONE, T. & CHANG, M.S. (1999). Novel neurotrophin-1/B cell-stimulating factor-3: a cytokine of the IL-6 family. *Proc Natl Acad Sci U S A*, **96,** 11458-63.

SERRELS, B., SANDILANDS, E., SERRELS, A., BAILLIE, G., HOUSLAY, M.D., BRUNTON, V.G., CANEL, M., MACHESKY, L.M., ANDERSON, K.I. & FRAME, M.C. A complex between FAK, RACK1, and PDE4D5 controls spreading initiation and cancer cell polarity. *Curr Biol*, **20,** 1086-92.

SETTE, C. & CONTI, M. (1996). Phosphorylation and activation of a cAMP-specific phosphodiesterase by the cAMP-dependent protein kinase. Involvement of serine 54 in the enzyme activation. *J Biol Chem*, **271,** 16526-34.

SETTE, C., VICINI, E. & CONTI, M. (1994). The ratPDE3/IVd phosphodiesterase gene codes for multiple proteins differentially activated by cAMP-dependent protein kinase. *J Biol Chem*, **269,** 18271-4.

SHARMA, R.K., SMITH, J.R. & MOORE, G.J. (1991). Inhibition of bovine brain calmodulin-dependent cGMP phosphodiesterase by peptide and non-peptide angiotensin receptor ligands. *Biochem Biophys Res Commun*, **179,** 85-9.

SHARMA, R.K. & WANG, J.H. (1986). Regulation of cAMP concentration by calmodulin-dependent cyclic nucleotide phosphodiesterase. *Biochem Cell Biol*, **64,** 1072-80.

SHARROCKS, A.D., YANG, S.H. & GALANIS, A. (2000). Docking domains and substrate-specificity determination for MAP kinases. *Trends Biochem Sci*, **25,** 448-53.

SHEPHERD, M., MCSORLEY, T., OLSEN, A.E., JOHNSTON, L.A., THOMSON, N.C., BAILLIE, G.S., HOUSLAY, M.D. & BOLGER, G.B. (2003). Molecular cloning and subcellular distribution of the novel PDE4B4 cAMP-specific phosphodiesterase isoform. *Biochem J*, **370,** 429-38.

SILVERMAN, R.E. & BRADSHAW, R.A. (1982). Nerve growth factor: subunit interactions in the mouse submaxillary gland 7S complex. *J Neurosci Res*, **8,** 127-36.

SIMON, M.I., STRATHMANN, M.P. & GAUTAM, N. (1991). Diversity of G proteins in signal transduction. *Science*, **252,** 802-8.

SINGH, T.P. Clinical use of sildenafil in pulmonary artery hypertension. *Expert Rev Respir Med*, **4,** 13-9.

SIUCIAK, J.A., MCCARTHY, S.A., CHAPIN, D.S. & MARTIN, A.N. (2008). Behavioral and neurochemical characterization of mice deficient in the phosphodiesterase-4B (PDE4B) enzyme. *Psychopharmacology (Berl)*, **197,** 115-26.

SIUCIAK, J.A., MCCARTHY, S.A., CHAPIN, D.S., MARTIN, A.N., HARMS, J.F. & SCHMIDT, C.J. (2008). Behavioral characterization of mice deficient in the phosphodiesterase-10A (PDE10A) enzyme on a C57/Bl6N congenic background. *Neuropharmacology*, **54,** 417-27.

SMITH, J.A., POTEET-SMITH, C.E., MALARKEY, K. & STURGILL, T.W. (1999). Identification of an extracellular signal-regulated kinase (ERK) docking site in ribosomal S6 kinase, a sequence critical for activation by ERK in vivo. *J Biol Chem*, **274,** 2893-8.

SMITH, S.J., BROOKES-FAZAKERLEY, S., DONNELLY, L.E., BARNES, P.J., BARNETTE, M.S. & GIEMBYCZ, M.A. (2003). Ubiquitous expression of phosphodiesterase 7A in human proinflammatory and immune cells. *Am J Physiol Lung Cell Mol Physiol*, **284,** L279-89.

SODERLING, S.H., BAYUGA, S.J. & BEAVO, J.A. (1998). Cloning and characterization of a cAMP-specific cyclic nucleotide phosphodiesterase. *Proc Natl Acad Sci U S A*, **95,** 8991-6.

SPINA, D. (2008). PDE4 inhibitors: current status. *Br J Pharmacol*, **155,** 308-15.

STARK, B., RISLING, M. & CARLSTEDT, T. (2001). Distribution of the neurotrophin receptors p75 and trkB in peripheral mechanoreceptors; observations on changes after injury. *Exp Brain Res*, **136,** 101-7.

STEPHENS, R.M., LOEB, D.M., COPELAND, T.D., PAWSON, T., GREENE, L.A. & KAPLAN, D.R. (1994). Trk receptors use redundant signal transduction pathways involving SHC and PLC-gamma 1 to mediate NGF responses. *Neuron*, **12,** 691-705.

STOKOE, D., CAMPBELL, D.G., NAKIELNY, S., HIDAKA, H., LEEVERS, S.J., MARSHALL, C. & COHEN, P. (1992). MAPKAP kinase-2; a novel protein kinase activated by mitogen-activated protein kinase. *Embo J*, **11,** 3985-94.

STOKOE, D., CAUDWELL, B., COHEN, P.T. & COHEN, P. (1993). The substrate

specificity and structure of mitogen-activated protein (MAP) kinase-activated protein kinase-2. *Biochem J*, **296 (Pt 3),** 843-9.

STRAUSFELD, U., LABBE, J.C., FESQUET, D., CAVADORE, J.C., PICARD, A., SADHU, K., RUSSELL, P. & DOREE, M. (1991). Dephosphorylation and activation of a p34cdc2/cyclin B complex in vitro by human CDC25 protein. *Nature*, **351,** 242-5.

STROHMAIER, C., CARTER, B.D., URFER, R., BARDE, Y.A. & DECHANT, G. (1996). A splice variant of the neurotrophin receptor trkB with increased specificity for brain-derived neurotrophic factor. *Embo J*, **15,** 3332-7.

SULLIVAN, M., OLSEN, A.S. & HOUSLAY, M.D. (1999). Genomic organisation of the human cyclic AMP-specific phosphodiesterase PDE4C gene and its chromosomal localisation to 19p13.1, between RAB3A and JUND. *Cell Signal*, **11,** 735-42.

SUN, P., YOSHIZUKA, N., NEW, L., MOSER, B.A., LI, Y., LIAO, R., XIE, C., CHEN, J., DENG, Q., YAMOUT, M., DONG, M.Q., FRANGOU, C.G., YATES, J.R., 3RD, WRIGHT, P.E. & HAN, J. (2007). PRAK is essential for ras-induced senescence and tumor suppression. *Cell*, **128,** 295-308.

SUTTER, A., RIOPELLE, R.J., HARRIS-WARRICK, R.M. & SHOOTER, E.M. (1979). The heterogeneity of nerve growth factor receptors. *Prog Clin Biol Res*, **31,** 659-67.

SWINNEN, J.V., JOSEPH, D.R. & CONTI, M. (1989). The mRNA encoding a high-affinity cAMP phosphodiesterase is regulated by hormones and cAMP. *Proc Natl Acad Sci U S A*, **86,** 8197-201.

SZPIRER, C., SZPIRER, J., RIVIERE, M., SWINNEN, J., VICINI, E. & CONTI, M. (1995). Chromosomal localization of the human and rat genes (PDE4D and

PDE4B) encoding the cAMP-specific phosphodiesterases 3 and 4. *Cytogenet Cell Genet*, **69,** 11-4.

TAKEDA, R., SUZUKI, E., SATONAKA, H., OBA, S., NISHIMATSU, H., OMATA, M., FUJITA, T., NAGAI, R. & HIRATA, Y. (2005). Blockade of endogenous cytokines mitigates neointimal formation in obese Zucker rats. *Circulation*, **111,** 1398-406.

TAN, Y., ROUSE, J., ZHANG, A., CARIATI, S., COHEN, P. & COMB, M.J. (1996). FGF and stress regulate CREB and ATF-1 via a pathway involving p38 MAP kinase and MAPKAP kinase-2. *Embo J*, **15,** 4629-42.

TASKEN, K. & AANDAHL, E.M. (2004). Localized effects of cAMP mediated by distinct routes of protein kinase A. *Physiol Rev*, **84,** 137-67.

TERMAN, J.R. & KOLODKIN, A.L. (2004). Nervy links protein kinase a to plexin-mediated semaphorin repulsion. *Science*, **303,** 1204-7.

TERRY, R., CHEUNG, Y.F., PRAESTEGAARD, M., BAILLIE, G.S., HUSTON, E., GALL, I., ADAMS, D.R. & HOUSLAY, M.D. (2003). Occupancy of the catalytic site of the PDE4A4 cyclic AMP phosphodiesterase by rolipram triggers the dynamic redistribution of this specific isoform in living cells through a cyclic AMP independent process. *Cell Signal*, **15,** 955-71.

THOMPSON, P.E., MANGANIELLO, V. & DEGERMAN, E. (2007). Re-discovering PDE3 inhibitors--new opportunities for a long neglected target. *Curr Top Med Chem*, **7,** 421-36.

THOMPSON, W.J. & APPLEMAN, M.M. (1971). Cyclic nucleotide phosphodiesterase and cyclic AMP. *Ann N Y Acad Sci*, **185,** 36-41.

TOKUOKA, S., TAKAHASHI, Y., MASUDA, T., TANAKA, H., FURUKAWA, S. & NAGAI, H. (2001). Disruption of antigen-induced airway inflammation and airway hyper-responsiveness in low affinity neurotrophin receptor p75 gene deficient mice. *Br J Pharmacol*, **134,** 1580-6.

TORCIA, M., BRACCI-LAUDIERO, L., LUCIBELLO, M., NENCIONI, L., LABARDI, D., RUBARTELLI, A., COZZOLINO, F., ALOE, L. & GARACI, E. (1996). Nerve growth factor is an autocrine survival factor for memory B lymphocytes. *Cell*, **85,** 345-56.

UHLIK, M.T., ABELL, A.N., JOHNSON, N.L., SUN, W., CUEVAS, B.D., LOBEL-RICE, K.E., HORNE, E.A., DELL'ACQUA, M.L. & JOHNSON, G.L. (2003). Rac-MEKK3-MKK3 scaffolding for p38 MAPK activation during hyperosmotic shock. *Nat Cell Biol*, **5,** 1104-10.

VAN DER STAAY, F.J., RUTTEN, K., BARFACKER, L., DEVRY, J., ERB, C., HECKROTH, H., KARTHAUS, D., TERSTEEGEN, A., VAN KAMPEN, M., BLOKLAND, A., PRICKAERTS, J., REYMANN, K.G., SCHRODER, U.H. & HENDRIX, M. (2008). The novel selective PDE9 inhibitor BAY 73-6691 improves learning and memory in rodents. *Neuropharmacology*, **55,** 908-18.

VASSALLO, R. & RYU, J.H. (2008). Tobacco smoke-related diffuse lung diseases. *Semin Respir Crit Care Med*, **29,** 643-50.

VECSEY, C.G., BAILLIE, G.S., JAGANATH, D., HAVEKES, R., DANIELS, A., WIMMER, M., HUANG, T., BROWN, K.M., LI, X.Y., DESCALZI, G., KIM, S.S., CHEN, T., SHANG, Y.Z., ZHUO, M., HOUSLAY, M.D. & ABEL, T. (2009). Sleep deprivation impairs cAMP signalling in the hippocampus. *Nature*, **461,** 1122-5.

VICINI, E. & CONTI, M. (1997). Characterization of an intronic promoter of a cyclic

adenosine 3',5'-monophosphate (cAMP)-specific phosphodiesterase gene that confers hormone and cAMP inducibility. *Mol Endocrinol*, **11,** 839-50.

VIDELA, S., VILASECA, J., MEDINA, C., MOURELLE, M., GUARNER, F., SALAS, A. & MALAGELADA, J.R. (2006). Selective inhibition of phosphodiesterase-4 ameliorates chronic colitis and prevents intestinal fibrosis. *J Pharmacol Exp Ther*, **316,** 940-5.

VONCKEN, J.W., NIESSEN, H., NEUFELD, B., RENNEFAHRT, U., DAHLMANS, V., KUBBEN, N., HOLZER, B., LUDWIG, S. & RAPP, U.R. (2005). MAPKAP kinase 3pK phosphorylates and regulates chromatin association of the polycomb group protein Bmi1. *J Biol Chem*, **280,** 5178-87.

WACHTEL, H. (1982). Characteristic behavioural alterations in rats induced by rolipram and other selective adenosine cyclic 3', 5'-monophosphate phosphodiesterase inhibitors. *Psychopharmacology (Berl)*, **77,** 309-16.

WAJANT, H. & SCHEURICH, P. (2001). Tumor necrosis factor receptor-associated factor (TRAF) 2 and its role in TNF signaling. *Int J Biochem Cell Biol*, **33,** 19-32.

WALL, E.A., ZAVZAVADJIAN, J.R., CHANG, M.S., RANDHAWA, B., ZHU, X., HSUEH, R.C., LIU, J., DRIVER, A., BAO, X.R., STERNWEIS, P.C., SIMON, M.I. & FRASER, I.D. (2009). Suppression of LPS-induced TNF-alpha production in macrophages by cAMP is mediated by PKA-AKAP95-p105. *Sci Signal*, **2,** ra28.

WALLACE, D.A., JOHNSTON, L.A., HUSTON, E., MACMASTER, D., HOUSLAY, T.M., CHEUNG, Y.F., CAMPBELL, L., MILLEN, J.E., SMITH, R.A., GALL, I., KNOWLES, R.G., SULLIVAN, M. & HOUSLAY, M.D. (2005). Identification and characterization of PDE4A11, a novel, widely expressed long

isoform encoded by the human PDE4A cAMP phosphodiesterase gene. *Mol Pharmacol*, **67,** 1920-34.

WANG, H., ROBINSON, H. & KE, H. (2007). The molecular basis for different recognition of substrates by phosphodiesterase families 4 and 10. *J Mol Biol*, **371,** 302-7.

WANG, H., YAN, Z., YANG, S., CAI, J., ROBINSON, H. & KE, H. (2008). Kinetic and structural studies of phosphodiesterase-8A and implication on the inhibitor selectivity. *Biochemistry*, **47,** 12760-8.

WANG, K.C., KIM, J.A., SIVASANKARAN, R., SEGAL, R. & HE, Z. (2002). P75 interacts with the Nogo receptor as a co-receptor for Nogo, MAG and OMgp. *Nature*, **420,** 74-8.

WANG, P., WU, P., EGAN, R.W. & BILLAH, M.M. (2001). Human phosphodiesterase 8A splice variants: cloning, gene organization, and tissue distribution. *Gene*, **280,** 183-94.

WASKIEWICZ, A.J., FLYNN, A., PROUD, C.G. & COOPER, J.A. (1997). Mitogen-activated protein kinases activate the serine/threonine kinases Mnk1 and Mnk2. *Embo J*, **16,** 1909-20.

WAYMAN, C., PHILLIPS, S., LUNNY, C., WEBB, T., FAWCETT, L., BAXENDALE, R. & BURGESS, G. (2005). Phosphodiesterase 11 (PDE11) regulation of spermatozoa physiology. *Int J Impot Res*, **17,** 216-23.

WEBER, H.O., LUDWIG, R.L., MORRISON, D., KOTLYAROV, A., GAESTEL, M. & VOUSDEN, K.H. (2005). HDM2 phosphorylation by MAPKAP kinase 2. *Oncogene*, **24,** 1965-72.

WECHSLER, J., CHOI, Y.H., KRALL, J., AHMAD, F., MANGANIELLO, V.C. & MOVSESIAN, M.A. (2002). Isoforms of cyclic nucleotide phosphodiesterase PDE3A in cardiac myocytes. *J Biol Chem*, **277,** 38072-8.

WEHRMAN, T., HE, X., RAAB, B., DUKIPATTI, A., BLAU, H. & GARCIA, K.C. (2007). Structural and mechanistic insights into nerve growth factor interactions with the TrkA and p75 receptors. *Neuron*, **53,** 25-38.

WEIER, H.U., RHEIN, A.P., SHADRAVAN, F., COLLINS, C. & POLIKOFF, D. (1995). Rapid physical mapping of the human trk protooncogene (NTRK1) to human chromosome 1q21-q22 by P1 clone selection, fluorescence in situ hybridization (FISH), and computer-assisted microscopy. *Genomics*, **26,** 390-3.

WIESMANN, C. & DE VOS, A.M. (2001). Nerve growth factor: structure and function. *Cell Mol Life Sci*, **58,** 748-59.

WINDISCH, J.M., MARKSTEINER, R. & SCHNEIDER, R. (1995). Nerve growth factor binding site on TrkA mapped to a single 24-amino acid leucine-rich motif. *J Biol Chem*, **270,** 28133-8.

WOLLBERG, P., LENNARTSSON, J., GOTTFRIDSSON, E., YOSHIMURA, A. & RONNSTRAND, L. (2003). The adapter protein APS associates with the multifunctional docking sites Tyr-568 and Tyr-936 in c-Kit. *Biochem J*, **370,** 1033-8.

WONG, W. & SCOTT, J.D. (2004). AKAP signalling complexes: focal points in space and time. *Nat Rev Mol Cell Biol*, **5,** 959-70.

XU, R.X., HASSELL, A.M., VANDERWALL, D., LAMBERT, M.H., HOLMES,

W.D., LUTHER, M.A., ROCQUE, W.J., MILBURN, M.V., ZHAO, Y., KE, H. & NOLTE, R.T. (2000). Atomic structure of PDE4: insights into phosphodiesterase mechanism and specificity. *Science*, **288,** 1822-5.

XU, Z., WANG, B.R., WANG, X., KUANG, F., DUAN, X.L., JIAO, X.Y. & JU, G. (2006). ERK1/2 and p38 mitogen-activated protein kinase mediate iNOS-induced spinal neuron degeneration after acute traumatic spinal cord injury. *Life Sci*, **79,** 1895-905.

YAMASHITA, T. & TOHYAMA, M. (2003). The p75 receptor acts as a displacement factor that releases Rho from Rho-GDI. *Nat Neurosci*, **6,** 461-7.

YAN, C., BENTLEY, J.K., SONNENBURG, W.K. & BEAVO, J.A. (1994). Differential expression of the 61 kDa and 63 kDa calmodulin-dependent phosphodiesterases in the mouse brain. *J Neurosci*, **14,** 973-84.

YAN, C., MILLER, C.L. & ABE, J. (2007). Regulation of phosphodiesterase 3 and inducible cAMP early repressor in the heart. *Circ Res*, **100,** 489-501.

YANAKA, N., KUROSAWA, Y., MINAMI, K., KAWAI, E. & OMORI, K. (2003). cGMP-phosphodiesterase activity is up-regulated in response to pressure overload of rat ventricles. *Biosci Biotechnol Biochem*, **67,** 973-9.

YANG, G., MCINTYRE, K.W., TOWNSEND, R.M., SHEN, H.H., PITTS, W.J., DODD, J.H., NADLER, S.G., MCKINNON, M. & WATSON, A.J. (2003). Phosphodiesterase 7A-deficient mice have functional T cells. *J Immunol*, **171,** 6414-20.

YARWOOD, S.J., STEELE, M.R., SCOTLAND, G., HOUSLAY, M.D. & BOLGER, G.B. (1999). The RACK1 signaling scaffold protein selectively interacts with the cAMP-specific phosphodiesterase PDE4D5 isoform. *J Biol Chem*, **274,** 14909-17.

YIN, D., GAVI, S., WANG, H.Y. & MALBON, C.C. (2004). Probing receptor structure/function with chimeric G-protein-coupled receptors. *Mol Pharmacol*, **65,** 1323-32.

YOON, S.O., CASACCIA-BONNEFIL, P., CARTER, B. & CHAO, M.V. (1998). Competitive signaling between TrkA and p75 nerve growth factor receptors determines cell survival. *J Neurosci*, **18,** 3273-81.

YORK, R.D., MOLLIVER, D.C., GREWAL, S.S., STENBERG, P.E., MCCLESKEY, E.W. & STORK, P.J. (2000). Role of phosphoinositide 3-kinase and endocytosis in nerve growth factor-induced extracellular signal-regulated kinase activation via Ras and Rap1. *Mol Cell Biol*, **20,** 8069-83.

YOU, H.J., WOO, C.H., CHOI, E.Y., CHO, S.H., YOO, Y.J. & KIM, J.H. (2005). Roles of Rac and p38 kinase in the activation of cytosolic phospholipase A2 in response to PMA. *Biochem J*, **388,** 527-35.

YUASA, K., KOTERA, J., FUJISHIGE, K., MICHIBATA, H., SASAKI, T. & OMORI, K. (2000). Isolation and characterization of two novel phosphodiesterase PDE11A variants showing unique structure and tissue-specific expression. *J Biol Chem*, **275,** 31469-79.

ZACCOLO, M., MAGALHAES, P. & POZZAN, T. (2002). Compartmentalisation of cAMP and Ca(2+) signals. *Curr Opin Cell Biol*, **14,** 160-6.

ZAKOWSKI, V., KERAMAS, G., KILIAN, K., RAPP, U.R. & LUDWIG, S. (2004). Mitogen-activated 3p kinase is active in the nucleus. *Exp Cell Res*, **299,** 101-9.

ZHANG, H.T., HUANG, Y., JIN, S.L., FRITH, S.A., SUVARNA, N., CONTI, M. & O'DONNELL, J.M. (2002). Antidepressant-like profile and reduced sensitivity to rolipram in mice deficient in the PDE4D phosphodiesterase enzyme. *Neuropsychopharmacology*, **27,** 587-95.

ZHANG, H.T., HUANG, Y., MASOOD, A., STOLINSKI, L.R., LI, Y., ZHANG, L., DLABOGA, D., JIN, S.L., CONTI, M. & O'DONNELL, J.M. (2008). Anxiogenic-like behavioral phenotype of mice deficient in phosphodiesterase 4B (PDE4B). *Neuropsychopharmacology*, **33,** 1611-23.

ZHANG, J., SHEN, B. & LIN, A. (2007). Novel strategies for inhibition of the p38 MAPK pathway. *Trends Pharmacol Sci*, **28,** 286-95.

ZHANG, K.Y., CARD, G.L., SUZUKI, Y., ARTIS, D.R., FONG, D., GILLETTE, S., HSIEH, D., NEIMAN, J., WEST, B.L., ZHANG, C., MILBURN, M.V., KIM, S.H., SCHLESSINGER, J. & BOLLAG, G. (2004). A glutamine switch mechanism for nucleotide selectivity by phosphodiesterases. *Mol Cell*, **15,** 279-86.

ZHANG, K.Y., IBRAHIM, P.N., GILLETTE, S. & BOLLAG, G. (2005). Phosphodiesterase-4 as a potential drug target. *Expert Opin Ther Targets*, **9,** 1283-305.

ZHANG, L., MURRAY, F., ZAHNO, A., KANTER, J.R., CHOU, D., SUDA, R., FENLON, M., RASSENTI, L., COTTAM, H., KIPPS, T.J. & INSEL, P.A. (2008). Cyclic nucleotide phosphodiesterase profiling reveals increased expression of phosphodiesterase 7B in chronic lymphocytic leukemia. *Proc Natl Acad Sci U S A*, **105,** 19532-7.

ZHANG, M., FRASER, D. & PHILLIPS, A. (2006). ERK, p38, and Smad signaling pathways differentially regulate transforming growth factor-beta1 autoinduction in proximal tubular epithelial cells. *Am J Pathol*, **169,** 1282-93.

ZHAO, A.Z., HUAN, J.N., GUPTA, S., PAL, R. & SAHU, A. (2002). A phosphatidylinositol 3-kinase phosphodiesterase 3B-cyclic AMP pathway in hypothalamic action of leptin on feeding. *Nat Neurosci*, **5,** 727-8.

ZIRRGIEBEL, U., OHGA, Y., CARTER, B., BERNINGER, B., INAGAKI, N., THOENEN, H. & LINDHOLM, D. (1995). Characterization of TrkB receptor-mediated signaling pathways in rat cerebellar granule neurons: involvement of protein kinase C in neuronal survival. *J Neurochem*, **65,** 2241-50.

ZORAGHI, R., CORBIN, J.D. & FRANCIS, S.H. (2004). Properties and functions of GAF domains in cyclic nucleotide phosphodiesterases and other proteins. *Mol Pharmacol*, **65,** 267-78.